Modification of poly(butylene terephthalate) by incorporation of comonomers in the solid state

Modification of poly(butylene terephthalate) by incorporation of comonomers in the solid state

Martinus Adrianus Gertrudus Jansen

CIP-DATA LIBRARY TECHNISCHE UNIVERSITEIT EINDHOVEN

Jansen, Martinus A.G.

Modification of poly(butylene terephthalate) by incorporation of comonomers
in the solid state / by Martinus A.G. Jansen. –
Eindhoven : Technische Universiteit Eindhoven, 2005.
Proefschrift. – ISBN 90-386-2827-7
NUR 913

Trefwoorden: vaste-stof polymerisatie / polycondensatie ; reactiekinetiek /
polyesters ; poly(butyleentereftalaat) / semi-kristallijne polymeren ; morfologie /
NMR spectroscopie
Subject headings: solid-state polymerization / polycondensation ; reaction
kinetics / polyesters ; poly(butylene terephthalate) / polymer morphology ;
crystallinity / NMR spectroscopy

Cover-design by Jan-Willem Luiten, JWL Producties
Printed by PrintPartners Ipskamp, The Netherlands

An electronic version of this thesis is downloadable in
PDF-format from the website of the Eindhoven
University of Technology (http://www.tue.nl/bib)

The work presented in this thesis was financially supported
by the Dutch Polymer Institute (DPI) under project #143.

Modification of poly(butylene terephthalate) by incorporation of comonomers in the solid state

PROEFSCHRIFT

ter verkrijging van de graad van doctor aan de
Technische Universiteit Eindhoven, op gezag van de
Rector Magnificus, prof.dr.ir. C.J. van Duijn, voor een
commissie aangewezen door het College voor
Promoties in het openbaar te verdedigen
op dinsdag 15 november 2005 om 16.00 uur

door

Martinus Adrianus Gertrudus Jansen

geboren te Helmond

Dit proefschrift is goedgekeurd door de promotor:

prof.dr. C.E. Koning

en copromotoren:

dr.ir. J.G.P. Goossens
en
dr. G. de Wit

Contents

Summary

Poly(butylene terephthalate) (PBT) is a semi-crystalline polycondensation polymer which is characterized by a high crystallization rate in combination with good thermal and mechanical properties. PBT is therefore very suitable for injection molding applications. The glass transition temperature is relatively low, i.e.$T_g \approx 45$ °C, so that the dimensional stability of unfilled PBT is low when used at elevated temperatures. It is generally known that the material properties of PBT can be modified by blending in the melt, e.g. with other polycondensates. Transesterification reactions, occurring in the melt, will first result in the formation of block copolymers, and with proceeding reaction time, copolymers with a random microstructure will be obtained. These random copolymers have shorter and more irregular homopolymer sequences and may therefore exhibit a decreased melting temperature, crystallization rate and crystallinity compared to pure PBT.

The aim of the research described in this thesis is to develop a modification method for PBT, which makes it possible to retain the high crystallization rate of PBT, whereas other properties can be enhanced. Here, one can think of an increase of the T_g, but also impact-strength and compatibility with other polymers could be improved. A modification method recently used to prepare copolymers from polycondensation homopolymers and diol comonomers is solid-state (co)polymerization (SSP). With SSP, a reaction temperature is used which is just below the melting temperature of the homopolymer. The result is that polymer chain segments present in the amorphous phase become sufficiently mobile to participate in transesterification reactions between the homopolymer chains and the mixed diol comonomer. The polymer chain segments present in the crystalline phase are not mobile enough at the used temperature and will remain unchanged. Therefore, solid-state polymerization can be used to selectively incorporate comonomers in the amorphous phase without modification of the crystalline phase. In this way, a blocky chemical microstructure is obtained and homopolymer PBT chain segments necessary for crystallization are retained, whereas thermal and mechanical properties can be adjusted.

Three diols appeared to be suitable for incorporation into PBT via SSP: 2,2-bis[4-(2-hydroxyethoxy)phenyl]propane (Dianol 220®), bis(2-hydroxyethyl)terephthalate (BHET) and 2,2'-biphenyldimethanol (BDM). PBT and the selected diol were mixed in different ratios to obtain copolymers of varying compositions using a solution blending route. For comparison, these diols were also incorporated into PBT via melt copolymerization (MP) resulting in random copolymers.

The reaction kinetics of the incorporation of Dianol into PBT was studied in detail. The incorporation occurred via two consecutive first-order reactions. Dianol first reacts by one

hydroxyl end group with amorphous PBT chains (i.e. first reaction) resulting in chain scission and concomitant decrease of the molecular weight. The PBT chain ends, encapped with Dianol, subsequently react with other PBT chain segments to result in chain recombination (i.e. second reaction) with 1,4-butanediol as the leaving group. It was shown that the first reaction proceeds at a higher rate than the second reaction. The morphology of the PBT-Dianol copolymers can be described by a three-phase model, consisting of a crystalline and an amorphous phase, which can be subdivided into a rigid amorphous fraction and a mobile amorphous fraction. A specially developed calculation method shows that only the mobile amorphous fraction is accessible for incorporation of Dianol via SSP, and also that Dianol is randomly incorporated into this mobile amorphous fraction. The PBT/Dianol mixtures used as a feed for SSP almost exclusively consist of a crystalline fraction and a rigid amorphous fraction. During the SSP-reaction, part of the rigid amorphous PBT chain segments get swollen by Dianol. As a result, the overall mobility of these chain segments significantly increases. This swollen fraction together with the small fraction of originally present mobile amorphous chain segments forms the total mobile amorphous fraction of the PBT/Dianol mixture. The PBT chain segments corresponding to this total mobile amorphous fraction have sufficient mobility to react via transesterification reactions with Dianol, resulting in randomly modified chain segments. These modified chain segments are no longer able to crystallize. The remaining rigid amorphous PBT chain segments, not swollen by Dianol, will partly transform into the crystalline phase as a result of crystal perfectioning. When increasing amounts of Dianol are used for incorporation, the fraction of swollen PBT chain segments at the initial stage of the SSP-reaction increases and consequently also the fraction in which transesterification reactions can occur increases. When no rigid amorphous chain segments are left for swelling, Dianol will dissolve the PBT crystals. This dissolution process proceeds at a low rate. The final result is that for sufficiently high fractions of Dianol, the copolymerization can no longer be considered as being performed in the solid-state, but is similar to copolymerization in the melt. The chemical microstructure is blocky for low fractions of incorporated Dianol, but becomes fully random for large fractions of incorporated Dianol. The latter result is in agreement with the random chemical microstructure obtained for the PBT-Dianol copolymers obtained by MP. Despite the differences in chemical microstructure, the observed thermal properties of the PBT-Dianol copolymers obtained by SSP are almost equal to those of the copolymers obtained by MP. The T_g of the PBT-Dianol copolymers obtained by SSP show directly after SSP a significantly increase compared to pure PBT. However when the copolymers are cooled from the melt and subsequently reheated, the T_g values decreased. This decrease is due to the full miscibility of the modified PBT chain segments with the unmodified chain segments when the PBT copolymer is in the molten state. Therefore, both crystallization rate and crystallinity significantly decrease during cooling from the melt. Consequently, an increased fraction of unmodified PBT chain

segments will contribute to the amorphous phase during the second heating run resulting in a reduction of the T_g.

Contrary to the PBT-Dianol copolymers, the blocky character of the chemical microstructure increases for the PBT-BHET copolymers when increasing fractions of BHET monomer are used for incorporation. Due to the presence of both hydroxyl and carbonyl groups, BHET is able to transesterify with other BHET monomers, resulting in the formation of PET homopolymers. It appears that BHET is only partly miscible with the amorphous PBT phase. Only this miscible BHET fraction is able to react with PBT. The BHET which is not miscible with PBT forms a separate phase and reacts to PET homopolymer during the SSP-reaction. When a large BHET fraction is present at the initial stage of the SSP-reaction, the formed PET homopolymers have sufficiently large chain lengths to crystallize during the SSP-reaction. Also for the PBT-BHET copolymers obtained by SSP, the thermal properties are similar to those of the PBT-BHET copolymers obtained by MP. As in the case for the PBT-Dianol copolymers, the unmodified PBT chain segments are fully miscible with the modified chain segments of the copolymers obtained by SSP when in the system is in the molten state.

Finally, the BDM monomer was incorporated into PBT via SSP and MP to result in copolymers of equal composition. BDM behaves similar to Dianol and hence swells the rigid amorphous PBT chain segments when mixed with PBT. However, due to the relatively high volatility, no more than 15 mol% BDM could be incorporated into the mobile amorphous PBT fraction via SSP. Examination of the thermal properties of these PBT-BDM copolymers obtained via SSP and MP show that for both methods a high nucleation rate is obtained when these copolymers are crystallized from the melt. Furthermore, the T_g increases for both copolymers approximately 15 °C compared to PBT homopolymer. The high nucleation rate is probably due to the rigid and rod-like structure of the BDM monomer resulting in an ordered structure of the PBT chain segments when the copolymers are in the molten state. For the PBT-BDM copolymer obtained by SSP, the crystallization temperature was even more than 10 °C higher than that of the PBT-BDM copolymer obtained by MP. In addition, the molecular weight of the PBT-BDM copolymer obtained by SSP was even slightly higher compared to that of the PBT-BDM copolymer obtained by MP. Hence, the non-random distribution of BDM in copolymer obtained by SSP results in an increased ordering in the molten state compared to the BDM-PBT copolymers obtained by MP. The ordering subsequently promotes nucleation when the copolymer is cooled from the melt. This result shows that SSP can be used to modify properties of semi-crystalline polymers with a better crystallization behavior compared to MP.

Chapter 1
Introduction

1.1 General introduction

In the late 1960s, Celanese introduced glass fiber-reinforced PBT compounds on the market. Because of its very easy processing and rapid crystallization, PBT became a widely used thermoplastic material. Nowadays, a broad range of injection moldable PBT grades is available. In addition to neat PBT grades, glass fiber-reinforced, impact-modified, mineral-filled and flame-retardant grades, as well as several blends based on PBT are available. Currently, the combined annual market of PBT in the United States, Western Europe, Japan and South-East Asia exceeds 350 ktons.[1] PBT is a semi-crystalline polymer and a member of the engineering thermoplastics. PBT is characterized by: 1) high stiffness and strength, 2) reasonable toughness at low temperatures, 3) high heat-deflection temperature, 4) high solvent resistance, 5) good dimensional stability, 6) high hydrolytic stability, and 7) electrical insulator properties.

1.2 Reactions to synthesize polyesters

Several reaction routes are possible to obtain polyesters. At least six routes can be distinguished:[2]

1. Direct esterification of diols with dicarboxylic acids or diacid derivatives.

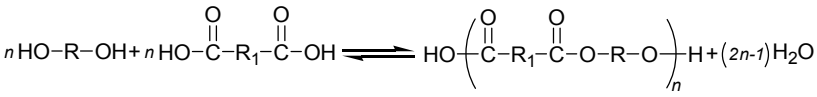

(1.1a)

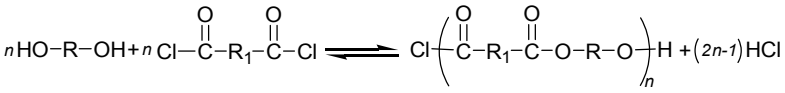

(1.1b)

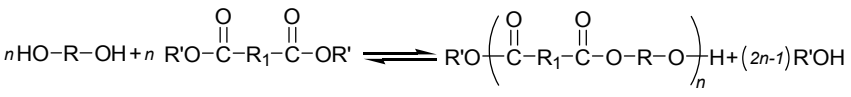

(1.1c)

The R' group of the di-ester may differ on either side

2. Self-condensation of hydroxy acids

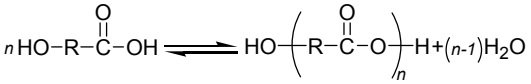

(1.2)

3. Reaction of alkane dihalides with dicarboxylic acid salts

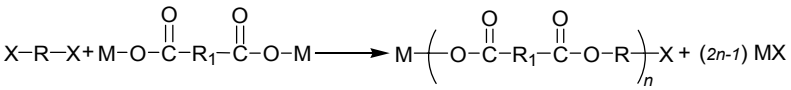

(1.3)

M = Ag, Na, K and X = Cl, Br, I

4. Reaction of diacids with diepoxides

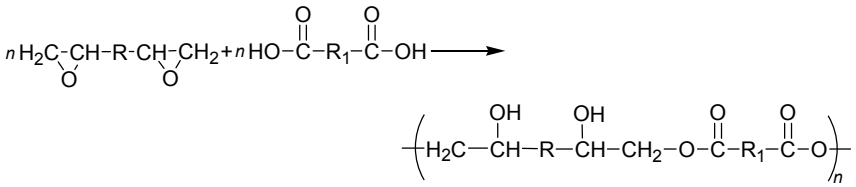

(1.4)

5. Ring-opening polymerization

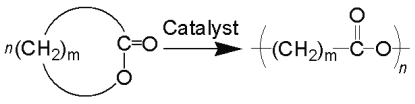

(1.5)

6. Ester interchange reactions

a) Alcoholysis

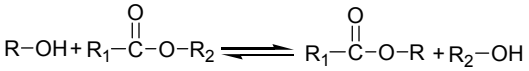

(1.6a)

b) Acidolysis

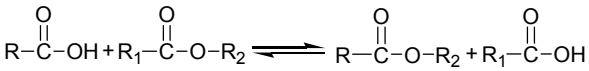

(1.6b)

c) Ester exchange

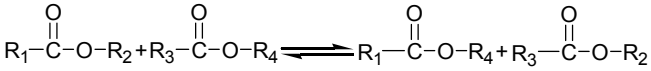

(1.6c)

It has to be mentioned that ester interchange reactions (eqs 1.6a-1.6c) only result in modification of the chemical structure of an existing polyester and thus cannot be used to synthesize polyesters as can be done by the other reaction mechanisms (eqs 1.1-1.5).

PBT is polymerized in a two-stage process. In the first stage, bis(4-hydroxybutyl)-terephthalate (BHBT) is formed by transesterification (i.e. alcoholysis; see eq 1.6a) of dimethyl terephthalate (DMT) with 1,4-butane diol. In the second stage, the BHBT further reacts by polycondensation to result in PBT homopolymer whereas 1,4-butanediol is the elimination product. The transesterification and polycondensation reaction are schematically presented in Figure 1.1a and 1.1b, respectively.

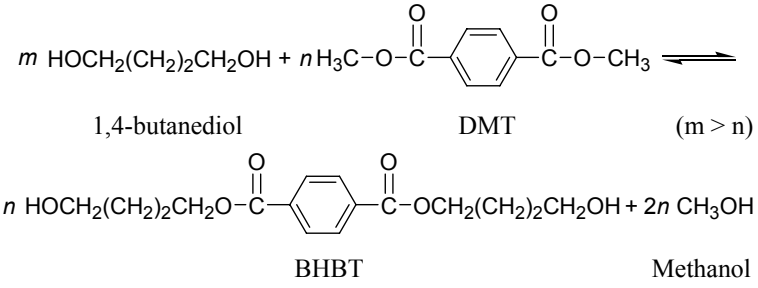

(a)

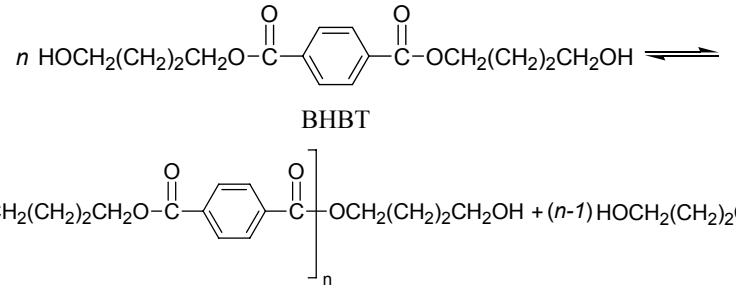

(b)

Figure 1.1. (a) Formation of BHBT by transesterification of DMT with 1,4-butanediol (b) polycondensation of BHBT to result in PBT.

In the transesterification stage, DMT reacts with an excess of approximately 30-50% 1,4-butanediol to form BHBT. During the transesterification reaction, the temperature is increased from 150 °C to approximately 210 °C. The pressure is atmospheric or slightly lower. The methanol formed as the elimination product is distilled off while the 1,4-butanediol is refluxed. The preferred catalysts are titanium or tin organic compounds. In the

polycondensation process, the temperature is increased to 250-260 °C and a high vacuum is applied (< 1 mBar). By applying these conditions, the BHBT formed during the transesterification process undergoes further polymerization to result in PBT homopolymer whereas 1,4-butanediol is formed as the elimination product. The 1,4-butanediol has to be removed to favor the polycondensation, which is an equilibrium reaction. The evaporation of 1,4-butanediol is promoted by intensive mixing of the melt and by the application of the high vacuum.

Besides the reactions resulting in PBT homopolymer, side reactions can occur. The most important side reaction is the formation of tetrahydrofuran (THF) which is formed by intramolecular dehydration of 1,4-butanediol (see Figure 1.2a). THF can also be formed by intramolecular elimination of hydroxybutyl ester end groups, which concomitantly results in the formation of a carboxylic end group (see Figure 1.2a). The formation of THF is acid-catalyzed. A second important side reaction is the thermal degradation of the ester bond resulting in formation of a carboxylic end group and a double bond (see Figure 1.2b).

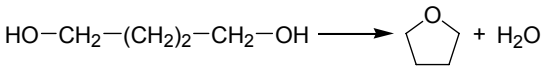

1,4-butanediol THF

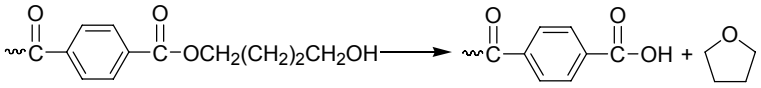

Butanediol end group carboxylic end group THF

(a)

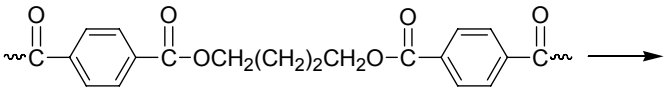

Butanediol (in polymer PBT chain)

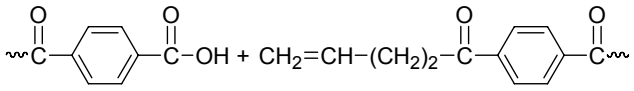

carboxylic end group vinyl end group

(b)

Figure 1.2. Side reactions during PBT formation: (a) THF formation and (b) vinyl end group formation.

1.3 Modification of polyesters

In general, the properties of bulk polymers do not always meet the demands for the application of the customer. Often, the bulk properties have to be modified. As a consequence, a "tailor approach" of polymer properties has been developed over the last decennia. In this way, heavy capital investments and long development times, usually associated with the development of new polymers, are not necessary. In the following paragraphs, several options to modify existing polyesters are discussed.

1.3.1 Reactive blending

One possibility to adjust the material properties of polyesters such as PBT is melt blending with other polymers. A basic requirement for obtaining a material with useful properties through blending is, at least partial, miscibility. However, most polymer blends are fully immiscible and consequently poor properties are obtained. Therefore, immiscible blends are usually compatibilized. In this way, the interfacial properties of an immiscible polymer blend are modified such that the desired morphology and concomitant properties are obtained. A generally used compatibilization method is reactive blending. With this method, a blend of two polyester homopolymers is kept in the molten state in the presence of a transesterification promoting catalyst. The subsequent ester-interchange reactions occurring in the melt first yield copolymers with a block-like structure, but as the reaction proceeds, a fully random copolymer is obtained.[3-9] Focusing on PBT blends, several studies related to transesterification and the concomitant crystallization behavior were performed e.g. on PBT/PC,[3,9] PBT/PAr,[4,7,10] and PBT/PET[5,6,8,11] blends.

1.3.2 Copolymerization in the melt (MP)

Another possibility to modify properties of homopolyesters, although not so often used on industrial scale, is melt copolymerization (MP). With MP, a diol monomer is mixed with a homopolyester. This mixture is subsequently molten in the presence of a transesterification promoting catalyst.[12] The diol to be incorporated should have a melting temperature (T_m) below that of the homopolyester and sufficiently thermally stable to prevent evaporation. Upon incorporation, the original diol of the homopolyester will evaporate and be removed from the reaction mixture by application of a high vacuum. Similar to the melt blending method as described previously, a fully random copolymer is obtained.[12]

1.3.3 Copolymerization in the solid state (SSP)

Although the material properties of polyesters can be modified with the previously discussed methods, both methods are less suitable for semi-crystalline polyesters. The resulting random copolyesters have shorter and more irregular homopolymer sequences. Consequently, when the material properties of semi-crystalline polyesters are modified by either of the previously discussed methods, a decrease in melting temperature, crystallinity and crystallization rate can be expected. It would therefore be desirable to develop a modification method in which the incorporation of diol monomer in semi-crystalline polyesters can be controlled in such a way that the crystallization behavior is retained, whereas other material properties, such as the glass transition temperature (T_g), impact strength and compatibility with other polymers, can be tailored. Hence, the chemical microstructure of the resulting copolyesters should consist of modified polymer chain segments and unmodified homopolymer chain segments of sufficient length being able to crystallize. Marchese and co-workers found that for PBT a length of at least 16 PBT repeat-units is necessary for crystallization to occur.[9]

This modification results in a non-random chemical microstructure. To illustrate the difference between a random and a non-random copolymer, a schematic representation of each chemical microstructure is shown in Figure 1.3a and 1.3b, respectively.

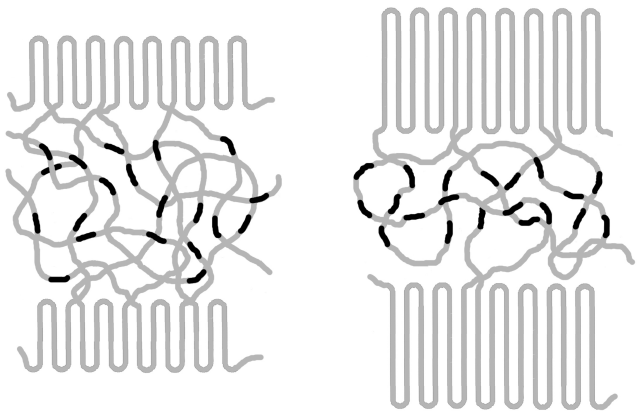

(a) (b)

Figure 1.3. (a) Random chemical microstructure with reduced crystallization behavior and (b) non-random chemical microstructure with retained crystallization behavior. The short dark connections represent the incorporated monomeric moieties.

A modification technique that recently has gained attention for preparing polycondensation copolymers is solid-state polymerization (SSP). SSP is traditionally used as a post-condensation technique to increase the molecular weight of semi-crystalline polycondensates, especially for the preparation of fiber grades of PET.[13] The essential point of SSP is that the reaction temperature is just below the melting temperature of the polymer and above its T_g. In practice, a temperature of 200-210 °C is used for solid-state polymerization of pure PBT homopolymer. A consequence of this high temperature is that the polymer chain segments in the amorphous phase become sufficiently mobile for transesterification reactions to take place. The polymer chain segments in the crystalline phase, however, are not mobile enough to participate in the transesterification reactions. During the SSP-reaction, recombination of mobile chain end groups by so-called outer-outer transesterification reactions[14] will occur, whereas low molecular weight side-products, notably 1,4-butanediol and water, evaporate. A vacuum or nitrogen flow is usually applied to remove these generated side-products from the polymer particles and thus drive the equilibrium to completion.

It was found in the early seventies by Lenz and Go[15,16] that transesterification reactions in random cis-trans poly(cyclohexylene 1,4-dimethylene terephthalate) polyesters also occur when the polyesters were kept below their melting temperature. The initial random chemical microstructure of these polyesters changed into a blocky chemical microstructure, whereas the overall chemical composition remained unchanged. In the early nineties, Backson and co-workers observed by ^{13}C-NMR sequence distribution analysis that a blocky microstructure was formed when a PBT-PET blend was kept for 6 h at 203 °C, which is below the melting temperature of PBT.[5] Sivaram and co-workers studied ester-carbonate interchange reactions in the solid state using oligomer mixtures of PET and poly(aryl carbonates) (PC).[17] SSP of these oligomer mixtures resulted in the formation of PET-PC copolyesters. They also used SSP to synthesize copolymers from blends of PET and poly(ethylene naphthalate) (PEN) oligomers.[18,19] The chemical microstructure of these PET-PEN copolymers was studied in detail via a ^{1}H-NMR sequence distribution analysis. A copolymer with a blocky microstructure was found after SSP.

1.4 Objectives of the thesis

The objective of this thesis is to modify the polymer properties of PBT in such a way that its good crystallization properties are retained. A method that might fulfill this aim is selective incorporation of diol monomers into PBT by solid-state polymerization. In this way, the diol monomer is expected to incorporate only in the polymer chain segments of the amorphous phase, whereas the PBT segments in the crystalline phase are not participating in the transesterification process. Large crystallizable PBT blocks should therefore be retained

whereas the modified amorphous chain segments contribute to an increase of the T_g.

To restrict the number of diol monomers to study for incorporation into PBT, the selection was made based on the following boundary conditions:

- The diol should increase the T_g of PBT after its incorporation. It is known that bulky aromatic groups have an enhancement effect on the T_g. Also groups that can lead to hydrogen bonding such as hydroxyl groups[20] and amides[21,22] increase the T_g. Furthermore, it is known that hydrogen bonding may improve the crystallization rate.[21,22]
- The diol should be commercially available. It is the aim of this work to study solid-state polymerization as a method for copolymerization. At this stage, existing diol monomers should provide the necessary scientific insight. In a later stage, specific diols might be synthesized to optimize the resulting polymer properties of the PBT copolyester.
- The diol should be sufficiently thermally stable. The temperatures used for SSP are in the range of 180 to 210 °C. Hence, the diol to be incorporated should not evaporate or degradate at these high temperatures.
- The T_m of the diol monomer should be lower than the T_m of PBT (< 220 °C), but higher than the T_g of PBT (> 45 °C).
- For transesterification reactions to occur, the diol to be incorporated should be sufficiently miscible with the amorphous PBT phase. If the miscibility is limited, then the reactive contact area between amorphous PBT chain segments and the diol monomer is low which will result in a decrease of the transesterification rate.
- The reactivity of the diol monomer itself should be sufficiently high. The diol should have two primary hydroxyl end groups. Secondary hydroxyl end groups are not reactive enough to react at the temperatures used for solid-state polymerization.

The previous mentioned list of boundary conditions resulted in the diol monomer selection as presented in Table 1.1. These diol monomers are incorporated in PBT via SSP and via MP. A difference in chemical microstructure (non-random versus random) is expected. The influence of the chemical microstructure on morphology and thermal properties should be well understood.

Table 1.1. Selected diol monomers for incorporation into PBT by SSP

Diol monomer	T_m [a]	Thermal stability[b]
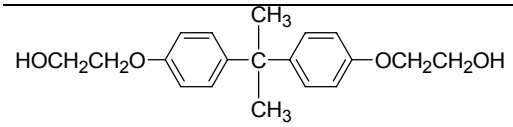 2,2-bis[4-(2-hydroxyethoxy)phenyl]propane: Dianol 220®	110 °C	100 % (200 °C)
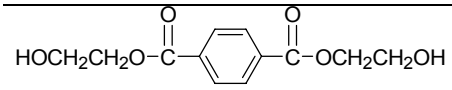 bis(2-hydroxyethyl)terephthalate: BHET	108 °C	90 % (200 °C)
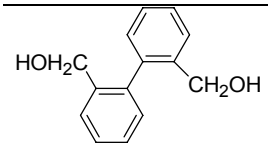 2,2'-biphenyldimethanol: BDM	110 °C	80.8 % (170 °C)

[a] as determined by differential scanning calorimetry (DSC)

[b] weight fraction of material left after holding isothermally for 1 h at the mentioned temperature in the presence of a nitrogen flow. Weight fractions were determined by thermogravimetric analysis (TGA).

1.5 Outline of the thesis

In **Chapter 2**, the kinetics of the incorporation of 2,2-bis[4-(2-hydroxyethoxy)phenyl]propane (Dianol 220®) in PBT via SSP is studied by variation of the reaction time under isothermal conditions. A reaction mechanism is proposed and the corresponding reaction rate constants are determined by fitting the calculated values with the experimentally obtained data using a least-square method. The incorporation is also studied by sequence distribution analysis using quantitative ^{13}C-NMR spectroscopy.

Chapter 3 focuses on the differences in chemical microstructure between PBT copolymers obtained by SSP and by melt polymerization (MP) for both Dianol and bis(2-hydroxyethyl)terephthalate (BHET). BHET can form PET homopolymer by self-transesterification. Hence, a different chemical microstructure is expected compared to incorporation of Dianol into PBT. The synthesis of PBT-Diol copolymers using different PBT-diol feed ratios by either SSP or MP is discussed in detail. The chemical microstructure is studied by quantitative ^{13}C-NMR sequence distribution analysis.

For the PBT-Dianol copolymers obtained by SSP, the chemical microstructure of the amorphous phase in which the modification takes place is examined in detail in **Chapter 4.** A calculation method is developed which adjusts the ^{13}C-NMR peak integral values of the dyad sequences in such a way that the contribution of the unchanged crystalline fraction is not taken into consideration. The calculation is first applied to a two-phase (crystallization and amorphous) morphology. In a second step, the amorphous phase is further divided into a rigid amorphous fraction and a mobile amorphous fraction. In **Chapter 5**, the morphology of the PBT-Dianol copolymers is studied by DSC and Small-Angle X-ray scattering (SAXS). The influence of Dianol on the initial morphology of PBT/Dianol feed mixtures used for SSP is examined. Furthermore, the morphology development during the SSP reaction (i.e. as a function of reaction time) is followed. The collected information is used to explain the final morphology of the PBT-Dianol copolymers obtained after SSP. In the second part of this chapter, the chemical microstructure of the PBT-Dianol copolymers obtained by SSP and MP is related to the thermal properties of these copolymers.

The BHET monomer incorporation into PBT, partly described in **Chapter 3**, is examined in more detail in **Chapter 6**. The chemical microstructure development and the morphology are revealed as a function of reaction time. The influence of BHET on the initial morphology of the PBT/BHET mixtures, used as feed for SSP, is examined. The final morphology of the PBT-BHET copolymers obtained by SSP is discussed and compared with the PBT-Dianol copolymers obtained by SSP (**Chapter 5**). The second part of this chapter focuses on the chemical microstructure of the PBT-BHET copolymers and the resulting thermal properties.

Chapter 7 focuses on the thermal properties of PBT-BDM copolymers obtained by SSP and MP. The obtained results are compared with the thermal properties of the PBT-Dianol and PBT-BHET copolymers (**Chapters 5** and **6**, respectively).

1.6 References and notes

1. van Berkel, R. W. M.; van Hartingsveldt, E. A. A.; van der Sluijs, C. L. In *Handbook of Thermoplastics*, Olabisi, O., Ed.; Marcel Dekker: New York: 1997, chapter 20, p465-490.
2. Fradet, A.; Maréchal, E. *Adv. Polym. Sci.* **1982**, 43, 51-142.
3. Devaux, J.; Godard, P.; Mercier, J. P.; Touillaux, R.; Dereppe, J. M. *J. Polym. Sci., Polym. Phys. Ed.* **1982**, *20*, 1881-1894.
4. Fernandez-Berridi, M. J.; Iruin, J. J.; Maiza, I. *Polymer* **1995**, *36*, 1357-1361.
5. Backson, S. C. E., Kenwright, A. M., Richards, R. W. *Polymer* **1995**, *36*, 1991-1998.
6. Jacques, B.; Devaux, J.; Legras, R.; Nield, E. *J. Polym. Sci., Polym. Chem. Ed.* **1996**, *34*, 1189-1194.
7. Denchev, Z.; Sarkissova, M.; Fakirov, S.; Yilmaz, F. *Macromol. Chem. Phys.* **1996**, *197*, 2869-2887.

8. Kim, J. H.; Lyoo, W. S.; Ha, W. S. *J. Appl. Polym. Sci.* **2001**, *82*, 159-168.
9. Marchese, P.; Celli, A.; Fiorini, M. *J. Polym. Sci., Polym. Phys. Ed.* **2004**, *42*, 2821-2832.
10. Kimura, M.; Porter. R. S. *J. Polym. Sci., Polym. Phys. Ed.* **1983**, *21*, 367-378.
11. Arivinthan, G.; Kale, D. D. *J. Appl. Polym. Sci.* **2005**, *98*, 75-82.
12. Berti C.; Colonna, M.; Fiorini M.; Lorenzetti, C.; Marchese P. *Macromol. Mat. Eng.* **2004**, *289*, 49-55.
13. Fakirov, S. In *Solid State Behavior of Linear Polyesters and Polyamides*, Schultz, J. M., Fakirov, S., Eds.; Prentice-Hall: Englewood Cliffs, NJ, 1990; Chapter 2, p 19-43.
14. Montaudo, G.; Puglisi, C.; Samperi, F. In *Transreactions in Condensation Polymers*, Fakirov, S., Ed.; Wiley-VCH: Weinheim, 1999; Chapter 4, p 159-193.
15. Lenz, R. W.; Go, S. *J. Polym. Sci., Polym. Chem. Ed.* **1973**, *11*, 2927-2946.
16. Lenz, R. W.; Go, S. *J. Polym. Sci., Polym. Chem. Ed.* **1974**, *12*, 1-10.
17. Hait, S.B.; Sivaram, S. *Macromol. Chem. Phys.* **1998**, *199*, 2689-2697.
18. James, N. R., Ramesh, C.; Sivaram, S. *Macromol. Chem. Phys.* **2001**, *202*, 1200.
19. James, N. R., Ramesh, C.; Sivaram, S. *Macromol. Chem. Phys.* **2001**, 202, 2689-2697.
20. Kuo, S.-W.; Xu, H.; Huang, C.-F.; Chang, F.-C. *J. Polym. Sci., Polym. Phys. Ed.* **2002**, *40*, 2313-2323.
21. Bennekom, A. C. M.; Gaymans, R. J. *Polymer* **1997**, *38*, 657-665.
22. Bouma, K.; De Wit, G.; Lohmeijer, J. H. G. M.; Gaymans, R. J. *Polymer* **2000**, *41*, 3965-3974.

Chapter 2

Reaction kinetics of the incorporation of 2,2-bis[4-(2-hydroxyethoxy)phenyl]propane in PBT via solid-state copolymerization*

2.1 Introduction

Poly(butylene terephthalate) (PBT) is an aromatic semi-crystalline polyester with a high crystallization rate. It is generally known that properties of polycondensates such as PBT can be easily modified by reactive blending in the melt with other polycondensates.[1] The transesterification reactions occurring in the melt convert the blends first into blocky copolymers and, as the reaction proceeds, a random copolymer will eventually be obtained.[2-7] This randomization process results in decreased homopolymer block lengths and may therefore have a large influence on the melting temperature, crystallization behavior and degree of crystallinity of the resulting copolymers. It would thus be desirable to develop a modification method that retains large crystallizable PBT blocks and concomitantly a high crystallization rate, whereas other material properties (e.g. increase of glass transition temperature and impact strength, compatibility with other polymers) can be enhanced. A method that recently has gained attention to prepare polyester copolymers is solid-state polymerization (SSP). SSP is a traditionally used technique to increase the molecular weight of polycondensates by heating the polymer just below its melting temperature in the presence of a nitrogen flow or vacuum.[8] At this temperature, the mobility of the polymer chains in the amorphous phase is sufficiently high for transesterification reactions to occur. In this way, it is possible to obtain copolymers from blends of polycondensates via SSP. Sivaram and co-workers[9,10] prepared copolymers via SSP using semi-crystalline oligomer blends from poly(ethylene terephthalate) (PET) and poly(ethylene naphthalate) (PEN) as starting material. They showed that transesterification occurred predominantly during the first 2 hours of the SSP reaction, whereas the molecular weight of the resulting copolymers still continued to increase for longer reaction times. Sequence distribution analysis via ^{1}H-NMR spectroscopy confirmed that the PET/PEN copolymers were non-random and hence homopolymer blocks were still present after SSP.

---

* This chapter is reproduced from: Jansen, M. A .G.; Goossens, J. G. P.; de Wit, G.; Bailly, C.; Koning C. E. *Macromolecules* **2005**, *38*, 2659-2664.

To our knowledge, no studies have been performed on the incorporation of monomers in a semi-crystalline homopolymer polycondensate via SSP. A different molecular microstructure might be obtained compared to copolymers obtained via SSP of oligomer blends.

In this study, a diol monomer was incorporated in the amorphous phase of PBT via SSP, leaving relatively long, crystallizable PBT sequences unchanged. A mixture consisting of 85 mol% PBT and 15 mol% 2,2-Bis[4-(2-hydroxyethoxy)phenyl]propane (Dianol 220®) was used as starting material. The kinetics of the incorporation via SSP was studied by variation of the reaction time under isothermal conditions. A reaction mechanism was proposed and the corresponding reaction rate constants were determined by fitting theoretical calculated values with experimentally obtained data using a least-square method. The incorporation was also studied by sequence distribution analysis using quantitative ^{13}C-NMR spectroscopy. Finally, the change in molecular weight and molecular weight distribution were determined as a function of reaction time. In **Chapter 4**, a detailed description will be given of the chemical microstructure of these PBT-Dianol copolymers made by SSP as a function of composition. In **Chapter 5**, the thermal properties will be discussed and compared to PBT-Dianol copolymers obtained via traditional melt copolymerization.

2.2 Experimental section

2.2.1 Materials

Poly(butylene terephthalate) (PBT) pellets ($\overline{M}_n$ = 15 kg/mol, $\overline{M}_w$ = 34 kg/mol, determined by size exclusion chromatography) were provided by GE Plastics (Bergen op Zoom, The Netherlands) and used as received. 2,2-Bis[4-(2-hydroxyethoxy)phenyl]propane (Dianol 220®) was provided by Air Liquide (Paris, France) and was recrystallized twice from acetone prior to use. 1,1,1,3,3,3-Hexafluoro-2-propanol (HFIP, 99%) and chloroform ($CHCl_3$, 99%), obtained from Biosolve (Valkenswaard, The Netherlands), were used for solution mixing of PBT with Dianol. For NMR measurements, deuterated trifluoroacetic acid (TFA-d, 99 % deuterated) was obtained from Aldrich and deuterated chloroform ($CDCl_3$, 99% deuterated) was obtained from Merck.

2.2.2 Solution preparation of a PBT-Dianol mixture from HFIP

First, PBT pellets were ground into powder by a mill (Retsch type ZM 100) after cooling with liquid nitrogen. The PBT powder was subsequently dried in a vacuum oven at 70 °C for 48 h. 19.944 g of PBT (0.0906 mol) and 5.057 g of Dianol (0.0160 mol) were dissolved in 50 mL HFIP at a temperature of approximately 55 °C. After complete dissolution, the temperature was raised to 65 °C and the HFIP was distilled off. As soon as the material started to

precipitate, a vacuum of 80-100 mBar was applied to enhance the removal of HFIP. Finally, the obtained lump of material was dried in an oven for 24 h and was then cooled in liquid nitrogen and subsequently ground into powder using an analytical laboratory mill (Waring, type 32BL80). This powder was subsequently dried in a vacuum oven for a period of 48 h prior to further analysis. The PBT/Dianol powder mixture, obtained via dissolution in HFIP, will be abbreviated in this article as $(BD_{85}Di_{15})_{feed}$ where BD_{85} denotes the mol percentage (mol%) of butanediol (BD) units and Di_{15} the mol% of Dianol (Di) units in the mixture.

2.2.3 Solid-state copolymerization (SSP)

The experimental setup for SSP consisted of a vessel with a heating element. A salt mixture of KNO_3 (53 wt%), $NaNO_2$ (40 wt%), and $NaNO_3$ (7 wt%) was used as heating medium.[11] The reactor comprised a glass tube (inner diameter = 2.4 cm) and a sintered glass plate at the bottom. A small heat exchange glass coil (inner diameter = 5 mm) surrounded the reactor and entered the inner glass tube at the bottom just below the glass plate. This coil was used to pass a nitrogen gas flow through. The gas flow was controlled by a flow meter. The reaction setup is schematically depicted in Figure 2.1.

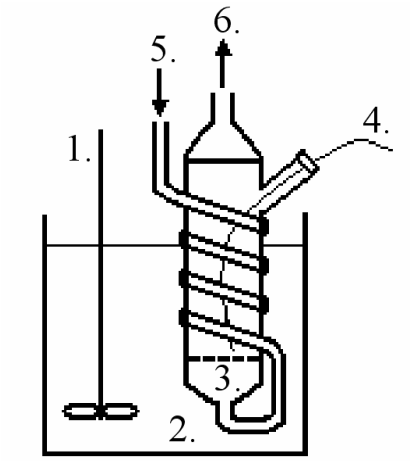

1. mechanical stirrer
2. salt bath
3. SSP-reactor
4. temperature sensor
5. nitrogen gas inlet
6. nitrogen gas outlet

Figure 2.1. Schematic representation of a reactor setup used for SSP.

For the SSP reactions as described in this chapter,[12] 3 g of $(BD_{85}Di_{15})_{feed}$ powder (mixed via dissolution in HFIP as described above) were placed on the sintered glass plate. The powder was fixed by addition of 18 g of glass pearls (d = 2 mm) on top of the powder. A nitrogen flow of 3 L/min was applied and the SSP temperature was kept at 180 °C. SSP reaction times

(t_{ssp}) were varied between 0 h and 24 h. For each t_{ssp}, a new SSP reaction mixture was prepared. After elapsing of t_{ssp}, the reactor was removed from the salt bath and quenched for 5 minutes in water of 80 °C and then further cooled in water of ambient temperature. The synthesized SSP copolymers will be abbreviated in this article as $(BD_{85}Di_{15})_{ssp}$ where BD_{85} and Di_{15} are respectively the mol% butanediol (BD) units and Dianol (Di) units as present in the initial $(BD_{85}Di_{15})_{feed}$ mixture being used for SSP.

2.2.4 Nuclear Magnetic Resonance Spectroscopy (NMR)

All solution ^{1}H-NMR spectra were recorded on a Varian 400 MHz spectrometer at 25 °C and at a resonance frequency of 400.164 MHz. For the ^{1}H-NMR measurements, 15 mg of polymer were dissolved in 0.8 mL of a 80:20 (v/v) $CDCl_3$:TFA-d mixture. All chemical shifts are reported in ppm downfield from tetramethylsilane (TMS), used as an internal standard. The spectra were acquired using 32 scans, a delay time (d1) of 5 s and a total number of data points of 64 k.

Quantitative proton-decoupled solution ^{13}C-NMR spectra were recorded on a Varian 300 MHz spectrometer, operated at a resonance frequency of 75.462 MHz. For ^{13}C-NMR measurements, 50 mg of polymer were dissolved in 0.8 mL pure TFA-d. TMS was used as internal standard. 3000-4000 scans were acquired with 64 k data points, a d1 of 12 s, a 90° pulse and a spectral width of 18.8 kHz. For the sequence distribution analysis, overlapping peaks were integrated after Lorentzian deconvolution of the spectra using the deconvolution option implemented in the Varian NMR-software.

2.2.5 Size Exclusion Chromatography (SEC)

The number-average molecular weight ($\overline{M}_n$) and the polydispersity index (PDI) of the synthesized $(BD_{85}Di_{15})_{ssp}$ copolymers and the $(BD_{85}Di_{15})_{feed}$ mixture were determined by SEC. The system was equipped with a Waters type 710B injector (injection volume = 50 µL) and two PFG linear XL columns from PSS (8×300 mm in size, 7 µm particles) thermostated by a Spark Holland Mistral thermostat at 30 °C. HFIP containing 0.4 wt% ammonium acetate was used as eluent. A Waters type 510 pump provided a flow rate of 0.4 mL/min. For detection, a Waters model 490 UV-detector (λ = 265 nm) was used. Prior to using HFIP as eluent, the SEC system was calibrated with polystyrene (PS) standards using THF as eluent. The remaining measuring conditions were kept equal. The obtained PS calibration curve was used to determine the relative $\overline{M}_n$ of the synthesized $(BD_{85}Di_{15})_{ssp}$ copolymers and $(BD_{85}Di_{15})_{feed}$ mixture. In addition, PBT homopolymer samples with known $\overline{M}_n$ values (determined by end group titration) were measured by the same SEC system. A fitting curve was made References and notes using the $\overline{M}_n$ values obtained by end group titration and the

$\overline{M}_n$ obtained via the PS calibration curve. The measured $\overline{M}_n$ of the $(BD_{85}Di_{15})_{feed}$ mixture and the $(BD_{85}Di_{15})_{ssp}$ copolymers were fitted using this calibration curve and corrected to obtain an absolute value. No correction was made for possible differences in hydrodynamic volumes for the $(BD_{85}Di_{15})_{ssp}$ copolymers versus PBT homopolymer.

2.2.6 High Performance Liquid Chromatography (HPLC)

The fraction of unreacted Dianol in $(BD_{85}Di_{15})_{feed}$ in each $(BD_{85}Di_{15})_{ssp}$ sample was determined via HPLC. The system was equipped with a Hewlett Packard 1100 series injector (injection volume = 25 μL), a Chrompack column (Chromsep 150×4.6 mm Intersil 5 ODS-3) thermostated at 35 °C. An Agilent diode array detector (λ = 240 nm) was used for detection. A solvent mixture consisting of acetonitrile (20 vol%) and water (80 vol%) was used as eluent. A HP 1100 series HPLC pump provided a flow of 1.0 mL/min.

Prior to measuring, a weighed amount of each $(BD_{85}Di_{15})_{ssp}$ sample was dissolved in HFIP and subsequently precipitated in acetonitrile. The HFIP/acetonitrile solution was filtered over a 0.45 μm filter and subsequently injected into the HPLC system. A calibration curve was used in order to determine the amount of free Dianol in each sample. Calibration samples were prepared by dissolution of a known amount of Dianol in a mixture of HFIP:acetonitrile (5:95 vol%) of known volume. The area of the peak corresponding to free Dianol in the $(BD_{85}Di_{15})_{ssp}$ samples was fitted with the calibration curve and converted into a weight fraction of free Dianol.

2.2.7 Differential Scanning Calorimetry (DSC)

The crystallinity ($\chi_{heating}$) of the synthesized $(BD_{85}Di_{15})_{ssp}$ copolymers was measured by a TA Instruments Q1000 DSC equipped with an autosampler and refrigerated cooling system (RCS). The DSC cell was purged with a nitrogen flow of 50 mL/min. The temperature was calibrated using the onset of melting for indium. The enthalpy was calibrated with the heat of fusion for indium. Samples of 5-7 mg were prepared in hermetically closed aluminum pans. Samples were measured in the temperature range from at 0 to 250 °C using a heating rate at 10 °C/min and isothermal periods of 3 min at 0 and at 250 °C, respectively.

2.3 Results and Discussion

In order to study the kinetics of the incorporation of Dianol in PBT, a $(BD_{85}Di_{15})_{feed}$ mixture was polymerized in the solid-state while the polymerization time (t_{ssp}) was varied between 0 to 24 h. The overall chemical structure of the resulting $(BD_{85}Di_{15})_{ssp}$ copolymer, consisting of BD-T and Di-T repeat-units, is shown in Figure 2.2.

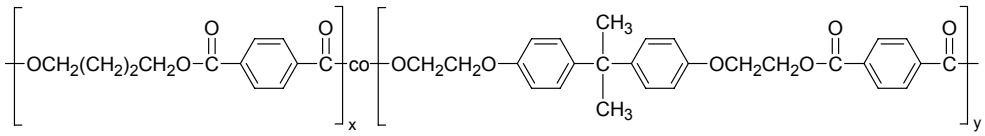

BD-T repeat-unit Di-T repeat-unit

Figure 2.2. Overall chemical structure of a $(BD_xDi_y)_{ssp}$ copolymer with BD-T and Di-T repeat-units.

2.3.1 Change in molecular weight as a function of reaction time (t_{ssp})

During SSP, transesterification reactions occur between the Dianol monomer and the PBT chains present in the amorphous phase, hence it can be expected that the molecular weight will change. The number-average molecular weight ($\overline{M}_n$) and the polydispersity index (PDI) of the $(BD_{85}Di_{15})_{ssp}$ copolymers were determined by Size Exclusion Chromatography (SEC). The change in molecular weight distribution as a function of reaction time (t_{ssp}) is shown in Figure 2.3a. The SEC chromatogram of $(BD_{85}Di_{15})_{feed}$ mixture (t_{ssp} = 0 h) shows the Dianol monomer as a sharp peak at an elution time of 56 min. The broad peak, starting at a lower elution time, represents the PBT homopolymer.

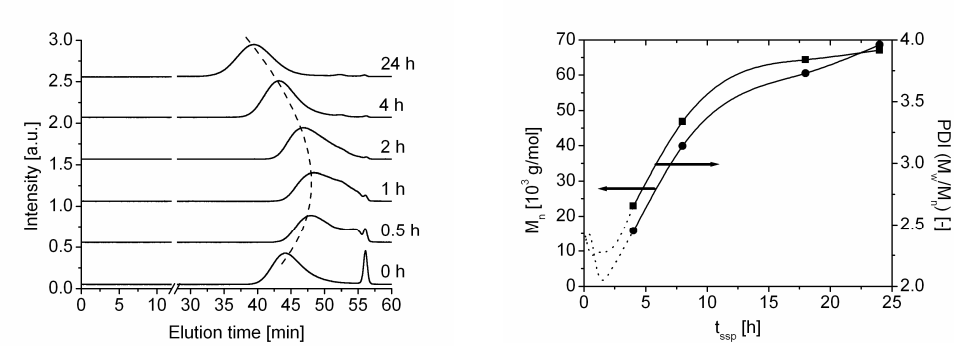

(a) (b)

Figure 2.3. (a) SEC chromatograms of $(BD_{85}Di_{15})_{ssp}$ samples with different t_{ssp} and (b) development of $\overline{M}_n$ and PDI as a function of t_{ssp}.

Already after 0.5 h of transesterification, the Dianol monomer peak becomes significantly smaller, while the peak originating from PBT shifts to higher elution times. This shift indicates that PBT chains are cleaved due to the transesterification reaction with one hydroxyl end group of free Dianol monomer. As a consequence, oligomers are formed which can be derived from the broadening of the polymer peak in the initial stage of the SSP reaction. At

t_{ssp} = 1 h, the polymer peak has its maximum broadness and highest elution time. After t_{ssp} = 2 h, the polymer peak becomes less broad and shifts back to lower elution times. Hence, recombination of polymer chains takes place resulting in higher $\overline{M}_n$ values. In the SEC chromatogram corresponding to t_{ssp} = 4 h, the Dianol monomer peak has almost completely disappeared, but some small traces of cyclic dimers and oligomers might still be present. This result is in agreement with the ^{1}H-NMR analysis of the sample with t_{ssp} = 4 h (Figure 2.5) and the HPLC measurements (F_F in Figure 2.6), which will be discussed in the next section. The $\overline{M}_n$ and PDI of each chromatogram, as shown in Figure 2.3a, are plotted as a function of t_{ssp} in Figure 2.3b. Due to overlap of the Dianol monomer peak with the broad PBT peak (Figure 2.3a), it was not possible to obtain an accurate $\overline{M}_n$ and PDI for $(BD_{85}Di_{15})_{ssp}$ samples with t_{ssp} less than 2 h. Therefore, the $\overline{M}_n$ and PDI curve for $t_{ssp} \leq 2$ h were plotted in Figure 2.3b as dotted lines. Figure 2.3b also shows that after completion of the Dianol incorporation around t_{ssp} = 4 h, the $\overline{M}_n$ of the $(BD_{85}Di_{15})_{ssp}$ copolymer steadily increases. Hydroxybutyl chain end groups are still present in high concentration and react with each other via alcoholysis upon releasing 1,4-butanediol. After ca. 20 h of SSP, the $\overline{M}_n$ levels off. Obviously, the hydroxybutyl end group concentration has become too low at this stage. After t_{ssp} = 24 h, $\overline{M}_n$ becomes close to 70 kg/mol. The PDI increases from 2.3 (t_{ssp} = 0 h) to 3.8 (t_{ssp} = 24 h). The increase in PDI can be explained by the absence of a Flory distribution[13] for SSP. The crystalline fraction of the $(BD_{85}Di_{15})_{ssp}$ copolymers cannot participate in the polycondensation reaction. However, this part does participate in the SEC analysis.

2.3.2 Quantitative discrimination between free Dianol monomer, Dianol mono-ester and Dianol di-ester

The chemical microstructure of the $(BD_{85}Di_{15})_{ssp}$ copolymers will have a blocky character consisting of unmodified homopolymer PBT blocks (only BD-T repeat units) which are predominantly present in the crystalline domains and amorphous parts consisting of both BD-T and Di-T repeat units. The Dianol monomer has two hydroxyl end groups which both can react with PBT. Consequently, during the SSP reaction, Dianol can be present in three forms: (1) as free monomer containing two hydroxyl end groups (= free Dianol, represented as F), (2) as Dianol containing one free hydroxyl end group (= mono-ester, represented as M) and 3) as fully incorporated Dianol (= di-ester, represented as D).

The three forms of Dianol are schematically depicted in Figure 2.4.

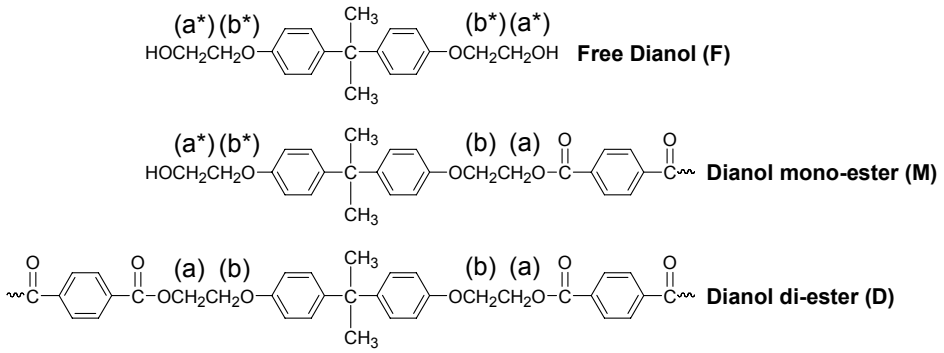

Figure 2.4. The three forms of Dianol that can be present during the SSP reaction: free Dianol monomer (F), Dianol mono-ester (M) and fully incorporated Dianol di-ester (D).

Figure 2.5 shows the 4-5 ppm region of a ^{1}H-NMR spectrum of the $(BD_{85}Di_{15})_{ssp}$ copolymers with different solid-state polymerization times (t_{ssp}). It can be observed that the multiplet peak intensities of (a*) and (b*) gradually decrease as the SSP reaction proceeds, while two new peaks appear more downfield at 4.43 (b) and 4.77 (a) ppm.

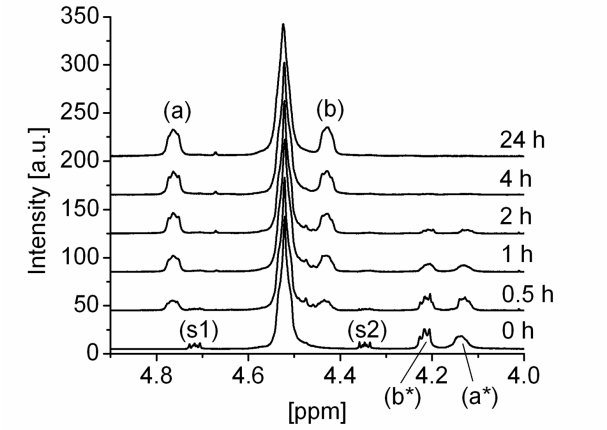

Figure 2.5. ^{1}H-NMR spectra: 4-5 ppm region shown at different t_{ssp} (see Figure 2.4 for the identification of peaks).

Peaks (a*) and (b*) originate from the two protons in the -CH_2- groups next to the free hydroxyl end groups of free Dianol (F) (see Figure 2.4). However, the protons in the -CH_2- group next to the free hydroxyl end group of the Dianol mono-ester (M) have an identical chemical shift as those in the -CH_2- groups of free Dianol. Hence, both free Dianol (F) and the

Dianol mono-ester (M) contribute to peaks (a*) and (b*). When the free hydroxyl end groups of free Dianol or Dianol mono-ester react via transesterification with PBT, a carbonyl group is formed close to the -CH_2- groups (Figure 2.4). The presence of the electron withdrawing carbonyl group close to the -CH_2- groups results in the formation of two new peaks (a) and (b), having a chemical shift more downfield with respect to peaks (a*) and (b*). Also here, the chemical shift of the protons in the -CH_2- groups close to a carbonyl bond is identical for Dianol mono-ester and Dianol di-ester. Consequently, both Dianol mono-ester and Dianol di-ester contribute to peaks (a) and (b). The small peaks at 4.35 and 4.70 ppm (s_1 and s_2) are the result from the ester formation between a small fraction of free hydroxyl end groups from (F) or (M) and deuterated trifluoroacetic acid,[14] used as NMR-solvent. When the fraction of free Dianol (F_F) is known as a function of t_{ssp}, the integrals of the peaks in the 4-5 ppm region can be used to obtain the fraction of Dianol mono-ester (F_M) and Dianol di-ester (F_D) as a function of t_{ssp}. The mol fraction of free Dianol (F_F) in $(BD_{85}Di_{15})_{feed}$ (t_{ssp} = 0 h) and each $(BD_{85}Di_{15})_{ssp}$ sample was determined via HPLC. The obtained value for F_F of the $(BD_{85}Di_{15})_{feed}$ mixture was 15.1 mol% and is thus in agreement with the mol fraction of Dianol used for the mixture (≈ 15 mol%, see Experimental Section). Subsequently, F_F was set at 1 and the F_F values for the samples after SSP were proportionally adjusted. Prior to calculation of the fractions F_M and F_D, the integrals in the 4-5 ppm region were used to express the total amount of Dianol (sum of F_F, F_M and F_D) as an integral value:

$$I(total\ Dianol) = I\left(\frac{(a^*)+(b^*)+(s_1+s_2)}{2}\right)+I(a) \tag{2.1a}$$

where:

$$I\left(\frac{(a^*)+(b^*)+(s_1+s_2)}{2}\right) = F+0.5M \tag{2.1b}$$

and

$$I(a) = D+0.5M \tag{2.1c}$$

The chemical shift of peak (a*) is closely positioned to that of peak (b*) making an accurate determination of the integral value of peak (a*) impossible. However, peaks (a*) and (b*) should have equal integral values and therefore the integral was taken over both (a*) and (b*) and subsequently divided by 2 (see eq 2.1a). Peak (s_2) was also taken into account because this peak originates from F or M. The integral values of peaks (s_2) are very small and were therefore added to the peak integral values of (s_1) and subsequently averaged (see eq 2.1a). It was already mentioned that, based on the number of protons, Dianol mono-ester (M) equally contributes to both peaks (a) and (a*) (2 protons for M versus 4 protons for F and D, see Figure 2.4). Now, the amounts of (F), (M) and (D) have to be expressed as an integral value.

The following equations were used:

$$F = F_F \cdot I(total\ Dianol) \tag{2.2}$$

$$1/2 \cdot M = I(total\ Dianol) - (a) - F \tag{2.3}$$

$$D = (a) - M \tag{2.4}$$

The fractions of free Dianol (F_F), Dianol mono-ester (F_M) and Dianol di-ester (F_D) can now be calculated by:

$$F_M = \frac{M}{I(total\ Dianol)} \tag{2.5}$$

$$F_D = \frac{D}{I(total\ Dianol)} \tag{2.6}$$

The fractions F_F, F_M and F_D, calculated via eqs 2.2, 2.5 and 2.6, are plotted as a function of t_{ssp} in Figure 2.6. F_F, obtained from HPLC measurements, rapidly decreases. Already after t_{ssp} = 1 h, 90% of free Dianol monomer (F_F) has reacted with PBT via alcoholysis reactions. At t_{ssp} = 4 h, no free Dianol monomer is left. The fraction of Dianol mono-ester (F_M) increases to a maximum at t_{ssp} = 1 h. This maximum clearly indicates that Dianol mono-ester (M) is an intermediate product that reacts with PBT via a consecutive alcoholysis reaction. At t_{ssp} = 4 h, all Dianol mono-ester has been fully incorporated (F_D = 100).

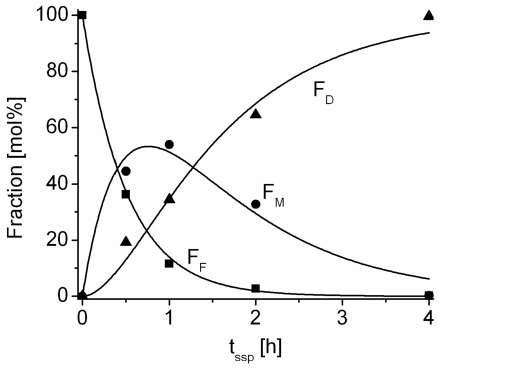

Figure 2.6. Experimentally determined values for F_F (■), F_M (●) and F_D (▲) using HPLC and ^{1}H-NMR spectroscopy measurements as a function of t_{ssp} and calculated values for F_F, F_M and F_D using k_1^f = 1.0 h^{-1} and k_2^f = 0.83 h^{-1} (—).

2.3.3 Reaction kinetics of SSP: two consecutive first-order reactions

As can be seen from Figure 2.6, the distribution of F_F, F_M and F_D as a function of t_{ssp} is typical for a series of two irreversible consecutive first-order reactions.[15] The corresponding reaction scheme is schematically given in eq 2.7a:

$$F \xrightarrow{k_1^f} M \xrightarrow{k_2^f} D \tag{2.7a}$$

where k_1^f and k_2^f are the reaction rate constants of the two consecutive reactions. F, M and D represent: free Dianol, Dianol mono-ester and Dianol di-ester respectively.

The reaction rate equations can be described by:

$$-\frac{dF_F}{dt} = k_1^f \cdot F_F \tag{2.7b}$$

$$\frac{dF_M}{dt} = k_1^f \cdot F_F - k_2^f \cdot F_M \tag{2.7c}$$

$$\frac{dF_D}{dt} = k_2^f \cdot F_M \tag{2.7d}$$

Solving the set of differential eqs 2.7b-2.7d results in:

$$F_F(t) = F_{F,t=0} \cdot e^{-k_1^f t} \tag{2.8}$$

$$F_M(t) = \frac{k_1^f}{k_2^f - k_1^f}(e^{-k_1^f t} - e^{-k_2^f t}) \cdot F_{F,t=0} \tag{2.9}$$

$$F_D(t) = (1 - \frac{k_2^f}{k_2^f - k_1^f} e^{-k_1^f t} + \frac{k_1^f}{k_2^f - k_1^f} e^{-k_2^f t}) \cdot F_{F,t=0} \tag{2.10}$$

where it is assumed that at t_{ssp}= 0 h, F_M = 0 and F_D = 0. Furthermore, eqs 2.7-2.10 are only valid when the reaction volume remains unchanged during the reaction and the Dianol monomer is homogenously distributed in the amorphous phase. To verify if the amorphous phase does not significantly change during the SSP reaction, the crystallinity ($\chi_{heating}$) of each $(BD_{85}Di_{15})_{ssp}$ sample was determined by Differential Scanning Calorimetry (DSC) using the first heating run. The obtained values for $\chi_{heating}$ were corrected in such a way that only the

crystallizable BD-T repeat-units were taken into account. The results are shown in Figure 2.7. It can be seen that the variation in $\chi_{heating}$ is ±5% for $0 \leq t_{ssp} \leq 4$ h and therefore within experimental error. When $t_{ssp} > 4$ h, all Dianol is fully incorporated (see Figure 2.6) and $\chi_{heating}$ only increases due to annealing.

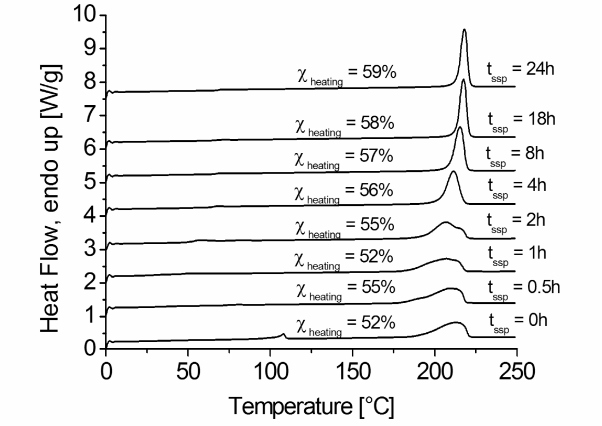

Figure 2.7. DSC traces (first heating run) of the synthesized $(BD_{85}Di_{15})_{ssp}$ copolymers as a function of t_{ssp}. Values for $\chi_{heating}$ are corrected for the weight fraction of crystallizable BD-T repeat-units present in each sample.

In addition, the results as will be discussed in **Chapter 3 and 5** show that Dianol also acts as a solvent for PBT crystals and therefore Dianol should be homogenously distributed in the amorphous phase of PBT once the Dianol monomer is molten. More details about the thermal properties of $(BD_xDi_y)_{ssp}$ copolymers will be described in **Chapter 5**.

Reaction rate constants k_1^f and k_2^f were obtained via a least-square fitting method. The fractions F_F, F_M and F_D were calculated for different t_{ssp} (0, 0.5, 1, 2 and 4 h) using eqs 2.8-2.10 with initial arbitrary values for k_1^f and k_2^f. A minimum total square error value was found for $k_1^f = 2.0$ h^{-1} and $k_2^f = 0.83$ h^{-1}. To validate the integrity of the values found, the fractions F_F, F_M, F_D were calculated as a function of t_{ssp}, using eqs 2.8-2.10 with $k_1^f = 2.0$ h^{-1} and $k_2^f = 0.83$ h^{-1}. These calculated values for fractions F_F, F_M and F_D are also plotted in Figure 2.6. It can be seen that the calculated fractions, based on k_1^f and k_2^f, are in good agreement with the experimentally obtained fractions (obtained via eqs 2.2, 2.5 and 2.6). However, the fractions F_F, F_M and F_D are expressed in mol fractions and because free Dianol has 2 reactive hydroxyl end groups, the value found for k_1^f has to be divided by 2 and consequently $k_1^f = 1$ h^{-1}. Because the obtained values for k_1^f and k_2^f are within experimental error, it can be concluded that the presence of a PBT chain on one side of Dianol (i.e. Dianol

mono-ester) results in a decreased hydroxyl end group reactivity compared to the end groups of free Dianol ($k_1^f / k_2^f > 1$). Flory[16] postulated that reactivity of functional end groups remains independent of molecular weight of the corresponding polymers. However, he remarked that for small molecules a higher end group reactivity is possible. This effect is clearly observed from the results described above.

2.3.4 Chemical microstructure as a function of reaction time (t_{ssp})

Besides ^{1}H-NMR spectroscopy, also ^{13}C-NMR spectroscopy was used to study the incorporation of Dianol in PBT via SSP. Kricheldorf[17] already showed in the early seventies that the ^{13}C-NMR shift of carbonyl carbon atoms present in terephthalate based polyesters is determined by adjacent monomeric units. Later, Newmark[18] used the same method for PBT-PET copolymers and found that the signal of the quaternary carbon atom of the terephthalate unit, i.e. the carbon atom to which the carboxylate group is attached, splits up into a total of four peaks. Each of these peaks represents a dyad sequence. In Figure 2.8, the 135-137 ppm region of the ^{13}C-NMR spectrum is shown for a $(BD_{85}Di_{15})_{ssp}$ copolymer with t_{ssp} = 4 h. Also for this copolymer, the signal of the quaternary carbon atom, adjacent to the carbonyl group, splits into four peaks.

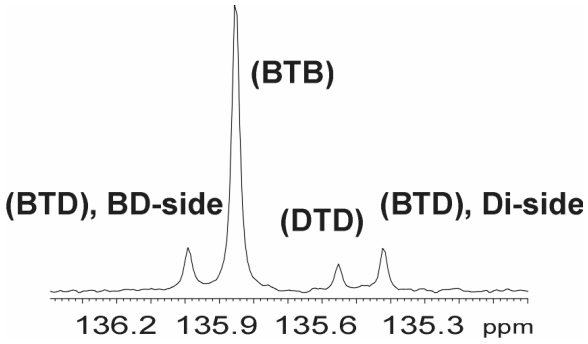

Figure 2.8. ^{13}C-NMR spectrum (135-137 ppm region) of a $(BD_{85}Di_{15})_{ssp}$ copolymer at t_{ssp} = 4 h: splitting of the quaternary carbon atom into four peaks with different chemical shifts and integral size.

The four corresponding dyad sequences, including chemical shifts, are shown in Figure 2.9. A schematic representation of a BTD sequence is shown for convenience.

Sequence	Chemical shift [ppm]
BTD, BD side	136.0
BTB	135.9
DTD	135.6
BTD, Di side	135.4

Schematic representation sequence BTD, BD-side

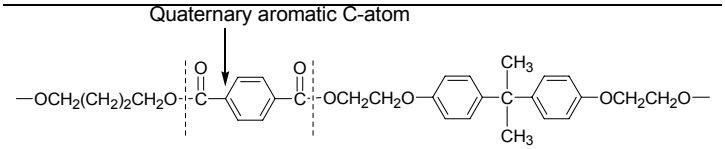

Figure 2.9. The four possible dyad sequences and corresponding chemical shifts. For convenience, a schematic representation of a BTD dyad sequence is included.

The peaks as shown in Figure 2.8 were integrated and the corresponding integral values were normalized to a total value of 1. It will be shown in **Chapter 3** and **Chapter 4** that the four peak signals in Figure 2.8, corresponding to the four dyad sequences, can be used in a quantitative way. The normalized integral values can be used to determine the degree of randomness (R) as a function of t_{ssp}. R is defined[19] by:

$$R = \frac{F_{BTD,\,tot}}{2 \cdot (F_{BD-T} \cdot F_{Di-T})} \tag{2.11a}$$

where:

$$F_{BD-T} = (F_{BTD,\,tot}/2 + F_{BTB}) \tag{2.11b}$$

$$F_{Di-T} = (F_{BTD,\,tot}/2 + F_{DTD}) \tag{2.11c}$$

$$F_{BTD,\,tot} = F_{BTD,\,BD\,side} + F_{BTD,\,Di\,side} \tag{2.11d}$$

where F_i denotes the normalized fraction of each sequence (i = BTD, BD side; BTB; DTD; BTD, Di side).

R should be 1 for a fully random copolymer[19,20] in which the repeat-units (in this study: BD-T and Di-T, see Figure 2.2) are randomly distributed over the copolymer. A value for R smaller than 1, indicates that similar repeat-units tend to form blocks. In Figure 2.10, the calculated degree of randomness is shown as a function of t_{ssp}.

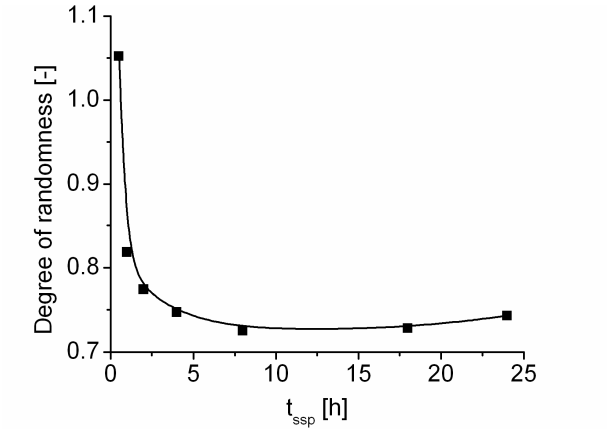

Figure 2.10. Degree of randomness (R) as a function of t_{ssp} obtained via quantitative ^{13}C-NMR spectroscopy measurements.

It was already mentioned that with SSP only the amorphous phase of PBT should be accessible for incorporation of Dianol, while the crystalline fraction should remain unchanged. As a consequence, the preserved crystallizable PBT homopolymer blocks result in a value for R below unity, which can clearly be observed in Figure 2.10. The degree of randomness rapidly decreases during the first hour and remains constant after t_{ssp} = 4 h. This stabilization of R implies that the final chemical microstructure of the $(BD_{85}Di_{15})_{ssp}$ copolymer does not change anymore. Hence, all Dianol should be fully incorporated around t_{ssp} = 4 h, which is in agreement with the results plotted in Figure 2.6. This stabilization of R implies that the final chemical microstructure of the $(BD_{85}Di_{15})_{ssp}$ copolymer does not change anymore. Hence, all Dianol should be fully incorporated around t_{ssp} = 4 h, which is in agreement with the results plotted in Figure 2.6.

2.4 Conclusions

Dianol was successfully incorporated in PBT via SSP using a reaction temperature of 180 °C. HPLC measurements in combination with ^{1}H-NMR spectroscopy showed that the incorporation of Dianol in PBT occurs via a series of two consecutive first-order transesterification reactions. The Dianol monomer first forms an intermediate species (Dianol

mono-ester) where PBT is attached on one side of the Dianol monomer. A second transesterification reaction results in Dianol di-ester. The reaction rate constants k_1^f and k_2^f were determined via a least-square fitting method which resulted in k_1^f = 1.0 h^{-1} and k_2^f = 0.83 h^{-1}. The fraction of amorphous phase did not considerably change during the SSP reaction and hence the obtained values for k_1^f and k_2^f are within experimental error. Because (k_1^f / k_2^f) > 1, it can be concluded that Dianol attached to a PBT chain (Dianol mono-ester) becomes less reactive towards transesterification compared to free Dianol monomer. Apparently, the hydroxyl end groups of Dianol mono-ester have a reduced reactivity compared to hydroxyl end groups of free Dianol monomer. It was also shown that the Dianol monomer was fully incorporated around t_{ssp} = 4 h. In agreement, ^{13}C-NMR sequence distribution analysis showed that the degree of transesterification did not significantly change after t_{ssp} = 4 h. SEC measurements showed that oligomers are formed in the initial stage of the SSP reaction. Alcoholysis results subsequently in an increase of the molecular weight. The broadening of the molecular weight distribution as a function of t_{ssp} can be explained by the absence of a Flory distribution during SSP.

2.5 References and notes

1. Denchev, Z. In *Handbook of Thermoplastic Polyesters*, Fakirov, S., Ed.; Wiley-VCH: Weinheim, 2002; Chapter 17, p 757-813.
2. Devaux, J.; Godard, P.; Mercier, J. P. *J. Polym. Sci., Polym. Phys. Ed.* **1982**, *20*, 1881-1894.
3. Fakirov, S.; Sarkissova, M.; Denchev, Z. *Macromol. Chem. Phys.* **1996**, *197*, 2837-2867.
4. Denchev, Z.; Sarkissova, M.; Fakirov, S.; Yilmaz, F. *Macromol. Chem. Phys.* **1996**, *197*, 2869-2887.
5. Fakirov, S.; Sarkissova, M.; Denchev, Z. *Macromol. Chem. Phys.* **1996**, *197*, 2889-2907.
6. Montaudo, G.; Montaudo, M. S.; Scamporrino, E.; Valatini, D. *Macromolecules* **1992**, *25*, 5099-5107.
7. Fernandez-Berridi, M. J.; Iruin, J. J.; Maiza, I. *Polymer* **1995**, *36*, 1357-1361.
8. Fakirov, S. In *Solid State Behavior of Linear Polyesters and Polyamides*, Schultz, J. M., Fakirov, S., Eds.; Prentice-Hall: Englewood Cliffs, 1990; Chapter 2, p 19-43.
9. James, N. R.; Ramesh, C.; Sivaram, S. *Macromol. Chem. Phys.* **2001**, *202*, 1200-1206.
10. James, N. R.; Ramesh, C.; Sivaram, S. *Macromol. Chem. Phys.* **2001**, *202*, 2267-2274.
11. Kirk, R. E.; Othmer, D. F. In *Kirk-Othmer Encyclopedia of Chemical Technology*, 4th ed.; Kroschwitz, J. I., Howe-Grant, M., Eds.; Wiley-Interscience: New York, 1997; Vol. 22, p 400.
12. The PBT as received already contained residuals of tetra-n-butyl titanate ($Ti(OBu)_4$) catalyst, so promoting the transesterification reaction by additional catalyst was not necessary.
13. Flory, P. J. In *Principles of Polymer Chemistry*, Cornell University Press: London, 1953; Chapter 8, p 317-326.
14. Kenwright, A. M.; Peace, S. K.; Richards, R. W.; Bunn, A.; MacDonald, W. A. *Polymer* **1999**, *40*, 2035-2040.

15. Santen van, R. A.; Niemantsverdriet, J. W. In *Chemical Kinetics and Catalysis*, Twigg, M. V., Spencer, M. S., Eds.; Plenum Press: New York, 1995; Chapter 2, p 38-41.
16. Flory, P. J. In *Principles of Polymer Chemistry*; Cornell University Press: London, 1953; Chapter 3, p 69-105.
17. Kricheldorf, H. R. *Makromol. Chem.* **1978**, *179*, 2133-2143.
18. Newmark, R. A. *J. Polym. Sci., Polym. Chem. Ed.* **1980**, 18, 559-563.
19. Yamadera, R.; Murano, M. *J. Polym. Sci. Part A-1* **1967**, *5*, 2259-2268.
20. Devaux, J.; Godard, P.; Mercier, J. P.; Touillaux, R.; Dereppe, J. M. *J. Polym. Sci., Polym. Phys. Ed.* **1982**, *20*, 1875-1880.

Chapter 3
The microstructure of PBT copolymers via ^{13}C-NMR sequence distribution analysis: solid-state copolymerization versus melt copolymerization*

3.1 Introduction

Poly(butylene terephthalate) (PBT) is a semi-crystalline aromatic polyester that is used in numerous applications. Its main advantage is a high crystallization rate combined with good mechanical properties and chemical resistance.[1] The glass transition temperature of PBT, however, is rather low ($T_g \approx 45°C$). It is generally known that material properties of PBT can be modified by reactive melt blending with other polycondensates.[2] The ester-interchange reactions will first yield copolymers with a block-like structure, but as the reaction proceeds, a fully random copolymer will be obtained.[3-8] These random copolymers have shorter and more irregular homopolymer sequences and consequently exhibit a lower melting temperature, crystallization rate and crystallinity. It would therefore be desirable to develop a modification method in which the microstructure can be controlled in such a way that the crystallization rate is retained while other material properties (T_g, but also impact strength and compatibility with other polymers) can be improved. A modification technique that recently has gained attention for preparing polycondensation copolymers is solid-state polymerization (SSP). SSP is traditionally used as a post-condensation technique to increase the molecular weight of semi-crystalline polycondensates.[9] The essential point of SSP is that the reaction temperature is just below the melting temperature of the polymer and far above its T_g. As a consequence, the polymer chain segments in the amorphous phase become mobile enough for transesterification reactions to take place, while the segments in the crystalline phase are not mobile enough. Sivaram and co-workers studied ester-carbonate interchange reactions in the solid state using oligomer mixtures of PET and poly(aryl carbonates) (PC).[10] SSP of these oligomer mixtures resulted in the formation of PET-PC copolyesters. They also used SSP to synthesize copolymers from oligomer blends of PET and poly(ethylene naphthalate)

* This chapter is reproduced from: Jansen, M. A. G.; Goossens, J. G. P.; de Wit, G.; Baily, C.; Koning, C. E. *Anal. Chim. Acta.* **2005**, in press.

(PEN).[11,12] The chemical microstructure of these PET-PEN copolymers was studied in detail via a ^{1}H-NMR sequence distribution analysis. A copolymer with a blocky microstructure was found after SSP.

Besides ^{1}H-NMR spectroscopy, ^{13}C-NMR spectroscopy can be used to study the sequence distribution. This method was first explored in the 1970's by Kricheldorf[13] who could make a clear distinction between homopolyesters and copolyesters, based on their difference in microstructure. Later, Newmark[14] used ^{13}C-NMR spectroscopy to study PET-PBT copolymers prepared via melt polycondensation. He observed that different dyad sequences could be distinguished due to the splitting of ^{13}C-NMR signals originating from both the quaternary aromatic carbon atom and the carbonyl carbon atom of the terephthalate unit into peaks with different chemical shifts. These peaks, having different integral values, were used to calculate the degree of randomness by a method proposed by Yamadera et al.[15] The same ^{13}C-NMR method was used by several authors to study the presence of transesterification reaction in blends of polycondensates[16,17] or to study the chemical microstructure of synthesized copolyesters.[3,18-21] In our previous work,[22] 2,2-Bis[4-(2-hydroxyethoxy)phenyl]-propane (Dianol 220®) was successfully incorporated in PBT via SSP, and the kinetics of the incorporation of this diol was studied in detail. In the present chapter, we focus on the analysis on the differences in chemical microstructure of PBT copolymers obtained by SSP and by melt polymerization (MP). Two diols were selected for incorporation in PBT: Dianol 220® and bis(2-hydroxyethyl)terephthalate (BHET). Both PBT-Dianol and PBT-BHET copolymers were synthesized by SSP and MP using different PBT/diol ratios and the chemical microstructures were studied by quantitative ^{13}C-NMR spectroscopy. The main difference between Dianol and BHET is that BHET can undergo self-transesterification, yielding poly(ethylene terephthalate) (PET). Hence, PBT-BHET copolymers obtained via SSP may result in a different chemical microstructure compared to PBT-Dianol copolymers obtained by SSP.

3.2 Experimental Section

3.2.1 Materials

Poly(butylene terephthalate) (PBT) pellets ($\overline{M}_n$ = 15 kg/mol and $\overline{M}_w$ = 34 kg/mol, determined by size exclusion chromatography) were provided by GE Plastics (Bergen op Zoom, The Netherlands) and used as received. 2,2-Bis[4-(2-hydroxyethoxy)phenyl]propane (Dianol 220®) was provided by Air Liquide (Paris, France) and was recrystallized twice from acetone prior to use. Bis(2-hydroxyethyl)terephthalate was obtained from Aldrich and recrystallized twice from acetone prior to use. 1,1,1,3,3,3-Hexafluoro-2-propanol (HFIP, 99

%), obtained from Biosolve (Valkenswaard, The Netherlands), was used as received for solution mixing of PBT with Dianol. For NMR measurements, deuterated trifluoro acetic acid (TFA-d, 99 % deuterated) was obtained from Aldrich and deuterated chloroform ($CDCl_3$, 99 % deuterated) was obtained from Merck.

3.2.2 Solution preparation of PBT-diol (Dianol or BHET) mixtures from HFIP

First, PBT pellets were ground into powder by a mill (Retsch, type ZM100) after cooling with liquid nitrogen. The PBT powder was subsequently dried in a vacuum oven at 70°C for 48 h. Mixtures of PBT/Dianol and PBT/BHET were prepared using different ratios of PBT and diol. These mixtures were used as feed for the SSP and MP reactions in order to obtain copolymers of different compositions. For the MP reactions, the PBT and Diol powder were mixed in a specific ratio in the melt (see Experimental Section: Melt polymerization). For the copolymers prepared by SSP, the PBT and Diol were mixed by dissolution in HFIP. As an example, the preparation of a mixture containing 15 mol% Dianol and 85 mol% PBT is described. 9.573 g PBT (0.0435 moles) and 2.431 g Dianol (0.00768 moles) (12 g powder in total) were dissolved in 24 mL HFIP at approximately 55°C. After complete dissolution, the temperature was raised to 65°C and HFIP was distilled off. As soon as the material started to precipitate, a vacuum of 80-100 mBar was applied to complete the removal of HFIP. Finally, the obtained lump of material was dried in an oven for 24 h, cooled in liquid nitrogen and subsequently ground into powder using an analytical laboratory mill (Waring, type 32BL80). This powder was subsequently dried in a vacuum oven for a period of 48 h prior to further analysis. The resulting PBT/Dianol mixtures are abbreviated as $(BD_xDi_y)_{feed}$ and the PBT/BHET mixtures as $(BD_xEG_y)_{feed}$. BD_x denotes the mol percentage (mol%) of PBT (expressed in 1,4-butanediol units) whereas Di_y and EG_y denote the mol% of Dianol and mol% of BHET units, respectively.

3.2.3 Solid-state polymerization (SSP)

The experimental setup for solid-state polymerization consisted of a heating vessel with a heating element. A salt mixture of KNO_3 (53 wt%), $NaNO_2$ (40 wt%), and $NaNO_3$ (7 wt%) was used as heating medium.[23] The reactor comprised a glass tube (inner diameter = 2.4 cm) with a sintered glass plate at the bottom. A small heat exchange glass coil (inner diameter = 5 mm) surrounded the reactor and entered the inner glass tube at the bottom just below the glass plate. The nitrogen gas was heated by passing through this coil prior to entering the reactor. The gas flow was controlled by a flow meter and was constantly kept at 3 L/min during the reaction. The procedure described below was used for both $(BD_xDi_y)_{feed}$ and $(BD_xEG_y)_{feed}$ mixtures. Typically, 5 g of a PBT/diol mixture[24] was placed on the sintered glass plate. The

powder was fixed by addition of 30 g of glass pearls (diameter = 2 mm) on top of the powder. For all SSP reactions, a reaction time of 9 h[22] was used in combination with a temperature of 180 °C for the $(BD_xDi_y)_{feed}$ mixtures and 185 °C for the $(BD_xEG_y)_{feed}$ mixtures. After completion of the reaction, the reactor was removed from the salt bath and gradually cooled down to room temperature by the nitrogen flow purging through the reactor. The (BD_xDi_y) and (BD_xEG_y) copolymers obtained via SSP are indicated as $(BD_xDi_y)_{ssp}$ and $(BD_xEG_y)_{ssp}$ copolymers, respectively. BD_x represents the mol% BD in the $(BD_xDi_y)_{feed}$ and $(BD_xEG_y)_{feed}$ mixtures used for SSP. Di_y and EG_y represent respectively the mol fractions Dianol and EG (2 mol EG per mol BHET) in the initial $(BD_xDi_y)_{feed}$ and $(BD_xEG_y)_{feed}$ mixtures used for SSP. The mol fractions of BD_x and Di_y/EG_y units after SSP slightly differ from the initially fractions present in the $(BD_xDi_y)_{feed}$ and the $(BD_xEG_y)_{feed}$ mixtures. This difference can be attributed to the evaporation of 1,4-butanediol or ethylene glycol during the SSP reaction.

3.2.4 Melt polymerization (MP)

The melt polymerizations were carried out in a typical melt polymerization setup consisting of a reactor tube, motorized stirrer and a distillation head connected to a cooler. A heating vessel, containing the same salt mixture as described previously, was used as heating equipment. The procedure described below was used for both $(BD_xDi_y)_{feed}$ and $(BD_xEG_y)_{feed}$ mixtures. The reactor tube was filled with 7.5 g of PBT/diol powder mixture (without HFIP dissolution treatment, see Experimental section: Solution preparation of PBT-diol mixtures from HFIP) and placed in the salt bath with a starting temperature of 220°C under continuous stirring and an argon flow of 1.5 L/min. The temperature was immediately raised and kept for 30 min at 230°C. The temperature was then further increased and kept for 1.5 h at 240°C for the $(BD_xDi_y)_{feed}$ mixtures and at 265°C for the $(BD_xEG_y)_{feed}$ mixtures. Simultaneously, the argon flow was replaced by a continuous high vacuum of 0.1 mBar. After this period, the vacuum was released and the tube was removed from the vessel and allowed to cool down to room temperature. The obtained copolymer was then dissolved in 15 mL of a 50:50 vol% HFIP:chloroform mixture and subsequently precipitated in cold methanol. The precipitated copolymer was dried in a vacuum oven at 65°C prior to further analysis. Melt polymerized (BD_xDi_y) and (BD_xEG_y) copolymers are denoted as $(BD_xDi_y)_{mp}$ and $(BD_xEG_y)_{mp}$ copolymers respectively. BD_x represents the initial mol% BD present in the $(BD_xDi_y)_{feed}$ and $(BD_xEG_y)_{feed}$ mixtures used for MP. Di_y and EG_y are the mol fractions of respectively Dianol and EG present in the $(BD_xDi_y)_{feed}$ and $(BD_xEG_y)_{feed}$ mixtures. Also here, the mol fractions of BD_x and Di_y/EG_y units after MP differ slightly from the initial fractions present in the $(BD_xDi_y)_{feed}$ and the $(BD_xEG_y)_{feed}$ mixtures.

3.2.5 Nuclear Magnetic Resonance (NMR) Spectroscopy

All solution ^{1}H-NMR spectra were recorded on a Varian 400 MHz spectrometer at 25°C at a resonance frequency of 400.164 MHz. For the ^{1}H-NMR measurements, 15 mg of polymer was dissolved in 0.8 mL of a 80:20 vol% $CDCl_3$:TFA-d mixture. All chemical shifts are reported in ppm downfield from tetramethylsilane (TMS), used as the internal standard. The spectra were acquired using 32 scans, a delay time (d1) of 5 s and a total number of data points of 64 k.

Quantitative proton-decoupled solution ^{13}C-NMR spectra were recorded on a Varian 300 MHz spectrometer, operated at a resonance frequency of 75.462 MHz. For copolymers with less then 10 mol% of incorporated Dianol or BHET, an Oxford 500 MHz spectrometer was used, operated at a resonance frequency of 125.685 MHz. For ^{13}C-NMR measurements, 50 mg of polymer was dissolved in 0.8 mL pure TFA-d. TMS was used as the internal standard. For spectra recorded with the 300 MHz spectrometer, 3000-4000 scans were acquired with 64 k data points, a d1 of 12 s, a 90° pulse and a spectral width of 18.8 kHz. For the spectra recorded with the 500 MHz spectrometer, 4000-5000 scans were acquired with 75 k data points, a d1 of 12 s, a 90° pulse and a spectral width of 25 kHz. Spinning was not used for the spectra recorded at the 500 MHz spectrometer.

For the sequence distribution analysis, overlapping peaks were integrated after Lorentzian deconvolution of the spectra using the deconvolution option implemented in the Varian NMR-software.

3.2.6 Size Exclusion Chromatography (SEC)

The number-average molecular weight ($\overline{M}_n$) and polydispersity index (PDI) of the synthesized (BD_xDi_y) and (BD_xEG_y) copolymers were determined by SEC. The system was equipped with a Hewlett Packard 1100 series injector (injection volume 10 µL) and a Hewlett Packard PL HFIP gel column (250×4.6 mm, part no: 1514-5900 HFIP) thermostated at 35°C. A mixture consisting of 5 vol% HFIP and 95 vol% chloroform was used as eluent. Acetophenone was used as flow marker. A HP 1100 series pump provided a flow rate of 0.3 mL/min. For detection, an Agilent diode array detector was used (λ = 295 nm). The SEC system was calibrated with polystyrene calibration standards ($\overline{M}_w$ range: 1000 - 900.000 g/mol). The obtained PS calibration curve was used to determine the $\overline{M}_n$ of the synthesized (BD_xDi_y) and (BD_xEG_y) copolymers. In addition, PBT homopolymer samples with known $\overline{M}_n$ values (determined by end group titration) were analyzed with the same SEC system. A fitting curve was prepared using the $\overline{M}_n$ values obtained by end group titration and the $\overline{M}_n$ obtained via the PS calibration curve. The measured $\overline{M}_n$ values of the (BD_xDi_y) and

(BD_xEG_y) copolymers were fitted using this calibration curve and corrected to obtain a more realistic value.

3.2.7 Differential Scanning Calorimetry (DSC)

The crystallinity ($\chi_{heating}$) of the $(BD_xDi_y)_{ssp}$ and $(BD_xEG_y)_{ssp}$ copolymers was measured with a TA Instruments Q1000 DSC equipped with an autosampler and refrigerated cooling system (RCS). The DSC cell was purged with a nitrogen flow of 50 mL/min. The temperature was calibrated using the onset of melting for indium. The enthalpy was calibrated with the heat of fusion of indium. Samples of 6-8 mg were prepared in crimped aluminum pans. Samples were measured from 0 to 250°C for the $(BD_xDi_y)_{ssp}$ copolymers and from 0 to 265°C for the $(BD_xEG_y)_{ssp}$ copolymers. A heating rate of 10 K/min was used and samples were kept isothermal for 3 min at 0 and 250°C/265°C, respectively.

3.3 Results and discussion

(BD_xDi_y) and (BD_xEG_y) copolymers were synthesized by SSP and MP using different PBT/diol ratios. The general chemical structures of (BD_xDi_y) and (BD_xEG_y) copolymers are shown in Figure 3.1.

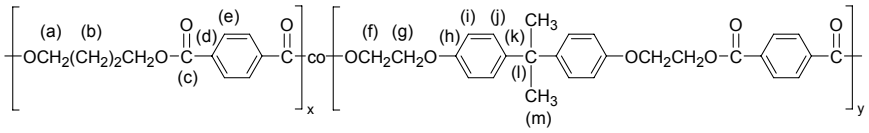

BD-T repeat-unit Di-T repeat-unit

(a)

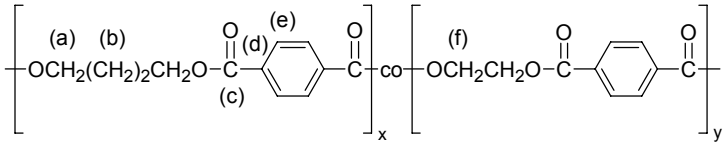

BD-T repeat-unit EG-T repeat-unit

(b)

Figure 3.1. Chemical structures of the synthesized PBT copolymers: (a) (BD_xDi_y) copolymer consisting of BD-T and Di-T repeat-units and (b) (BD_xEG_y) copolymer consisting of BD-T and EG-T repeat-units. Labeling used for NMR peak assignments is also shown.

The $(BD_xDi_y)_{mp}$ and $(BD_xEG_y)_{mp}$ copolymers were prepared via copolymerization (transesterification) of the Dianol and BHET monomer, respectively with PBT in the melt.[25] The transesterification reactions occurring in the melt will result in chain scission of the homopolymer PBT. As a consequence, oligomers will be formed during the melt polymerization reaction. A high vacuum is applied in order to remove 1,4-butanediol (BD) or ethylene glycol (EG) formed during the reaction. In this way, the excess of diol with respect to terephthalate will decrease, which drives the transesterification reaction to completion. Consequently, after an initial drop, an increase of the molecular weight is obtained later on. The kinetics of the incorporation of Dianol into PBT via SSP was already described in **Chapter 2**.[22] In that study, a $(BD_{85}Di_{15})_{feed}$ mixture was polymerized in the solid state at a temperature of 180°C, while the solid-state polymerization time (t_{ssp}) was varied. ^{1}H-NMR spectroscopy measurements showed, that after t_{ssp} = 4 h virtually all Dianol monomer had been incorporated. ^{13}C-NMR sequence distribution analysis showed that the final microstructure of the resulting $(BD_{85}Di_{15})_{ssp}$ copolymer did not change anymore after t_{ssp} = 4 h. The molecular weight reached its maximum after t_{ssp} = 18 h.

3.3.1 Characterization of synthesized PBT-Dianol and PBT-BHET copolymers

All synthesized (BD_xDi_y) and (BD_xEG_y) copolymers were characterized by ^{1}H-NMR spectroscopy. Typical ^{1}H-NMR spectra for a (BD_xDi_y) and a (BD_xEG_y) copolymer are shown in Figure 3.2a and 3.2b, respectively. Table 3.1 shows the chemical shift of the corresponding peaks.

Table 3.1. ^{1}H-NMR chemical shifts of corresponding peaks for (BD_xDi_y) and (BD_xEG_y).

(BD_xDi_y) copolymer								
Proton	Hm	Hb	Hg	Ha	Hf	Hj	Hi	He
Chemical shift	1.65	2.04	4.43	4.52	4.76	6.90	7.19	8.14
(BD_xEG_y) copolymer								
Proton	Hm	Hb	Hg	Ha	Hf	Hj	Hi	He
Chemical shift		2.05		4.52	4.81			8.14

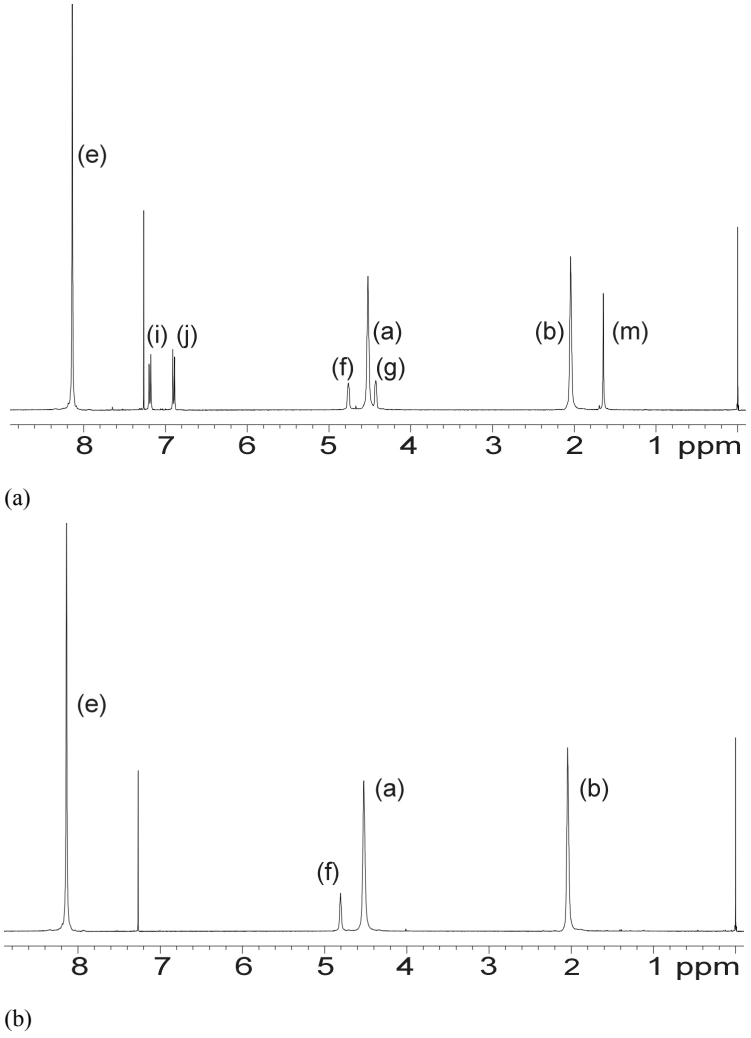

Figure 3.2. Typical ^{1}H-NMR spectra including peak assignments for (a) (BD_xDi_y) copolymer and (b) (BD_xEG_y) copolymer.

The composition of the (BD_xDi_y) copolymers was calculated with eq 3.1a using the ^{1}H-NMR peak integrals in the 4-5 ppm region (see Figure 3.2a):

$$F_{Di-T,total} = \frac{(f)}{(a)+(f)} \tag{3.1a}$$

and hence:

$$F_{BD-T,total} = 1 - F_{Di-T,total} \tag{3.1b}$$

where $F_{Di\text{-}T,\ total}$ and $F_{BD\text{-}T,\ total}$ denote the mol fractions of Di-T and BD-T repeat-units in the (BD_xDi_y) copolymer, respectively. Integral (f) corresponds to incorporated Dianol next to an ester group, whereas integral ((a)+(f)) represents the total amount of diol (both Dianol and 1,4-butanediol).

In a similar way, the compositions of the (BD_xEG_y) copolymers were calculated with Equation 3.2a using the ^{1}H-NMR peak integrals in the 4-5 ppm region (see Figure 2b):

$$F_{EG-T,total} = \frac{(f)}{(a)+(f)} \tag{3.2a}$$

and hence:

$$F_{BD-T,total} = 1 - F_{EG-T,total} \tag{3.2b}$$

where $F_{EG\text{-}T,\ total}$ and $F_{BD\text{-}T,\ total}$ denote the mol fractions of EG-T and BD-T repeat-units in the (BD_xEG_y) copolymer, respectively. Integral (f) corresponds to incorporated ethylene glycol whereas integral ((a)+(f)) represents the total amount of incorporated diol (both ethylene glycol and 1,4-butanediol).

The compositions of the $(BD_xDi_y)_{ssp}$ and the $(BD_xDi_y)_{mp}$ copolymers are listed in Table 3.2 and Table 3.3, respectively together with the obtained number-average molecular weights ($\overline{M}_n$) and the polydispersity indices (PDI).

Table 3.2. Overview of all synthesized $(BD_xDi_y)_{ssp}$ copolymers. Compositions were obtained by ^{1}H-NMR spectroscopy. $\overline{M}_n$ and PDI were measured by SEC

$(BD_xDi_y)_{ssp}$ copolymers					
Composition Feed		Composition after SSP		SEC	
$F_{BD\text{-}T,\ feed}$ (mol%)	$F_{Di,\ feed}$ (mol%)	$F_{BD\text{-}T,\ total}$ (mol%)	$F_{Di\text{-}T,\ total}$ (mol%)	$\overline{M}_n$ (kg/mol)	PDI
Pure PBT		100	0	15	2.3
100	0	100	0	42	2.7
95	5	96	4	35	3
90	10	90	10	38	3.3
85	15	84	16	35	3
80	20	76	24	34	3
75	25	69	31	10	2.6
70	30	61	39	12	3
65	35	54	46	8	3

The pure PBT homopolymer, used as feed material for all (BD_xDi_y) copolymer preparations, is also listed in the table. $(BD_{100}Di_0)_{ssp}$ is a PBT homopolymer for which the same procedure was applied as for the $(BD_xDi_y)_{ssp}$ copolymers (HFIP dissolution + SSP at 180°C respectively, see Experimental Section).

Table 3.3. Overview of all synthesized $(BD_xDi_y)_{mp}$ copolymers. Compositions were obtained by ^{1}H-NMR spectroscopy. $\overline{M}_n$ and PDI were measured by SEC

$(BD_xDi_y)_{mp}$ copolymers					
Composition Feed		Composition after MP		SEC	
$F_{BD\text{-}T,\ feed}$ (mol%)	$F_{Di,\ feed}$ (mol%)	$F_{BD\text{-}T,\ total}$ (mol%)	$F_{Di\text{-}T,\ total}$ (mol%)	$\overline{M}_n$ (kg/mol)	PDI
95	5	96	4	17	2.3
90	10	90	10	15	2.4
85	15	81	19	12	2.3
80	20	74	26	11	2.2
75	25	70	30	11	2.2

The compositions of the $(BD_xEG_y)_{ssp}$ and the $(BD_xEG_y)_{mp}$ copolymers are listed in Table 3.4 and Table 3.5, respectively together with the obtained number-average molecular weights ($\overline{M}_n$) and the polydispersity indices (PDI).

Table 3.4. Overview of all synthesized $(BD_xEG_y)_{ssp}$ copolymers. Compositions were obtained by ^{1}H-NMR spectroscopy. $\overline{M}_n$ and PDI were measured by SEC

$(BD_xEG_y)_{ssp}$ copolymers					
Composition Feed		Composition after SSP		SEC	
$F_{BD\text{-}T,\ feed}$ (mol%)	$F_{EG,\ feed}$ (mol%)	$F_{BD\text{-}T,\ total}$ (mol%)	$F_{EG\text{-}T,\ total}$ (mol%)	$\overline{M}_n$ (kg/mol)	PDI
90	10	95	5	68	2.9
80	20	91	9	76	2.9
70	30	84	16	76	3.0
60	40	76	24	41	3.0
50	50	68	32	25	3.2
40	60	59	41	15	3.8
30	70	47	53	19	4.0

Table 3.5. Overview of all synthesized $(BD_xEG_y)_{ssp}$ copolymers. Compositions were obtained by ^{1}H-NMR spectroscopy. $\overline{M}_n$ and PDI were measured by SEC

$(BD_xEG_y)_{mp}$ copolymers					
Composition Feed		Composition after MP		SEC	
$F_{BD\text{-}T,\ feed}$ (mol%)	$F_{EG,\ feed}$ (mol%)	$F_{BD\text{-}T,\ total}$ (mol%)	$F_{EG\text{-}T,\ total}$ (mol%)	$\overline{M}_n$ (kg/mol)	PDI
90	10	93	7	20	2.8
80	20	84	16	22	2.8
70	30	79	21	16	2.7
60	40	69	31	19	3.0
50	50	60	40	20	3.0

3.3.2 Real copolymer composition versus theoretical composition

The amounts of PBT and comonomer (Dianol and BHET) as present in the $(BD_xDi_y)_{feed}$ and $(BD_xEG_y)_{feed}$ used for SSP and MP were accurately weighed. These amounts were subsequently used to calculate the theoretical compositions of the synthesized (BD_xDi_y) and (BD_xEG_y) copolymers. For the (BD_xDi_y) copolymers, the theoretical end composition is obtained by assuming that all weighed Dianol is fully incorporated and only 1,4-butanediol is removed during the polymerization reaction. For the (BD_xEG_y) copolymers however, the theoretical composition can vary between two limits. One limit (**limit 1**) is obtained when during the SSP reaction only 1,4-butanediol is removed during the polymerization reaction. This implies that BHET will be incorporated as a whole molecule (similar to Dianol) and thus the ester linkages in BHET will not be broken. The second limit (**limit 2**) is obtained when only ethylene glycol is removed during the melt polymerization reaction. In Figure 3.3, the end compositions (expressed as $F_{BD\text{-}T,\ total}$) of the synthesized $(BD_xDi_y)_{ssp}$ (■) and $(BD_xDi_y)_{mp}$ (●) copolymers are plotted as a function of F_{PBT}, which is the mol fraction of BD-T repeat-units present in the $(BD_xDi_y)_{feed}$ mixture used for SSP or MP. It can be seen that for the $(BD_xDi_y)_{mp}$ copolymers the experimentally obtained values for $F_{BD\text{-}T,\ total}$ are close to the theoretical values of $F_{BD\text{-}T,\ total}$ (-). For the $(BD_xDi_y)_{ssp}$ copolymers, the experimentally obtained values for $F_{BD\text{-}T,\ total}$ are also close to the theoretical values, except when large amounts of Dianol are used for incorporation (F_{PBT} < 75 mol%). In addition, the $\overline{M}_n$ of the $(BD_xDi_y)_{ssp}$ copolymers decreases when F_{PBT} is below 75 mol%. During the SSP reaction, the PBT chains in the amorphous phase will be cleaved due to alcoholysis reactions with the Dianol monomer. These alcoholysis reactions can be specified as outer-inner reactions,[26] because the outer hydroxyl end group of Dianol reacts with an inner carbonyl group of PBT.

In our previous work,[22] it was shown that $\overline{M}_n$ decreased during the first hour of the SSP reaction due to chain scission. $\overline{M}_n$ can only increase via (outer-outer) alcoholysis reactions. The initial excess of diol will then decrease via the release of 1,4-butanediol. When a $(BD_xDi_y)_{feed}$ mixture with F_{PBT} < 75 mol% is polymerized in the solid state, the polymer chains in the amorphous phase are endcapped with Dianol. (outer-outer) Alcoholysis can still take place but results in the release of free Dianol monomer instead of 1,4-butanediol. The Dianol monomer however doesn't evaporate at the used SSP temperature (T_{ssp}) of 180°C and reacts with other polymer chains by a new alcoholysis resulting in new Dianol endcapped polymer chains. In this way, an increase of the number-average molecular weight cannot occur. A similar effect occurs for the $(BD_xDi_y)_{mp}$ copolymers, although it is less pronounced.

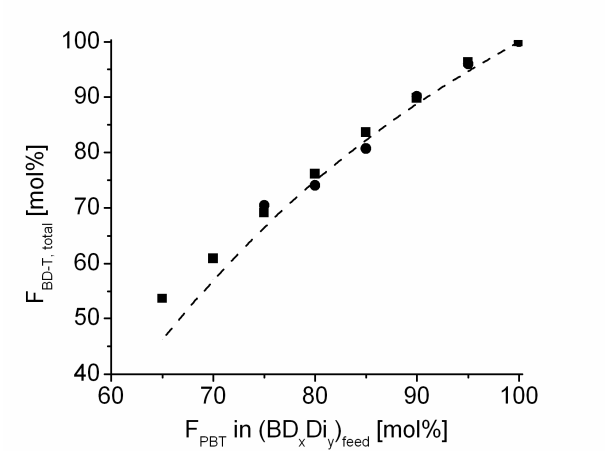

Figure 3.3. Experimentally obtained values of $F_{BD\text{-}T,\ total}$ for the synthesized $(BD_xDi_y)_{ssp}$ (■) and $(BD_xDi_y)_{mp}$ (●) copolymers as a function of the initially used mol fraction F_{PBT} in the feed. The theoretical end composition is denoted as $F_{BD\text{-}T,\ total}$ (-).

In Figure 3.4, the experimentally obtained end composition (expressed as $F_{BD\text{-}T,\ total}$) of the synthesized $(BD_xEG_y)_{ssp}$ and (■) $(BD_xEG_y)_{mp}$ (●) copolymers are plotted as a function of F_{PBT} together with the theoretical values for $F_{BD\text{-}T,\ total}$ (**limit 1** (-) and **limit 2** (-)) It can be seen that the compositions for the $(BD_xEG_y)_{ssp}$ copolymers coincide with the values of **limit 1**. The $(BD_xEG_y)_{mp}$ copolymers, however, have compositions with larger fractions of EG. The relatively low T_{ssp} (185°C) used for SSP is very close to the boiling point of ethylene glycol ($T_{boiling}$ = 196°C). Therefore, the equilibrium of the SSP reaction prefers the removal of ethylene glycol over 1,4-butanediol ($T_{boiling}$ = 220°C).

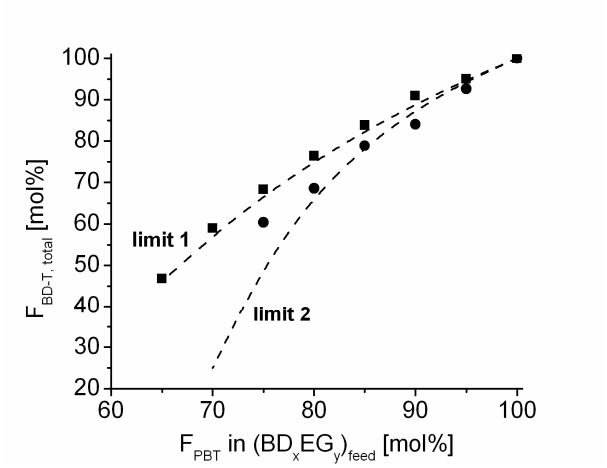

Figure 3.4. Experimentally obtained values of $F_{BD\text{-}T,\ total}$ for the synthesized $(BD_xEG_y)_{ssp}$ (■) and $(BD_xEG_y)_{mp}$ (●) copolymers as a function of the initially used mol fraction F_{PBT} in the feed. The theoretical values for $F_{BD\text{-}T,\ total}$ (-) are between two limits (**limit 1**: only ethylene glycol removed; **limit 2**: only 1,4-butanediol removed).

The melt polymerization was done at a final temperature of 265°C. At this temperature, there is no preference for either 1,4-butanediol or ethylene glycol. The PDI values of the $(BD_xDi_y)_{ssp}$ copolymers are all close to 3, whereas for the $(BD_xDi_y)_{mp}$ copolymers, the PDI values are closer to the theoretical value of 2, calculated by Flory.[27] In our previous work,[22] it was shown that the PDI gradually increases with increasing t_{ssp}. This is due to the absence of a Flory distribution during the SSP reaction, since the crystalline fraction is not able to participate in the polycondensation process.

3.3.3 ^{13}C-NMR dyad sequence distribution analysis

3.3.3.1 PBT-Dianol copolymers obtained by SSP and MP

^{13}C-NMR dyad sequence distribution analysis can be used to determine the chemical microstructure of the synthesized $(BD_xDi_y)_{ssp}$ and $(BD_xDi_y)_{mp}$ copolymers. The chemical microstructure is defined as the total distribution of Di-T and BD-T repeat-units in a (BD_xDi_y) copolymer. The microstructure has therefore a large influence on the macroscopic properties of the (BD_xDi_y) copolymers. As explained in the introduction, the selective incorporation of Dianol into PBT via SSP should give a different microstructure compared to incorporation via MP. The chemical microstructure of the $(BD_xDi_y)_{ssp}$ and $(BD_xDi_y)_{mp}$ copolymers was determined via ^{13}C-NMR dyad sequence distribution analysis. A ^{13}C-NMR spectrum of a $(BD_{85}Di_{15})_{ssp}$ copolymer with assignment of the peaks is shown in Figure 3.5. The

corresponding chemical shift of each peak is shown in Table 3.6. The chemical shift of the aromatic quaternary carbon atom (d in Figure 3.1) present in the 135-136 ppm region is magnified and shown in insert (a) of Figure 3.5. It can be seen that this peak splits up into four different peaks. Kricheldorf[13] observed that for copolyesters the shift of the peak corresponding to the carbonyl group is determined by the presence of different adjacent monomeric units. Later, Newmark[14] showed for PBT-PET copolymers (eg. $(BD_xEG_y)_{mp}$ copolymers) that also the peak corresponding to the quaternary aromatic carbon atom splits up into four different peaks. Each peak originates from a different dyad sequence. The possible dyad sequences for the (BD_xDi_y) copolymers together with their abbreviation and corresponding chemical shifts are shown in Figure 3.6. The BTD (BD-side) and BTD (Di-side) are equal and have therefore the same integral values. Because the four peaks shown in insert (a) of Figure 3.5 are slightly overlapping, a deconvolution procedure assuming Gaussian peak shapes was applied for a clear peak separation and subsequent determination of the integral value of each peak. The obtained integral values were normalized to a total value of 100 for convenience and are also listed in insert (a) and (b). Deducing quantitative information from ^{13}C-NMR spectra is only allowed when the peaks involved have equal relaxation times and Nuclear Overhauser enhancements (nOes).[28] Newmark[14] showed that for linear PBT-PET copolymers the different chemical shifts originating from peak splitting of the quaternary carbon atoms and the carbonyl carbon atoms have identical relaxation times and nOes. The (BD_xDi_y) and (BD_xEG_y) copolymers are also linear and it can therefore be assumed that the obtained peak integrals are quantitative. It will be shown later that the mol fractions $F_{BD\text{-}T,\ total}$, $F_{Di\text{-}T,\ total}$ and $F_{EG\text{-}T,\ total}$ obtained via ^{13}C-NMR measurements give similar values as the compositions obtained via ^{1}H-NMR (shown in Table 3.2 - Table 3.5). Insert (b) of Figure 3.5 also shows the same ppm region but then for a $(BD_{85}Di_{15})_{mp}$ copolymer. The $(BD_{85}Di_{15})_{ssp}$ and the $(BD_{85}Di_{15})_{mp}$ copolymer only vary slightly in composition (see Table 3.2 and Table 3.3, respectively), but the peak integral values as listed in insert (a) and (b) are remarkably different.

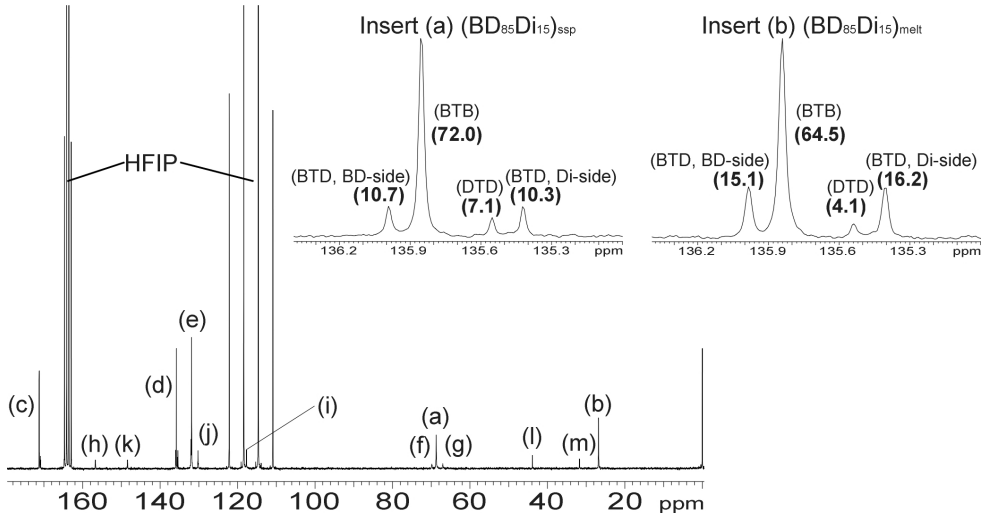

Figure 3.5. ^{13}C-NMR spectrum of $(BD_{85}Di_{15})_{ssp}$ with peak assignments. Insert (a) shows the 135-136.3 ppm region of $(BD_{85}Di_{15})_{ssp}$ with the splitting of the quaternary C-atom chemical shift and corresponding peak integrals. Insert (b) shows the same ppm region for a $(BD_{85}Di_{15})_{mp}$ copolymer.

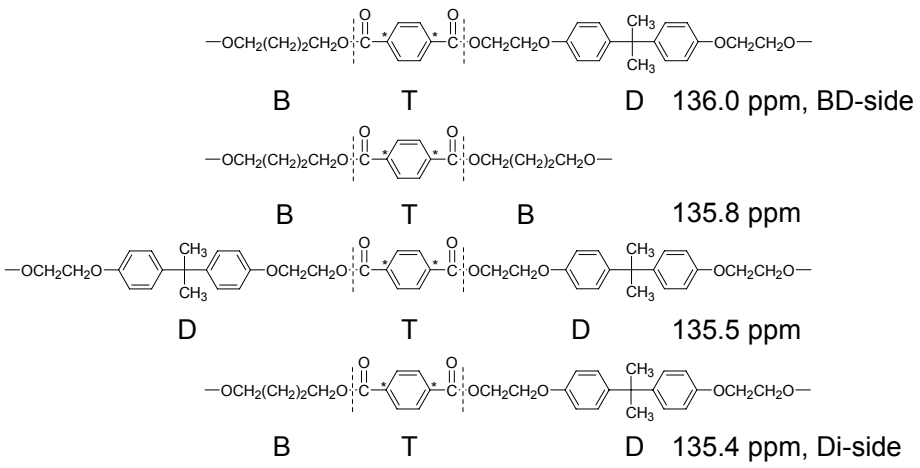

Figure 3.6. Possible dyad sequences and corresponding chemical shifts for a (BD_xDi_y) copolymer due to peak splitting of the quaternary carbon atom (*).

Table 3.6. (BD_xDi_y) copolymers: chemical shifts of corresponding peaks as measured via ^{13}C-NMR spectroscopy

	(BD_xDi_y) copolymer												
Carbon	Cb	Cm	Cl	Cg	Ca	Cf	Ci	Cj	Ce	Cd	Ck	Ch	Cc
Chemical Shift	26.8	31.7	43.9	67.03	68.7	69.9	117.7	130.2	131.9	135.8	148.4	156.7	171.3

When normalized, the peak integral values can be used to calculate the end composition (mol fractions $F_{BD\text{-}T,\ total}$ and $F_{Di\text{-}T,\ total}$) and the degree of randomness (R) of the $(BD_xDi_y)_{ssp}$ and the $(BD_xDi_y)_{mp}$ copolymers. The following equations[15] were used:

$$F_{BTD,\ total} = F_{BTD,\ BD-side} + F_{BTD,\ Di-side} \tag{3.3}$$

$$F_{BD-T,\ total} = (F_{BTD,\ total}/2 + F_{BTB}) \tag{3.4}$$

$$F_{Di-T,\ total} = (F_{BTD,\ total}/2 + F_{DTD}) \tag{3.5}$$

$$R_{total} = \frac{F_{BTD,\ total}}{2 \cdot (F_{BD-T,\ total} \cdot F_{Di-T,\ total})} \tag{3.6}$$

where F_i denotes the mol fraction of each sequence (i = BTD, BD-side; BTB; DTD and BTD, Di-side), while $F_{BD\text{-}T,\ total}$ and $F_{Di\text{-}T,\ total}$ denote the total mol fractions of BD-T and Di-T units, respectively. From eqs 3.5 and 3.6, it follows that $F_{BD\text{-}T,\ total} = 0.825$ and $F_{Di\text{-}T,\ total} = 0.175$ for $(BD_{85}Di_{15})_{ssp}$, and $F_{BD\text{-}T,\ total} = 0.802$ and $F_{Di\text{-}T,\ total} = 0.198$ for $(BD_{85}Di_{15})_{mp}$. The values are in agreement with the values calculated from the ^1H-NMR measurements ($F_{BD\text{-}T,\ total} = 0.836$ for $(BD_{85}Di_{15})_{ssp}$ and $F_{BD\text{-}T,\ total} = 0.807$ for $(BD_{85}Di_{15})_{mp}$, see also Table 3.2 and Table 3.3, respectively) and hence the ^{13}C-NMR measurements can be considered as being quantitative. For a fully random copolyester, the distribution of the two different BD-T and Di-T repeat-units should obey Bernoullian statistics.[15,29] The degree of randomness (R_{total}) in eq 3.5 should then be equal to 1. If R_{total} is below 1, the repeat-units are supposed to be arranged in blocks. Calculation of R_{total} for $(BD_{85}Di_{15})_{mp}$ using eq 3.5 gives $R_{total,\ melt} = 0.99$; thus a random copolyester is obtained. The same calculation for $(BD_{85}Di_{15})_{ssp}$, however, gives $R_{total,\ ssp} = 0.73$ and therefore a non-random distribution of Di-T repeat-units is present after SSP. The latter result is as expected, since the crystallized BD-T repeat-units do not participate in the transesterification reaction.

The chemical microstructure of the $(BD_{85}Di_{15})_{mp}$ copolymer and $(BD_{85}Di_{15})_{ssp}$ copolymer is schematically depicted in Figure 3.7a and 3.7b, respectively. DSC measurements show that the $(BD_{85}Di_{15})_{mp}$ copolymer still has a crystalline fraction (denoted as $\chi_{heating}$; $\chi_{heating}$ = 0.18 obtained from second heating run).

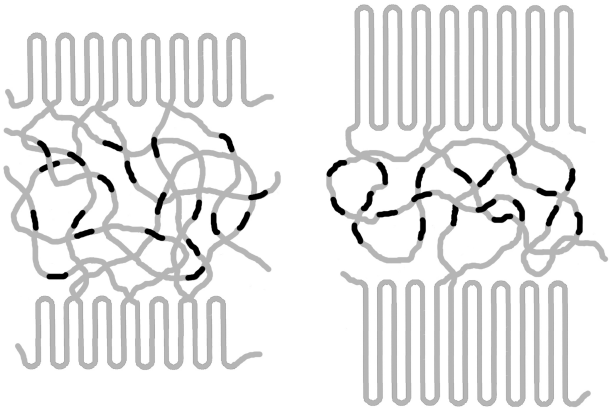

(a) (b)

Figure 3.7. Schematic representation of the microstructure of (a) $(BD_{85}Di_{15})_{mp}$ (random) and (b) $(BD_{85}Di_{15})_{ssp}$ copolymer (non-random).

3.3.3.2 PBT-BHET copolymers obtained by SSP and MP

A ^{13}C-NMR spectrum of a $(BD_{70}EG_{30})_{ssp}$ copolymer with assignment of the peaks is shown in Figure 3.8. The corresponding chemical shift of each peak is shown in Table 3.7. The possible dyad sequences for the (BD_xEG_y) copolymers together with their abbreviation and corresponding chemical shifts are shown in Figure 3.9. The chemical shift of the aromatic quaternary carbon atom (d in Figure 3.2), present in the 133-134 ppm region of Figure 3.8, is magnified and shown in insert (a). Insert (b) shows the same ppm region for a $(BD_{70}EG_{30})_{mp}$ copolymer. According to ^{1}H-NMR measurements (see Table 3.4 and 3.5, respectively), the composition of the $(BD_{70}EG_{30})_{ssp}$ copolymer and the $(BD_{70}EG_{30})_{mp}$ copolymer is almost equal ($F_{BD\text{-}T,\ total}$ = 83.8 mol% for $(BD_{70}EG_{30})_{ssp}$ and $F_{BD\text{-}T,\ total}$ = 78.9 mol% for $(BD_{70}EG_{30})_{mp}$. From the normalized peak integral values, shown in inserts (a) and (b), it can be directly observed that the $(BD_{70}EG_{30})_{ssp}$ copolymer and the $(BD_{70}EG_{30})_{mp}$ copolymer have a different chemical microstructure.

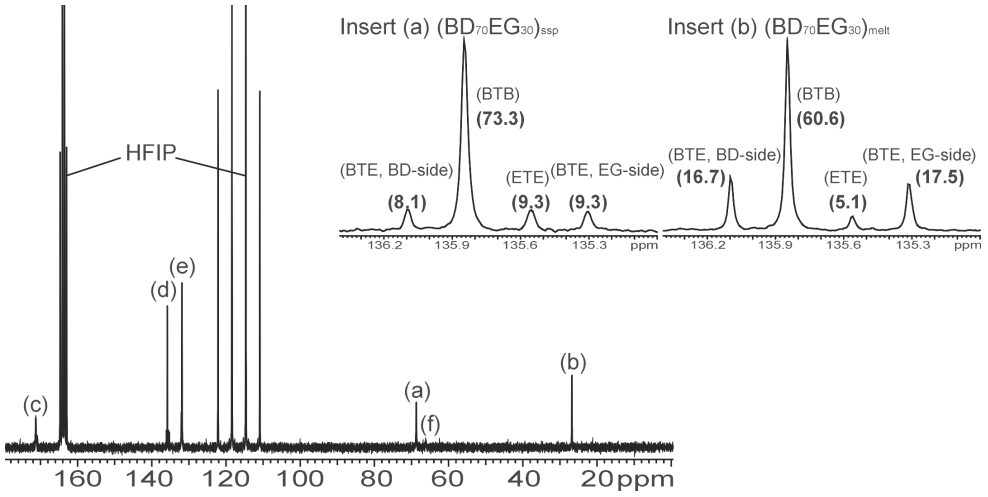

Figure 3.8. ^{13}C-NMR spectrum of $(BD_{70}EG_{30})_{ssp}$ with peak assignments. Insert (a) shows the 133-134 ppm region of $(BD_{70}EG_{30})_{ssp}$ with the splitting of the quaternary C-atom chemical shift and corresponding peak integrals. Insert (b) shows the same ppm region for a $(BD_{70}EG_{30})_{mp}$ copolymer.

Table 3.7 (BD_xEG_y) copolymers: chemical shifts of corresponding peaks as measured via ^{13}C-NMR spectroscopy

	(BD_xEG_y) copolymer					
Carbon	Cb	Ca	Cf	Ce	Cd	Cc
Chemical Shift	26.8	68.8	66.2	131.9	135.9	171.3

The normalized peak integral values as shown in insert (a) and (b) of Figure 3.8 were used in eqs 3.3-3.6 (D-T-D is replaced by E-T-E; B-T-D by B-T-E and Di-T by EG-T) to calculate the end compositions (mol fractions $F_{BD\text{-}T,\ total}$ and $F_{EG\text{-}T,\ total}$) and degrees of randomness (R) of the $(BD_{70}EG_{30})_{ssp}$ and the $(BD_{70}EG_{30})_{mp}$ copolymers. $F_{BD\text{-}T,\ total}$ = 82.0 mol% for the $(BD_{70}EG_{30})_{ssp}$ copolymer and 77.8 mol% for the $(BD_{70}EG_{30})_{mp}$ copolymer. Also here, the values for $F_{BD\text{-}T,\ total}$ as found by ^{13}C-NMR are within experimental error in agreement with the values obtained by ^{1}H-NMR (see Table 3.4 and Table 3.5, respectively).

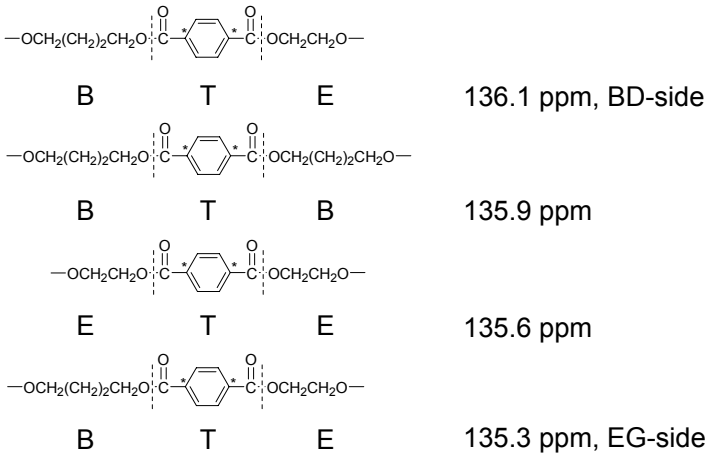

Figure 3.9. Possible dyad sequences and corresponding chemical shifts for a (BD_xEG_y) copolymer due to peak splitting of the quaternary carbon atom (*).

3.3.4 Chemical microstructure: PBT-Dianol copolymers versus PBT-BHET copolymers

$R_{total,\ ssp}$ and $R_{total,\ mp}$ were also determined for the remaining (BD_xDi_y) copolymers listed in Table 3.2 and Table 3.3. The obtained values for $R_{total,\ ssp}$ and $R_{total,\ mp}$ are plotted in Figure 3.10 as a function of $F_{BD\text{-}T,\ total}$.

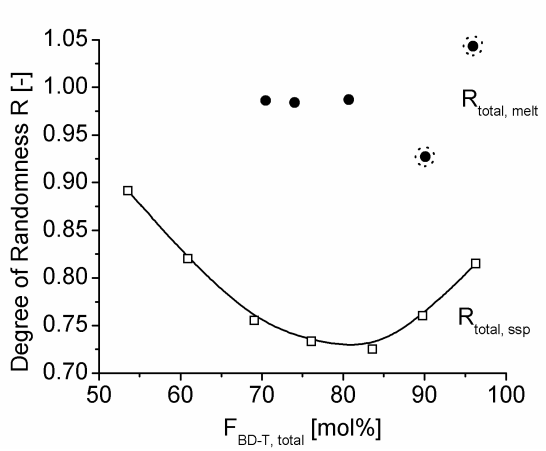

Figure 3.10. Degree of randomness of the synthesized $(BD_xDi_y)_{ssp}$ (□) and $(BD_xDi_y)_{mp}$ (●) copolymers, $R_{total,\ ssp}$ and $R_{total,\ mp}$ respectively, as a function of $F_{BD\text{-}T,\ total}$.

It can be seen that all values for $R_{total,\ mp}$ are close to unity. When a small fraction of Dianol is incorporated (< 10 mol%), the peak integral of the DTD sequence (F_{DTD}) could not be accurately determined due to its low intensity, and it therefore has a larger error. As a consequence, the corresponding (encircled) values for $R_{total,\ mp}$ (1.05 and 0.93) deviate slightly from unity. For the $(BD_xDi_y)_{ssp}$ copolymers, $R_{total,\ ssp}$ has a parabolic shape with a minimum value of 0.73 at $F_{BD\text{-}T,\ total}$ = 83 mol%. All measured values for $R_{total,\ ssp}$ are below unity. Apparently, the $(BD_xDi_y)_{ssp}$ copolymers have a non-random overall microstructure, which can be subscribed to the selective incorporation of Dianol in the amorphous phase, resulting in a blocky structure. In addition, $R_{total,\ ssp}$ increases for $F_{BD\text{-}T,\ total}$ < 83 mol%. This result indicates that Dianol monomer is incorporated more randomly when the initial fraction of Dianol in the $(BD_xDi_y)_{feed}$ mixtures is increased. Figure 3.11 shows the crystallinity ($\chi_{heating}$, ■) of the $(BD_xDi_y)_{ssp}$ copolymers as a function of $F_{BD\text{-}T,\ total}$. The horizontal dotted line ($\chi_{PBT,\ HFIP\ treatment}$ = 39%) represents the crystallinity of PBT after HFIP dissolution treatment. It can be seen that for $F_{BD\text{-}T,\ total}$ < 90 mol%, $\chi_{heating}$ is linearly dependent on $F_{BD\text{-}T,\ total}$. When the linear part of the curve is extrapolated to $F_{BD\text{-}T,\ total}$ = 45 mol%, a value of 0% is found for $\chi_{heating}$, which corresponds to a fully amorphous $(BD_xDi_y)_{ssp}$ copolymer. The observed decrease in $\chi_{heating}$ as a function of composition can be partly explained by the fact that the $(BD_xDi_y)_{ssp}$ copolymers consist of a certain fraction Di-T repeat-units. Finelli et al.[25] showed that a $(BD_0Di_{100})_{mp}$ homopolymer, consisting of only Di-T repeat-units, is fully amorphous. Hence, only the PBT fraction contributes to the crystallinity of the $(BD_xDi_y)_{ssp}$ copolymers. When $\chi_{heating}$ is divided by the weight fraction BD-T repeat-units ($W_{BD\text{-}T,\ total}$) of each $(BD_xDi_y)_{ssp}$ copolymer, the crystallinity of the PBT fraction only ($\chi_{heating,\ PBT\ only}$, ●) is obtained. $\chi_{heating,\ PBT\ only}$ is also shown in Figure 3.11 as a function of $F_{BD\text{-}T,\ total}$. It can be seen that with decreasing BD-T content, $\chi_{heating,\ PBT\ only}$ has a maximum at $F_{BD\text{-}T,\ total}$ = 83 mol% and subsequently decreases with increasing Di-T content. $\chi_{heating,\ PBT\ only}$ even decreases below $\chi_{heating}$ = 39%. This decrease is remarkable, because it implies that the crystalline fraction is not retained during the SSP reaction. Apparently, Dianol residues in the amorphous phase dissolve PBT during the SSP reaction. The dissolution properties of Dianol will be presented in **Chapter 5**.

The degree of randomness of the synthesized $(BD_xEG_y)_{ssp}$ (□) and $(BD_xEG_y)_{mp}$ (●) copolymers, $R_{total,\ ssp}$ and $R_{total,\ mp}$ respectively, are plotted in Figure 3.12 as a function of $F_{BD\text{-}T,\ total}$.

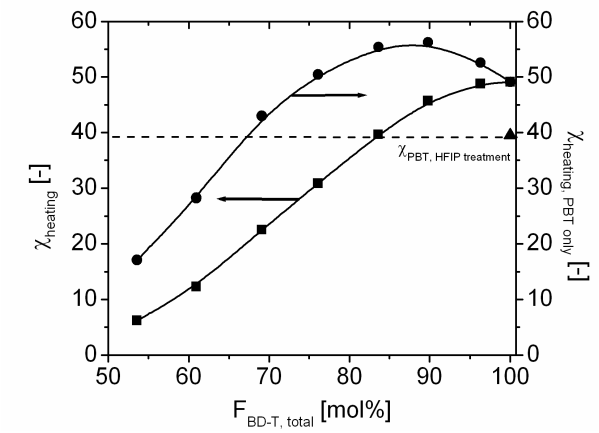

Figure 3.11. Total crystallinity ($\chi_{heating}$, ■) and crystallinity of the PBT fraction only ($\chi_{heating, PBT\ only}$, ●) of the $(BD_xDi_y)_{ssp}$ copolymers as a function of $F_{BD\text{-}T, total}$. The dotted line represents the crystallinity of PBT after HFIP treatment ($\chi_{PBT, HFIP\ treatment}$).

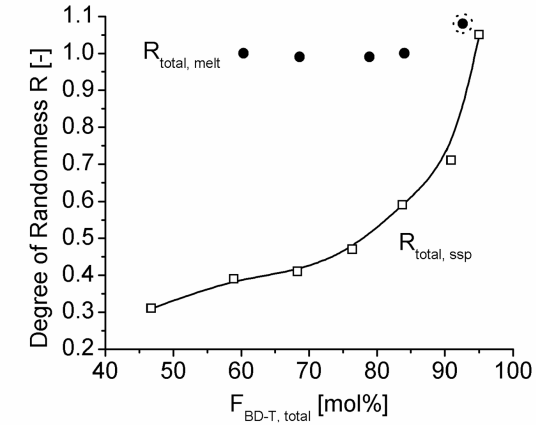

Figure 3.12. Degree of randomness of the synthesized $(BD_xEG_y)_{ssp}$ (□) and $(BD_xEG_y)_{mp}$ (●) copolymers ($R_{total, ssp}$ and $R_{total, melt}$ respectively) as a function of $F_{BD\text{-}T, total}$.

From Figure 3.12, it can be seen that the chemical microstructure $(BD_xEG_y)_{mp}$ copolymers is fully random for all synthesized compositions. The $(BD_xEG_y)_{ssp}$ copolymers have a non-random distribution. In addition, contrary to the observation for the $(BD_xDi_y)_{mp}$ copolymers, $R_{total, ssp}$ continually decreases with decreasing values of $F_{BD\text{-}T, total}$. Apparently, homopolymer PET blocks are formed during the SSP reaction. The crystallinity ($\chi_{heating}$, ■) of the $(BD_xEG_y)_{ssp}$ copolymers is plotted in Figure 3.13 as a function of $F_{BD\text{-}T, total}$.

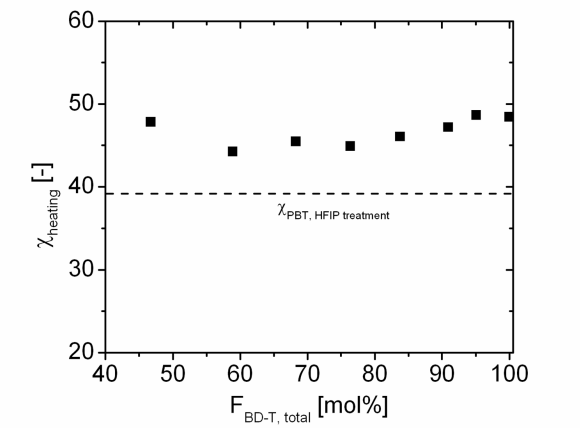

Figure 3.13. Total crystallinity ($\chi_{heating}$, ■) of the $(BD_xEG_y)_{ssp}$ copolymers as a function of $F_{BD\text{-}T,\ total}$. The dotted line represents the crystallinity of PBT after HFIP treatment ($\chi_{PBT,\ HFIP\ treatment}$).

It can be seen that the $\chi_{heating}$ is almost constant over the whole composition range. Apparently, the formed PET blocks crystallize during the SSP reaction. Consequently, BHET does not act as a solvent for PBT, thereby gradually decreasing $\chi_{heating}$, as was observed for Dianol.

3.4 Conclusions

(BD_xDi_y) and (BD_xEG_y) copolymers with different PBT/diol ratios were synthesized via solid-state polymerization and via melt polymerization. For both $(BD_xDi_y)_{ssp}$ and $(BD_xDi_y)_{mp}$ copolymers, the $\overline{M}_n$ decreases when larger amounts of Dianol are incorporated into PBT. This decrease is due to the endcapping of PBT chains with Dianol resulting in an excess of diol, which cannot be easily removed. When the $(BD_xDi_y)_{feed}$ mixtures were polymerized in the solid-state, only ethylene glycol was removed during the reaction whereas during melt polymerization of the $(BD_xEG_y)_{feed}$ mixtures, both ethylene glycol and 1,4-butanediol were evaporated. The PDI values for the $(BD_xDi_y)_{ssp}$ and $(BD_xEG_y)_{ssp}$ copolymers were all around 3 whereas PDI values found for the $(BD_xDi_y)_{mp}$ and $(BD_xEG_y)_{mp}$ copolymers were all close to the theoretical value of 2. Quantitative ^{13}C-NMR spectroscopy was used to determine the end composition of the synthesized (BD_xDi_y) and (BD_xEG_y) copolymers. The obtained results were verified by ^{1}H-NMR spectroscopy. Furthermore, the ^{13}C-NMR measurements showed that the $(BD_xDi_y)_{mp}$ and $(BD_xEG_y)_{mp}$ copolymers are fully random ($R_{total,\ mp} \approx 1$). The $(BD_xDi_y)_{ssp}$ copolymers, have a non-random distribution ($R_{total,\ ssp} < 1$) but $R_{total,\ ssp}$ increases to 1 for large fractions of incorporated Dianol. Crystallinity measurements show that Dianol

is, besides a reactant, also a solvent for PBT. For the $(BD_xEG_y)_{ssp}$, the degree of randomness continually decreases with increased fraction of incorporated ethylene glycol. During the SSP reaction, PET blocks are formed which subsequently crystallize as was verified by DSC measurements.

3.5 References and notes

1. Radusch, H.-J. In *Handbook of Thermoplastic Polyesters*; Fakirov, S., Ed.; Wiley-VCH: Weinheim, 2002, Chapter 8, p 389-419.
2. Radusch, H.-J., Androsch, R. In *Handbook of Thermoplastic Polyesters*; Fakirov, S., Ed.; Wiley-VCH: Weinheim, 2002, Chapter 20, p 895-925.
3. Devaux, J.; Godard, P.; Mercier, J. P.; Touillaux, R.; Dereppe, J. M. *J. Polym. Sci., Polym. Phys. Ed.* **1982**, *20*, 1881-1894.
4. Fakirov, S.; Sarkissova, M.; Denchev, Z. *Macromol. Chem. Phys.* **1996**, *197*, 2837-2867.
5. Denchev, Z.; Sarkissova, M.; Fakirov, S.; Yilmaz, F. *Macromol. Chem. Phys.* **1996**, *197*, 2869-2887.
6. Fakirov, S.; Sarkissova, M.; Denchev, Z. *Macromol. Chem. Phys.* **1996**, *197*, 2889-2907.
7. Montaudo, G.; Montaudo, M. S.; Scamporrino, E.; Vitalini, D. *Macromolecules* **1992**, *25*, 5099-5107.
8. Fernandez-Berridi, M. J.; Iruin, J. J.; Maiza, I. *Polymer* **1995**, *36*, 1357-1361.
9. Fakirov, S. In *Solid State Behavior of Linear Polyesters and Polyamides*; Schultz, J. M., Fakirov, S., Eds.; Prentice-Hall: Englewood Cliffs, NJ, 1990; Chapter 2, p 19-43.
10. Hait, S. B.; Sivaram, S. *Macromol. Chem. Phys.* **1998**, *199*, 2689-2697.
11. James, N. R., Ramesh, C.; Sivaram, S. *Macromol. Chem. Phys.* **2001**, *202*, 1200-1206.
12. James, N. R., Ramesh, C.; Sivaram, S. *Macromol. Chem. Phys.* **2001**, *202*, 2267-2274.
13. Kricheldorf, H. R. *Makromol. Chem.* **1978**, *179*, 2133-2143.
14. Newmark, R. A. *J. Polym. Sci., Polym. Chem. Ed.* **1980**, *18*, 559-563.
15. Yamadera, R.; Murano, M. *J. Polym. Sci., Part A-1* **1967**, *5*, 2259-2268.
16. Backson, S. C. E.; Kenwright, A. M.; Richards, R. W. *Polymer* **1995**, *36*, 1991-1998.
17. Jacques, A.; Devaux. J.; Legras, R.; Nield, E. *J. Polym. Sci., Polym. Chem. Ed.* **1996**, *34*, 1189-1194.
18. Martínez de Ilarduya, A.; Kint, D. P. R.; Muñoz-Guerra, S. *Macromolecules* **2000**, *33*, 4596-4598.
19. Kint, D. P. R.; Martínez de Ilarduya, A.; Muñoz-Guerra, S. *J. Polym. Sci., Polym. Chem. Ed.* **2001**, *39*, 1994-.
20. Kint, D. P. R.; Martínez de Ilarduya, A.; Muñoz-Guerra, S. *Macromolecules* **2002**, *35*, 314-317.
21. Sandhya, T. E.; Ramesh, C.; Sivaram, S. *Macromol. Symp.* **2003**, *199*, 467-482.
22. Jansen, M. A. G.; Goossens, J. G. P.; de Wit, G.; Bailly C.; Koning, C. E. *Macromolecules* **2005**, *38*, 2659-2664.
23. Kirk, R. E.; Othmer, D. F. In *Kirk-Othmer Encyclopedia of Chemical Technology*, 4th ed.; Kroschwitz, J. I., Howe-Grant, M., Eds.; Wiley-Interscience: New York, 1997; Vol. 22, p 400.
24. PBT as received already contained residuals of tetra-n-butyl titanate ($Ti(OBu)_4$) catalyst, so promoting the transesterification reaction by additional catalyst was not necessary.

25. Finelli, L.; Lotti, N.; Munari, A.; Berti, C.; Colonna, M.; Lorenzetti, C. *Polymer* **2003**, *44*, 1409-1420.

26. Montaudo, G.; Puglisi, C.; Samperi, F. In *Transreactions in Condensation Polymers*; Fakirov, S., Ed.; Wiley-VCH: Weinheim, 1999; Chapter 4, p 159-193.

27. Flory, P. J. In *Principles of Polymer Chemistry*; Cornell University Press: London, 1953; Chapter 8, p 317-326.

28. Randall, J. C. In *Polymer sequence determination carbon 13 nmr method*; Academic Press: New York, 1977, p 39.

29. Devaux, J.; Godard, P.; Mercier, J. P. ; Touillaux, R. ; Dereppe, J. M. *J. Polym. Sci., Polym. Phys. Ed.* **1982**, *20*, 1875-1880.

Chapter 4

^{13}C-NMR sequence distribution analysis applied on a three phase model for determination of the chemical microstructure*

4.1 Introduction

Poly(butylene terephthalate) (PBT) is a semi-crystalline aromatic polyester with a high crystallization rate in combination with good mechanical properties.[1] However, its relatively low glass transition temperature makes unfilled PBT less suitable for use at elevated temperatures. It is generally known that material properties of PBT can be modified by reactive melt blending with other polycondensates.[2] Transesterification reactions in the melt first result in the formation of block copolymers, and with proceeding reaction times copolymers with a random microstructure are obtained.[3-8] These random copolymers have shorter and more irregular homopolymer sequences and may therefore exhibit a decreased melting temperature, crystallization rate and crystallinity compared to pure PBT. A method suitable for preparation of copolymers from polycondensates with retention of long homopolymer blocks is solid-state polymerization (SSP).[9] With SSP, the PBT homopolymer is heated just below its melting temperature (T_m) but far above its glass transition temperature (T_g) so that the crystalline fraction, consisting of homopolymer PBT blocks, will be retained. As a result of the high reaction temperature close to T_m, the amorphous fraction will become mobile enough for transesterification reactions to occur here. Polymer chain ends present in the amorphous phase will react with each other by transesterification resulting in a recombination of polymer chains. Similarly, when a mixture of different semi-crystalline homopolymer polycondensates is heated below the T_m of the lowest melting homopolymer a copolymer will be obtained. In this way, Sivaram and co-workers prepared several copolymers.[10-12] In **Chapters 2** and **3**, it was shown that SSP can also be used to incorporate diol monomers into semi-crystalline polycondensates.[13-14] 2,2-bis[4-(2-hydroxyethoxy)-phenyl]propane (Dianol 220®) was successfully incorporated into PBT via SSP. Copolymers of different compositions were obtained using different PBT/diol ratios. Quantitative ^{13}C-NMR sequence distribution analysis[15-20] was used to study the difference in chemical microstructure between PBT-Dianol copolymers obtained via SSP and via MP.[14] A clear

* This chapter is reproduced from: Jansen, M. A. G.; Goossens, J. G. P.; de Wit, G.; Bailly, C.; Schick, C.; Koning, C. E. *Macromolecules* **2005**, in press

difference in chemical microstructure was observed: the copolymers obtained by MP have a fully random microstructure, whereas the SSP copolymers have a non-random microstructure. The latter result is due to the presence of homopolymer PBT blocks. For tailoring the overall properties of copolymers obtained by SSP, it is important to know how the diol is incorporated and distributed in the amorphous phase. However, the total chemical microstructure as obtained by quantitative ^{13}C-NMR sequence distribution analysis includes both the crystalline and amorphous phase and hence does not give exclusive information about the chemical microstructure of the amorphous phase only.

In the present chapter, a calculation method is discussed which reveals the chemical microstructure of the amorphous phase using the peak integral values of the dyad sequences as obtained from the quantitative ^{13}C-NMR sequence distribution analysis. Initially, a two-phase model (based on a crystalline and an amorphous phase) will be used to describe the morphology of the semi-crystalline PBT-Dianol copolymers obtained by SSP. Crystallinity measurements are performed by DSC and implemented in the calculation method to determine the chemical microstructure of the amorphous phase. In the second part, the morphology of the semi-crystalline PBT-Dianol copolymers will be described by a three-phase model (crystalline, rigid amorphous and mobile amorphous phase) and the calculation method will be accordingly adjusted to exclusively determine the chemical microstructure of the mobile amorphous fraction.

4.2 Experimental Section

4.2.1 Materials

Poly(butylene terephthalate) (PBT) pellets ($\overline{M}_n$ = 15 kg/mol and $\overline{M}_w$ = 34 kg/mol, determined by size exclusion chromatography) were provided by GE Plastics (Bergen op Zoom, The Netherlands) and used as received. 2,2-bis[4-(2-hydroxyethoxy)phenyl]propane (Dianol 220®) was provided by Air Liquide (Paris, France) and was recrystallized twice from acetone prior to use. For NMR measurements, deuterated trifluoro acetic acid (TFA-d, 99 % deuterated) was obtained from Aldrich and deuterated chloroform ($CDCl_3$, 99 % deuterated) was obtained from Merck.

4.2.2 Synthesis of PBT-Dianol copolymers: Solid-state copolymerization (SSP) and melt copolymerization (MP)

The synthesis of PBT-Dianol copolymers by SSP and MP was described in detail in **Chapter 2**.[14] Powder mixtures of different PBT/Dianol ratios were used as feed for the SSP and MP reactions in order to obtain copolymers of different compositions. For the SSP reactions, the

PBT and Dianol powder were mixed by dissolution in 1,1,1,3,3,3-hexafluoro-2-propanol (HFIP) prior to SSP. After complete dissolution, the HFIP was evaporated and the obtained lump of material was ground into powder. The PBT/Dianol mixtures used for MP or SSP are abbreviated as $(BD_xDi_y)_{feed}$. BD_x denotes the mole percentage (mol%) of PBT (expressed in 1,4-butanediol units), whereas Di_y denotes the mole percentage of Dianol (expressed in Di units) in the $(BD_xDi_y)_{feed}$ mixtures. Solid-state polymerized (BD_xDi_y) copolymers are indicated as $(BD_xDi_y)_{ssp}$ copolymers, where BD_x and Di_y represent the initial mol% PBT and Dianol present in the $(BD_xDi_y)_{feed}$ mixture being used for SSP. The actual mole fractions of BD and Di units after SSP differ only slightly from the initial fractions present in the $(BD_xDi_y)_{feed}$ mixtures. These differences can be attributed to the evaporation of 1,4-butanediol during the SSP reaction. For all $(BD_xDi_y)_{ssp}$ copolymers, a solid-state polymerization temperature (T_{ssp}) of 180 °C was used in combination with a solid-state polymerization time (t_{ssp}) of 9 h. This time proved to be long enough for complete incorporation of the Dianol into the PBT. Furthermore, after this reaction time, it was shown that the molecular weight of the resulting $(BD_xDi_y)_{ssp}$ copolymers did not significantly increase anymore.[13] Melt polymerized samples (BD_xDi_y) copolymers are denoted as $(BD_xDi_y)_{mp}$, where BD_x and Di_y respectively represent the initial mol% PBT and Dianol present in the $(BD_xDi_y)_{feed}$ powder mixture being used for MP. Also here, the mole fractions of BD and Di units after MP slightly differ from the reactions initially present in the $(BD_xDi_y)_{feed}$ mixtures.

4.2.3 Nuclear Magnetic Resonance (NMR) Spectroscopy.

All solution ^{1}H-NMR spectra were recorded on a Varian 400 MHz spectrometer at 25 °C at a resonance frequency of 400.164 MHz. For the ^{1}H-NMR measurements, 15 mg of polymer was dissolved in 0.8 mL of a 80:20 vol% $CDCl_3$:TFA-d mixture. All chemical shifts are reported in ppm downfield from tetramethylsilane (TMS), used as the internal standard. The spectra were acquired using 32 scans, a delay time (d1) of 5 s and a total number of data points of 64 k.

Quantitative proton-decoupled solution ^{13}C-NMR spectra were recorded on a Varian 300 MHz spectrometer, operated at a resonance frequency of 75.462 MHz. For copolymers with less then 10 mol% of incorporated Dianol, an Oxford 500 MHz spectrometer was used, operated at a resonance frequency of 125.685 MHz. For ^{13}C-NMR measurements, 50 mg of polymer was dissolved in 0.8 mL pure TFA-d. TMS was used as the internal standard. For spectra recorded with the 300 MHz spectrometer, 3000-4000 scans were acquired with 64 k data points, a d1 of 12 s, a 90° pulse and a spectral width of 18.8 kHz. For the spectra recorded with the 500 MHz spectrometer, 4000-5000 scans were acquired with 75 k data points, a d1 of 12 s, a 90° pulse and a spectral width of 25 kHz. Spinning was not used for the

spectra recorded at the 500 MHz-spectrometer. Overlapping peaks were integrated after Lorentzian deconvolution of the spectra using the deconvolution option implemented in the Varian NMR-software.

4.2.4 Differential Scanning Calorimetry (DSC)

Specific heat capacity measurements were done on a Perkin Elmer Pyris Diamond DSC equipped with an Intracooler II. Nitrogen was used as purge gas. $(BD_xDi_y)_{ssp}$ copolymer samples of 18-20 mg were wrapped in approximately 5 mg aluminum foil where the aluminum weights of the sample and reference were closely matched. Crystallinity was estimated from the heat of fusion from scan measurements at 20 K/min from 0 to 260 °C. The peak area was obtained using a linear baseline for integration. Heat of fusion of the infinite crystal was assumed to be 145 J/g (32 kJ/mol).[21-23] Specific heat capacity in the vicinity of the glass transition was calculated from StepScan™ DSC measurements with steps of 1 K and isothermal waiting times of 1 minute. The mobile amorphous fraction was determined as the ratio of the increase of heat capacity at the glass transition for the sample under investigation and that for the amorphous PBT of 0.35 J/g K.[21,24] The step in heat capacity for the semi-crystalline samples was obtained using tangents to the measured curves below and above the glass transition. The tangents above T_g were constructed as linear superposition of the heat capacities for crystalline and liquid PBT according to ATHAS database.[21] The crystalline heat capacity was used as the tangent below T_g. Details about the calculation of the crystallinity as well as mobile and rigid amorphous fraction, are given below.

4.3 Results and discussion

$(BD_xDi_y)_{ssp}$ and $(BD_xDi_y)_{mp}$ copolymers were synthesized using different PBT/Dianol ratios. The procedures to synthesize these copolymers were explained in **Chapters 2** and **3**.[13,14] The general chemical structure of the (BD_xDi_y) copolymer is shown in Figure 4.1.

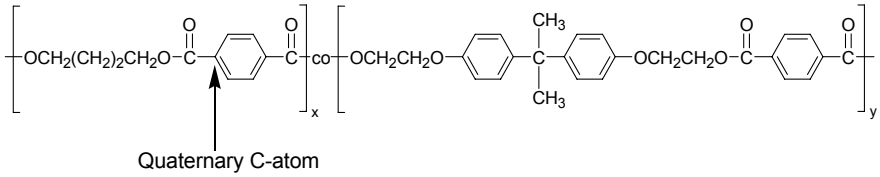

Figure 4.1. Chemical structure of a (BD_xDi_y) copolymer, consisting of BD-T and Di-T repeat-units. The arrow marks the quaternary carbon atom which ^{13}C-NMR signal is used in the sequence distribution analysis.

4.3.1 Chemical microstructure of PBT-Dianol copolymers obtained by SSP

The overall chemical compositions of both $(BD_xDi_y)_{ssp}$ and $(BD_xDi_y)_{mp}$ copolymers, obtained from ^{1}H-NMR measurements are listed in Table 4.1.

Table 4.1. Overview of the used $(BD_xDi_y)_{feed}$ mixtures and the resulting $(BD_xDi_y)_{ssp}$ copolymers.

Composition feed[a] $(BD_xDi_y)_{feed}$		Composition after SSP[b] $(BD_xDi_y)_{ssp}$		Degree of Randomness[c]	Crystallinity[d]	
$F_{BD\text{-}T,\ feed}$ (x) (mol%)	$F_{Di,\ feed}$ (y) (mol%)	$F_{BD\text{-}T,\ total}$ (mol%)	$F_{Di\text{-}T,\ total}$ (mol%)	$R_{ssp,\ total}$	$\chi_{heating,\ total}$	$\chi_{heating.\ PBT\ only}$
100	0	100	0		54.5	54.5
95	5	96	4	0.82	51.8	55.8
90	10	90	10	0.76	46.6	57.3
85	15	84	16	0.73	41.1	57.4
80	20	76	24	0.73	33.4	54.7
75	25	69	31	0.76	25.6	48.8
70	30	61	39	0.82	15.5	35.7
65	35	54	46	0.89	5.7	15.7

Composition feed[a] $(BD_xDi_y)_{feed}$		Composition after MP[b] $(BD_xDi_y)_{mp}$		Degree of Randomness[c]
$F_{BD\text{-}T,\ feed}$ (x) (mol%)	$F_{Di,\ feed}$ (y) (mol%)	$F_{BD\text{-}T,\ total}$ (mol%)	$F_{Di\text{-}T,\ total}$ (mol%)	$R_{mp,\ total}$
95	5	96	4	1.04
90	10	90	10	0.93
85	15	81	19	0.99
80	20	74	26	0.98
75	25	70	30	0.99

[a] Composition of the feed mixtures used for SSP and MP (amounts of PBT and Dianol were weighed so that a specific mole ratio PBT:Dianol was obtained.

[b] Compositions of the $(BD_xDi_y)_{ssp}$ and $(BD_xDi_y)_{mp}$ copolymers were determined by ^{1}H-NMR spectroscopy.

[c] $R_{ssp,\ total}$ and $R_{mp,\ total}$ were obtained by quantitative ^{13}C-NMR spectroscopy.

[d] $\chi_{heating,\ total}$ is the total crystallinity, based on $\Delta H_{melting}$. $\chi_{heating,\ PBT\ only}$ is obtained by dividing $\chi_{heating,\ total}$ by the present weight fraction of BD-T repeat-units.

The chemical microstructure of the synthesized $(BD_xDi_y)_{ssp}$ and $(BD_xDi_y)_{mp}$ copolymers, studied by ^{13}C-NMR dyad sequence distribution using the chemical shift of the aromatic quaternary carbon atom (marked with the arrow in Figure 4.1), was described in detail in

Chapters 2 and **3**.[13,14] This peak, positioned in the 135-136 ppm region of the ^{13}C-NMR spectrum, splits up into four different peaks as is shown in Figure 4.2 for a $(BD_{85}Di_{15})_{ssp}$ copolymer.

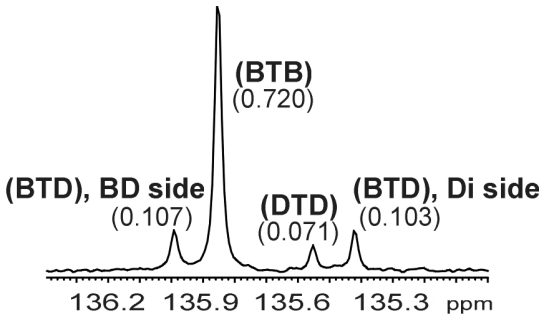

Figure 4.2. ^{13}C-NMR spectrum (135-136 ppm) of a $(BD_{85}Di_{15})_{ssp}$ copolymer: splitting of the quaternary carbon atom (marked by the arrow in Figure 4.1) into four peaks. Peak integral values are also listed.

Each peak originates from a different dyad sequence. Because the four peaks are slightly overlapping, a Gaussian deconvolution procedure was applied for a clear peak separation. Subsequently, the integral value of each peak was determined. The obtained integral values were normalized to a total value of 100. These values are also listed in Figure 4.2. The normalized peak integral values can be used to calculate the composition and the degree of randomness (R) of each (BD_xDi_y) copolymer. The latter parameter represents the sequence distribution of a copolymer. The following equations[15] were used:

$$F_{BTD,\,total} = F_{BTD,\,BD-side} + F_{BTD,\,Di-side} \tag{4.1}$$

$$F_{BD-T,\,total} = (F_{BTD,\,total}/2 + F_{BTB}) \tag{4.2}$$

$$F_{Di-T,\,total} = (F_{BTD,\,total}/2 + F_{DTD}) \tag{4.3}$$

$$R_{total} = \frac{F_{BTD,\,total}}{2 \cdot (F_{BD-T,\,total} \cdot F_{Di-T,\,total})} \tag{4.4}$$

where $F_{BTD,\,BD\text{-}side}$, F_{BTB}, F_{DTD}, $F_{BTD,\,Di\text{-}side}$ represent the integral values of the dyad sequences. $F_{BD\text{-}T,\,total}$ and $F_{Di\text{-}T,\,total}$ denote the total mole fractions of BD-T and Di-T units, respectively. For a fully random copolyester, the distribution of the two different BD-T and Di-T repeat units should obey Bernoullian statistics.[15,25] The degree of randomness (R_{total}) as calculated

using eq 4.4 should then be equal to 1. If R_{total} is smaller than 1, this implies that the repeat units tend to be arranged in block-like structures. Schematic representations of copolymers obtained by MP (random: $R_{mp,\ total} = 1$) and by SSP (non-random: $R_{ssp,\ total} < 1$) are shown in Figures 4.3a and 4.3b, respectively.

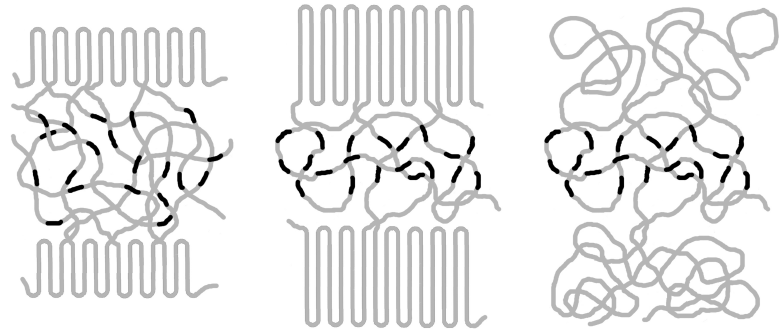

(a) (b) (c)

Figure 4.3. Schematic representation of the chemical microstructures (a) $(BD_xDi_y)_{mp}$: random distribution of BD-T and Di-T repeat units: $R_{mp,\ total} = 1$, (b) $(BD_xDi_y)_{ssp}$: non-random distribution of Di-T repeat units: $R_{ssp,\ total} < 1$, (c) After dissolution of a $(BD_xDi_y)_{ssp}$ copolymer in TFA-d.

The values for $R_{ssp,\ total}$ and $R_{mp,\ total}$ for all synthesized $(BD_xDi_y)_{ssp}$ copolymers respectively $(BD_xDi_y)_{mp}$ copolymers are also listed in Table 4.1. It can be seen that all synthesized $(BD_xDi_y)_{mp}$ copolymers have a fully random distribution ($R_{mp,\ total} = 1$) for the whole composition range. Only for the $(BD_{95}Di_5)_{mp}$ and $(BD_{90}Di_{10})_{mp}$ copolymer, the obtained values for $R_{mp,\ total}$ slightly deviate from unity, which is due to the low peak signal intensity of the DTD dyad sequence for these low Dianol concentrations.

The microstructure of the $(BD_xDi_y)_{ssp}$ copolymers, represented by $R_{ssp,\ total}$, depends on the mole fraction of incorporated Dianol. $R_{ssp,\ total}$ decreases to a minimum value of 0.73 at $F_{BD\text{-}T,\ total} = 83$ mol% and then gradually increases to unity with increasing Dianol content. DSC measurements showed that the total crystallinity ($\chi_{heating}$) of the $(BD_xDi_y)_{ssp}$ copolymers decreased for increasing fractions of incorporated Dianol. Lotti et al.[26] synthesized a $(BD_0Di_{100})_{mp}$ copolymer and observed that this homopolymer was fully amorphous. Hence, Di-T repeat units are not able to crystallize. To obtain the crystallinity of the PBT-segments only, $\chi_{heating}$ was divided by the weight fraction of BD-T repeat units ($W_{BD\text{-}T,\ total}$). Both $\chi_{heating}$ and $\chi_{heating,\ PBT\ only}$ are listed in Table 4.1 for the $(BD_xDi_y)_{ssp}$ copolymers. It can be seen that $\chi_{heating,\ PBT\ only}$ initially shows a small increase for $(BD_xDi_y)_{ssp}$ copolymers with $F_{BD\text{-}T,\ total} > 90$ mol% compared to $\chi_{heating,\ PBT\ only}$ of a $(BD_{100}Di_0)_{ssp}$ homopolymer. For $F_{BD\text{-}T,\ total} < 63$ mol%, $\chi_{heating,\ PBT\ only}$ decreases to a value which is even below $\chi_{heating}$ of a $(BD_{100}Di_0)_{feed}$

homopolymer (i.e. PBT homopolymer after HFIP treatment; $\chi_{heating} = \chi_{heating,\ PBT\ only} = 0.38$, see **Chapter 3**). This result is remarkable because it was assumed that the crystalline fraction is preserved during SSP and that modifications only take place in the amorphous phase. This decrease of $\chi_{heating,\ PBT\ only}$ for increasing fractions of Dianol monomer might already occur during the preparation of the $(BD_xDi_y)_{feed}$ mixtures. Another possibility is that $\chi_{heating,\ PBT\ only}$ decreases during the SSP reaction. The small increase of $\chi_{heating,\ only}$ for $F_{BD\text{-}T,\ total} > 90$ mol% with respect to pure PBT may be the result of the solvent induced crystallization effect of Dianol, when present in small amounts during the SSP reaction. The increased mobility will favor the crystallization, simultaneously occurring with SSP over the dissolution of the crystalline PBT fraction. Once the crystalline PBT blocks are dissolved, all polymer chain segments will have sufficient mobility to participate in the transesterification reactions. Hence, the degree of randomness of the $(BD_xDi_y)_{ssp}$ copolymers will gradually increase when the Dianol concentration is higher in the $(BD_xDi_y)_{feed}$ mixtures used for SSP (Table 4.1).

Because the ^{13}C-NMR sequence distribution analysis is based on solution NMR, the $(BD_xDi_y)_{ssp}$ copolymers have to be completely dissolved prior to measuring. The microstructure of a dissolved $(BD_xDi_y)_{ssp}$ copolymer is schematically depicted in Figure 4.3c. For clarity, the homopolymer blocks of the former crystalline part and the modified former amorphous part are drawn separately, although realizing that this conformation is unlikely. In this way however, it can be clearly seen that the obtained degree of randomness for the $(BD_xDi_y)_{ssp}$ copolymers ($R_{ssp,\ total}$) is an *overall* degree of randomness, in which both the former crystalline and former amorphous parts contribute to the total signal intensity. Therefore, $R_{ssp,\ total}$ does not give exclusive information on the chemical microstructure of the amorphous phase, the only part of the material that can participate in the transesterification process during SSP. The presence of large homopolymer PBT blocks, originating from the crystalline parts during SSP, results in a decrease of $R_{ssp,\ total}$ compared to $R_{mp,\ total}$. Knowledge about the chemical microstructure of the amorphous phase is important because it influences the thermal properties of the corresponding copolymer. In order to reveal the chemical microstructure of the amorphous phase after SSP, it is necessary to correct the obtained peak integral values of the different dyad sequences in such a way that only the amorphous part is taken into consideration. Hence, the relationship between crystallinity of the $(BD_xDi_y)_{ssp}$ copolymers and the peak integral values of the dyad sequences has to be established in order to proportionally adjust these values. The corrected peak integral values should then represent the microstructure of the amorphous phase. A method to correct the peak integral values of the dyad sequences will be discussed below. The morphology of the semi-crystalline $(BD_xDi_y)_{ssp}$ copolymers will first be represented by a two-phase (crystalline/amorphous) model.

4.3.2 Chemical microstructure based on the two-phase model

The calculation method described below consists of three steps. First, the ratio of BD-T and Di-T repeat units in the amorphous phase are calculated. Subsequently, a mole balance is made in relation to the total copolymer. Finally, the peak integral values are corrected by taking previous calculations into account. The data for a $(BD_{85}Di_{15})_{ssp}$ copolymer are used to illustrate the calculation method.

4.3.2.1 Mole ratio of BD-T and Di-T repeat units in the amorphous phase

The degree of randomness (Rssp, total), as calculated using eq 4.4, is based on the overall mole fractions of BD-T and Di-T repeat units in the copolymer. When this equation is used to calculate the degree of randomness of the amorphous phase only, then the mole fractions of BD-T and Di-T repeat units present in the amorphous phase have to be considered. Therefore, the crystallinity of the $(BD_{85}Di_{15})_{ssp}$ copolymer should be known. The crystallinity (denoted as $\chi_{heating}$) was determined by dividing the melting enthalpy ($\Delta H_{melting}$) of the first heating run (obtained via DSC measurements) by the melting enthalpy (ΔH^0_{fuse}) for 100% crystalline PBT. For ΔH^0_{fuse}, values of 145[21-23] J/g (32 kJ/mol) 140[27] J/g (31 kJ/mol) are reported in literature. In this study, a value of 145 J/g was used for ΔH^0_{fuse}. For $(BD_{85}Di_{15})_{ssp}$, $\Delta H_{melting}$ has a value of 59.4 J/g which corresponds to $\chi_{heating} = 0.41$ and hence the amorphous fraction $\alpha_{heating} = 0.59$. It has to be mentioned that during the SSP reaction annealing may occur which results in PBT crystals with a larger lamellar thickness and an increased crystallinity. Furthermore, the DSC traces of the first heating run of the SSP samples gave sharp melting peaks and did not show any reorganization upon heating. Hence, $\chi_{heating}$ as obtained from the first DSC heating run should represent the crystallinity of the $(BD_xDi_y)_{ssp}$ copolymers directly after SSP. Now, a BD-T mass balance with respect to the total $(BD_{85}Di_{15})_{ssp}$ copolymer can be made:

$$\chi_{heating} \cdot W_{BD-T,\,\chi} + \alpha_{heating} \cdot W_{BD-T,\,\alpha} = W_{BD-T,\,total} \qquad (4.5)$$

where $\chi_{heating}$ and $\alpha_{heating}$ represent the fractions of the crystalline and amorphous phase based upon $\Delta H_{melting}$ of the first heating run. $W_{BD\text{-}T,\,\chi}$ and $W_{BD\text{-}T,\,\alpha}$ are the weight fractions of BD-T repeat units in the crystalline phase and amorphous phase, whereas $W_{BD\text{-}T,\,total}$ is the total weight fraction of BD-T repeat units based on the entire copolymer. $W_{BD\text{-}T,\,total}$ was calculated using $F_{BD\text{-}T,\,total}$ (obtained via ^{1}H-NMR measurements; values are shown in Table 4.1):

$F_{BD\text{-}T,\,total} = 0.836 \cong W_{BD\text{-}T,\,total} = 0.716$ ($M_{BD\text{-}T} = 220.2$ g/mol)

$F_{Di\text{-}T,\,total} = 0.164 \cong W_{Di\text{-}T,\,total} = 0.284$ ($M_{Di\text{-}T} = 446$ g/mol)

It is assumed that the crystalline fraction only consists of PBT homopolymer segments (BD-T repeat units) and thus for this fraction $W_{BD\text{-}T,\,\chi} = 1$. This assumption also implies that Dianol is only incorporated into the amorphous phase (present as Di-T repeat units). Using $W_{BD\text{-}T,\,\chi} = 1$ together with $\chi_{heating} = 0.411$, $\alpha_{heating} = 0.589$ and $W_{BD\text{-}T,\,total} = 0.716$, gives $W_{BD\text{-}T,\,\alpha} = 0.518$, i.e., the amorphous copolyester PBT phase consists of 51.8 wt% BD-T repeat units and thus of 48.2 wt% Di-T repeat units. Recalculation in mole fractions gives:

$W_{BD\text{-}T,\,\alpha} = 0.518 \cong F_{BD\text{-}T,\,\alpha} = 0.685$ BD-T

$W_{Di\text{-}T,\,\alpha} = 0.482 \cong F_{Di\text{-}T,\,\alpha} = 0.315$ Di-T

Consequently, for the $(BD_{85}Di_{15})_{ssp}$ copolyester the mole ratio in the amorphous phase is $(F_{BD\text{-}T,\,\alpha}/F_{Di\text{-}T,\,\alpha}) = 2.18$.

4.3.2.2 Total mole fraction of BD-T and Di-T repeat units based on the total copolymer (crystalline and amorphous fraction)

The next step is to calculate the overall mole fractions of BD-T and Di-T repeat units in the total copolymer. It was already mentioned that Di-T repeat units are assumed to be present only in the amorphous phase, whereas the BD-T repeat units are distributed over both the amorphous and crystalline phase. A composition balance based on the total $(BD_{85}Di_{15})_{ssp}$ copolymer can be made:

$$F_{Di-T,\,\alpha\,(total)} + F_{BD-T,\,\alpha\,(total)} + F_{BD-T,\,\chi\,(total)} = 1 \qquad (4.6)$$

where $F_{Di\text{-}T,\,\alpha\,(total)}$ and $F_{BD\text{-}T,\,\alpha\,(total)}$ are the mole fractions of Di-T and BD-T repeat units in the amorphous phase, and $F_{BD\text{-}T,\,\chi\,(total)}$ is the mole fraction of BD-T repeat units in the crystalline phase. All fractions mentioned in eq 4.6 are based on the total copolymer composition. From the earlier mentioned assumption that all Di-T repeat units are exclusively present in the amorphous phase, it follows that $F_{Di\text{-}T,\,\alpha\,(total)} = 0.164 = F_{Di\text{-}T,\,total}$. By using the earlier calculated mole ratio $(F_{BD\text{-}T,\,\alpha}/F_{Di\text{-}T,\,\alpha}) = 2.18$, a value of $F_{BD\text{-}T,\,\alpha\,(total)} = 0.357$ is found. This latter mentioned value will be used to determine the degree of randomness of the amorphous phase as is shown in the next part. Using $F_{BD\text{-}T,\,\alpha\,(total)} = 0.357$ in eq 4.6, results in $F_{BD\text{-}T,\,\chi\,(total)} = 0.480$.

4.3.2.3 Correction of ^{13}C-NMR peak integral values of dyad sequences to obtain the chemical microstructure of the amorphous phase

The peak integral values of the four dyad sequences (as shown in Figure 4.2) have to be corrected in such a way that these values only give information about the distribution of BD-T and Di-T repeat units in the amorphous phase. Therefore, the fraction of each sequence in the amorphous phase has to be known. Based on the assumption that all Di-T repeat units are present in the amorphous phase and by definition of eqs 4.1 and 4.3, sequences (DTD), (BTD, Di-side) and (BTD, BD-side), determining the degree of randomness, should be present in the amorphous phase. For simplicity, all DTD and BTD sequences present at the boundary of the crystalline and amorphous phase are in this calculation method added to the amorphous phase. Consequently, the peak integrals of the previously mentioned dyad sequences remain unchanged and hence the mole fractions of sequences in the amorphous phase are: $F_{DTD,\,\alpha}$ = 0.071, $F_{BTD,\,BD\text{-}side,\,\alpha}$ = 0.107 and $F_{BTD,\,Di\text{-}side,\,\alpha}$ = 0.103 (see Figure 4.2). The only unknown parameter is the mole fraction of (BTB) sequences in the amorphous phase ($F_{BTB,\,\alpha}$). This value can be obtained using the earlier calculated value for the total mole fraction of BD-T repeat units in the amorphous phase, $F_{BD\text{-}T,\,\alpha\,(total)}$, together with eq 4.2 applied to the amorphous phase:

$$F_{BD-T,\,\alpha\,(total)} = ((F_{BTD,\,BD-side,\,\alpha} + F_{BTD,\,Di-side,\,\alpha})/2 + F_{BTB,\,\alpha}) \tag{4.7}$$

where $F_{BD\text{-}T,\,\alpha\,(total)}$ = 0.357, $F_{BTD,\,BD\text{-}side,\,\alpha}$ = 0.107, $F_{BTD,\,Di\text{-}side,\,\alpha}$ = 0.103. Using these values in eq 4.7 results in $F_{BTB,\,\alpha}$ = 0.252.

4.3.2.4 Calculation of corrected degree of randomness ($R_{ssp,\,\alpha}$)

The final step is to normalize the corrected integral values of the four dyad sequences to a total value of 1. The thus obtained integral values can subsequently be used with eq 4.4 to give the degree of randomness of the amorphous phase ($R_{ssp,\,\alpha}$) which results in: $R_{ssp,\,\alpha}$ = 0.89. Because during SSP the crystalline fraction is no longer participating, the value of $R_{ssp,\,\alpha}$ is larger than $R_{ssp,\,total}$, which has a value of 0.73. The results of the described calculations are summarized in Table 4.2.

The previously described calculation method was also applied to the other synthesized $(BD_xDi_y)_{ssp}$ copolymers given in Table 4.1. The uncorrected values of $R_{ssp,\,total}$ and the values obtained after application of the correction method, $R_{ssp,\,\alpha}$, are plotted in Figure 4.4 as a function of $F_{BD\text{-}T,\,total}$ The degree of randomness of the mobile amorphous fraction ($R_{ssp,\,mobile\,\alpha}$), which will be discussed later, is also shown.

Table 4.2. Calculated parameters and the resulting degree of randomness of the amorphous phase using the two-phase model for the $(BD_{85}Di_{15})_{ssp}$ copolymer.

Sequences total copolymer	$F_{BTD,\ BD\text{-}side}$	F_{BTB}	F_{DTD}	$F_{BTD,\ Di\text{-}side}$
Normalized peak integral values by ^{13}C-NMR	0.107	0.720	0.071	0.103
Total composition by ^{13}C-NMR	$F_{BD\text{-}T,\ total} = 0.825$		$F_{Di\text{-}T,\ total} = 0.175$	
Crystalline fraction, total	$F_{BD\text{-}T,\ \chi\ (total)} = 0.480$			
Amorphous fraction, total	$F_{BD\text{-}T,\ \alpha\ (total)} = 0.357$		$F_{Di\text{-}T,\ \alpha\ (total)} = 0.164$	
Amorphous fraction only	$F_{BD\text{-}T,\ \alpha} = 0.685$		$F_{Di\text{-}T,\ \alpha} = 0.315$	
Sequences amorphous phase	$F_{BTD,\ BD\text{-}side,\ \alpha}$	$F_{BTB,\ \alpha}$	$F_{DTD,\ \alpha}$	$F_{BTD,\ Di\text{-}side,\ \alpha}$
Corrected peak integral values	0.107	0.252	0.071	0.103
Normalized corrected peak integral values	20.1	47.3	13.3	19.3
Degree of randomness before correction	$R_{ssp,\ total} = 0.73$			
Degree of randomness after correction (two- phase model)	$R_{ssp,\ \alpha} = 0.89$			

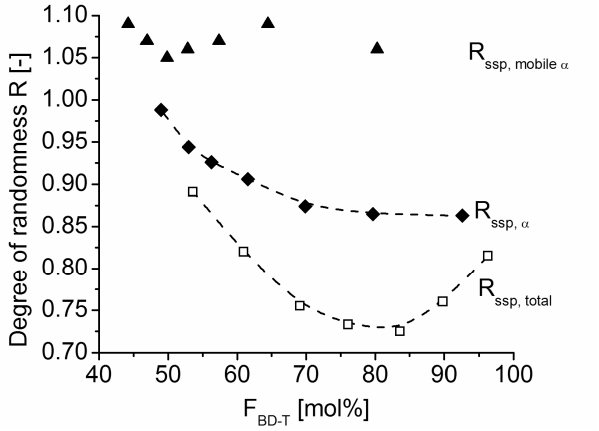

Figure 4.4. Sequence distribution analysis of $(BD_xDi_y)_{ssp}$ copolymers: total degree of randomness $R_{ssp,\ total}$ (□, based on the total microstructure), corrected degree of randomness $R_{ssp,\ \alpha}$ (◆, based on the two-phase model) and $R_{ssp,\ mobile\ \alpha}$ (▲, based on the three-phase model) as a function of $F_{BD\text{-}T,\ total}$.

It can be seen that the values for $R_{ssp,\ \alpha}$ are higher compared to the original values of $R_{ssp,\ total}$, which is expected because the PBT segments, during SSP present in the crystalline fraction,

and not participating in the transesterification reactions, are no longer taken into account. Furthermore like $R_{ssp,\,total}$, $R_{ssp,\,\alpha}$ is dependent on the fraction of incorporated Dianol. It can be seen that the values for $R_{ssp,\,\alpha}$ are still below unity over a large composition range. Only when the crystallinity $\chi_{heating} = 0$ (and hence $F_{BD\text{-}T,\,\alpha} = F_{BD\text{-}T,\,total}$), $R_{ssp,\,\alpha} = R_{ssp,\,total} \approx 1$. Apparently, the values of $R_{ssp,\,\alpha}$ are only below unity when the $(BD_xDi_y)_{ssp}$ copolymers have a crystalline fraction. A possible explanation is that a small fraction of the amorphous phase, close to the crystal surface, is not accessible for the transesterification reactions. Wunderlich and co-workers[28-32] proposed a model in which the amorphous phase in several semi-crystalline polymers, including PBT, is divided into a mobile amorphous sub-phase (α_{mobile}) and a rigid amorphous sub-phase (α_{rigid}). Two models are often used to describe this rigid amorphous sub-phase.[32] One model is based on adjacent reentry folds of polymer chains, whereas the other model is based on fringed micelles. It is assumed for PBT that the rigid amorphous sub-phase does not become mobile until fusion.[24] Consequently, it might be possible that the PBT parts in this rigid amorphous sub-phase are still not mobile enough for participation in the transesterification process at the applied SSP temperature (T_{ssp}) of 180 °C. The values for the amorphous fraction ($\alpha_{heating}$) as used in eq 4.5 may therefore be overestimated. In that case, an additional correction for $R_{ssp,\,\alpha}$ is necessary.

The mobile amorphous fraction (α_{mobile}) can be calculated by eq 4.8a. In this equation, the Δc_p is the heat capacity increase at T_g and $\Delta c_p^{\,0}{}_{\alpha}$ is the Δc_p increase for 100% amorphous PBT at T_g. The literature value for $\Delta c_p^{\,0}{}_{\alpha}$ is 77 J/mol·K (0.35 J/g·K) at T_g = 320 K.[21,24] The rigid amorphous fraction α_{rigid} does not contribute to the increase of Δc_p at the T_g. The crystallinity can be obtained by eq 4.8b, where ΔH^0_{fuse} = 145 J/g.[21-23]

$$\alpha_{mobile} = \Delta c_p / \Delta c_p{}^{0}{}_{\alpha} \tag{4.8a}$$

$$\chi_{heating} = \Delta H_{melting} / \Delta H^{0}{}_{fuse} \tag{4.8b}$$

Hence, α_{rigid} can be described by:

$$\alpha_{rigid} = 1 - \chi_{heating} - \alpha_{mobile} \tag{4.8c}$$

Figure 4.5 shows the obtained values for the fractions α_{mobile}, $\chi_{heating}$ and α_{rigid} as a function of $F_{BD\text{-}T,\,total}$ for the $(BD_xDi_y)_{ssp}$ copolymers. The curves are guides to the eye only and were obtained after polynomial fitting of the obtained data points.

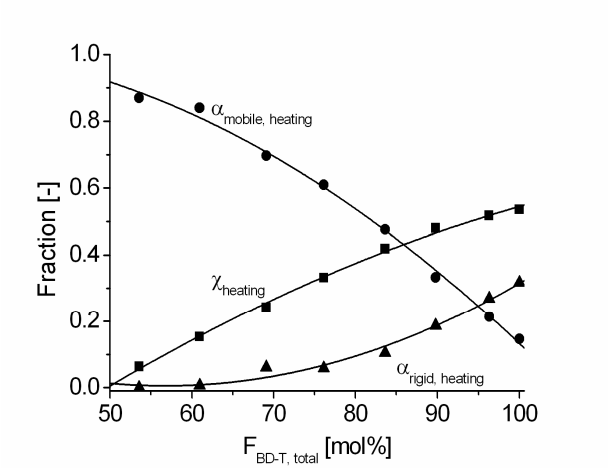

Figure 4.5. Crystalline ($\chi_{heating}$, ■), rigid amorphous ($\alpha_{rigid,\ heating}$, ▲) and mobile amorphous ($\alpha_{mobile,\ heating}$, ●) fractions as a function of $F_{BD\text{-}T,\ total}$.

Hence, correction of $R_{ssp,\ \alpha}$ by subtracting the contribution of the rigid amorphous fraction α_{rigid}, presumably not participating in the transesterification process, should give the degree of randomness of the mobile amorphous fraction which is independent of composition. Of course, the required correction gets smaller with increasing mol% of incorporated Dianol. It can be seen that α_{rigid} increases with increasing $F_{BD\text{-}T,\ total}$, whereas, according to Figure 4.4, $R_{ssp,\ \alpha}$ decreases with increasing $F_{BD\text{-}T,\ total}$.

4.3.3 Chemical microstructure based on the three-phase model

Now that all fractions ($\chi_{heating}$, α_{mobile} and α_{rigid}; Figure 4.5) are known as a function of the $(BD_xDi_y)_{ssp}$ copolymer composition, the correction method for the integral values of the quaternary carbon atom can be adjusted for the three-phase model. Also here, the $(BD_{85}Di_{15})_{ssp}$ copolyester is used to illustrate the calculation model. The first step is to adjust the BD-T mass balance as previously described by eq 4.5. The term $\alpha_{heating}$ in eq 4.5 has to be replaced by a rigid amorphous component and a mobile amorphous component:

$$\chi_{heating} \cdot W_{BD-T,\ \chi} + \alpha_{rigid} \cdot W_{BD-T,\ \alpha\ rigid} + \alpha_{mobile} \cdot W_{BD-T,\ \alpha\ mobile} = W_{BD-T,\ total} \qquad (4.9a)$$

where $\chi_{heating}$ is the crystalline fraction and α_{mobile} and α_{rigid} are the mobile and rigid amorphous fractions, respectively. $W_{BD\text{-}T,\chi}$, $W_{BD\text{-}T,\ \alpha\ rigid}$ and $W_{BD\text{-}T,\ \alpha\ mobile}$ are respectively the weight fractions of BD-T repeat units in the crystalline, rigid amorphous and mobile

amorphous fraction. $W_{BD\text{-}T,\ total}$ is the total weight fraction of BD-T repeat units based on the whole copolymer. The remaining crystalline fraction ($\chi_{heating}$) after SSP should only consist of BD-T repeat units and hence $W_{BD\text{-}T,\ \chi} = 1$. When calculating $R_{ssp,\ \alpha}$, it was assumed that the polymer chains in the rigid amorphous fraction α_{rigid} are still not mobile enough at $T_{ssp} = 180$ °C to participate in the transesterification reactions. Hence, α_{rigid} should also only consist of BD-T repeat units and consequently $W_{BD\text{-}T,\ \alpha\ rigid} = 1$. All Dianol should be present in α_{mobile} and thus eq 4.9a can be simplified to:

$$\chi_{heating} + \alpha_{rigid} + \alpha_{mobile} \cdot W_{BD-T,\ \alpha\ mobile} = W_{BD-T,\ total} \tag{4.9b}$$

According to Figure 4.5, for the $(BD_{85}Di_{15})_{ssp}$ copolymer $\chi_{heating} = 0.411$, $\alpha_{mobile} = 0.473$ and $\alpha_{rigid} = 0.116$. Using these values together with $W_{BD\text{-}T,\ total} = 0.716$ (see earlier) in eq 9b yields $W_{BD\text{-}T,\ \alpha\ mobile} = 0.399$. Hence, α_{mobile} consists of ca. 40 wt% BD-T and ca. 60 wt% Di-T repeat units. Recalculation into mole fractions results in: $F_{BD\text{-}T,\ \alpha\ mobile} = 0.574$ and $F_{Di\text{-}T,\ \alpha\ mobile} = 0.426$. The mole ratio $(F_{BD\text{-}T,\ \alpha\ mobile})/(F_{Di\text{-}T,\ \alpha\ mobile})$ is equal to 1.35.

The assumption that Dianol is only incorporated in the mobile amorphous fraction implies that $F_{Di\text{-}T,\ \chi\ (total)} = 0$ and $F_{Di\text{-}T,\ \alpha\ rigid\ (total)} = 0$ and $F_{Di\text{-}T,\ \alpha\ mobile\ (total)} = F_{Di\text{-}T,\ total} = 0.164$. Using this latter mentioned value in the previously calculated mole ratio $(F_{BD\text{-}T,\ \alpha\ mobile})/(F_{Di\text{-}T,\ \alpha\ mobile}) = 1.35$ results in $F_{BD\text{-}T,\ \alpha\ mobile\ (total)} = 0.221$. Latter mentioned value will be used to calculate the degree of randomness for the mobile amorphous fraction. Furthermore, $F_{BD\text{-}T,\ \alpha\ rigid\ mobile\ (total)}$ and $F_{BD\text{-}T,\ \chi\ (total)}$ can be calculated by combining a total BD-T composition balance with the ratio between α_{rigid} and $\chi_{heating}$:

$$F_{BD-T,\ \alpha\ mobile\ (total)} + F_{BD-T,\ \alpha\ rigid\ (total)} + F_{BD-T,\ \chi\ (total)} = F_{BD-T,\ total} \tag{4.10a}$$

$$\frac{\alpha_{rigid}}{\chi_{heating}} = \frac{F_{BD-T,\ \alpha\ rigid\ (total)}}{F_{BD-T,\ \chi\ (total)}} \tag{4.10b}$$

where $F_{BD\text{-}T,\ \alpha\ mobile\ (total)} = 0.221$, $F_{BD\text{-}T,\ (total)} = 0.836$, $\alpha_{rigid} = 0.116$ and $\chi_{heating} = 0.411$. Hence, for the $(BD_{85}Di_{15})_{ssp}$ copolymer $F_{BD\text{-}T,\ \alpha\ rigid\ (total)} = 0.480$ and $F_{BD\text{-}T,\ \chi\ (total)} = 0.136$.

The last step is to correct the integral values of the dyad sequences in such a way that they represent the sequence distribution of the mobile amorphous fraction ($R_{ssp,\ \alpha\ mobile}$).

Because $F_{Di\text{-}T,\ \alpha\ mobile\ (total)} = F_{Di\text{-}T,\ total}$, the integral values F_{DTD}, $F_{BTD,\ Di\text{-}side}$ and $F_{BTD,\ BD\text{-}side}$ remain unchanged. The only integral value that needs to be corrected is $F_{BTB,\ \alpha\ mobile}$. This

value can be obtained by applying eq 4.2 to the mobile amorphous fraction:

$$F_{BD-T,\,\alpha\ mobile\,(total)} = (F_{BTD,\,total}/2 + F_{BTB,\,\alpha\ mobile}) \tag{4.11}$$

Using $F_{BD\text{-}T,\ \alpha\ mobile\ (total)} = 0.221$ and $F_{BTD,\ total} = 0.210$ in eq 4.11 results in: $F_{BTB,\ \alpha\ mobile} = 0.116$.

The values found for $F_{DTD,\ \alpha\ mobile}$ (0.071), $F_{BTD,\ Di\text{-}side,\ \alpha\ mobile}$ (0.103), $F_{BTD,\ BD\text{-}side,\ \alpha\ mobile}$ (0.107) and $F_{BTB,\ \alpha\ mobile}$ (0.12) are normalized and subsequently used in eq 4.4 to give the degree of randomness of the mobile amorphous fraction: $R_{ssp,\ \alpha\ mobile} = 1.07$. The calculated parameters are summarized in Table 4.3.

Table 4.3. Calculated parameters and the resulting degree of randomness of the accessible amorphous fraction using the three-phase model for the $(BD_{85}Di_{15})_{ssp}$ copolymer.

Sequences total copolymer	$F_{BTD,\ BD\text{-}side}$	F_{BTB}	F_{DTD}	$F_{BTD,\ Di\text{-}side}$
Normalized peak integral values by ^{13}C-NMR	0.107	0.720	0.071	0.103
Total composition by ^{13}C-NMR	$F_{BD\text{-}T,\ total} = 0.825$		$F_{Di\text{-}T,\ total} = 0.175$	
Crystalline fraction	$F_{BD\text{-}T,\ \chi} = 1$		$F_{Di\text{-}T,\ \chi} = 0$ (assumed)	
Rigid amorphous fraction	$F_{BD\text{-}T,\ \alpha\ rigid} = 1$		$F_{Di\text{-}T,\ \alpha\ rigid} = 0$ (assumed)	
Mobile amorphous fraction	$F_{BD\text{-}T,\ \alpha\ mobile} = 0.574$		$F_{Di\text{-}T,\ \alpha\ mobile} = 0.426$	
Mobile amorphous fraction, total	$F_{BD\text{-}T,\ \alpha\ mobile\ (total)} = 0.221$		$F_{Di\text{-}T,\ \alpha\ mobile\ (total)} = 0.164$	
Rigid amorphous fraction, total	$F_{BD\text{-}T,\ \alpha\ rigid\ (total)} = 0.136$		$F_{Di\text{-}T,\ \alpha\ rigid\ (total)} = 0$	
Crystalline fraction, total	$F_{BD\text{-}T,\ \chi\ (total)} = 0.480$		$F_{Di\text{-}T,\ \chi\ (total)} = 0$	
Sequences mobile amorphous fraction	$F_{BTD,\ BD\text{-}side,\ \alpha\ mobile}$	$F_{BTB,\ \alpha\ mobile}$	$F_{DTD,\ \alpha\ mobile}$	$F_{BTD,\ Di\text{-}side,\ \alpha\ mobile}$
Corrected peak integral values	0.107	0.116	0.071	0.103
Normalized corrected peak integral values	0.270	0.292	0.178	0.257
Degree of randomness before correction	$R_{ssp,\ total} = 0.73$			
Degree of randomness after correction (three-phase model)	$R_{ssp,\ \alpha\ mobile} = 1.07$			

Similar calculations were done for the remaining $(BD_xDi_y)_{ssp}$ copolymers. The distribution of BD-T and Di-T repeat-units over the crystalline, rigid amorphous and mobile amorphous fraction as a function of $F_{BD\text{-}T,\ total}$ is shown in Figure 4.6. $F_{Di\text{-}T,\ \alpha\ mobile\ (total)}$ decreases linearly as a function of $F_{BD\text{-}T,\ total}$ because $F_{Di\text{-}T,\ \alpha\ mobile\ (total)} = F_{Di\text{-}T,\ total}$ and $F_{Di\text{-}T,\ total} + F_{BD\text{-}T,\ total} = 1$. The fraction of $F_{BD\text{-}T,\ \alpha\ mobile\ (total)}$ decreases linearly as a function of $F_{BD\text{-}T,\ total}$, but the linearity is lost when $F_{BD\text{-}T,\ total} < 75$ mol%. For these values of $F_{BD\text{-}T,\ total}$, a leveling off is observed. Dianol will not evaporate at $T_{ssp} = 180$ °C and hence, the fraction of polymer chain segments endcapped with Dianol gradually increases when the fraction of Dianol present in the initial $(BD_xDi_y)_{feed}$ mixtures increases. As a consequence, the polymer chain segments in the amorphous phase cannot efficiently recombine anymore because the elimination of the condensation product (i.e. Dianol) is stagnating. Hence, the molecular weight will decrease.

In **Chapter 3**, it was shown that for $F_{BD\text{-}T,\ total} < 75$ mol% the number-average molecular weight ($\overline{M}_n$) indeed decreases.[14] The polymer chains present in the mobile amorphous fraction become endcapped with Dianol and recombination of polymer chains with elimination of Dianol is no longer possible. Furthermore, it can be seen that for values of $F_{BD\text{-}T,\ total} < 75$ mol%, a large fraction of BD-T is still present in the crystalline phase, whereas rigid amorphous BD-T is almost absent. This result is an indication that Dianol dissolves the rigid amorphous fraction during the SSP reaction so that the BD-T repeat units in this rigid amorphous fraction become sufficiently mobile to participate in the transesterification reactions. Further research by DSC and Small-Angle X-ray scattering (SAXS) experiments have to be done to verify this hypothesis.

In Figure 4.6, the calculated values for $R_{ssp,\ \alpha\ mobile}$ are shown as a function of $F_{BD\text{-}T,\ total}$. These degrees of randomness have now been corrected for the crystalline and the rigid amorphous fraction, both not participating in the transesterification reactions. It can be seen that all values for $R_{ssp,\ \alpha\ mobile}$ are very close to one, pointing to a fully random copolyester structure in the mobile amorphous fraction, which is comparable to the results obtained for the $(BD_xDi_y)_{mp}$ copolyesters.

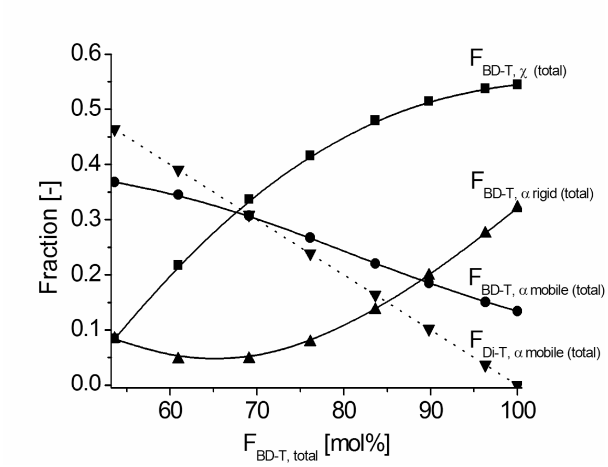

Figure 4.6. Distribution of BD-T and Di-T repeat units in $(BD_xDi_y)_{ssp}$ copolymer based on the three-phase model: mole fraction of BD-T repeat-units in the crystalline fraction ($F_{BD\text{-}T,\ \chi\ (total)}$, ■), mobile amorphous fraction ($F_{BD\text{-}T,\ \alpha\ mobile\ (total)}$, ●) and rigid amorphous fraction ($F_{BD\text{-}T,\ \alpha\ rigid\ (total)}$, ▲) as a function of $F_{BD\text{-}T,\ total}$ and mole fraction of Di-T repeat-units in the mobile amorphous fraction ($F_{Di\text{-}T,\ \alpha\ mobile\ (total)}$, ▼) as a function of $F_{BD\text{-}T,\ total}$. $F_{Di\text{-}T,\ \alpha\ rigid\ (total)}$ and $F_{Di\text{-}T,\ \chi\ (total)}$ are assumed to be 0.

The observation that these values for $R_{ssp,\ \alpha\ mobile}$ are slightly higher than unity is probably not the result of errors in our measurements. It might be possible that at the interface between mobile and rigid amorphous fraction, which is not strictly defined, some Di-T repeat units are present. With the calculation method previously described, the Di-T repeat units were all assumed to be part of the mobile amorphous fraction. This consequent error might result in values for $R_{ssp,\ \alpha\ mobile}$ slightly larger than unity.

4.4 Conclusions

The calculation method as presented in this chapter shows that it is possible to determine the chemical microstructure of the amorphous phase using the peak integral values from the ^{13}C-NMR dyad sequences originating from the quaternary carbon atom. When the morphology of the $(BD_xDi_y)_{ssp}$ copolymers is represented by the traditional two-phase (crystalline/ amorphous) model, the values of $R_{ssp,\ \alpha}$ are still below unity for a large composition range. Only when the $(BD_xDi_y)_{ssp}$ copolymers are fully amorphous ($\chi_{heating} = 0$), $R_{ssp,\ \alpha} = R_{ssp,\ total} = 1$. Hence, the presence of a crystalline fraction ($\chi_{heating} > 0$) results in a decrease of $R_{ssp,\ \alpha}$. Heat capacity measurements showed that, in the presence of a crystalline fraction, the amorphous phase consists of a mobile amorphous fraction and a rigid amorphous fraction. The calculation method, based on the two-phase model, was extended by taking the mobile and

rigid amorphous fraction into account. The degree of randomness of the mobile amorphous fraction ($R_{ssp,\ \alpha\ mobile}$) was calculated with the assumption that the PBT chains in the rigid amorphous fraction are not mobile enough to participate in the transesterification reactions and thus all Dianol is only incorporated into the mobile amorphous fraction. This assumption results in values for $R_{ssp,\ \alpha\ mobile}$ between 1.05 and 1.09. These values show that the chemical microstructure of the mobile amorphous phase is fully random. Hence, Dianol is incorporated in a similar way as with melt polymerization although with SSP only the most mobile chain segments are participating in the transesterification reaction.

The slightly larger values found for $R_{ssp,\ \alpha\ mobile}$ are possibly the result of a consequent error during the calculation. Most likely, the interface between mobile and rigid amorphous fraction is not so well defined. In the calculation method as described in this article, all Di-T repeat units were assumed to be present in the mobile amorphous fraction. This assumption results therefore values for $R_{ssp,\ \alpha\ mobile}$ slightly larger than unity.

4.5 References and notes

1. Radusch, H.-J. In *Handbook of Thermoplastic Polyesters*; Fakirov S., Ed.; Wiley-VCH: Weinheim, 2002; Chapter 8, p 389-419.
2. Radusch, H.-J.; Androsch, R. In *Handbook of Thermoplastic Polyesters*; Fakirov S., Ed.; Wiley-VCH: Weinheim, 2002; Chapter 20, p 895-925.
3. Devaux, J.; Godard, P.; Mercier, J. P. *J. Polym. Sci., Polym. Phys. Ed.* **1982**, *20*, 1881-1894.
4. Fakirov, S.; Sarkissova, M.; Denchev, Z. *Macromol. Chem. Phys.* **1996**, *197*, 2837-2867.
5. Denchev, Z.; Sarkissova, M.; Fakirov, S.; Yilmaz, F. *Macromol. Chem. Phys.* **1996**, *197*, 2869-2887.
6. Fakirov, S.; Sarkissova, M.; Denchev, Z. *Macromol. Chem. Phys.* **1996**, *197*, 2889-2907.
7. Montaudo, G.; Montaudo, M. S.; Scamporrino, E.; Vitalini, D. *Macromolecules* **1992**, *25*, 5099-5107.
8. Fernandez-Berridi, M. J.; Iruin, J. J.; Maiza, I. *Polymer* **1995**, *36*, 1357-1361.
9. Fakirov, S. In *Solid State Behavior of Linear Polyesters and Polyamides*; Schultz, J. M., Fakirov, S., Eds.; Prentice-Hall: Englewood Cliffs, NJ, 1990; Chapter 2, pp 19-43.
10. Hait, S. B.; Sivaram, S. *Macromol. Chem. Phys.* **1998**, *199*, 2689-2697.
11. James, N. R.; Ramesh, C.; Sivaram, S. *Macromol. Chem. Phys.* **2001**, *202*, 1200-1206.
12. James, N. R.; Ramesh, C.; Sivaram, S. *Macromol. Chem. Phys.* **2001**, *202*, 2267-2274.
13. Jansen, M. A. G.; Goossens, J. G. P.; de Wit, G.; Bailly, C.; Koning, C. E. *Macromolecules* **2005**, *38*, 2659-2664**.**
14. Jansen, M. A. G.; Goossens, J. G. P.; de Wit, G.; Bailly, C.; Koning, C. E. *Anal. Chim. Acta* **2005**, in press.
15. Yamadera, R.; Murano, M. *J. Polym. Sci., Part A-1* **1967**, *5*, 2259-2268.
16. Kricheldorf, H. R. *Makromol. Chem.* **1978**, *179*, 2133-2143.
17. Newmark, R. A. *J. Polym. Sci., Polym. Chem. Ed.* **1980**, *18*, 559-563.

18. Devaux, J.; Godard, P.; Mercier, J. P. *J. Polym. Sci., Polym. Phys. Ed.* **1982**, *20*, 1881-1894.
19. Martínez de Ilarduya, A.; Kint, D. P. R.; Muñoz-Guerra, S. *Macromolecules* **2000**, *33*, 4596-4598.
20. Kint, D. P. R.; Martínez de Ilarduya, A.; Muñoz-Guerra, S. *Macromolecules* **2002**, *35*, 314-317.
21. ATHAS database: Wunderlich, B. *Pure and Applied Chemistry* **1995**, *67*, 1019-1026.
22. Conix, A.; Van Kerpel, R. *J. Polym. Sci.* **1959**, *40*, 521-532.
23. Kirshenbaum, I. J. *J. Polym. Sci., Part A* **1965**, *3*, 1869-1875.
24. Cheng, S. Z. D.; Pan, R.; Wunderlich, B. *Makromol. Chem.* **1988**, *189*, 2443-2458.
25. Devaux, J.; Godard, P.; Mercier, J. P. *J. Polym. Sci., Polym. Phys. Ed.* **1982**, *20*, 1875-1880.
26. Finelli, L.; Lotti, N.; Munari A.; Berti, C.; Colonna, M.; Lorenzetti, C. *Polymer* **2003**, *44*, 1409-1420.
27. Illers, K.-H. *Colloid Polym. Sci.* **1980**, *258*, 117-124.140
28. Cheng, S. Z. D.; Cao, M.-Y.; Wunderlich, B. *Macromolecules* **1986**, *19*, 1868-1876.
29. Cheng, S. Z. D.; Wunderlich, B. *Macromolecules* **1987**, *20*, 1630-1637.
30. Cheng, S. Z. D.; Wu, Z. Q.; Wunderlich, B. *Macromolecules* **1987**, *20*, 2802-2810.
31. Cheng, S. Z. D.; Wunderlich, B. *Macromolecules* **1988**, *21*, 789-797.
32. Wunderlich, B. In *Macromolecular Physics, Vol 1. Crystal Structure, Morphology, Defects;* Academic Press: New York, 1973; Chapter 4.2, p 435-452.

Chapter 5
Influence of Dianol on the chemical microstructure and thermal properties of PBT-Dianol copolymers obtained by solid-state copolymerization

5.1 Introduction

Traditionally, solid-state polymerization (SSP) is used to increase the molecular weight of polycondensates after their preparation by melt polymerization.[1] The temperature used for SSP is just below the melting temperature of the semi-crystalline polycondensate. The polymer chain segments present in the amorphous phase will become very mobile and can therefore participate in transesterification reactions. (Outer-outer) alcoholysis reactions[2] between polymer chain-ends result in recombination of polymer chains whereas low molecular weight condensation products are removed by application of a nitrogen flow or a vacuum.

In the previous chapters, it was shown that solid-state copolymerization (SSP) can also be used to incorporate diol monomers in semi-crystalline poly(butylene terephthalate) (PBT).[3,4] The main advantage of copolymerization in the solid state, compared to copolymerization in the melt, is that the incorporation only occurs in the mobile polymer chain segments, i.e. the amorphous phase, whereas the polymer chain segments in the lamellar crystals are not mobile enough for participation in the transesterification reactions, and thus remain unchanged. In this way, polymer properties may be enhanced by selective modification of the amorphous phase while the crystallization behavior is more or less preserved due to the presence of large crystallizable homopolymer blocks.

In **Chapters 2** and **3**, the incorporation of 2,2-Bis[4-(2-hydroxyethoxy)phenyl]propane (Dianol 220®) into PBT via SSP was described in detail.[3,4] For comparison, Dianol was also incorporated into PBT via copolymerization in the melt (MP). Feed mixtures of varying PBT/Dianol ratios were used to obtain copolymers by SSP and MP having different compositions. Finelli and co-workers also prepared PBT-Dianol copolymers by MP.[5,6] These copolymers had an increased glass-transition temperature (T_g) compared to pure PBT. However, due to the random microstructure of these PBT-Dianol copolymers, only short residual homopolymer PBT blocks were obtained. Consequently, a decrease of the

crystallinity and crystallization rate of these copolymers was observed. In addition, it was found that Dianol-terephthalate repeat-units were not able to crystallize. Hence co-crystallization processes upon cooling from the melt did not occur.

In **Chapter 3**, quantitative ^{13}C-NMR sequence distribution analysis was used to study the difference in chemical microstructure between PBT-Dianol copolymers obtained via SSP and via MP.[4] for the copolymers obtained via MP, a random distribution of Dianol in PBT was found, while the chemical microstructure for the SSP copolymers can be represented by a non-random, blockwise distribution of Dianol in PBT. This non-random overall distribution was mainly due to the existence of unmodified PBT chain segments, during the SSP-process present in the crystalline phase, in which no incorporation of Dianol occurred. For increased ratios of Dianol/PBT in the feed mixtures, it was observed that the randomness of the chemical microstructure of the resulting SSP copolyesters increased until a fully random chemical microstructure was obtained. A fully random microstructure can only be obtained when all polymer chain segments can participate in the transesterification reaction, implying that no crystalline PBT fraction should be present at the initial stage of the SSP-reaction. Differential Scanning Calorimetry (DSC) measurements showed that the crystalline PBT fraction indeed decreased when the fraction of incorporated Dianol increased. It was shown in **Chapter 4** that the morphology of the PBT-Dianol copolymers obtained by SSP can be represented by a three-phase model consisting of a crystalline phase and an amorphous phase, which can be subdivided into a mobile amorphous fraction and a rigid amorphous fraction.[7] For many semi-crystalline homopolymers the three-phase model gives a more accurate description of the morphology than a two-phase model.[8-12] The developed calculation method, described in **Chapter 4**, showed that Dianol is only incorporated in the mobile amorphous fraction. This mobile amorphous fraction increased with increasing amounts of Dianol used for incorporation. Consequently, Dianol has a large influence on the initial morphology of the PBT-Dianol mixtures, used as feed for SSP, and therefore also on the final chemical microstructure after SSP.

In the present chapter, the role of Dianol on the morphology is studied in detail for the PBT-Dianol copolyesters obtained by SSP. The influence of the Dianol fraction on the morphology of the PBT-Dianol mixtures used as feed samples for SSP is studied by DSC. The development of the morphology is examined as a function of solid-state polymerization time by DSC and Small-Angle X-ray Scattering (SAXS). In this way, a relation can be made between morphological changes and the chemical microstructure as presented in **Chapters 2** and **3**. Furthermore, the influence of the chemical microstructure (random versus non-random) of the PBT-Dianol copolymers on the resulting thermal properties is examined.

5.2 Experimental Section

5.2.1 Materials

Poly(butylene terephthalate) (PBT) pellets ($\overline{M}_n$ = 15 kg/mol and $\overline{M}_w$ = 34 kg/mol; determined by size exclusion chromatography) were provided by GE Plastics (Bergen op Zoom, The Netherlands) and used as received. 2,2-Bis[4-(2-hydroxyethoxy)phenyl]propane (Dianol 220®) was provided by Air Liquide (Paris, France) and was recrystallized twice from acetone prior to use.

5.2.2 Solid-state polymerization (SSP) and melt copolymerization (MP)

Copolyesters of PBT and Dianol were synthesized via SSP and MP. A detailed description of the preparation method can be found in **Chapter 2**.[3] Powder mixtures of different PBT/Dianol ratios were used as feed for the SSP and MP reactions in order to obtain copolymers of different compositions. For the preparation of the SSP copolymers, the PBT and Dianol were mixed by dissolution in 1,1,1,3,3,3-hexafluoro-2-propanol (HFIP). After complete dissolution, the HFIP was evaporated and the obtained, partial crystalline lump of material was ground into powder. The PBT/Dianol mixtures used feed for MP or SSP are abbreviated as $(BD_xDi_y)_{feed}$. BD_x denotes the mole percentage (mol%) of PBT (expressed as 1,4-butanediol units), whereas Di_y denotes the mol% of Dianol (expressed as Di units) in the $(BD_xDi_y)_{feed}$ mixtures. Solid-state polymerized (BD_xDi_y) copolymers are indicated as $(BD_xDi_y)_{ssp}$ copolymers, in which x and y represent the initial mol% PBT and Dianol present in the $(BD_xDi_y)_{feed}$ mixture being used for SSP. The actual mole fractions of BD and Di units after SSP differ only slightly from the initial fractions present in the $(BD_xDi_y)_{feed}$ mixtures. These differences were attributed to the evaporation of 1,4-butanediol during the SSP reaction (see **Chapter 3**).[4] For all $(BD_xDi_y)_{ssp}$ copolymers, a solid-state polymerization temperature (T_{ssp}) of 180 °C was used in combination with a solid-state polymerization time (t_{ssp}) of 9 h. This time proved to be long enough for complete incorporation of Dianol into PBT and to result in $(BD_xDi_y)_{ssp}$ copolymers with a sufficiently high molecular weight (see **Chapter 2**).[3] Melt polymerized (BD_xDi_y) copolymers are denoted as $(BD_xDi_y)_{mp}$, in which x and y respectively represent the initial mol% PBT and Dianol present in the $(BD_xDi_y)_{feed}$ powder mixtures being used for MP. Also here, the mole fractions of BD and Di units after MP slightly differ from the reactions initially present in the $(BD_xDi_y)_{feed}$ mixtures.

5.2.3 Differential Scanning Calorimetry (DSC)

The melting and crystallization enthalpies ($\Delta H_{melting}$ and $\Delta H_{crystallization}$ respectively) were measured by a TA Instruments Q1000 DSC equipped with an autosampler and refrigerated cooling system (RCS). The DSC cell was purged with a nitrogen flow of 50 mL/min. The temperature was calibrated using the onset of melting for indium. The enthalpy was calibrated with the heat of fusion of indium. For the $(BD_xDi_y)_{ssp}$ and $(BD_xDi_y)_{mp}$ copolymers, samples of 6-8 mg were prepared in crimped aluminum pans. All samples were measured in the temperature range from 0 to 250 °C using heating and cooling rates of 10 °C/min and isothermal periods of 3 min at 0 and 250 °C, respectively. The crystallinity ($\chi_{heating}$) was defined as the ratio of $\Delta H_{melting}$ and the heat of fusion for 100% PBT (ΔH^0_{fuse} = 145 J/g).[13-15]

The glass transition temperature (T_g) of the $(BD_xDi_y)_{ssp}$ copolymers was measured in temperature modulated DSC (TMDSC®) mode using the same TA Q1000 DSC as previously described. The DSC cell was purged with a nitrogen flow of 50 mL/min. For the $(BD_xDi_y)_{ssp}$ copolymers, samples of 6-8 mg were prepared in crimped aluminum pans. An oscillating heat flow signal with a period of 60 seconds and amplitude of 0.5 °C was used. Samples were measured in the temperature range from 0 °C to 180 °C using an underlying heating rate of 2 °C/min.

For the $(BD_xDi_y)_{feed}$ mixtures, samples of 5-7 mg were prepared in hermetically closed aluminum pans due to possible formation of 1,4-butanediol by transesterification reactions occurring upon heating. The samples were first heated from 0 to 120 °C, which is approximately 10 °C above the T_m of Dianol, and kept for 10 minutes at this temperature. The samples were then cooled to -80 °C and subsequently reheated to 240 °C using cooling and heating rates of 10 °C/min, respectively. $\Delta H_{melting}$ was taken from the second heating run.

The T_g of the $(BD_xDi_y)_{feed}$ mixtures and the corresponding heat capacity increase at half-step T_g (Δc_p) were determined in modulated DSC mode. The $(BD_xDi_y)_{feed}$ mixtures were first heated in normal DSC mode from 0 to 120 °C and subsequently kept at this temperature for 10 minutes. The samples were then cooled to -80 °C using a rate of 10 °C/min and reheated from -80 to 120 °C in modulated DSC mode, using an underlying rate of 2 °C/min and a temperature with a period of 60 s and amplitude of 0.5 °C. The T_g values were taken from the reversing heat capacity signal. The step increase of the heat capacity at T_g (Δc_p) was determined using tangents to the measured curve below and above the T_g. The value obtained for Δc_p was used to determine the mobile amorphous fraction (α_{mobile}) of the $(BD_xDi_y)_{feed}$ mixtures. α_{mobile} is defined as the ratio between the measured Δc_p and that of fully amorphous PBT ($\Delta c_p{}^0{}_\alpha$ = 0.35 J/g K).[12,15]

5.2.4 Small-Angle X-ray Scattering (SAXS)

SAXS experiments were performed on the DUBBLE beamline (BM 26B) at the European Radiation Synchrotron Facility (ESRF) in Grenoble (France). A wavelength of 1.218 Å was used. The SAXS data were collected on a gas-filled multiwire two-dimensional (2D) detector positioned at 4.5 m from the sample. Approximately 18-20 mg (BD_xDi_y) copolymer material was placed in a crimped aluminum DSC pan. A Linkam THMS600 hotstage with controller was used for heating/cooling of the samples. For calibration of the SAXS detector, the scattering pattern from an oriented specimen of wet collagen (rat-tail tendon) was used. The experimental data were corrected for background scattering, i.e. subtraction of the scattering from an empty DSC pan. The two-dimensional SAXS data were transformed into one-dimensional plots by performing integration along the azimuthal angle using the FIT2D program of Dr. Hammersley of ESRF. The exposure time of each single shot experiment was 30 s and for the time-resolved measurements this was 5 s per frame.

For analysis of the SAXS patterns, the one-dimensional correlation function ($\gamma_1(x)$) was applied. The morphology of the $(BD_xDi_y)_{ssp}$ copolymers can be represented by a finite lamellar stacking model. This model consists of a finite number of crystalline lamellae separated by interlamellar amorphous layers. The correlation function ($\gamma_1(x)$) is defined as:[16]

$$\gamma_1(x) = \frac{1}{Q}\int_0^\infty I(q)q^2\cos(qx)dq \tag{5.1}$$

where I(q) is the scattering intensity, q (= $4\pi/\lambda\sin(\theta/2)$ with θ being the scattering angle) is the scattering vector. The scattering invariant Q is expressed as:

$$Q = \int_0^\infty Iq^2dq \tag{5.2}$$

$\gamma_1(x)$ is normalized by $Q(\gamma_1(0) = 1)$. The SAXS pattern could only be collected in a limited angular range ($0.1\ nm^{-1} < q < 2.5\ nm^{-1}$) and consequently, the scattering vector q has to be extrapolated to $q = 0$ and $q = \infty$ prior to application of the Fourier transform. The extrapolation to the high q-values was done by using the Porod-Ruland model.[17] I(q) can then be described by:

$$I(q) = I_b(q) + K_p\frac{\left(\exp(-\sigma^2q^2)\right)}{q^4} \tag{5.3}$$

where $I_b(q)$ is the background intensity arising from thermal density fluctuation. σ is related to the width of the crystalline-amorphous interphase and K_p is the Porod constant. The exponential term corrects for the contribution of the crystal-amorphous interphase. The extrapolation to zero q-values was obtained by fitting the intensity curve at low q-range with

the Debye-Bueche model:[18,19]

$$I(q) = \frac{I(0)}{(1+q^2\xi^2)^2} \tag{5.4}$$

where ξ is the correlation length. The long period (L_p) can be estimated from the first maximum of the correlation function. The analysis of the correlation function further yields the average lamellar crystal thickness l_χ and the average amorphous thickness l_α. Determination of the rigid amorphous layer thickness and mobile amorphous layer thickness, as was done by Hong and co-workers,[20] did not give accurate results and was therefore not performed. However, it can be assumed that the average electron density of the rigid amorphous layer is slightly higher than that of the mobile amorphous layer. Hence, the rigid amorphous layer thickness will mainly contribute to l_χ whereas the mobile amorphous layer will predominantly contribute to l_α.

5.3 Results and discussion

In **Chapter 3**, the incorporation of Dianol into PBT via SSP and MP was described in detail. Different Dianol/PBT mole ratios were used to obtain copolyesters of different compositions. The chemical structure of a (BD_xDi_y) copolymer is schematically represented in Figure 5.1.

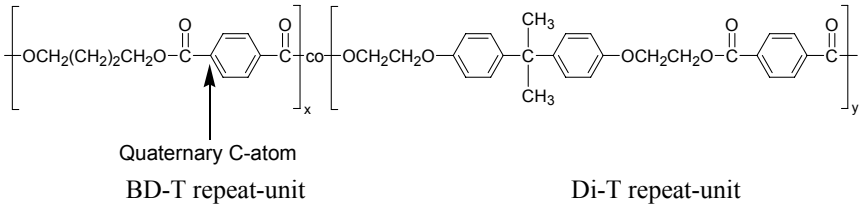

Figure 5.1. Chemical structure of a (BD_xDi_y) copolymer, consisting of BD-T and Di-T repeat-units. The arrow denotes the quaternary carbon atom which signal is used in ^{13}C-NMR sequence distribution analysis.

5.3.1 Miscibility study of Dianol in PBT

In **Chapters 3** and **4**, the chemical microstructure of the synthesized $(BD_xDi_y)_{ssp}$ and $(BD_xDi_y)_{mp}$ copolymers was studied by ^{13}C-NMR sequence distribution analysis. The ^{13}C-NMR peak corresponding to the quaternary carbon atom (marked by the arrow in Figure 5.1) is positioned at a chemical shift of 136.0 ppm and splits up into 4 peaks with different chemical shifts and integral values. Each peak represents a dyad sequence (BTD, BD-side; BTB, DTD and BTD, Di-side with BTD, BD-side and BTD, Di-side being equal). After normalization, the integral values of the four peaks were used to determine the degree of

randomness (R) of the synthesized $(BD_xDi_y)_{ssp}$ and $(BD_xDi_y)_{mp}$ copolymers. This parameter gives information about the chemical microstructure of the corresponding (BD_xDi_y) copolymer.

For a fully random copolyester, the distribution of the two different BD-T and Di-T repeat-units should obey Bernoullian statistics.[21,22] The degree of randomness (R_{total}) should then be equal to 1. If R_{total} is smaller than 1, the repeat-units have arranged themselves in blocks. The values for the degree of randomness of the $(BD_xDi_y)_{mp}$ and $(BD_xDi_y)_{ssp}$ copolymers were already presented in **Chapter 3**. The values for the degree of randomness obtained for the $(BD_xDi_y)_{mp}$ copolymers ($R_{mp,\ total}$) were all close to one whereas for the synthesized $(BD_xDi_y)_{ssp}$ copolymers, the obtained values for the degree of randomness $R_{ssp,\ total}$ were dependent on the fraction of incorporated Dianol. When the fraction of incorporated Dianol was close to 15 mol%, (i.e. $F_{BD\text{-}T,\ total}$ = 85 mol%), $R_{ssp,\ total}$ reached a minimum value of 0.83 and subsequently increased for decreasing values of $F_{BD\text{-}total}$ to approach a final value of 1 for $F_{BD\text{-}T,\ total} \approx 45$ mol%. Hence the fraction of mobile PBT homopolymer chain segments participating in the transesterification reactions during SSP increases for increasing fractions of Dianol. It was already explained in the introduction of this chapter that the fraction of Dianol used in the initial stage of the SSP-reaction has a large influence on the mobile amorphous fraction present after SSP. To study this influence in more detail, $(BD_xDi_y)_{feed}$ mixtures with different PBT/Dianol ratios were examined by DSC. These non-transesterified $(BD_xDi_y)_{feed}$ samples were kept for 10 min at 120 °C, which is approximately 10 °C above the T_m of the Dianol monomer (i.e. T_m = 110 °C) , to allow the molten Dianol to diffuse into the rubbery amorphous phase. Transesterification reactions can be considered as negligible at this low temperature. The samples were then cooled to -80 °C and subsequently reheated to 240 °C (above the T_m of PBT) using respectively cooling and heating rates of 10 °C/min. The resulting DSC heating traces of these second heating runs are shown in Figure 5.2a. The corresponding T_g values were measured separately by modulated DSC and are shown in Figure 5.2b as a function of F_{PBT}, which is the mole fraction of PBT in the $(BD_xDi_y)_{feed}$ mixtures (i.e. $F_{PBT} = x$). The $(BD_{100}Di_0)_{feed}$ sample is the abbreviation of a PBT homopolymer which has undergone the same HFIP dissolution treatment used for preparation of the $(BD_xDi_y)_{feed}$ mixtures. For $(BD_{100}Di_0)_{feed}$, $\chi_{heating}$ = 0.38 (see **Chapter 3**).

From Figure 5.2a, it can be seen that the melting endotherm of the Dianol monomer, which should be present at T_m = 110 °C, is completely absent for all examined $(BD_xDi_y)_{feed}$ mixtures. In addition, the T_m of PBT decreases when the ratio PBT/Dianol decreases. This melting temperature depression can be attributed to both thermodynamic and kinetic effects. Furthermore, the decreasing values of the T_g for increasing fractions of Dianol, plotted in Figure 5.2b, show that the amorphous PBT chain segments increase in mobility. The T_g

values rapidly decrease to a minimum value of approximately -8 °C for increased fractions of Dianol. This decrease shows that the mobility of the amorphous PBT chain segments increases due to swelling by molten Dianol monomer. Apparently, Dianol acts as a plasticizer by swelling amorphous PBT chain segments. The limited T_g value indicates that the concentration of Dianol in the amorphous phase becomes constant. Such a constant Dianol concentration can only be obtained when the fraction of swollen amorphous PBT chain segments concomitantly increases with the increasing amounts of Dianol used for mixing.

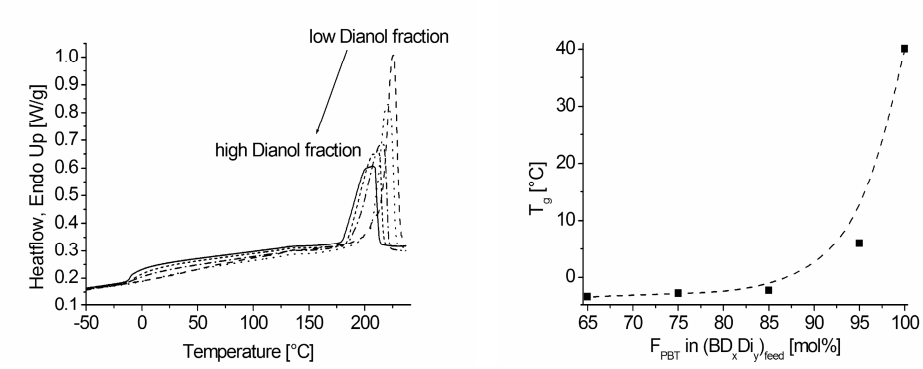

(a) (b)

Figure 5.2. (a) DSC heating traces of non-transesterified $(BD_xDi_y)_{feed}$ mixtures as a function of temperature: $(BD_{100}Di_0)_{feed}$ i.e. PBT homopolymer after HFIP treatment (– – –), $(BD_{95}Di_5)_{feed}$ (·····), $(BD_{85}Di_{15})_{feed}$) (·–·–·), $(BD_{75}Di_{25})_{feed}$ (-----), $(BD_{65}Di_{35})_{feed}$ (——) and (b) T_g of the $(BD_xDi_y)_{feed}$ mixtures as a function of the mole fraction PBT present in the mixtures (F_{PBT}).

Looking again at Figure 5.2a, it can be seen that the Δc_p at the half-step T_g increases when the mole ratio PBT/Dianol of the $(BD_xDi_y)_{feed}$ mixtures decreases. The melting enthalpy ($\Delta H_{melting}$) and the heat capacity increase Δc_p at half-step T_g, as observed from the DSC traces shown in Figure 5.2b, can be used to determine the fractions $\chi_{heating}$, α_{rigid} and α_{mobile} of each $(BD_xDi_y)_{feed}$ mixture. The following equations were used:

$$\alpha_{mobile} = \Delta c_p / \Delta c_p{}^0{}_{\alpha} \tag{5.5a}$$

$$\chi_{heating} = \Delta H_{melting} / \Delta H^0{}_{fuse} \tag{5.5b}$$

$$\alpha_{rigid} = 1 - \chi_{heating} - \alpha_{mobile} \tag{5.5c}$$

where Δc_p in eq 5.5a is the heat capacity increase at the half-step T_g of the non-transesterified

$(BD_xDi_y)_{feed}$ mixture, whereas $\Delta c_p^0{}_{\alpha}$ is the heat capacity increase for 100% amorphous PBT at the half-step T_g ($\Delta c_p^0{}_{\alpha}$ is 77 J/mol K (0.35 J/g K) at T_g = 320 K).[12,15] ΔH^0_{fuse} is the crystallinity of 100% crystalline PBT (ΔH^0_{fuse} = 145 J/g).[13-15] The value of $\Delta c_p^0{}_{\alpha}$ for 100% amorphous PBT was assumed to be independent of the added Dianol monomer. In practice, $\Delta c_p^0{}_{\alpha}$ is slightly influenced by the presence of Dianol. However, it was shown by Lotti and co-workers that an amorphous $(BD_0Di_{100})_{mp}$ homopolymer consisting of only Di-T repeat-units has a Δc_p value of 0.35 J/g K which is equal to that of a 100% amorphous PBT homopolymer.[5] Hence, the $\Delta c_p^0{}_{\alpha}$ value for 100% PBT in the vicinity of molten Dianol monomer may only slightly differ.

The obtained values for the fractions $\chi_{heating}$, α_{rigid} and α_{mobile} are plotted in Figure 5.3 as a function of F_{PBT} in the $(BD_xDi_y)_{feed}$ mixtures.

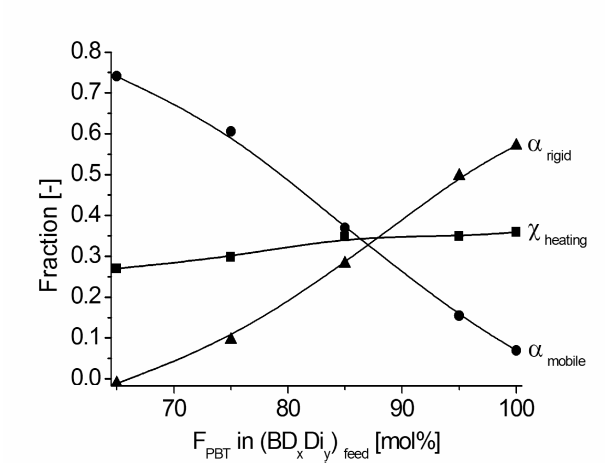

Figure 5.3. Crystalline ($\chi_{heating}$ ■), rigid amorphous fraction (α_{rigid} ▲) and mobile amorphous fraction (α_{mobile} ●) as a function of F_{PBT} in the $(BD_xDi_y)_{feed}$ mixtures.

For the $(BD_{100}Di_0)_{feed}$ sample (PBT after HFIP treatment), no Δc_p at half-step T_g could be observed from the DSC trace shown in Figure 5.2. Apparently, no mobile amorphous fraction is present in the PBT after HFIP treatment. Hence by definition of eq 5.5a, α_{mobile} = 0. $\Delta H_{melting}$ of the $(BD_0Di_{100})_{feed}$ sample was equal to 55 J/g and corresponds to $\chi_{heating}$ = 0.38. Using this value together with α_{mobile} = 0 in eq 5.5c results in α_{rigid} = 0.62. For comparison, bulk PBT (PBT without HFIP treatment) has α_{mobile} = 0.51, $\chi_{heating}$ = 0.32, α_{rigid} = 0.17. Hence, the HFIP treatment results in a large increase of the rigid amorphous PBT fraction. It can be observed from Figure 5.3 that an increasing fraction of Dianol in the $(BD_xDi_y)_{feed}$ mixtures results in a continuous decrease of α_{rigid}, whereas α_{rigid} concomitantly increases. The decrease of $\chi_{heating}$ is only small. In addition, α_{rigid} approaches 0 at F_{PBT} = 65 mol%, whereas a

crystalline fraction $\chi_{heating}$ is still present. Apparently, molten Dianol swells the rigid amorphous chain segments which subsequently increase in mobility. This mobility increase was already observed from the decreasing T_g values shown in Figure 5.2b. These swollen amorphous chain segments have a sufficiently high mobility and subsequently contribute to the mobile amorphous fraction (increase of Δc_p at the half-step T_g as shown in Figure 5.2a). When large amounts of Dianol are used, all rigid amorphous chain segments are swollen and Dianol subsequently dissolves the PBT crystals. The dissolution process proceeds at a much lower rate and initially only dissolves the crystals with the smallest lamellar thickness and concomitant lowest melting temperatures.

5.3.2 Development of the morphology during solid-state polymerization.

To get more insight in how the morphology develops during the SSP reaction, $(BD_{85}Di_{15})_{feed}$ mixtures were polymerized in the solid state using polymerization times (t_{ssp}) varying from 0 to 24 h. The resulting $(BD_{85}Di_{15})_{ssp}$ samples with different values for t_{ssp} were also used to determine the kinetics of the Dianol incorporation into PBT via SSP (see **Chapter 2**). For these $(BD_{85}Di_{15})_{ssp}$ samples, the Δc_p values to calculate α_{mobile} by eq 5.5a were obtained from the first heating run in contrast to the values for α_{mobile} of the $(BD_xDi_y)_{feed}$ mixtures shown in Figure 5.2, which were obtained from the second heating run (after an isothermal period of 10 minutes at 120 °C). $\chi_{heating}$ was determined from $\Delta H_{melting}$ using eq 5.5b whereas α_{rigid} was determined by eq 5.5c. The results are shown in Figure 5.4.

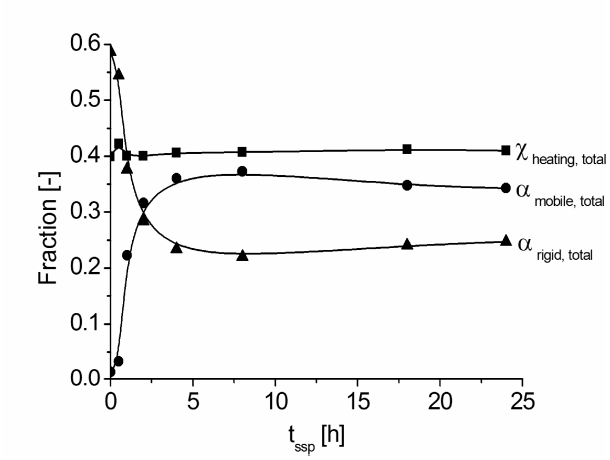

Figure 5.4. Morphology development during SSP of the $(BD_{85}Di_{15})_{feed}$ mixture: fractions of $\chi_{heating}$ (■), α_{rigid} (▲) and α_{mobile} (●) as a function of t_{ssp}.

It can be seen that the $(BD_{85}Di_{15})_{feed}$ mixture present at $t_{ssp} = 0$ h almost exclusively consists of $\chi_{heating}$ and α_{rigid}. A similar result was observed in Figure 5.3 for a $(BD_{100}Di_0)_{feed}$ mixture (i.e. a PBT homopolymer after dissolution in HFIP). Apparently, the solution mixing of PBT and Dianol in HFIP, necessary for the preparation of $(BD_xDi_y)_{feed}$ mixtures, results in a solvent-induced crystallization effect during evaporation of the HFIP. As soon as the SSP reaction starts, α_{rigid} is converted into α_{mobile}, whereas $\chi_{heating}$ almost remains constant. It was already shown in **Chapter 2** that the cleavage of PBT chain segments by free Dianol predominantly takes place during the first 2 hours of the SSP-reaction ($0 < t_{ssp} \leq 2$ h).[3] It can be observed from Figure 5.4 that the major conversion of α_{rigid} into α_{mobile} occurs in the same period. Consequently, the fraction of free Dianol in the $(BD_{85}Di_{15})_{feed}$ mixture swells the rigid amorphous PBT chain segments as soon as Dianol is in its molten state ($T_m > 110$ °C) These swollen PBT chain segments will therefore become sufficiently mobile for (outer-inner) alcoholysis reactions with Dianol to take place. These alcoholysis reactions will result in cleavage of the PBT chain segments and thus contribute to a further increase of the chain mobility. The conversion of α_{rigid} into α_{mobile} stops as soon as all Dianol has been fully incorporated into the polymer chains. The fraction $\chi_{heating}$ will not significantly decrease during the SSP-reaction as long as there is a rigid amorphous PBT fraction available which can, after swelling by Dianol monomer, participate in the transesterification reactions. When α_{rigid} of the $(BD_xDi_y)_{feed}$ mixtures is close to 0, the remaining crystalline PBT fraction will be dissolved by Dianol and corresponding PBT chain segments subsequently become available for transesterification. This dissolution process is very slow as was already mentioned.

For low fractions of Dianol monomer, $\chi_{heating}$ may even increase due to annealing of PBT crystals during the SSP process. The increased mobility, due to the swelling of rigid amorphous chain segments by Dianol, may enhance the crystal perfection.

5.3.3 Morphological parameters of the PBT-Dianol copolymers

The previous results clearly show that Dianol is not only a reactant during the SSP process, but also acts as a swelling agent for the rigid amorphous fraction. This dual role of both reactant and swelling agent has a large influence on both chemical microstructure and morphology of the $(BD_xDi_y)_{ssp}$ copolymers. The morphology of the $(BD_xDi_y)_{ssp}$ copolymers was also studied by SAXS. For each $(BD_xDi_y)_{ssp}$ copolymer, the long period L_p was determined and the average crystal thickness l_χ and amorphous layer thickness l_α were calculated, using a finite lamellar stack model in which a finite number of lamellae is arranged in stacks separated by interlamellar amorphous layers. It was already explained in the Experimental Section that a distinction between rigid amorphous fraction and mobile amorphous fraction could not obtained from SAXS measurements following this approach. It

is assumed that the electron density of the rigid amorphous fraction is slightly higher than the mobile amorphous fraction and, as a result, the contribution of the rigid amorphous fraction to l_χ is larger than its contribution to l_α. The morphological parameters, L_p, l_χ, and l_α, are plotted as a function of $F_{BD\text{-}T,\ total}$ in Figure 5.5.

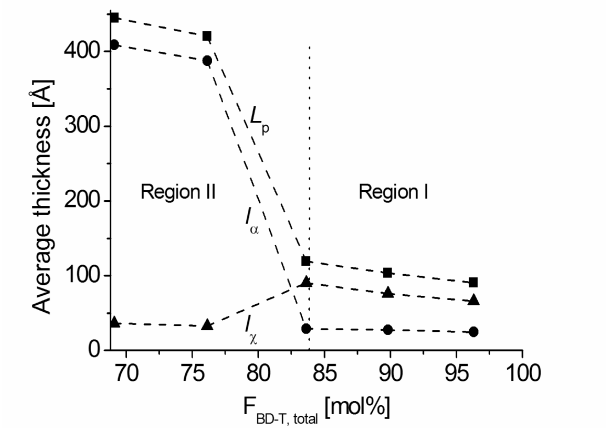

Figure 5.5. Morphological parameters obtained from SAXS: long period L_p, average crystal thickness l_χ and average amorphous layer thickness l_α as a function of $F_{BD\text{-}T,\ total}$ in the $(BD_xDi_y)_{ssp}$ copolymer.

Two different regions can be observed in Figure 5.5. In the first region, for $100 \leq F_{BD\text{-}T,\ total} \leq 83$ mol%, the morphological parameters L_p and l_χ slightly increase with increasing Dianol contents whereas l_α remains constant. For the second region, where $F_{BD\text{-}T,\ total} < 83$ mol%, L_p and l_α both rapidly increase, whereas l_χ decreases. The fast transition between regions I and II is remarkable. It is known that the molecular weight $\overline{M}_n$ can have a significant influence on the long period and average crystal thickness. It was shown in **Chapter 3** that for $F_{BD\text{-}T,\ total} \geq 76$ mol%, the $(BD_xDi_y)_{ssp}$ copolymers have $\overline{M}_n$ values ≥ 34 kg/mol. Hence, the sudden increase of L_p and l_α for $F_{BD\text{-}T,\ total} < 83$ mol% cannot be assigned to a change in $\overline{M}_n$. It was already mentioned that a small fraction of Dianol promotes the crystal perfectioning during the SSP-reaction. Apparently, two processes occur simultaneously during the initial stage of the SSP-reaction: in the first process, a specific fraction of the rigid amorphous chain segments swells by the molten Dianol monomer. These swollen amorphous chain segments have an overall increased mobility and will thus contribute to the mobile amorphous fraction of the $(BD_xDi_y)_{feed}$ mixtures (as shown in Figure 5.3). Due to the increased mobility, these chain segments may react with Dianol via (outer-inner) alcoholysis reactions.[2] In the second process, rigid amorphous chain segments are transferred into the lamellar crystal as a result of crystal perfectioning. For the first region ($100 \leq F_{BD\text{-}T,\ total} \leq 83$ mol%), the fraction of Dianol is so low that only a small fraction of rigid PBT chain segments is swollen. Hence, crystal

perfectioning occurs at higher extent compared to transesterification, which only takes place in the mobile (i.e. swollen) amorphous chain segments. As a consequence, L_p and l_χ slightly increase in the first region as a function of $F_{BD\text{-}T,\ total}$. For the second region, when $F_{BD\text{-}T,\ total}$ is less than 83 mol%, the fraction of swollen rigid amorphous chain segments is significantly larger than the fraction of rigid amorphous chain segments. Hence transesterification occurs to a higher extent than transference of rigid amorphous PBT chain segments into the crystal phase. The result is that L_p and l_α both rapidly increase with decreasing fraction $F_{BD\text{-}T,\ total}$. l_χ decreases, which may be a result of the ability of Dianol to partially dissolve the PBT lamellae when present in large excess. These two regions can also be distinguished in the values for $R_{ssp,\ total}$ shown in **Chapters 3** and **4**.[3,4] For $F_{BD\text{-}T,\ total} \geq 83$ mol%, $R_{ssp,\ total}$ continuously decreases with increasing Dianol content to 0.83, whereas for $F_{BD\text{-}T,\ total} < 83$ mol% $R_{ssp,\ total}$ increases again to a value close to unity

5.3.4 Thermal properties of the PBT-Dianol copolymers

The difference in chemical microstructure between $(BD_xDi_y)_{ssp}$ and $(BD_xDi_y)_{mp}$ copolymers may be reflected in the thermal properties. The glass transition temperature (T_g), melting temperature (T_m) and crystallization behavior of these (BD_xDi_y) copolymers were therefore studied by DSC. The DSC traces of the first heating run of the synthesized $(BD_xDi_y)_{ssp}$ copolymers are plotted in Figure 5.6.

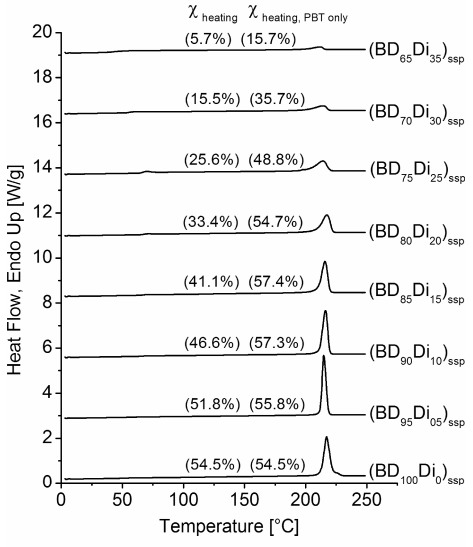

Figure 5.6. DSC first heating runs of the synthesized $(BD_xDi_y)_{ssp}$ copolymers. DSC curves are shifted vertically for clarity.

The thermal properties of the $(BD_xDi_y)_{ssp}$ copolymers, obtained from the DSC measurements, are summarized in Table 5.1

Table 5.1. Thermal properties of the synthesized $(BD_xDi_y)_{ssp}$ copolymers.

$(BD_xDi_y)_{feed}$ mixtures		$(BD_xDi_y)_{ssp}$ copolymers		Heating run 1[a,b,c]		Cooling run 1[b,c]	heating run 2[a]	(T_m-T_c)
x	y	$F_{BD\text{-}T,\ total}$	$F_{Di\text{-}T,\ total}$	T_g	T_m	T_c	T_g	
[mol%]	[mol%]	[mol%]	[mol%]	[°C]	[°C]	[°C]	[°C]	[°C]
100	0	100	0	54.9	217.1	185.2	40.8	35.7
95	5	96	4	60.5	214.8	175.1	45.2	30.9
90	10	90	10	66.8	216.2	147.3	49.6	50.2
85	15	84	16	67.1	215.8	113.0	48.9	71.2
80	20	76	24	68.0	217.5	-	53.6	-
75	25	69	31	65.9	214.4	-	56.5	-
70	30	61	39	60.9	214.4	-	55.7	-
65	35	54	46	54.1	212.4	-	45.7	-

[a] The T_g values were determined in modulated DSC mode

[b] T_m and T_c were determined in normal DSC mode using heating/cooling rates of 10 °C/min.

[c] The T_m and T_c values shown are the peak values of the melting endotherms and crystallization exotherms, respectively.

The $(BD_{100}Di_0)_{ssp}$ material is the abbreviation used for a PBT homopolymer after HFIP treatment and subsequent SSP. For all DSC traces, no recrystallization was observed upon heating above the T_g. The values for $\chi_{heating}$ and $\chi_{heating,\ PBT\ only}$ are also given in Figure 5.6. $\chi_{heating,\ PBT\ only}$ is the crystallinity which is corrected for the weight percentage of present BD-T units in the $(BD_xDi_y)_{ssp}$ copolymer, taking into consideration that the Di-T repeat units are not able to crystallize. The decrease of $\chi_{heating}$ and $\chi_{heating,\ PBT\ only}$ was already partly discussed in **Chapter 3**. It can be seen that the values for $\chi_{heating,\ PBT\ only}$ increase until a maximum value ($\chi_{heating,\ PBT\ only}$ = 0.57) is obtained for the $(BD_{90}Di_{10})_{ssp}$ and $(BD_{85}Di_{15})_{ssp}$ copolymers. This increase is due to the transformation of rigid amorphous chain segments into the lamellar crystal phase during the initial stages of the SSP-reaction, as was already explained when analyzing the SAXS measurements (see Figure 5.5). For $(BD_xDi_y)_{ssp}$ copolymers with x < 85 (i.e. $F_{BD\text{-}T,\ total}$ < 83 mol%), $\chi_{heating,\ PBT\ only}$ decreases because the transesterification rate of Dianol with swollen amorphous PBT segments is higher than the rate of lamellar crystal thickening. The DSC results shown in Figure 5.6 are therefore also in agreement with the observed values for $R_{ssp,\ total}$ showing a minimum for $F_{BD\text{-}T,\ total}$ = 83 mol% (see **Chapter 4**). It can be observed from Figure 5.6 and Table 5.1 that the T_m value of the $(BD_{100}Di_0)_{ssp}$

homopolymer is significantly lower than generally reported in literature (220 °C < T_m < 230 °C).[12] It was already mentioned in this chapter, that a PBT homopolymer after HFIP treatment, denoted as $(BD_{100}Di_0)_{feed}$, has a mobile amorphous fraction (α_{mobile}) which is close to zero whereas $\alpha_{rigid} = 0.62$ and thus also $\chi_{heating} = 0.38$. Apparently, the absence of a mobile amorphous PBT fraction does not result in the reorganization process leading to melting and recrystallization of the PBT crystal, which normally occurs during heating. It will be shown later in this paragraph that after cooling from the melt and subsequent reheating, the T_m value is in agreement with the values mentioned in literature.

The cooling runs of the synthesized $(BD_xDi_y)_{ssp}$ copolymers and $(BD_xDi_y)_{mp}$ copolymers are shown in Figures 5.7a and 5.7b, respectively. The thermal properties derived from the DSC traces of the $(BD_xDi_y)_{mp}$ copolymers are summarized in Table 5.2.

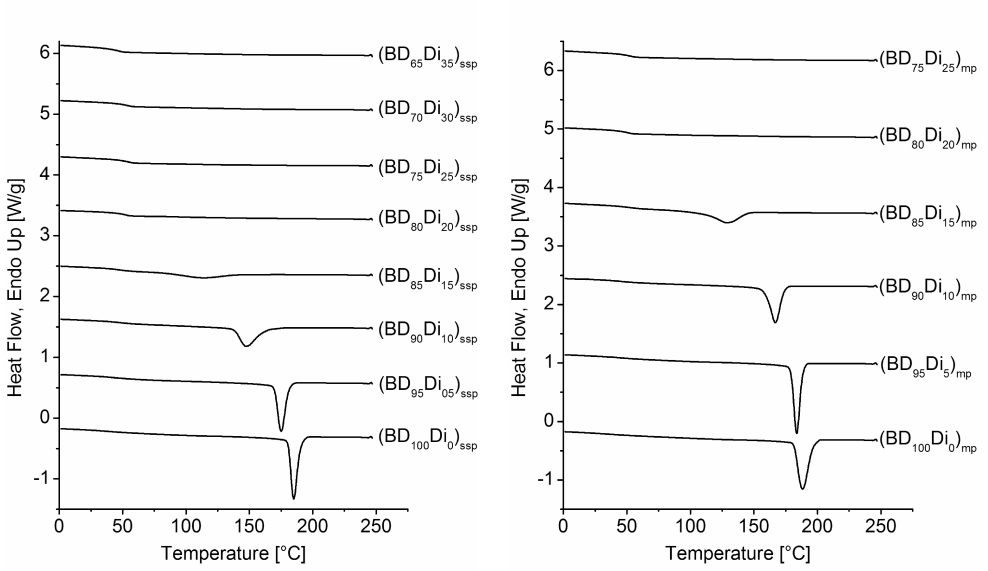

(a) (b)

Figure 5.7. (a) DSC cooling runs of the synthesized $(BD_xDi_y)_{ssp}$ copolymers and (b) of the synthesized $(BD_xDi_y)_{mp}$ copolymers. DSC curves are shifted vertically for clarity.

It can be observed that the difference in chemical microstructure between $(BD_xDi_y)_{ssp}$ and $(BD_xDi_y)_{mp}$ copolymers does not have a significant influence on the thermal properties. For both $(BD_xD_y)_{ssp}$ and $(BD_xDi_y)_{mp}$ copolymers, the crystallization peaks shift to lower temperatures and become broader for higher fractions of incorporated Dianol. Apparently, once the $(BD_xDi_y)_{ssp}$ copolymers are in the molten state, the former crystalline homopolymer

PBT segments are fully miscible with the modified chain segments consisting of both BD-T and Di-T repeat units.

Table 5.2. Thermal properties of the synthesized $(BD_xDi_y)_{mp}$ copolymers.

$(BD_xDi_y)_{feed}$ mixtures		$(BD_xDi_y)_{mp}$ copolymers		Cooling run 1	Heating run 2	(T_m-T_c)
x	y	$F_{BD\text{-}T,total}$	$F_{Di\text{-}T,total}$	T_c	T_g	
[mol%]	[mol%]	[mol%]	[mol%]	[°C]	[°C]	[°C]
100	0	100	0	188.3	39.1	34.8
95	5	96	4	183.8	43.6	31.3
90	10	90	10	166.9	47.7	37.3
85	15	81	19	128.15	54.9	55.2
80	20	74	26	-	52.0	-
75	25	70	30	-	54.8	-

[a] The T_g values were determined in modulated DSC mode, whereas $\Delta H_{melting}$, T_m, $\Delta H_{crystallization}$ and T_c were determined in normal DSC mode using heating/cooling rates of 10 °C/min.

[b] The T_m and T_c values shown are the peak values of the melting endotherms and crystallization exotherms, respectively.

This miscibility behavior comparable with the miscibility of PBT and polyarylate, having a similar structure to Dianol.[23,24] The miscibility in the melt imparts the formation of nuclei and the result is a decrease of the T_c (see Table 5.1 and 5.2). The broad crystallization peaks, observed for both $(BD_xDi_y)_{ssp}$ and $(BD_xDi_y)_{mp}$ copolymers, indicate that crystal growth is retarded because the diffusion of homopolymer PBT chain segments to the crystal growth front is hampered due to the presence of the non-crystallizable Di-T repeat-units in the PBT chain segments. These Di-T repeat-units are completely excluded from the crystalline phase, as was shown by Lotti and co-workers.[5] It was shown in **Chapter 3** that the $\overline{M}_n$ values and polydispersity indices (PDI) of the $(BD_xDi_y)_{ssp}$ copolymers are generally higher than for the $(BD_xDi_y)_{mp}$ copolymers. Only the $(BD_{75}Di_{25})_{ssp}$, $(BD_{70}Di_{30})_{ssp}$ and $(BD_{65}Di_{35})_{ssp}$ copolymers have $\overline{M}_n$ values in the same range as the $(BD_xDi_y)_{mp}$ copolymers. The $(BD_xDi_y)_{ssp}$ copolymers with higher $\overline{M}_n$ values also have a higher melt viscosity resulting in slightly lower values for the T_c values compared to those of the $(BD_xDi_y)_{mp}$ copolymers.

The second heating runs of the synthesized $(BD_xDi_y)_{ssp}$ copolymers and $(BD_xDi_y)_{mp}$ copolymers are shown in Figures 5.8a and 5.8b, respectively. For low fractions of incorporated Dianol, a double melting peak is observed. This double melting peak for PBT has already been studied in detail and several explanations were given in literature. Some authors assigned this double melting peak behavior to different types of spherulites, each

having their own melting peak.[25] Other authors assigned the double melting peak behavior to the formation of a bimodal distribution of crystals formed during cooling from the melt.[26-28] Most recent research showed that most likely the double melting peak behavior is due to a reorganization process occurring during the DSC heating run, resulting in melting and recrystallization of less perfect crystals into thicker and more perfect crystals.[12,29,30] It can also be observed that the T_m of the $(BD_{100}Di_0)_{ssp}$ homopolymer is now approximately 221 °C and hence is in agreement with the values mentioned in literature.[9]

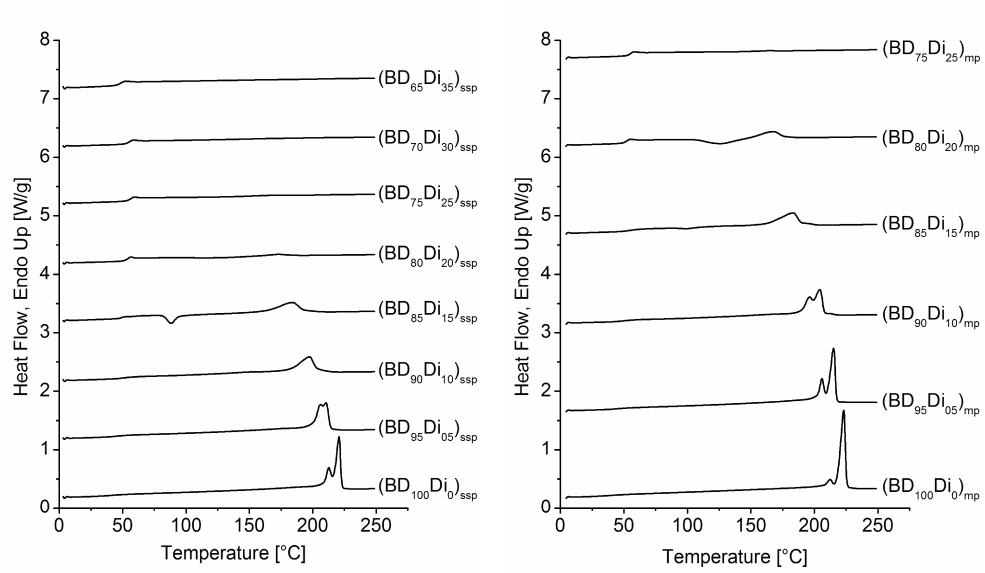

(a) (b)

Figure 5.8. (a) DSC second heating runs of the synthesized $(BD_xDi_y)_{ssp}$ copolymers and (b) of the synthesized $(BD_xDi_y)_{mp}$ copolymers. DSC curves are shifted vertically for clarity.

The T_g values of the synthesized $(BD_xDi_y)_{ssp}$ and $(BD_xDi_y)_{mp}$ copolymers were examined by modulated DSC. For each $(BD_xDi_y)_{ssp}$ copolymer, the reversing c_p signal obtained from the first heating run is shown in Figure 5.9a. The corresponding T_g values are summarized in Table 5.1. The derivatives of the reversing c_p signal are plotted in Figure 5.9b. It can be observed that the incorporation of Dianol via SSP results in a considerable increase of the T_g. The observed decrease of the T_g for the $(BD_xDi_y)_{ssp}$ copolymers with $x \leq 75$ (i.e. $F_{BD\text{-}T,\ total} \leq$ 69 mol%) can be assigned to the concomitant decrease of the $\overline{M}_n$ (see **Chapter 3**). In addition, the derivatives of the c_p signals which are plotted in Figure 5.9b, show a bimodal T_g distribution for the $(BD_xDi_y)_{ssp}$ copolymers with $x \leq 75$ mol%. The highest T_g values are in the region of 70-75 °C whereas the bulk T_g is around 60-65 °C. Lotti and co-workers

measured a T_g of 83 °C for a $(BD_0Di_{100})_{mp}$ homopolymer, consisting of only Di-T repeat-units.[5] Furthermore, Lodge and McLeish showed that the T_g is strongly dependent on the local environment.[31] The local region for the endcapped PBT chain segments is different compared to the bulk chain segments and may thus result in a slightly higher T_g value.

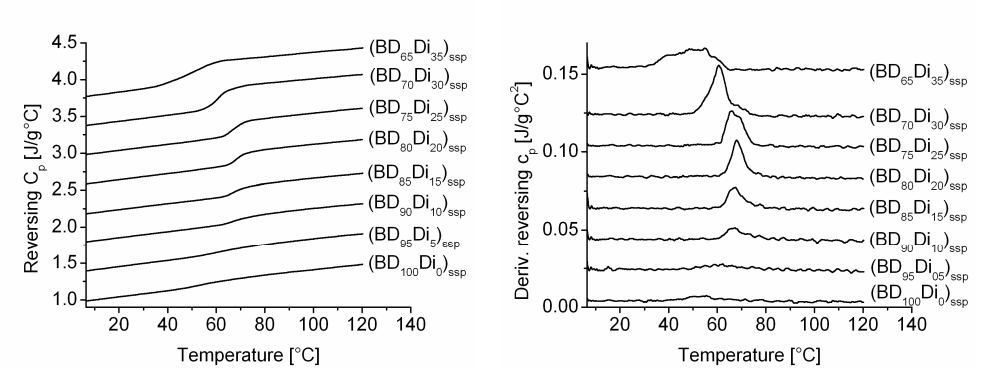

(a) (b)

Figure 5.9. a) First heating run reversing c_p traces and (b) corresponding derivative values of the synthesized $(BD_xDi_y)_{ssp}$ copolymers. Traces are shifted vertically for clarity.

When the $(BD_xDi_y)_{ssp}$ copolymers are crystallized from the melt (with a rate of 10 °C/min) and subsequently reheated in modulated mode, the c_p traces shown in Figure 5.10a are obtained. Due to the low crystallinity obtained upon cooling from the melt, an additional fraction of homopolymer PBT chain segments will contribute to the amorphous phase. As a consequence, the PBT/Dianol ratio of the amorphous phase will increase and hence result in lower values for the T_g. The derivatives of the c_p values, plotted in Figure 5.10b, show a broad peak for the $(BD_xDi_y)_{ssp}$ copolymers with $x \geq 80$, indicating that the amorphous phase is not homogeneous in mobility. For the $(BD_xDi_y)_{ssp}$ copolymer with $x \leq 75$, the peaks are Gaussian and hence a homogeneous amorphous phase is present. The homogenous amorphous phase for the $(BD_xDi_y)_{ssp}$ copolymers with $x \leq 75$, is a direct result from the absence of a crystallization peak as can be observed from Figure 5.7a. Hence, the homogeneity of the polymer melt is frozen during cooling into the glassy state. Reheating of the $(BD_xDi_y)_{ssp}$ copolymer results then in a Gaussian distribution of T_g values. For the $(BD_xDi_y)_{ssp}$ copolymers with $x \geq 80$, having a crystallization endotherm, the homopolymer unmodified PBT chain segments which are no longer present in the crystalline fraction will still be located close to the crystal surface.

These localized homopolymer amorphous PBT blocks result in a broad distribution of T_g values upon heating the $(BD_xDi_y)_{ssp}$ copolymer from the glassy state.

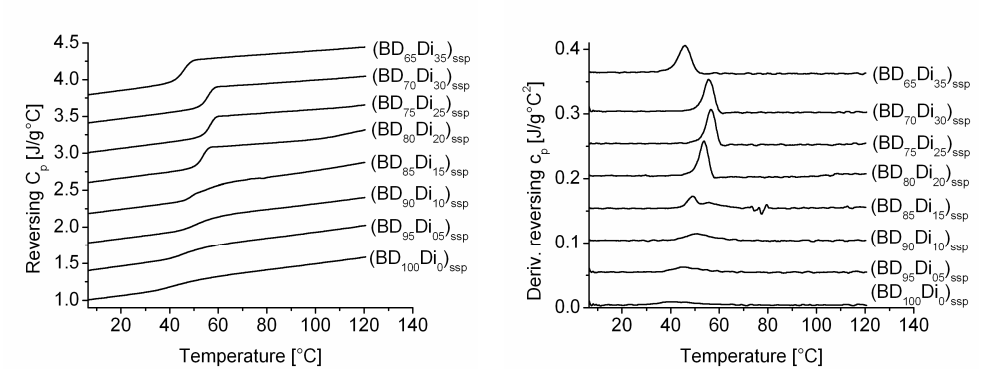

(a) (b)

Figure 5.10. a) Second heating run reversing c_p traces and (b) corresponding derivative values of the synthesized $(BD_xDi_y)_{ssp}$ copolymers. Traces are shifted vertically for clarity.

In Figures 5.11a and 5.11b, the reversing c_p traces and corresponding derivative values of the second heating run are plotted for the $(BD_xDi_y)_{mp}$ copolymers. It can be seen that the difference with the traces of the $(BD_xDi_y)_{ssp}$ copolymers is small which is mainly due to the full miscibility in the melt of modified and unmodified PBT chain segments.

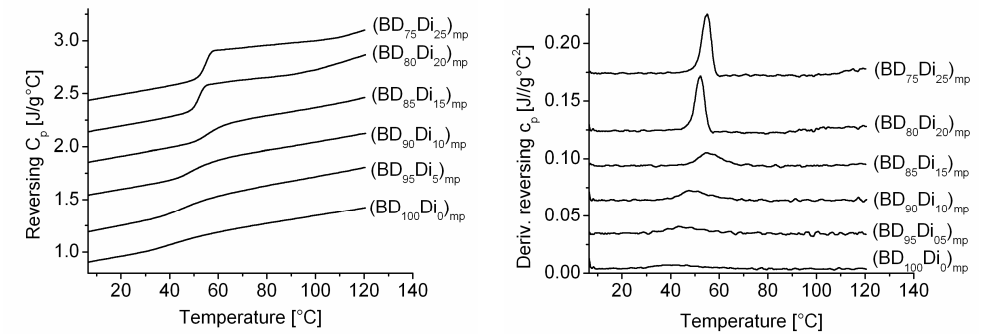

(a) (b)

Figure 5.11. Second heating run reversing c_p traces and (b) corresponding derivative values of the synthesized $(BD_xDi_y)_{mp}$ copolymers. Traces are shifted vertically for clarity.

5.4 Conclusions

The influence of Dianol monomer on the material morphology during its incorporation into PBT via SSP has been revealed. Dianol has a dual role during the SSP-reaction by acting as a

reactant for transesterification but also as a swelling agent (i.e. plasticizer) of rigid amorphous PBT chain segments. The swelling of these rigid amorphous chain segments by Dianol occurs in the initial stage of the SSP reaction, resulting in an increased chain mobility. These mobile swollen polymer chain segments can no longer be considered as rigid and therefore contribute to the mobile amorphous fraction of the $(BD_xDi_y)_{feed}$ mixture. The swollen polymer chain segments will subsequently become reactive for incorporation of Dianol via transesterification.

It was observed that two processes occur simultaneously during the SSP-reaction. One process involves the transesterification reaction of Dianol with the swollen amorphous chain segments. The other process is crystal perfectioning by transformation of non-swollen rigid amorphous chain segments into the crystal phase. When the fraction of Dianol in the $(BD_xDi_y)_{feed}$ mixtures is below 15 mol%, the fraction of swollen amorphous chain segments is sufficiently low so that predominantly crystal thickening occurs as observed by SAXS and DSC. When the fraction of Dianol in the $(BD_xDi_y)_{feed}$ mixtures exceeds 15 mol%, the remaining fraction of non-swollen rigid amorphous chain segments is so small that no significant crystal thickening can take place and hence only transesterification occurs. In addition, Dianol will dissolve the PBT crystals during the SSP-reaction when nearly all rigid amorphous chain segments are swollen and consequently no rigid amorphous chain segments are left. This dissolution process proceeds at a much lower rate than the transesterification process. The dissolved PBT homopolymer chain segments will also participate in the transesterification process so that eventually a fully random $(BD_xDi_y)_{ssp}$ is obtained (for $F_{BD\text{-}T,\ total} \approx 45$ mol%). The initial thickening of the crystalline lamellae for small fractions of Dianol and dissolution of the lamellae for large fractions of Dianol is in agreement with the results obtained from the ^{13}C-NMR sequence distribution analysis. The chemical microstructure of the $(BD_xDi_y)_{ssp}$ copolymers has a maximum in blocky character (minimum value for $R_{ssp,\ total}$) for $F_{BD\text{-}T,\ total} = 83$ mol%.

Analysis of the thermal properties by DSC shows that copolymers obtained via SSP and via MP almost have an equal thermal behavior despite the differences in chemical microstructure. This result is due to the full miscibility of unmodified PBT homopolymer blocks with modified copolyester chain segments when the $(BD_xDi_y)_{ssp}$ copolymers are in the molten state. As a consequence the nucleation rate and crystallization enthalpy decrease. The decrease in crystallinity subsequently results in an increased fraction of amorphous PBT blocks and therefore in a decrease of the T_g when the $(BD_xDi_y)_{ssp}$ copolymers are reheated from the glassy state. Consequently, a blocky chemical microstructure over a broad composition range can only be obtained when the diol monomer being used for incorporation is partly miscible with the amorphous PBT phase. In this way, a sufficient fraction of non-

swollen rigid amorphous chain segments will be retained which will not react with the diol monomer but will participate in the lamellar crystal thickening process (i.e. annealing) during SSP. For a diol monomer which is fully miscible with the amorphous phase, such as Dianol, the blocky character of the chemical microstructure depends on the morphology present during the SSP-reaction. Furthermore, in order to retain a high crystallization rate in combination with an increased T_g, it is necessary that the modified PBT chain segments, containing the incorporated diol, are not miscible in the melt with the unmodified homopolymer PBT blocks.

5.5 References and notes

1. Fakirov, S. In *Solid-state Behavior of Linear Polyesters and Polyamides*, Schultz, J. M., Fakirov, S., Eds.; Prentice-Hall: EngleWood Cliffs, NJ, 1990; Chapter 2, p 19-43.
2. Montaudo, G.; Puglisi, C.; Samperi, F. In Transreactions in Condensation Polymers, Fakirov, S., Ed.; Wiley-VCH: Weinheim, 1999, Chapter 4, p 159-193.
3. Jansen, M. A. G.; Goossens, J. G. P.; de Wit, G.; Bailly, C.; Koning, C. E. *Macromolecules* **2005**, *38*, 2659-2664.
4. Jansen, M. A. G.; Goossens, J. G. P.; de Wit, G.; Bailly, C.; Koning, C. E. *Anal. Chim. Acta* **2005**, in press
5. Finelli, L.; Lotti, N.; Munari, A.; Berti, C.; Colonna, M.; Lorenzetti, C. *Polymer* **2003**, *44*, 1409-1420.
6. Berti, C.; Colonna, M.; Fiorini, M.; Lorenzetti, C.; Marchese, P. *Macromol. Mater. Eng.* **2004**, *289*, 49-55.
7. Jansen, M. A. G.; Goossens, J. G. P.; de Wit, G.; Bailly, C.; Schick, C.; Koning, C. E. *Macromolecules* **2005**, accepted.
8. Cheng, S. Z. D.; Cao, M.-Y.; Wunderlich, B. *Macromolecules* **1986**, *19*, 1868-1876.
9. Cheng, S. Z. D.; Wunderlich, B. *Macromolecules* **1987**, *20*, 1630-1637.
10. Cheng, S. Z. D.; Wu, Z. Q.; Wunderlich, B. *Macromolecules* **1987**, *20*, 2802-2810.
11. Cheng, S. Z. D.; Wunderlich, B. *Macromolecules* **1988**, *21*, 789-797.
12. Cheng, S. Z. D.; Pan, R.; Wunderlich, B. *Makromol. Chem.* **1988**, 189, 2443-2458.
13. Conix, A.; Van Kerpel, R. *J. Polym. Sci.* **1959**, *40*, 521-532.
14. Kirshenbaum, I. J. *J. Polym. Sci., Part A* **1965**, *3*, 1869-1875.
15. ATHAS database: Wunderlich, B. *Pure and Applied Chemistry* **1995**, *67*, 1019-1026.
16. Strobl, G. R.; Schneider, M. *J. Polym. Sci., Polym. Chem. Ed.* **1980**, *18*, 1343-1359.
17. Ruland, W. *Colloid Polym. Sci.* **1977**, *255*, 417-427.
18. Debye, P.; Bueche, A. M. *J. Appl. Phys.* **1949**, *20*, 518-525.
19. Debye, P.; Anderson Jr., H. R.; Brumberger, H. *J. Appl. Phys.* **1957**, *28*, 679-683.
20. Hong, P-D.; Chuang, W-T.; Yeh, W-J; Lin, T-L. *Polymer* **2002**, *43*, 6879-6886.
21. Yamadera, R.; Murano, M. *J. Polym. Sci., Part A-1* **1967**, *5*, 2259-2268.
22. Devaux, J.; Godard, P.; Mercier, J. P. *J. Polym. Sci., Polym. Phys. Ed.* **1982**, *20*, 1875-1881.
23. Kimura, M.; Porter, R. S. *J. Polym. Sci., Polym. Phys. Ed.* **1983**, *21*, 367-378.

24. Denchev, Z.; Sarkissova, M.; Fakirov, S.; Yilmaz, F. *Macromol. Chem. Phys.* **1996**, *197*, 2869-2887.

25. Stein, R. S.; Misra, A. *J. Polym. Sci., Polym. Phys. Ed.* **1980**, *18*, 327-342.

26. Nichols, M. E.; Robertson, R. E. *J. Polym. Sci., Polym. Phys. Ed.* **1992**, *30*, 305-307.

27. Nichols, M. E.; Robertson, R. E. *J. Polym. Sci., Polym. Phys. Ed.* **1992**, *30*, 755-768.

28. Kim, H. G.; Robertson, R. E. *J. Polym. Sci., Polym. Phys. Ed.* **1998**, *36*, 1757-1767.

29. Yeh, J. T.; Runt, J. *J. Polym. Sci., Polym. Phys. Ed.* **1989**, *27*, 1543-1550.

30. Yasuniwa, M.; Tsubakihara, S.; Ohoshita, K.; Tokudome, S. *J. Polym. Sci., Polym. Phys. Ed.* **2001**, *39*, 2005-2015.

31. Lodge, T. P.; McLeish, T. C. B. *Macromolecules* **2002**, *33*, 5278-5284.

Chapter 6
Incorporation of bis(2-hydroxyethyl)terephthalate into PBT by solid-state copolymerization

6.1 Introduction

Poly(butylene terephthalate) (PBT) and poly(ethylene terephthalate) (PET) are two semi-crystalline polycondensates which are used in widespread applications. The main advantage of PBT is its high crystallization rate, making it suitable for injection molding applications due to short molding cycle times.[1] PET, however, has a considerably lower crystallization rate and is therefore mainly used for fiber applications and packaging.[2] The glass transition temperature of PBT is rather low compared to PET ($T_g \approx 45$ °C for PBT and $T_g \approx 80$ °C for PET). As a consequence, PBT is less suitable for applications where elevated temperatures are involved due to a loss of dimensional stability. For commercial injection molding purposes for which a higher T_g than 45 °C is required, PBT and PET can be reactively blended in the melt. The ester-interchange reactions occurring in the melt first result in block copolymers and as the reaction proceeds, random PBT-PET copolymers are obtained.[3-5] These random PBT-PET copolymers have a T_g in between that of PBT and PET.[6] However, the shorter and more irregular homopolymer sequences of these random copolymers consequently lead to a decrease of the melting temperature, crystallization rate and crystallinity with respect to pure PBT. It would therefore be desirable to synthesize PBT-PET copolymers having a T_g higher than PBT homopolymer, but with a crystallization behavior comparable to that of PBT. To get a copolymer based on PBT with a sufficient crystallization behavior, a copolymerization method should be used with which it is possible to retain large crystallizable homopolymer PBT blocks. Consequently, a blocky (non-random) chemical microstructure should be present after copolymerization. Misra et al.[7] synthesized PET-PBT block copolymers by end group reaction of a PET-PBT oligomer mixture in the melt using a short reaction time. Triphenyl phosphate was added to this mixture of oligomers to quench the transesterification catalysts used for the synthesis of the PBT and PET oligomers. However, transesterification was not fully prevented. Later, Backson et al.[3] studied transesterification reactions during melt blending of PBT-PET mixtures for a period of 30 minutes at 300 °C. ^{13}C-NMR sequence distribution analysis showed that random copolymers were obtained. On the contrary, when the PBT-PET mixtures were kept for 6 hours at 200 °C, which is below the T_m of both PBT

and PET, a PBT-PET copolymer with a blocky chemical microstructure was obtained. No further details were given about the thermal properties of these blocky copolymers. These transesterification reactions, occurring below the melting temperature and thus in the solid state of the semi-crystalline polyesters, are generally used as a post-condensation process to increase the molecular weight of semi-crystalline polycondensates. This process is often referred to as solid-state polymerization (SSP).[8] The transesterification reactions (predominantly alcoholysis and acidolysis) occurring in the amorphous fraction of the semi-crystalline polyesters result in coupling of amorphous polymer chain segments and consequently in a increase of the molecular weight. Sivaram and co-workers used SSP to synthesize poly(ethylene terephthalate)-poly(ethylene naphthalate) copolymers from corresponding semi-crystalline oligomer mixtures.[9-10] The PET-PEN copolymers formed after SSP had a blocky chemical microstructure.

In **Chapter 3**, PBT-PET copolymers were made by copolymerization (i.e. transesterification) in the melt (MP) of bis(2-hydroxyethyl)terephthalate (BHET) with PBT.[11] BHET can react by self-condensation (**Chapter 1**, eq 1.2) to result in PET homopolymer.[12,13] The chemical microstructure of the resulting PBT-PET copolymers was examined by ^{13}C-NMR spectroscopy sequence distribution analysis. As expected, the chemical microstructure of the PBT-PET copolymers obtained by MP was fully random. However, when BHET was incorporated into PBT via SSP, a non-random blocky chemical microstructure was obtained. When the fraction of BHET used for incorporation in PBT was increased, the blocky character of the chemical microstructure became more pronounced. This result was a clear indication that BHET may react by self-condensation to form homopolymer PET blocks. In addition, ^{13}C-NMR sequence distribution analysis also showed that transesterification reactions occurred between BHET monomer and PBT. Up to now, it is not fully understood which parameters determine whether BHET reacts by self-condensation or by transesterification with PBT. Furthermore, it is not clear if the formed homopolymer PET blocks are present as a separate phase or if these blocks are incorporated in the amorphous PBT phase.

In this chapter, the incorporation of BHET into PBT via SSP is studied in more detail. The kinetics of the incorporation via SSP is studied by variation of the reaction time under isothermal conditions. In this way, the development of the chemical microstructure during the SSP-reaction can be examined. Furthermore, the miscibility of BHET and PBT is examined by differential scanning calorimetry (DSC). From these results, the relation between the used BHET/PBT ratio and the resulting chemical microstructure of the PBT copolymers after SSP can be revealed. The morphology of the PBT copolymers obtained by SSP was examined by Small-Angle X-ray Spectroscopy (SAXS). Furthermore, the influence of the chemical

microstructure (random versus non-random) of the PBT copolymers on the thermal properties i.e. crystallization behavior and glass-transition increase, is studied by DSC.

6.2 Experimental Section

6.2.1 Materials

Poly(butylene terephthalate) (PBT) pellets ($\overline{M}_n$ = 15 kg/mol and $\overline{M}_w$ = 34 kg/mol, determined by size exclusion chromatography) were provided by GE Plastics (Bergen op Zoom, The Netherlands) and used as received. Bis(2-hydroxyethyl)terephthalate (BHET) was obtained from Aldrich and recrystallized twice from acetone prior to use. 1,1,1,3,3,3-Hexafluoro-2-propanol (HFIP, 99 %) and chloroform ($CHCl_3$, 99 %), obtained from Biosolve (Valkenswaard, The Netherlands), were used as received for solution mixing of PBT with BHET. For NMR measurements, deuterated trifluoro acetic acid (TFA-d, 99 % deuterated) was obtained from Aldrich and deuterated chloroform ($CDCl_3$, 99 % deuterated) was obtained from Merck.

6.2.2 Solid-state copolymerization (SSP) and melt copolymerization (MP)

Copolyesters of PBT and BHET were synthesized via SSP and MP. The corresponding preparation methods are described in detail in **Chapter 3** of this thesis. Powder mixtures of different PBT/BHET ratios were used as feed for the SSP and MP reactions in order to obtain copolymers of different compositions. The PBT/BHET mixtures to be used for the SSP reaction were first dissolved in HFIP. After complete dissolution, the HFIP was evaporated and the resulting lump of material was dried and subsequently ground into powder. The PBT/BHET mixtures are abbreviated as $(BD_xEG_y)_{feed}$ mixtures. BD_x represents the initial mol% PBT and EG_y the mol% of BHET hydroxyl end groups (1 mole BHET contains 2 moles hydroxyl end groups). The (BD_xEG_y) copolymers obtained via SSP are indicated as $(BD_xEG_y)_{ssp}$ copolymers, whereas (BD_xEG_y) samples obtained by MP are denoted as $(BD_xEG_y)_{mp}$ copolymers. The actual fractions of BD_x and EG_y units after SSP and MP slightly differ from the initial fractions present in the $(BD_xEG_y)_{feed}$ mixtures. This difference can be attributed to the evaporation of ethylene glycol and/or 1,4-butanediol during the SSP and MP reaction (see **Chapter 3**).[11]

6.2.3 Kinetics experiments

The kinetics experiments were done in a similar way as described in **Chapter 2** for a $(BD_{85}Di_{15})_{feed}$ mixture. A $(BD_{70}EG_{30})_{feed}$ mixture was prepared by solution mixing in HFIP as

described previously. Samples of approximately 3 g $(BD_{70}EG_{30})_{feed}$ powder mixture were transesterified in the solid state at a constant temperature of 180 °C, whereas the reaction time (t_{ssp}) was varied for each sample. A nitrogen flow of 3 L/min was used for all samples. After elapsing of t_{ssp}, the reactor was removed from the salt bath (used as heating medium) and quenched for 5 min in water of 80 °C and then further cooled in water of ambient temperature.

6.2.4 Nuclear Magnetic Resonance (NMR) Spectroscopy

All solution ^{1}H-NMR spectra were recorded on a Varian 400 MHz spectrometer at 25 °C at a resonance frequency of 400.164 MHz. For the ^{1}H-NMR measurements, 15 mg of polymer was dissolved in 0.8 mL of a 80:20 vol% $CDCl_3$:TFA-d mixture. All chemical shifts are reported in ppm downfield from tetramethylsilane (TMS), used as the internal standard. The spectra were acquired using 32 scans, a delay time (d1) of 5 s and a total number of data points of 64 k.

Quantitative proton-decoupled solution ^{13}C-NMR spectra were recorded on a Varian 300 MHz spectrometer, operated at a resonance frequency of 75.462 MHz. 3000-4000 scans were acquired with 64 k data points, a d1 of 12 s, a 90° pulse and a spectral width of 18.8 kHz. For the sequence distribution analysis, overlapping peaks were integrated after Lorentzian deconvolution of the spectra using the deconvolution option implemented in the Varian NMR-software.

6.2.5 Size Exclusion Chromatography (SEC)

The number-average molecular weight ($\overline{M}_n$) and polydispersity index (PDI) of the $(BD_{70}EG_{30})_{feed}$ mixture (t_{ssp} = 0 h) and the $(BDEG)_{ssp}$ samples with 0 h < t_{ssp} ≤ 24 h were determined by SEC. The system was equipped with a Hewlett Packard 1100 series injector (injection volume 10 µl) and a Hewlett Packard PL HFIP gel column (250 × 4.6 mm, part no: 1514-5900 HFIP) thermostated at 35 °C. A mixture consisting of 5 vol% HFIP and 95 vol% chloroform was used as eluent. Acetophenone was used as flow marker. A HP 1100 series pump provided a flow rate of 0.3 mL/min. For detection, an Agilent diode array detector was used (λ = 295 nm). The SEC system was calibrated with polystyrene calibration standards ($\overline{M}_w$ range: 1000 - 900.000 g/mol). The obtained PS calibration curve was used to determine the $\overline{M}_n$ and PDI of the $(BD_{70}EG_{30})_{feed}$ mixture and the synthesized $(BD_{70}EG_{30})_{ssp}$ copolymers. In addition, PBT homopolymer samples with known $\overline{M}_n$ values (determined by end group titration) were analyzed with the same SEC system. A fitting curve was prepared using the $\overline{M}_n$ values obtained by end group titration and the $\overline{M}_n$ obtained via the PS calibration curve. The measured $\overline{M}_n$ of the $(BD_{70}EG_{30})_{feed}$ mixture and $(BD_{70}EG_{30})_{ssp}$

copolymers were fitted using this calibration curve and corrected to obtain a more realistic value. No additional corrections were made for changes in hydrodynamic volumes for the $(BD_{70}EG_{30})_{ssp}$ copolymers versus pure PBT.

6.2.6 Small-Angle X-ray Scattering (SAXS)

SAXS experiments were performed on the DUBBLE beamline (BM 26B) at the European Radiation Synchrotron Facility (ESRF) in Grenoble (France). A wavelength of 1.218 Å was used. The SAXS data were collected on a gas-filled multiwire two-dimensional (2D) detector positioned at 4.5 m from the sample. Approximately 18-20 mg (BD_xEG_y) copolymer material was placed in crimped aluminum DSC pans. A Linkam THMS600 hotstage with controller was used for heating/cooling of the samples. For calibration of the SAXS detector, the scattering pattern from an oriented specimen of wet collagen (rat-tail tendon) was used. The experimental data were corrected for background scattering, i.e. subtraction of the scattering from the hotstage and DSC pan. The two-dimensional SAXS data were transformed into one-dimensional plots by performing integration along the azimuthal angle using the FIT2D program of Dr. Hammersley of ESRF. The exposure time of each single shot experiment was 30 s, and for the time-resolved measurements 5 s per frame. The procedure to determine the long period, average lamellar crystal thickness and thickness of the amorphous layer has been described in **Chapter 5**.

6.2.7 Differential Scanning Calorimetry (DSC)

The melting and crystallization enthalpy ($\Delta H_{melting}$ and $\Delta H_{crystallization}$ respectively) were measured by a TA Instruments Q1000 DSC equipped with an autosampler and refrigerated cooling system (RCS). The DSC cell was purged with a nitrogen flow of 50 mL/min. The temperature was calibrated using the onset of melting for indium. The enthalpy was calibrated with the heat of fusion of indium. For the $(BD_xEG_y)_{ssp}$ and $(BD_xEG_y)_{mp}$ copolymers, samples of 6-8 mg were prepared in crimped aluminum pans. The $(BD_{70}EG_{30})$ samples, used to study the kinetics, were prepared in hermetically closed aluminum pans using sample weights of 5-7 mg. All samples were measured in the temperature range from 0 to 265 °C using heating and cooling rates of 10 °C/min, respectively and isothermal periods of 3 min at respectively 0 and 265 °C (for the $(BD_{70}EG_{30})$ kinetics samples, only the first heating run was used). The crystallinity was defined as the ratio of $\Delta H_{melting}$ and the heat of fusion for 100% PBT (ΔH^0_{fuse} = 145 J/g).[14-16]

The glass transition temperature (T_g) and corresponding heat capacity increase (Δc_p) of the (BD_xEG_y) copolymers were measured in modulated DSC (TMDSC®) mode using the same TA Q1000 DSC as previously described.

The DSC cell was purged with a nitrogen flow of 30 mL/min. For all modulated DSC measurements, samples of approximately 6-8 mg were prepared in crimped aluminum pans. An oscillating temperature with a period of 60 seconds and amplitude of 0.5 °C was used. The $(BD_xEG_y)_{ssp}$, $(BD_xEG_y)_{mp}$ and $(BD_{70}EG_{30})$ kinetics samples were measured in the temperature range from 0 to 180 °C using an underlying heating rate of 2 °C/min.

The $(BD_xEG_y)_{feed}$ mixtures, used to study the miscibility of PBT and BHET, were first heated in normal mode from 20 to 120 °C, which is approximately 10 °C above the T_m of BHET, and kept for 10 minutes at this temperature. The samples were then cooled to -80 °C and subsequently reheated to 240 °C using cooling and heating rates of 10 °C/min, respectively. $\Delta H_{melting}$ was taken from the second heating run.

The glass transition temperatures (T_g) of the $(BD_xEG_y)_{feed}$ mixtures were measured in modulated DSC. The samples were first heated in normal DSC-mode from 0 to 120 °C and kept at this temperature for 10 minutes. The samples were subsequently cooled at a rate of 10 °C/min to -80 °C and then reheated in modulated mode from -80 to 140 °C using an underlying heating rate of 2 °C/min and an oscillating temperature with a period of 60 s with an amplitude of 0.5 °C. The T_g values were taken from the reversing heat capacity signal. The step increase of the heat capacity (Δc_p) at half-step T_g was determined using tangents to the measured curve below and above the T_g. The obtained Δc_p-values were used to obtain the mobile amorphous fraction which is defined as the ratio between the measured Δc_p and that of fully amorphous PBT (Δc_p^0 = 0.35 J/g K).[16,17]

6.3 Results and discussion

6.3.1 Miscibility limit of BHET in PBT

The synthetic aspects of the incorporation of BHET into PBT via SSP and MP were already described in detail in **Chapter 3**. The (BD_xEG_y) copolymers were synthesized by SSP and MP using different PBT/BHET ratios. The chemical structure of a BHET monomer and a (BD_xEG_y) copolymer are shown in Figures 6.1a and 6.1b respectively. The chemical microstructure of these $(BD_xEG_y)_{ssp}$ and $(BD_xEG_y)_{mp}$ copolymers was determined by quantitative ^{13}C-NMR sequence distribution analysis. The corresponding results of this analysis are described in **Chapter 3**. The ^{13}C-NMR peak corresponding to the quaternary carbon atom (marked by the arrow in Figure 6.1) is positioned at 135.8 ppm.

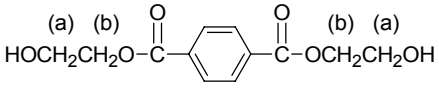

(a) BHET monomer

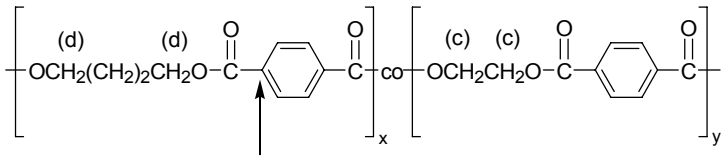

BD-T repeat-unit EG-T repeat-unit

(b) (BD_xEG_y) copolymer

Figure 6.1. a) Chemical structure of a (BD_xEG_y) copolymer, consisting of BD-T and EG-T repeat-units. ^{1}H-NMR peak assignments are also shown. The arrow denotes the quaternary carbon atom used in ^{13}C-NMR sequence distribution analysis.

Due to long range coupling of adjacent chemical groups, the quaternary carbon peak splits up into four peaks with different chemical shift and peak integral values. Each peak represents a dyad sequence (BTE BD-side, BTB, ETE and BTE EG-side). After normalization, the integral values of the four peaks can be used to determine the chemical microstructure of the (BD_xEG_y) copolymers. The following equations were used:

$$F_{BTE,\,total} = F_{BTE,\,BD-side} + F_{BTE,\,EG-side} \tag{6.1}$$

$$F_{BD-T,\,total} = (F_{BTE,\,total}/2 + F_{BTB}) \tag{6.2}$$

$$F_{EG-T,\,total} = (F_{BTE,\,total}/2 + F_{ETE}) \tag{6.3}$$

$$R_{total} = \frac{F_{BTE,\,total}}{2 \cdot (F_{BD-T,\,total} \cdot F_{EG-T,\,total})} \tag{6.4}$$

where F_i denotes the mol fraction of each sequence (i = BTE, BD-side; BTB; ETE or BTE, EG-side), while $F_{BD\text{-}T,\,total}$ and $F_{EG\text{-}T,\,total}$ denote the total mol fractions of BD-T and EG-T units, respectively.

From the results described in **Chapter 3**, it was already observed that all synthesized $(BD_xEG_y)_{mp}$ copolymers have a degree of randomness ($R_{total,\,mp}$) equal to unity, which represents a fully random distribution of BD-T and EG-T repeat units. For the $(BD_xEG_y)_{ssp}$ copolymers, however, $R_{total,\,ssp}$ decreased when the fraction of EG-T repeat units ($F_{EG\text{-}T,\,total}$) in the $(BD_xEG_y)_{ssp}$ copolyesters increased. An interesting result is found when the dyad fractions F_{ETE}, F_{BTB} and $F_{BTE,\,total}$ (i.e. $F_{BTE,\,BD\text{-}side} + F_{BTE,\,EG\text{-}side}$) are plotted as a function of $F_{BD\text{-}T,\,total}$ as done in Figure 6.2. The sum of F_{ETE}, F_{BTB} and $F_{BTE,\,total}$ was set at a value of 1.

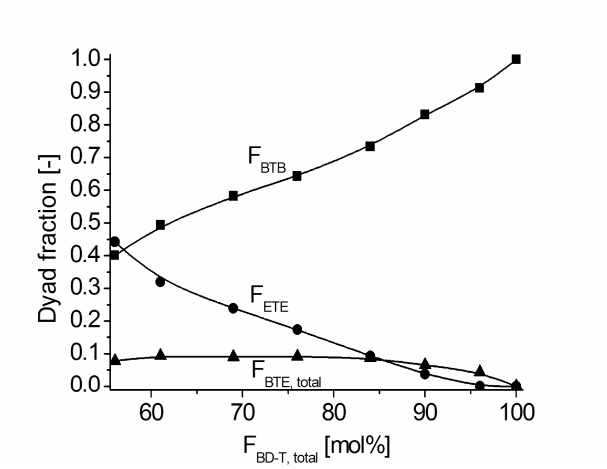

Figure 6.2. Dyad sequence distribution analysis of the $(BD_xEG_y)_{ssp}$ copolymers: Dyad fractions F_{BTB}, F_{ETE}, $F_{BTE,\ total}$ as a function of $F_{BD\text{-}T,\ total}$ in the $(BD_xEG_y)_{ssp}$ copolymer.

It can be seen that for decreasing fractions of $F_{BD\text{-}T,\ total}$, the fraction F_{ETE} continuously increases. It is known that BHET can undergo self-condensation to result in PET homopolymer.[12,13] The formation of PET homopolymer blocks, consisting of only ETE-sequences, will have a reducing effect on the value of the degree of randomness $R_{ssp,\ total}$. In addition, the observed values for $R_{ssp,\ total}$ were above 0 for all synthesized $(BD_xEG_y)_{ssp}$ copolymers. Hence, for all synthesized $(BD_xEG_y)_{ssp}$ copolymers, a BTE fraction was present ($F_{BTE,\ total} > 0$; see eq 6.1). It can therefore be concluded that, besides self-condensation, BHET monomer also reacts by (outer-inner) alcoholysis reactions[18] with the amorphous PBT chain segments.

For the occurrence of transesterification reactions, the BHET monomer should be miscible with the amorphous PBT fraction. The observed maximum attainable value for $F_{BTE,\ total}$ with increasing fraction of incorporated BHET has a value of 0.1 at $F_{BD\text{-}T,\ total}$ = 84 mol%. Apparently, the miscibility of BHET with the amorphous PBT phase is limited. To yield a $(BD_xEG_y)_{ssp}$ copolymer with $F_{BD\text{-}T,\ total}$ = 84 mol%, a $(BD_xEG_y)_{feed}$ mixture with a PBT fraction (F_{PBT}) = 84 mol% and a BHET fraction (F_{BHET}) = 16 mol% (i.e. x = 72.4 mol% BD and y = 27.6 mol% EG) should be used for SSP (see **Chapter 3**).[11] Hence, when F_{BHET} in the $(BD_xEG_y)_{feed}$ mixture exceeds 16 mol%, a separate BHET phase should be formed. To verify this miscibility limit, several $(BD_xEG_y)_{feed}$ mixtures were examined by DSC. The mixtures were first kept for 10 min at 120 °C, which is approximately 10 °C above the T_m of BHET monomer, to allow the molten BHET to diffuse into the rubbery amorphous PBT phase. It is assumed that at 120 °C the rate of transesterification is sufficiently small to have no

significant effect on the measurement. The samples were subsequently cooled to -80 °C at a rate of 10 °C/min and then reheated with 10 °C/min to 250 °C. The resulting DSC heating traces of these second heating runs are shown in Figure 6.3a. The corresponding glass transition temperatures were measured separately by modulated DSC and are shown in Figure 6.3b.

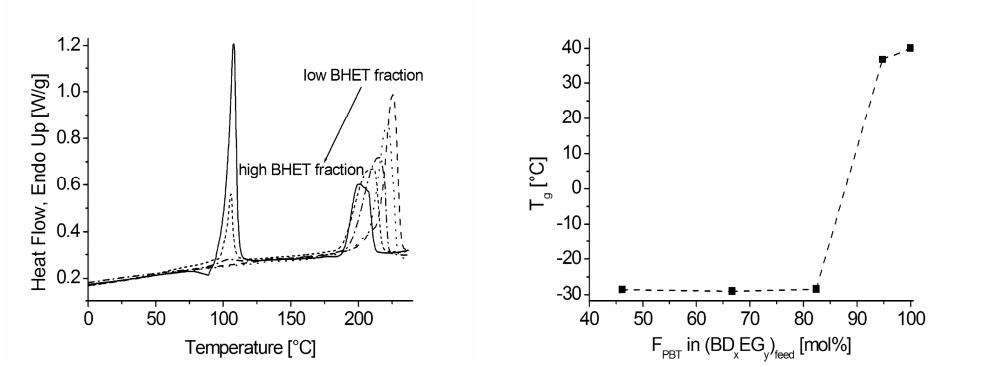

(a) (b)

Figure 6.3. (a) DSC heating traces of $(BD_xEG_y)_{feed}$ mixtures as a function of $F_{BD\text{-}total}$: $(BD_{100}EG_0)_{feed}$ (– – –), $(BD_{90}EG_{10})_{feed}$ (·····), $(BD_{70}Di_{30})_{feed}$ (·–·–·), $(BD_{50}Di_{50})_{feed}$ (-----), $(BD_{30}Di_{70})_{feed}$ (——) and (b) T_g of the $(BD_xEG_y)_{feed}$ mixtures as a function of fraction PBT present in the mixtures (F_{PBT}).

From Figure 6.3a, it can be observed that the PBT melting peak shifts to lower temperature when the ratio PBT/BHET of the $(BD_xEG_y)_{feed}$ mixtures decreases. This melting temperature depression is an indication that BHET is at least partly miscible with PBT. In addition, the BHET melting peak is completely absent in the DSC trace of the $(BD_{90}EG_{10})_{feed}$ mixture and appears only in the DSC traces of $(BD_xEG_y)_{feed}$ mixtures with 70 mol% BD or less ($x \leq 70$ mol%). The composition of a $(BD_{70}EG_{30})_{feed}$ mixture (x = 70 mol% BD and y = 30 mol% EG) is in agreement with miscibility limit as was previously calculated from the composition at which $F_{BTE,\ total}$ reaches its maximum value (see Figure 6.2). The BHET monomer, which is not miscible with PBT, is present as a separate phase. Upon heating, the BHET melts and will react by self-condensation resulting in PET homopolymer.[12,13]

The T_g values plotted in Figure 6.3b rapidly decrease with decreasing values for F_{PBT}. A limit is obtained for the T_g when $80 < F_{PBT} < 90$ mol%. This composition roughly corresponds to a $(BD_{70}EG_{30})_{feed}$ mixture with F_{PBT} = 84 mol% as was already shown and hence is close to the miscibility limit as previously calculated.

The rather constant value of $F_{BTE,\ total}$ for $F_{BD\text{-}T,\ total} \leq 84$ mol% as observed in Figure 6.2 implies that the fraction of BHET which reacts with PBT during SSP is almost independent on the amount of BHET used in the $(BD_xEG_y)_{feed}$ mixtures. Hence, when the fraction of BHET in the $(BD_xEG_y)_{feed}$ mixtures (F_{BHET}) increases, the amorphous PBT fraction available for mixing with BHET prior to SSP should increase as well. From the results discussed in **Chapters 4** and **5**, it is known that the amorphous fraction of PBT can be divided into a rigid amorphous subfraction (α_{rigid}) and a mobile amorphous subfraction (α_{mobile}).[19] It was shown that only the mobile PBT chain segments are accessible for incorporation of comonomers by SSP. The rigid amorphous PBT segments were not mobile enough at the used SSP-temperature of 180 °C for transesterification reactions to occur. The maximum attainable value for the $F_{BTE,\ total}$ as observed in Figure 6.2 suggests that for BHET monomer only a limited mobile amorphous fraction is available for incorporation. This fraction should then remain constant over a broad composition range. To verify this statement, α_{mobile} was determined for the $(BD_xEG_y)_{feed}$ mixtures, previously used to study the miscibility (see Figure 6.3). α_{mobile} is calculated by eq 6.5a, where Δc_p is the heat capacity increase at half-step T_g obtained by modulated DSC and $\Delta c_p^{\ 0}$ is the heat capacity increase for 100% amorphous PBT (i.e. $\Delta c_p^{\ 0} = 0.35$ J/g K).[16,17] The crystalline fraction ($\chi_{heating}$) was obtained by eq 6.5b, where $\Delta H_{melting}$ is the melting enthalpy of the PBT melting endotherm (obtained from Figure 6.3a) and ΔH^0_{fuse} is the crystallinity of 100% crystalline PBT ($\Delta H^0_{fuse} = 145$ J/g).[14-16]

$$\alpha_{mobile} = \Delta c_p / \Delta c_p^{\ 0}{}_{\alpha} \tag{6.5a}$$

$$\chi_{heating} = \Delta H_{melting} / \Delta H^{0}{}_{fuse} \tag{6.5b}$$

Hence, α_{rigid} can be described by:

$$\alpha_{rigid} = 1 - \chi_{heating} - \alpha_{mobile} \tag{6.5c}$$

The obtained values for the fractions $\chi_{heating}$, α_{rigid} and α_{mobile} are plotted in Figure 6.4 as a function of F_{PBT} in the $(BD_xEG_y)_{feed}$ mixtures.

From Figure 6.4, it can be seen that $\chi_{heating}$ continually decreases as a function of F_{PBT} in the $(BD_xEG_y)_{feed}$ mixtures. This decrease of $\chi_{heating}$ is due to the decreased ratio PBT/BHET in the $(BD_xEG_y)_{feed}$ mixtures. α_{mobile} slightly decreases to 0.1 for $85 < F_{PBT} < 100$ mol%. For $F_{PBT} <$ 85 mol%, α_{mobile} does not significantly change anymore which is in agreement with the maximum attainable value for $F_{BTE,\ total}$ as was presented in Figure 6.2.

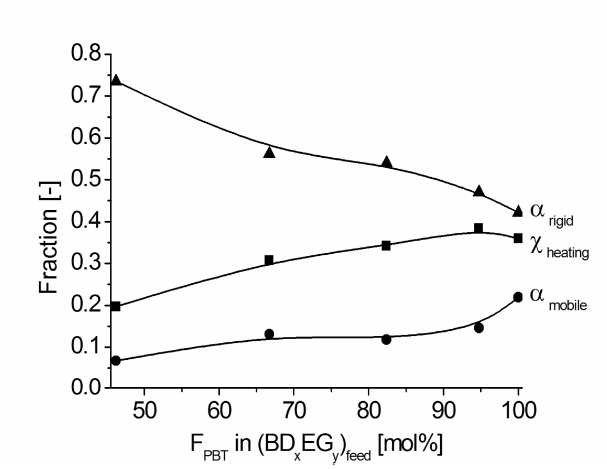

Figure 6.4. Crystalline ($\chi_{heating}$ ■), rigid amorphous (α_{rigid} ▲) and mobile amorphous (α_{mobile} ●) fraction as a function of F_{PBT} in the $(BD_xEG_y)_{feed}$ mixtures.

6.3.2 Development of chemical microstructure as a function of solid-state polymerization time

The previously discussed results show that the final chemical microstructure of the $(BD_xEG_y)_{ssp}$ copolymers is already influenced by the morphology of the $(BD_xEG_y)_{feed}$ mixtures used as feed for SSP. In addition, the development of the chemical microstructure was also studied as a function of solid-state polymerization time. Therefore, a $(BD_{70}EG_{30})_{feed}$ mixture was polymerized in the solid state at a temperature of 180 °C, while the solid-state polymerization time (t_{ssp}) was varied. The number-average molecular weight ($\overline{M}_n$) and polydispersity index (PDI) of the $(BD_{70}EG_{30})_{ssp}$ samples with different values for t_{ssp} were determined by Size Exclusion Chromatography (SEC). The SEC chromatograms are shown in Figure 6.5a. The molecular weight ($\overline{M}_n$) and polydispersity index (PDI) of each SEC chromatogram are plotted in Figure 6.5b as a function of t_{ssp}. The $(BD_{70}EG_{30})_{feed}$ mixture has a solid-state polymerization time of 0 h. The sharp peak, present at an elution time around 11 min, represents the free BHET monomer whereas the broad peak at a lower elution time originates from the PBT homopolymer. The peak, present at an elution time of 11.5 minutes originates from acetophenone, which is added as flow marker. In the same period during which the free BHET monomer reacts ($0 \leq t_{ssp} \leq 1$ h), the $\overline{M}_n$ of the PBT rapidly decreases. This decrease proves that BHET monomer reacts by (outer-inner) alcoholysis reactions with amorphous PBT chain segments. The transesterification reactions result in cleavage of the amorphous PBT chain segments and hence in a decrease of the molecular weight. After t_{ssp} = 1 h, the $\overline{M}_n$ increases again, which is a result of recombination of polymer chain segments.

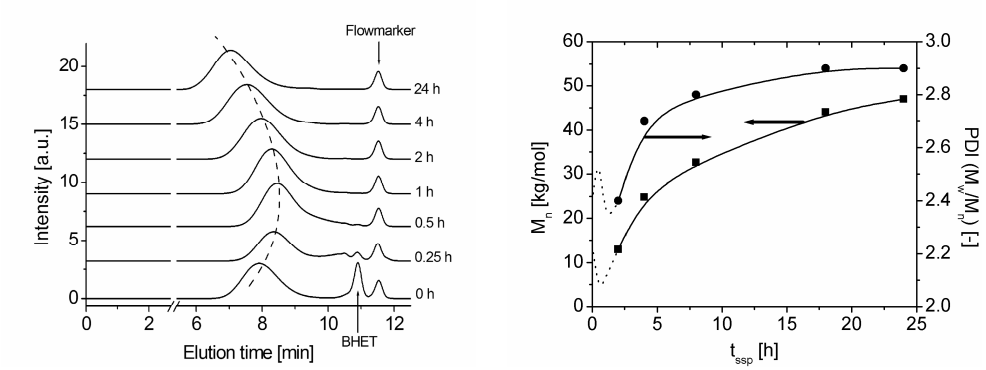

(a) (b)

Figure 6.5. (a) SEC chromatograms of $(BD_{70}Di_{30})_{ssp}$ samples with different solid-state polymerization times and (b) development of the molecular weight ($\overline{M}_n$) and polydispersity index (PDI) as a function of t_{ssp}. The acetophenone flowmarker signal has an elution time of 11.5 min.

The development of the $\overline{M}_n$ as a function of t_{ssp} is therefore similar to the development of the $\overline{M}_n$ observed during incorporation of Dianol monomer into PBT by SSP, as discussed in **Chapter 2**.[20] Hence, the SEC measurements do not provide evidence that separate PET homopolymer formation occurs during the SSP reaction of $(BD_xEG_y)_{feed}$ mixtures. To get more insight into the changes of the chemical microstructure as a function of t_{ssp}, the $(BD_{70}EG_{30})_{feed}$ mixture and $(BD_{70}EG_{30})_{ssp}$ samples were also studied by ^{1}H-NMR spectroscopy. The ^{1}H-NMR spectra (4-5 ppm region) of the $(BD_{70}EG_{30})_{feed}$ mixture and $(BD_{70}EG_{30})_{ssp}$ copolymers are shown in Figure 6.6a. Peaks (a) and (b) originate from free BHET monomer (see Figure 6.1 for peak assignments). In agreement with the previously discussed SEC results, shown in Figure 6.5a, it can be observed that the free PBT monomer rapidly decreases as the SSP reaction proceeds. After t_{ssp} = 15 min, peak (a) and (b) have disappeared almost completely, whereas a new peak (c) has formed at 4.8 ppm. Peaks (c) originate from CH_2 protons situated between two carbonyl groups (see Figure 6.1). For each $(BD_{70}EG_{30})_{ssp}$ sample, this set of overlapping peaks is magnified and shown in Figure 6.6b. It can be seen that as the SSP reaction proceeds, peak (c) splits up into a triplet. This peak splitting was already observed by Asakura and co-workers, who used ^{1}H-NMR triad sequence distribution analysis to study the transesterification reactions in molten PET-PBT blends as a function of reaction time.[21-22]

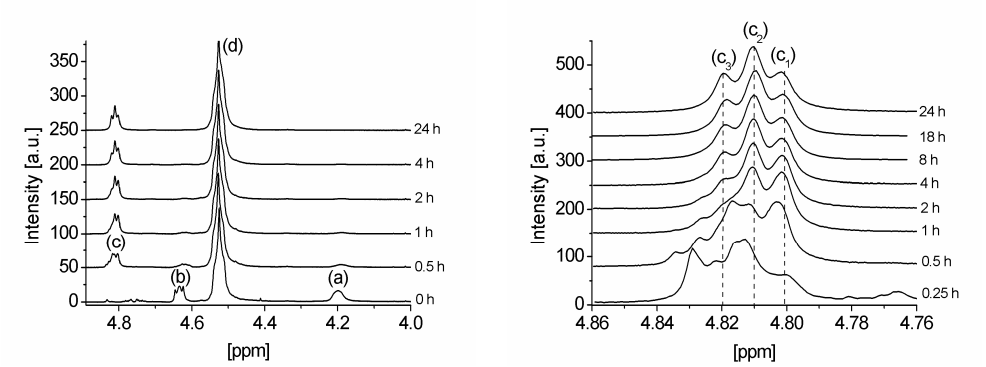

(a) (b)

Figure 6.6. (a) ^{1}H-NMR spectra of the $(BD_{70}EG_{30})_{ssp}$ copolymers with different values for t_{ssp}: (a) 4-5 ppm region (b) Magnification of ^{1}H-NMR peak (c) present at 4.81 ppm. For identification of the peaks is referred to Figure 6.1.

Each peak corresponds to a triad sequence: c_1 = ETETE, c_2 = ETETB, c_3 = BTETB, where E represents an ethylene glycol unit, B a butane-diol unit and T a terephthalate unit. The chemical resolution of the spectra shown in Figure 6.6a is not as high as the spectra presented in the work of Asakura and co-workers who used an operating frequency of 600 MHz. They could also observe that the proton signal of the -CH2- group originating from the BD-T repeat-unit (peak (d) in Figure 6.6a) split up into multiple peaks due to long-range coupling of adjacent moieties. This peak splitting is not observed in the ^{1}H-NMR spectra shown in Figure 6.6a. In addition, the resolution of the peak splitting as shown in Figure 6.6b is not high enough to use the results in a quantitative way. However, the observed change in triplet shape as a function of t_{ssp} gives qualitative information about the mechanism of the BHET incorporation into PBT. From the $(BD_{70}EG_{30})_{ssp}$ sample with t_{ssp} = 15 min it can be seen that first peak c_1 is formed, indicating that self-condensation of BHET occurs in the initial stage of the reaction. The sharp peak present at 4.83 ppm is probably the result from triad sequences with a hydroxyl end groups attached to it. At t_{ssp} = 0.5 h, peak c_1 has tremendously increased whereas the peak at 4.83 ppm has almost disappeared. Also peak c_2, representing ETETB sequences, has just appeared which is an indication that BHET has reacted with amorphous PBT chain segments by (outer-inner) alcoholysis reactions. These alcoholysis reactions result in chain scission of the amorphous homopolymer PBT chain segments. As the reaction proceeds, the peak ratio $(c_1)/(c_2)$ slowly decreases. Hence, peak c_2 gradually increases with respect to peak c_1. This result indicates that the (outer-inner) alcoholysis reaction between BHET monomer and amorphous PBT chain segments proceeds at a slower rate than the self-

condensation of BHET monomer. At t_{ssp} = 1 h, all free BHET monomer has disappeared (see SEC chromatograms in Figure 6.5a), and peak c_3, representing BTETB sequences, appears. The size of peak c_3 gradually increases as the SSP-reaction proceeds which might result from the coupling of amorphous PBT chain segments. The molecular weight should then increase which is also observed from the SEC measurements, presented in Figure 6.5.

The reaction mechanism of the BHET incorporation into PBT was also studied by quantitative ^{13}C-NMR sequence distribution analysis. In Figure 6.7, the degree of randomness $R_{ssp,\ total}$ (see eq 6.4) is plotted as a function of t_{ssp}.

The initial low value for $R_{ssp,\ total}$ at t_{ssp} = 0.5 h is due to the presence of a large fraction of ETE dyad sequences (see eq 6.4) which is in agreement with the results from the ^{1}H-NMR triad sequence analysis. However, $R_{ssp,\ total}$ rapidly increases between $0 < t_{ssp} \leq 2$ h. This increase is due to the formation of BTE sequences (see eq 6.4), which was also observed as an increase of peak c_2 in Figure 6.6b. When $t_{ssp} > 2$ h, $R_{ssp,\ total}$ still increases but at a lower rate. This might be attributed to a continuous chain coupling of short amorphous PBT chain segments which is supported by the increase of the continuous increase of the $\overline{M}_n$ (see Figure 6.5a and b) and increase of the BTETB sequence (peak c_3 in Figure 6.6b).

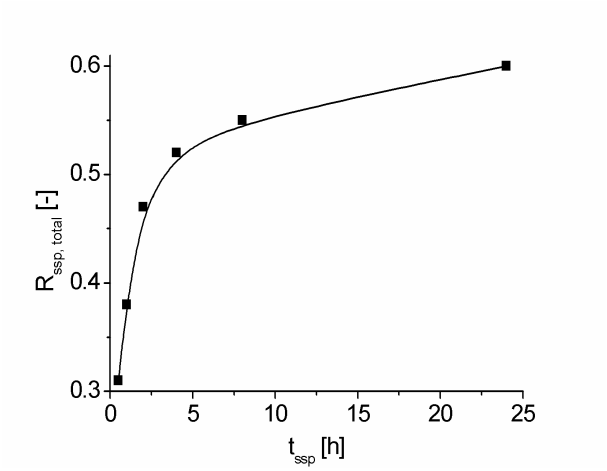

Figure 6.7. Degree of randomness $R_{ssp,\ total}$ as a function of t_{ssp} obtained via quantitative ^{13}C-NMR spectroscopy measurements.

6.3.3 Thermal properties of PBT-BHET copolymers

The aim of the work presented in this thesis is to obtain a copolymer based on PBT that has a higher T_g than the homopolymer, but with a similar crystallization behavior. The results from the ^{1}H-NMR and ^{13}C-NMR sequence distribution analysis showed that the chemical

microstructure of the $(BD_xEG_y)_{ssp}$ copolymers differs from the $(BD_xEG_y)_{mp}$ copolymers. It can therefore be expected that also a difference in thermal properties will be observed. The glass transition temperature (T_g), melting temperature (T_m) and crystallization behavior were studied in detail by DSC. The first DSC heating runs of the synthesized $(BD_xEG_y)_{ssp}$ copolymers are shown in Figure 6.8. The crystalline fractions ($\chi_{heating}$) of the $(BD_xEG_y)_{ssp}$ copolymers are also given in the same figure. The $(BD_{100}EG_0)_{ssp}$ copolymer represents a PBT homopolymer after HFIP solvent treatment and subsequent polymerization in the solid state. For all DSC traces shown in Figure 6.8, no recrystallization was observed upon heating.

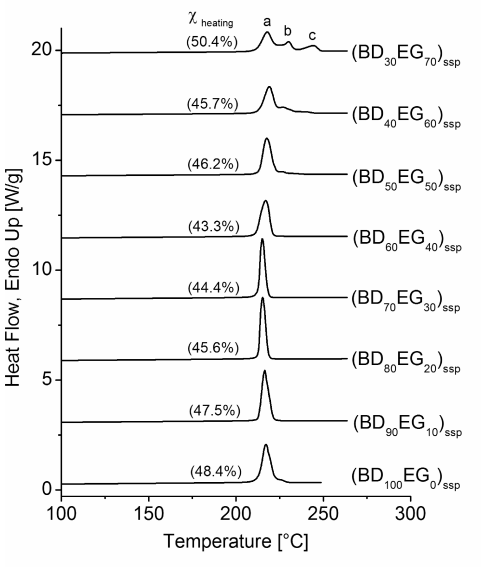

Figure 6.8. First DSC heating runs of the synthesized $(BD_xEG_y)_{ssp}$ copolymers. DSC curves are shifted vertically for clarity. For each DSC-trace, the crystallinity $\chi_{heating}$ is given.

It can be seen T_m value of the $(BD_{100}Di_0)_{ssp}$ homopolymer is significantly lower than generally reported in literature (220 °C < T_m < 230 °C).[17] A similar result was observed for the $(BD_xDi_y)_{ssp}$ copolymers, discussed in **Chapter 5**. It was shown in **Chapter 4** that the $(BD_{100}Di_0)_{ssp}$ homopolymer has a very low mobile amorphous fraction ($\alpha_{mobile} \approx 0.15$) after SSP. Apparently, this low fraction of mobile amorphous PBT does not lead to the reorganization process resulting in melting and recrystallization, which normally occurs during heating. It will be shown later in this paragraph that after cooling from the melt and subsequent reheating, the T_m value is in agreement with the values mentioned in literature.

For the $(BD_xEG_y)_{ssp}$ copolymers with $100 < x \leq 70$ (i.e. $100 < F_{BD\text{-}T,\ total}\ x \leq 84$ mol%), the width of the PBT melting peak gradually narrows, whereas for $x \leq 40$ the melting peak

broadens again. The sharpening of the melting peaks indicates a narrower lamellar thickness distribution. As previously discussed, BHET monomer is fully miscible with the amorphous PBT phase for $(BD_xEG_y)_{feed}$ mixtures with x ≥ 70 mol% BD (i.e. F_{PBT} ≥ 84 mol%). The miscible fraction of BHET will react by (outer-inner) alcoholysis reactions with the PBT chain segments present in the mobile amorphous fraction (α_{mobile}) in the initial stages of the SSP-process. The mobile amorphous PBT chains will be cleaved resulting in an overall increased mobility of the PBT system. During the SSP-reaction, this increased mobility may promote the crystal perfectioning process resulting in narrower melting endotherms.

As observed from the miscibility study (see Figure 6.3), a separate BHET phase is formed for $(BD_xEG_y)_{feed}$ mixtures with x < 70 mol% BD (i.e. F_{PBT} < 84 mol%). The BHET present in this phase forms homopolymer PET blocks during SSP as verified by the ^{1}H-NMR and ^{13}C-NMR sequence distribution analyses. When these PET blocks are of sufficient length, lamellar crystals may be formed. Marchese and co-workers found for PET that the minimum block length for crystallization is 31 repeat-units.[23] Small crystalline PET crystals, having low melting temperatures, may be formed for the $(BD_{60}EG_{40})_{ssp}$ copolymer. The presence of small PET crystals becomes more pronounced for the $(BD_xEG_y)_{ssp}$ copolymers with x < 60 for which small endotherms become visible after the melting endotherm of PBT. This tail subsequently develops into two clearly separated endotherms as the BHET fraction used for incorporation is further increased (see DSC trace of the $(BD_{30}EG_{70})_{ssp}$ copolymer). These two additional peaks are denoted as peak (b) and peak (c) and have a T_m of 230 °C and 244 °C respectively. Probably two different populations of crystals are formed.

The previously mentioned increase of the lamellar crystal thickness for $(BD_xEG_y)_{ssp}$ copolymers with x ≥ 70 and the formation of PET crystals for $(BD_xEG_y)_{ssp}$ copolymers with x ≤ 60 may be observed from Small-Angle X-ray Scattering measurements (SAXS). The SAXS patterns were analyzed by the one-dimensional correlation function[24] applied to a finite lamellar stack model to result in the long period (L_p), the average crystal thickness (l_χ) and average amorphous thickness (l_α) of the $(BD_xEG_y)_{ssp}$ copolymers. These morphological parameters are plotted in Figure 6.9 as a function of $F_{BD\text{-}T,\ total}$ in the $(BD_xEG_y)_{ssp}$ copolymer.

The analysis of the SAXS patterns is described in detail in **Chapter 5**. It has to be mentioned here that the SAXS patterns used in this chapter could not give a distinction between mobile amorphous phase and rigid amorphous phase as was done by Hong and co-workers for poly(trimethylene terephthalate).[25] The rigid amorphous fraction should have a slightly higher electron density than the mobile amorphous fraction. For the SAXS analysis, described in **Chapter 5**, it was therefore assumed that the rigid amorphous thickness should mainly contribute to the average crystal thickness l_χ. The ratio l_χ / L_p, which is often used as the value for crystallinity obtained by SAXS, is larger than the crystallinity values obtained via the

melting enthalpies of the DSC heating traces (see Figure 6.8). Hence, the assumption that the average thickness of the rigid amorphous fraction predominantly contributes to l_χ may be justified.

From Figure 6.9, it can be seen that L_p gradually increases for decreasing values of $F_{BD\text{-}T,\ total}$ to reach a maximum value for $F_{BD\text{-}T,\ total} \approx 76$ mol%. This composition corresponds to a $(BD_{60}EG_{40})_{ssp}$ copolymer. Similarly, l_χ reaches a maximum value for $F_{BD\text{-}T,\ total} \approx 76$ mol%, whereas l_α does not significantly change over the analyzed composition range.

The increase of L_p and concomitant increase of l_χ for $100 \leq F_{BD\text{-}T,\ total} \leq 76$ mol% may be due to crystal perfectioning, which is in agreement with the DSC results shown in Figure 6.8. The decrease of L_p and l_χ for $F_{BD\text{-}T,\ total} < 76$ mol% is due to the formation of small PET crystals (see DSC traces in Figure 6.8), present in a separate phase with its own electron density distribution, between the lamellar PBT stacks.

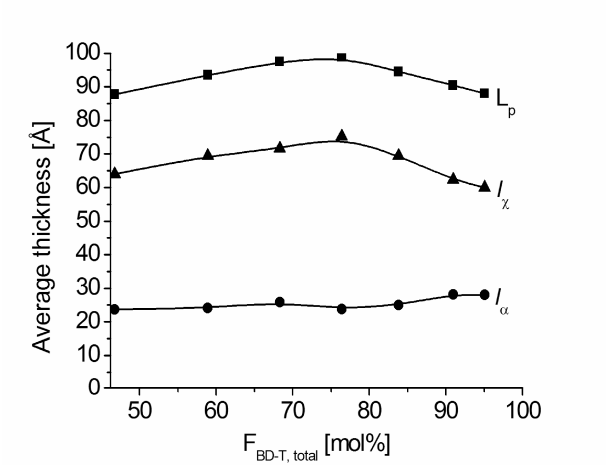

Figure 6.9. Long period (L_p), average crystal thickness (l_χ), average mobile thickness (l_α) of the synthesized $(BD_xEG_y)_{ssp}$ copolymers as obtained from SAXS measurements.

The DSC cooling runs of the synthesized $(BD_xEG_y)_{ssp}$ copolymers are shown in Figure 6.10a. It can be seen that the crystallization peak shifts to lower temperatures and becomes broader when more BHET is incorporated. On the contrary, Avramova[6] showed that for blends of PBT and PET, which are fully miscible in the melt, separate PBT and PET crystals are formed without disturbing the crystallization process of the other component. For the $(BD_xEG_y)_{ssp}$ copolymers however, the decrease of the crystallization temperature (T_c) as is observed from the DSC cooling runs presented in Figure 6.10a, indicates that nucleation is delayed upon

cooling from the melt. Hence, the former crystalline homopolymer PBT segments, which adopt a random coil configuration in the molten state, have difficulties to organize themselves in lamellar crystals upon cooling due to the miscibility with the modified polymer chain segments. Furthermore, the peak broadening, which increases with increasing fraction of incorporated BHET, shows that diffusion of homopolymer PBT chain segments to the crystal growth front is hindered. This limited diffusion process is also due to the miscibility of the homopolymer PBT blocks with the modified polymer chain segments consisting of both BD-T and EG-T repeat units.

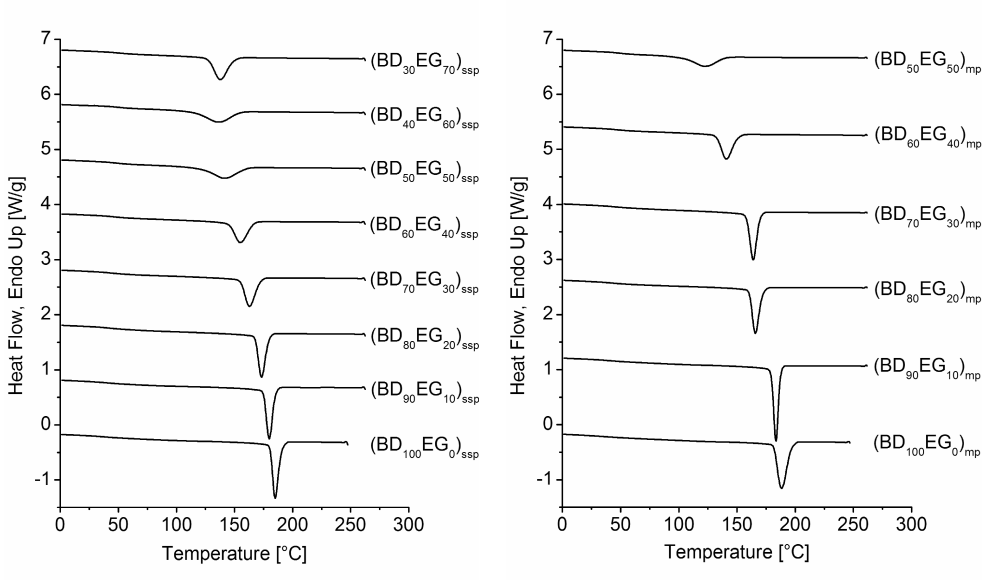

(a) (b)

Figure 6.10. DSC cooling runs of (a) the synthesized $(BD_xEG_y)_{ssp}$ copolymers and (b) of the synthesized $(BD_xEG_y)_{mp}$ copolymers. DSC curves are shifted vertically for clarity.

An interesting crystallization behavior is observed for the $(BD_{30}EG_{70})_{ssp}$ copolymer. The crystallization peak is sharper and appears at a higher temperature than the peaks of the $(BD_{40}EG_{60})_{ssp}$ and $(BD_{50}EG_{50})_{ssp}$ copolymers. Apparently, the crystallization process of the PET homopolymer fraction is enhanced by faster-crystallizing PBT blocks which act as nucleation sites for the subsequent crystallization of PET. This synergistic effect was also observed by Misra et al.[7] for PBT-PET block copolymers. When these block copolymers contained a small fraction of PBT blocks (approximately 5 wt%), the PET homopolymer crystallized about 5 times faster than pure PET. Although beyond the scope of this research project, the incorporation of a small fraction of bis(4-hydroxybutyl)terephthalate (BHBT)

monomer in homopolymer PET using the solid-state copolymerization process as described in this chapter for the PBT-BHET system, may easily improve the crystallization behavior of PET.

The DSC cooling runs of the synthesized $(BD_xEG_y)_{mp}$ copolymers are shown in Figure 6.10b. Also here, the crystallization temperature of the peaks decreases for an increased fraction of incorporated BHET. However, the crystallization peaks of the $(BD_xEG_y)_{mp}$ copolymers are in general less broad than those of $(BD_xEG_y)_{ssp}$ copolymers with similar composition. This difference is due to the significantly lower $\overline{M}_n$-value of the $(BD_xEG_y)_{mp}$ copolymers (see **Chapter 3**),[11] resulting in a decreased melt viscosity.

The second heating runs of the $(BD_xEG_y)_{ssp}$ copolymers and $(BD_xEG_y)_{mp}$ copolymers are shown in Figures 6.11a and 6.11b, respectively.

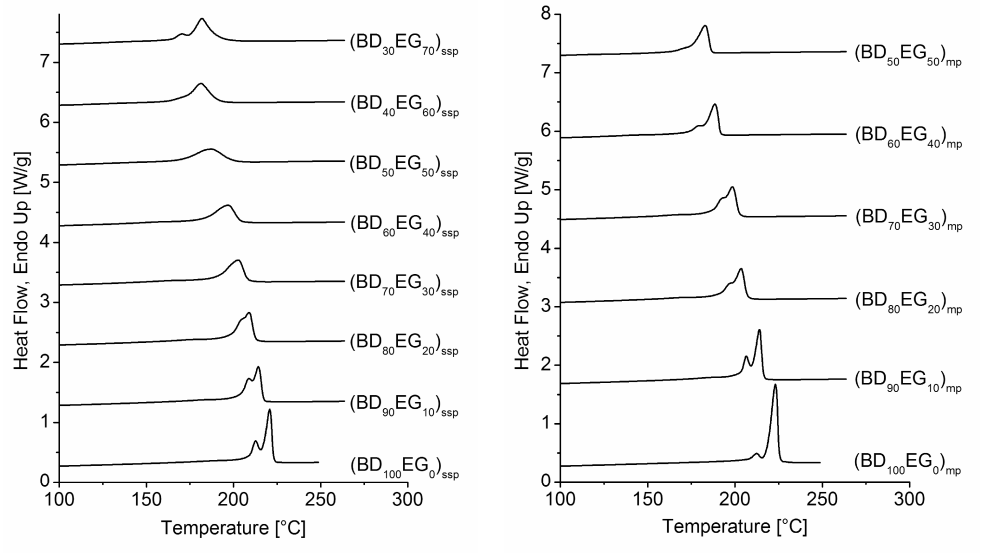

(a) (b)

Figure 6.11. Second DSC heating runs of (a) the synthesized $(BD_xEG_y)_{ssp}$ copolymers and (b) of the synthesized $(BD_xEG_y)_{mp}$ copolymers. DSC curves are shifted vertically for clarity.

It can be seen that the melting behavior of the $(BD_xEG_y)_{ssp}$ copolymers closely resembles the melting behavior of the $(BD_xEG_y)_{mp}$ copolymers. This result is remarkable because it was expected that incorporation of BHET by solid-state copolymerization results in a better crystallization behavior compared to that of $(BD_xEG_y)_{mp}$ copolymers. Hence, a blocky chemical microstructure is not sufficient to result in a retained crystallization behavior. Once

in the molten state, the unmodified former crystalline homopolymer PBT blocks should not be miscible with the modified former mobile amorphous chain segments to successively result in a high crystallization rate. A double PBT melting peak is observed in the DSC traces of the $(BD_{100}EG_0)_{ssp}$ and $(BD_{100}EG_0)_{mp}$ copolymer but also in the DSC traces of the (BD_xEG_y) copolymers with a low fraction of incorporated BHET. Most recent research showed that the double melting peak behavior is probably due to a reorganization process occurring during the DSC heating run, resulting in melting and recrystallization of less perfect crystals into thicker and more perfect crystals.[17,26-27] It can also be observed that the T_m of the $(BD_{100}Di_0)_{ssp}$ homopolymer is approximately 221 °C for the second heating run and hence is in agreement with the values mentioned in literature.[17]

The synthesized $(BD_xEG_y)_{ssp}$ and $(BD_xEG_y)_{mp}$ copolymers were also measured by modulated DSC. The reversing c_p signals of the $(BD_xEG_y)_{ssp}$ copolymers are plotted in Figure 6.12a. The corresponding values for the T_g are shown in Table 6.1. Also the end composition of each copolymer, obtained via ^{1}H-NMR spectroscopy (see **Chapter 3**) is given in this table.

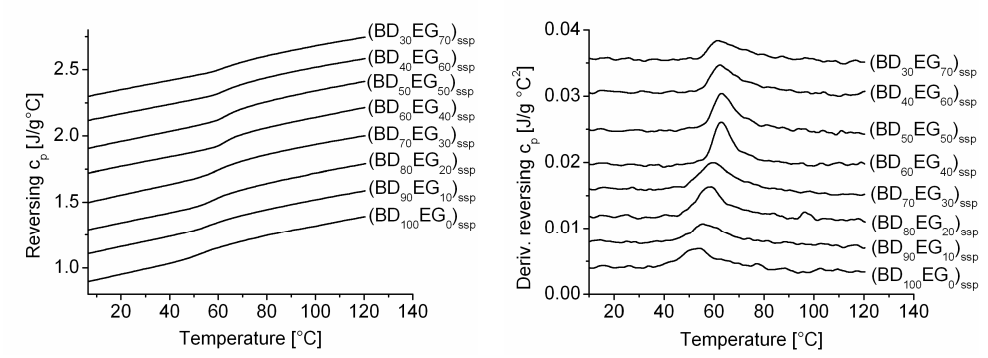

(a) (b)

Figure 6.12. (a) First heating run reversing c_p traces and (b) corresponding derivative values of the synthesized $(BD_xEG_y)_{ssp}$ copolymers. Traces are shifted vertically for clarity.

It can be seen that the T_g gradually increases as more BHET is incorporated. As soon as the homopolymer PET folds into lamellar crystals, as observed for $(BD_xEG_y)_{ssp}$ copolymers with $x \leq 60$ (see DSC traces shown in Figure 6.8), the T_g decreases again. Furthermore, it can be seen that the derivative values of the reversing c_p traces, presented in Figure 6.12b, form a Gaussian peak shape for the $(BD_xEG_y)_{ssp}$ copolymers with a low fraction of incorporated BHET (i.e. $x > 70$; $F_{BD\text{-}T,\,total} > 84$ mol%).

Table 6.1. T_g values obtained by modulated DSC for the $(BD_xEG_y)_{ssp}$ and $(BD_xEG_y)_{mp}$ copolymers.

Composition $(BD_xEG_y)_{feed}$ mixtures		Composition		heating run 1 T_g [°C]	heating run 2 T_g [°C]	
		$(BD_xEG_y)_{ssp}$	$(BD_xEG_y)_{mp}$			
x	y	$F_{BD\text{-}T,\ total}$	$F_{BD\text{-}T,\ total}$	SSP	SSP	MP
100	0	100	100	54.9	40.7	39.1
90	10	95	93	54.9	42.4	43.8
80	20	91	84	57.8	43.6	43.5
70	30	84	79	60.1	46.7	46.5
60	40	76	69	62.6	50.9	49.3
50	50	68	60	62.5	53.0	53.6
40	60	59		61.8	53.0	
30	70	47		61.5	53.4	

When the fraction of incorporated BHET increases, it can be seen that a sharp peak is formed on top of the initially present broad peak. Hence a bimodal distribution is present which is due to the formation of a separate fraction of PET homopolymer. The peak becomes broader again when the PET homopolymer forms its own crystalline phase (see derivative reversing c_p traces of $(BD_{40}EG_{60})_{ssp}$ and $(BD_{30}EG_{70})_{ssp}$ copolymers in Figure 6.12b).

In Figure 6.13a and b, the reversing c_p traces and the derivative values of the reversing c_p signal corresponding to the second heating run are shown for the $(BD_xEG_y)_{ssp}$ copolymers. For the second heating run, the (BD_xEG_y) copolymers were crystallized from the melt using a cooling rate of 10 °C/min and subsequently reheated in modulated mode. For all (BD_xEG_y) copolymers, only one T_g was observed. Also Avramova, who studied the miscibility of PET-PBT blends, observed one T_g for these blends upon heating.[6] Hence, PET and PBT are fully miscible in the amorphous phase. From Table 6.1, it can be observed that the T_g values of the $(BD_xEG_y)_{ssp}$ copolymers are considerably lower for the second heating runs compared to the first heating runs. This decrease of the T_g values is due to the lower crystallinity of the $(BD_xEG_y)_{ssp}$ copolymers after crystallization from the melt compared to the crystallinity present directly after SSP (compare DSC traces of Figure 6.8 and 6.11a). As a consequence, the fraction of homopolymer PBT chain segments present in the amorphous phase is higher for the second heating run compared to the first heating run, resulting in lower T_g values.

The T_g values of the $(BD_xEG_y)_{ssp}$ copolymers for the second heating run are not so much different from the values obtained for the $(BD_xEG_y)_{mp}$ copolymers as can be observed from Figure 6.14a. Also the derivative curvatures of the reversing c_p traces, shown in 6.13b, are comparable to those of the $(BD_xEG_y)_{mp}$ copolymers which are plotted in 6.14b. Hence, the T_g

increasing effect of BHET does not only depend on the chemical microstructure when copolymers, obtained by SSP, are fully miscible in the melt.

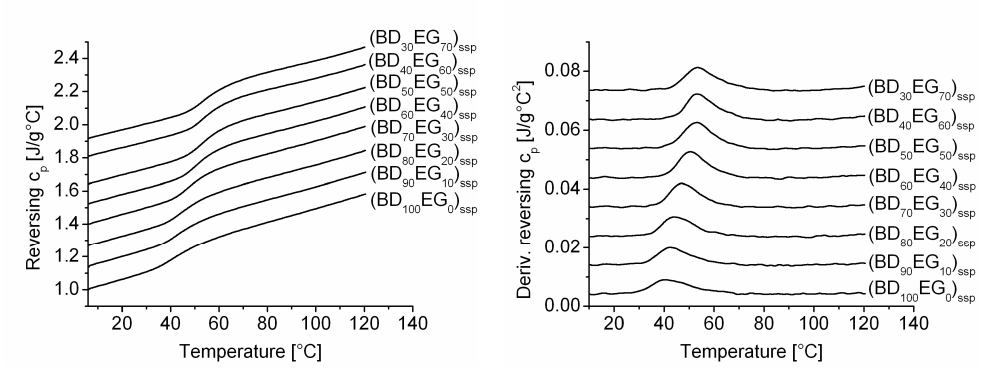

(a) (b)

Figure 6.13. (a) Second heating run reversing c_p traces and (b) corresponding derivative values of the synthesized $(BD_xEG_y)_{ssp}$ copolymers. Traces are shifted vertically for clarity.

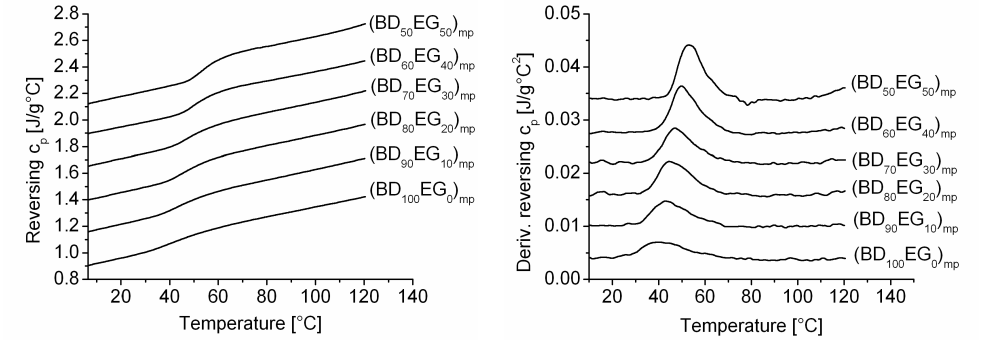

(a) (b)

Figure 6.14. (a) Second heating run reversing c_p traces and (b) corresponding derivative values of the synthesized $(BD_xEG_y)_{mp}$ copolymers. Traces are shifted vertically for clarity.

6.4 Conclusions

^{13}C-NMR sequence distribution analysis of $(BD_xEG_y)_{ssp}$ copolymers showed that the BHET fraction incorporated in the amorphous PBT phase was constant over a broad composition range (for 55 mol% < $F_{BD\text{-}T,\ total}$ < 84 mol %). From DSC-measurements, it was observed for $(BD_xEG_y)_{feed}$ mixtures, used as feed for SSP, that BHET monomer is only partly miscible

with the amorphous PBT phase. The BHET fraction not miscible forms a separate phase. During SSP, only the miscible BHET fraction reacts with PBT chain segments via transesterification reactions. The BHET fraction present as a separate phase forms PET homopolymer by self-polycondensation reactions. SEC-measurements show that the BHET monomer, present in the $(BD_xEG_y)_{feed}$ mixtures, has completely reacted within 1 hour. It was observed from ^{1}H-NMR sequence distribution analysis that the self-condensation of BHET, resulting into PET homopolymer, proceeds at a higher rate than the transesterification of BHET monomer with amorphous PBT chain segments. Quantitative ^{13}C-NMR sequence distribution analysis showed that a blocky microstructure is present in the initial stage of the SSP-reaction, which rapidly becomes more random. The initial blocky microstructure ($R_{ssp, total} \approx 0.31$) is a clear indication that PET homopolymer chain segments are formed in the initial stage of the SSP-reaction. A similar microstructure development was observed from the ^{1}H-NMR sequence distribution analysis. In addition, $R_{ssp, total}$ rapidly increases during the first 2 hours of the reaction which is due to the transesterification reactions of the miscible BHET fraction with the amorphous PBT chain segments. After approximately 2 hours of reaction, the increase of $R_{ssp, total}$ proceeded more gradually. This gradual increase is due to chain recombination in the amorphous PBT phase, which is also observed from the continuous increase of the $\overline{M}_n$ values.

SAXS measurements showed for $(BD_xEG_y)_{ssp}$ copolymers with small fractions of incorporated BHET an increase of the lamellar crystal thickness and concomitant increase of the long period. When $(BD_xEG_y)_{feed}$ mixtures with large fractions of BHET are polymerized in the solid state, the homopolymer PET chain segments formed during SSP become large enough to form separate crystals. This formation of PET crystals results in a decrease of the long period as observed from the SAXS measurements. The formation of PET crystals for large fractions of BHET was also observed from DSC-measurements of a $(BD_{40}EG_{60})_{ssp}$ and $(BD_{30}EG_{70})_{ssp}$ copolymer which show additional melting endotherms at approximately 230 and 240 °C for the first heating run. These two melting endotherms may be due to different populations of PET crystals. Although clear differences in chemical microstructure were obtained between $(BD_xEG_y)_{ssp}$ copolymers and $(BD_xEG_y)_{mp}$ copolymers (non-random and random, respectively), the thermal behavior observed by DSC was not significantly different. Similar to the PBT-Dianol copolymers discussed in **Chapter 5**, the modified PBT segments of the $(BD_xEG_y)_{ssp}$ copolymers are fully miscible with the unmodified homopolymer PBT chain segments when the copolymers are in the molten state. Due to the significantly higher $\overline{M}_n$ values of the $(BD_xEG_y)_{ssp}$ copolymers compared to the $(BD_xEG_y)_{mp}$ copolymers, even a slightly higher nucleation temperature and crystal growth rate were observed for the random $(BD_xEG_y)_{mp}$ copolymers. Modulated DSC measurements showed that for the $(BD_{60}EG_{40})_{ssp}$ and $(BD_{50}EG_{50})_{ssp}$ copolymers, two overlapping T_g's were observed from the first heating run.

Hence, the formed homopolymer PET chain segments, present in a separate phase, are still amorphous and consequently exhibit its own T_g. As soon as the PET chain segments become long enough to form separate crystals, the two T_g's are no longer visible. The T_g values corresponding to the second heating run are for both $(BD_xEG_y)_{ssp}$ and $(BD_xEG_y)_{mp}$ copolymers in the same range.

In conclusion, a high crystallization rate in combination with a high T_g may only be obtained when the modified chain segments in the molten state are immiscible with the unmodified homopolymer PBT blocks.

6.5 References and notes

1. Radusch, H.-J. in *Handbook of Thermoplastic Polyesters*, Fakirov, S., Ed.; Wiley-VCH, Weinheim, 2002, Chapter 8, p 389-418.
2. Gupta, V. B.; Bashir, Z. In *Handbook of Thermoplastic Polyesters*, Fakirov, S., Ed.; Wiley-VCH, Weinheim, 2002, Chapter 7, p 317-382.
3. Backson, S. C. E., Kenwright, A. M., Richards, R. W. *Polymer* **1995**, *36*, 1991-1998.
4. Jacques, B.; Devaux J.; Legras R.; Nield, E. *J. Polym. Sci., Polym. Chem. Ed.* **1996**, *34*, 1189-1194.
5. Kim, J. H.; Lyoo, W. S.; Ha, W. S. *J. Appl. Polym. Sci.* **2001**, *82*, 159-168.
6. Avramova, N. *Polymer* **1995**, *36*, 801-808.
7. Misra, A.; Garg, S. N. *J. Polym. Sci., Polym. Phys. Ed.* **1986**, *24*, 983-997.
8. Fakirov, S. In *Solid State Behavior of Linear Polyesters and Polyamides*, Schultz, J. M., Fakirov, S., Eds.; Prentice Hall: Englewood Cliffs, NJ, 1990; Chapter 2, p 19-43.
9. James, N. R., Ramesh, C.; Sivaram, S. *Macromol. Chem. Phys.* **2001**, *202*, 1200-1206.
10. James, N. R., Ramesh, C.; Sivaram, S. *Macromol. Chem. Phys.* **2001**, *202*, 2267-2274.
11. Jansen, M. A. G.; Goossens, J. G. P.; de Wit, G.; Bailly C.; Koning, C. E. *Anal. Chim. Acta* **2005**, in press.
12. Tomita, K. *Polymer* **1973**, *14*, 50-54.
13. Lin, C.-C.; Baliga, S. *J. Appl. Polym. Sci.* **1986**, *31*, 2483-2489.
14. Conix, A.; Van Kerpel, R. *J. Polym. Sci.* **1959**, *40*, 521-532.
15. Kirshenbaum, I. J. *J. Polym. Sci., Part A* **1965**, *3*, 1869-1875.
16. ATHAS database: Wunderlich, B. *Pure and Applied Chemistry* **1995**, *67*, 1019-1026
17. Cheng, S. Z. D.; Pan, R.; Wunderlich, B. *Makromol. Chem.* **1988**, *21*, 789-797.
18. Montaudo, G.; Puglisi, C.; Samperi, F. In *Transreactions in Condensation Polymers*, Fakirov S., Ed.; Wiley-VCH: Weinheim, 1999; Chapter 4, p 159-193.
19. Jansen, M. A. G.; Goossens, J. G. P.; de Wit, G.; Bailly, C.; Schick, C.; Koning, C. E. *Macromolecules* **2005**, accepted.
20. Jansen, M. A. G.; Goossens, J. G. P.; de Wit, G.; Bailly, C.; Koning, C. E. *Macromolecules* **2005**, *38*, 2659-2664.
21. Matsuda, H.; Asakura, T.; Miki, T. *Macromolecules* **2002**, *35*, 4664-4668.
22. Matsuda, H.; Asakura, T.; Nagasaki, B.; Sato, K. *Macromolecules* **2004**, *37*, 4651-4657.

23. Marchese, P.; Celli, A.; Fiorini, M. *J. Polym. Sci., Polym. Phys. Ed.* **2004**, *42*, 2821-2832.
24. Strobl, G. R.; Schneider, M. *J. Polym. Sci., Polym. Chem. Ed.* **1980**, *18*, 1343-1359.
25. Hong, P.-D.; Chuang, W.-T.; Yeh, W.-J.; Lin, T.-L. *Polymer* **2002**, *43*, 6879-6886.
26. Yeh, J. T.; Runt, J. *J. Polym. Sci., Polym. Phys. Ed.* **1989**, *27*, 1543-1550.
27. Yasuniwa, M.; Tsubakihara, S.; Ohoshita, K.; Tokudome, S. *J. Polym. Sci., Polym. Phys. Ed.* **2001**, *39*, 2005-2015.

Chapter 7
Incorporation of 2,2'-biphenyldimethanol in PBT via solid-state copolymerization and melt copolymerization

7.1 Introduction

Hitherto, solid-state polymerization (SSP) has mainly been used to increase the molecular weight of semi-crystalline polycondensates.[1] With SSP, the used reaction temperature is just below the melting temperature (T_m) of the polymer but far above its glass transition temperature (T_g). Consequently, polymer chain segments present in the amorphous phase become sufficiently mobile for transesterification reactions to occur, whereas the chain segments present in the crystalline phase are not mobile enough for participation in the transesterification process. Hence, the crystalline polymer chain segments will remain unchanged.

In the previous chapters, it was shown that SSP can also be used to synthesize copolymers by incorporation of diol monomers in semi-crystalline poly(butylene terephthalate) (PBT).[2,3] The main advantage of copolymerization in the solid state is that the diol monomer is only incorporated in the mobile amorphous polymer chain segments whereas the crystalline chain segments remain unchanged. In this way, polymer properties can be enhanced by selective modification of the amorphous phase, while the crystallization behavior is expected to be preserved due to the presence of large crystallizable homopolymer blocks.

In **Chapters 2** and **3**, the incorporation of 2,2-bis[4-(2-hydroxyethoxy)phenyl]propane (Dianol 220®) and bis(2-hydroxyethyl)terephthalate (BHET) into PBT via SSP was described in detail.[2,3] For comparison, these diols were also incorporated by copolymerization in the melt (MP). The ^{13}C-NMR sequence distribution analysis showed that the copolymers obtained by MP have a fully random chemical microstructure, while the copolymers obtained by SSP have a non-random and more blocky chemical microstructure.[3]

It was shown in **Chapter 4** that the morphology of the PBT copolymers obtained by SSP can be represented by a three-phase model,[4] which is often used to describe the morphology of semi-crystalline polymers, consisting of a crystalline phase and an amorphous phase which can be subdivided into a rigid amorphous fraction and a mobile amorphous fraction.[5-9]

Furthermore, the calculation method developed and explained in **Chapter 4** showed that both Dianol and BHET are only incorporated in the mobile amorphous PBT chain segments, whereas the rigid amorphous chain segments remained unchanged.[4]

In **Chapters 5** and **6**, it was shown by Differential Scanning Calorimetry (DSC) measurements that the final chemical microstructure of the SSP copolymers partly depends on the initial mobile amorphous and rigid amorphous fractions of the PBT-diol powder mixtures used as feed material for the SSP-reactions. These fractions are mainly determined by the miscibility of the diol monomer with the amorphous PBT phase. Consequently, the diol monomers used for incorporation indirectly have a large influence on the final chemical microstructure and therefore also on the final thermal properties of the copolymer obtained after SSP. It has to be remarked here that also the way of mixing PBT with Dianol (solution mixing or pre-melt mixing) has an influence on the initial size of the crystalline fraction, rigid amorphous fraction and mobile amorphous fraction and thus also on the final chemical microstructure present after SSP.

A DSC study of the thermal properties showed that the difference in thermal properties between PBT copolymers obtained by SSP and MP was much less than expected. For both PBT-Dianol and PBT-BHET copolymers obtained by SSP, a decrease in crystallinity and crystallization rate with respect to PBT homopolymer was observed. This effect was more pronounced for increased fractions of incorporated comonomer. Hence, the presence of long crystallizable PBT blocks as verified from the ^{13}C-NMR measurements could not preserve the original crystallization behavior of PBT. The decreased crystallinity and crystallization rate can predominantly be ascribed to the miscibility of these homopolymer PBT blocks with the modified PBT segments when the copolymer is in the molten state. Upon cooling, the nucleation is delayed and the growth of these nuclei to lamellar crystal structures is retarded.

Sakaguchi and co-workers[10] incorporated rigid rod-like 4.4'-biphenol monomers in polyethylene terephthalate (PET). The chemical microstructure of these copolymers was fully random. A significant increase of the nucleation rate was observed when these copolymers were cooled from the melt. Isothermal crystallization from the melt at different crystallization temperatures was studied by time-resolved Small-Angle Light Scattering (SALS) measurements. An intense scattering at low angles was observed for the PET copolymer with 8 mol% of incorporated 4,4'-biphenol monomer when the copolymer was still in its molten state. The enhanced nucleation rate of PET was explained by local ordering of the polymer chains, containing the rigid comonomer segments, in the melt.

In the present chapter, the incorporation of 2,2'-biphenyldimethanol (BDM) into PBT via SSP and MP is discussed. The rigid rod-like structure of BDM may increase the glass transition temperature (T_g) after incorporation and concomitantly may increase the nucleation rate upon

cooling the copolymer from the melt. The influence of BDM on the morphology of the PBT-BDM mixtures used as feed for the SSP-reactions is studied by Differential Scanning Calorimetry (DSC). The thermal properties of the PBT-BDM copolymers obtained via SSP and MP are examined by DSC and compared with the earlier examined PBT-Dianol and PBT-BHET copolymers. During cooling from the melt, the expected BDM-containing blocky microstructure may trigger a local ordering of the melt and subsequently result in a higher nucleation rate from the melt compared to the previously synthesized PBT-Dianol and PBT-BHET copolymers.

7.2 Experimental Section

7.2.1 Materials

Poly(butylene terephthalate) (PBT) pellets ($\overline{M}_n$ = 15 kg/mol and $\overline{M}_w$ = 34 kg/mol, determined by size exclusion chromatography) were provided by GE Plastics (Bergen op Zoom, The Netherlands) and used as received. 2,2'-biphenyldimethanol (98%) was obtained from Aldrich and used as received. For NMR measurements, deuterated trifluoro acetic acid (TFA-d, 99 % deuterated) was obtained from Aldrich and deuterated chloroform ($CDCl_3$, 99 % deuterated) was obtained from Merck.

7.2.2 Synthesis of PBT-BDM copolymers: solid-state copolymerization (SSP) and melt copolymerization (MP

Copolyesters of PBT and BDM were obtained via SSP and MP. Both SSP and MP methods were described in detail in **Chapter 3** and will be only briefly discussed here. Powder mixtures of PBT and BDM monomer were used as feed for the SSP and MP reactions. These PBT/BDM mixtures are abbreviated as $(BD_xBDM_y)_{feed}$. BD_x denotes the mole percentage (mol%) of PBT (expressed as 1,4-butanediol units), whereas BDM_y denotes the mol% of BDM (expressed as BDM units) in the $(BD_xBDM_y)_{feed}$ mixtures. The $(BD_xBDM_y)_{feed}$ mixtures used for the SSP-reaction were obtained by dissolution of both PBT and BDM in 1,1,1,3,3,3-hexafluoro-2-isopropanol (HFIP). After complete dissolution, the HFIP was evaporated and the obtained lump of material was ground into powder. For the SSP-reaction, 3 g of $(BD_xBDM_y)_{feed}$ mixture was used. An amount of 18 g glass pearls was added on top of the powder mixture to keep the powder in its position at the bottom of the SSP-reactor. A temperature of 170 °C was used in combination with a solid-state polymerization time of 24 h. The nitrogen flow, purging through the reactor during the SSP reaction, was set at 0.5 L/min for the first 1 h and was increased to 2 L/min for the remaining 23 h of the SSP-reaction. The solid-state polymerized (BD_xBDM_y) copolymers are indicated as

$(BD_xBDM_y)_{ssp}$, in which BD_x and BDM_y represent the initial mol% PBT and BDM present in the $(BD_xBDM_y)_{feed}$ mixture being used for SSP. The actual mole percentages of BD and BDM units after SSP slightly differ from the initial mol% present in the $(BD_xBDM_y)_{feed}$ mixtures. These differences can be attributed to the evaporation of 1,4-butanediol and some BDM monomer during the SSP reaction.

The MP reaction of the $(BD_xBDM_y)_{feed}$ mixtures was done in a melt reactor. Typically, approximately 7.5 g of a $(BD_xBDM_y)_{feed}$ powder mixture was molten and subsequently stirred in the melt reactor for 0.5 h at a temperature of 230 °C in the presence of an argon flow of 1.5 L/min. The temperature was then further increased and kept for 1.5 h at 240 °C. Simultaneously, the argon flow was replaced by a continuous high vacuum of 0.1 mBar. After this period, the vacuum was released and the melt reactor was removed from the vessel. The obtained copolymer was then dissolved in approximately 25 mL 50:50 vol% HFIP:chloroform mixture and subsequently precipitated in cold methanol. Melt polymerized (BD_xBDM_y) copolymers are denoted as $(BD_xBDM_y)_{mp}$ copolymers, where BD_x and BDM_y represent the initial mol% PBT and BDM present in the $(BD_xBDM_y)_{feed}$ mixture being used for MP.

7.2.3 Nuclear Magnetic Resonance (NMR) Spectroscopy

All solution ^{1}H-NMR spectra were recorded on a Varian 400 MHz spectrometer at 25 °C at a resonance frequency of 400.164 MHz. For the ^{1}H-NMR measurements, 15 mg of polymer was dissolved in 0.8 mL of a 80:20 vol% $CDCl_3$:TFA-d mixture. All chemical shifts are reported in ppm downfield from tetramethylsilane (TMS), used as the internal standard. The spectra were acquired using 32 scans, a delay time (d1) of 5 s and a total number of data points of 64 k.

7.2.4 Size Exclusion Chromatography (SEC)

The number-average molecular weight ($\overline{M}_n$) and polydispersity index (PDI) of the synthesized (BD_xBDM_y) copolymers were determined by SEC. The system was equipped with a Hewlett Packard 1100 series injector (injection volume 10 μL) and a Hewlett Packard PL HFIP gel column (250×4.6 mm, part no: 1514-5900 HFIP) thermostated at 35 °C. A mixture consisting of 5 vol% HFIP and 95 vol% chloroform was used as eluent. Acetophenone was used as flow marker. A HP 1100 series pump provided a flow rate of 0.3 mL/min. For detection, an Agilent diode array detector was used (λ = 295 nm). The SEC system was calibrated with polystyrene calibration standards ($\overline{M}_w$ range: 1000 - 900.000 g/mol). The obtained PS calibration curve was used to determine the $\overline{M}_n$ of the synthesized (BD_xBDM_y) copolymers. In addition, PBT homopolymer samples with known $\overline{M}_n$ values

(determined by end group titration) were analyzed with the same SEC system. A fitting curve was prepared using the $\overline{M}_n$ values obtained by end group titration and the $\overline{M}_n$ obtained via the PS calibration curve. The measured $\overline{M}_n$ vales of the (BD_xBDM_y) copolymers were fitted using this calibration curve and corrected to obtain a more realistic value.

7.2.5 Differential Scanning Calorimetry (DSC)

The melting and crystallization enthalpy ($\Delta H_{melting}$ and $\Delta H_{crystallization}$, respectively) were measured with a TA Instruments Q1000 DSC equipped with an autosampler and a refrigerated cooling system (RCS). The DSC cell was purged with a nitrogen flow of 50 mL/min. The temperature was calibrated using the onset of melting for indium. The enthalpy was calibrated with the heat of fusion of indium. For the (BD_xBDM_y) copolymers, samples of 6-8 mg were prepared in crimped aluminum pans. These samples were measured in the temperature range from 0 to 250 °C using heating and cooling rates of 10 °C/min and isothermal periods of 3 min at 0 and 250 °C, respectively.

For the $(BD_xBDM_y)_{feed}$ mixtures, samples of 5-7 mg were prepared in hermetically closed aluminum pans. The samples were first heated from 0 °C to 120 °C, which is 10 °C above the T_m of BDM, and kept for 10 minutes at this temperature. The samples were then cooled to -80 °C and subsequently reheated to 240 °C using cooling and heating rates of 10 °C/min, respectively. $\Delta H_{melting}$ was taken from the second heating run.

The glass transition temperature (T_g) of the $(BD_xBDM_y)_{feed}$ mixtures was measured in temperature modulated DSC (TMDSC®) mode using the same TA Q1000 DSC as previously described. The DSC cell was purged with a nitrogen flow of 50 mL/min. Samples of 6-8 mg were prepared in crimped aluminum pans. The samples were first heated in normal DSC mode from 0 to 120 °C and subsequently kept at this temperature for 10 minutes. The samples were subsequently cooled down with 10 °C/min to -60 °C and reheated from -60 to 100 °C in modulated DSC mode, using an underlying heating rate of 2 °C/min and an oscillating temperature with a period of 60 seconds and amplitude of 0.5 °C. The T_g values were taken from the reversing heat capacity signal. The step increase of the heat capacity at T_g (Δc_p) was determined using tangents to the measured curve below and above the T_g. The value obtained for Δc_p was used to determine the mobile amorphous fraction (α_{mobile}) of the $(BD_xBDM_y)_{feed}$ mixtures. α_{mobile} is defined as the ratio between the measured Δc_p and that of fully amorphous PBT ($\Delta c_p{}^0{}_\alpha = 0.35$ J/g K).[9,11]

7.3 Results and discussion

(BD_xBDM_y) copolymers were synthesized via SSP and via MP. The general chemical structure of a (BD_xBDM_y) copolymer is shown in Figure 7.1.

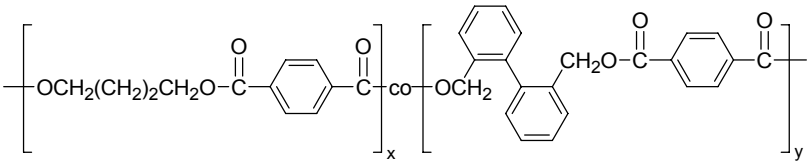

Figure 7.1. Chemical structure of a (BD_xBDM_y) copolymer, consisting of BD-T and BDM-T repeat-units.

7.3.1 Miscibility study of PBT-BDM mixtures

To study the influence of BDM monomer on the morphology of the $(BD_xBDM_y)_{feed}$ mixtures, similar DSC measurements were performed as previously described in **Chapter 5** for the $(BD_xDi_y)_{feed}$ mixtures. Therefore, several $(BD_xBDM_y)_{feed}$ mixtures with different PBT/BDM ratios were first kept at 120 °C, which is approximately 10 °C above the T_m of the BDM monomer. At this rather low temperature, transesterification reactions are negligible. In this way, the molten BDM is allowed to diffuse into the amorphous phase of PBT. The samples were subsequently cooled to -80 °C and then reheated at 10 °C/min to 240 °C. The DSC traces of the second heating runs are shown in Figure 7.2a. The corresponding T_g values were measured by modulated DSC and are plotted in Figure 7.2b as a function of F_{PBT}, representing the PBT fraction present in each $(BD_xBDM_y)_{feed}$ mixture.

From the DSC traces shown in Figure 7.2a, it can be observed that the BDM melting endotherm is completely absent in the DSC-traces. Furthermore, the PBT melting endotherm shifts to lower temperatures as the fraction of BDM in the mixture increases. This melting temperature depression is a clear indication that BDM is at least partly miscible with PBT. Also the Δc_p values at the half-step T_g increase for increasing amounts of BDM used for mixing. Similar to the $(BD_xDi_y)_{feed}$ mixtures, this increase is attributed to the swelling of the rigid amorphous PBT chain segments by BDM monomer, which obviously acts as a plasticizer. As a consequence, the mobility of these swollen chain segments increases. The T_g values shown in Figure 7.2b rapidly decrease to a minimum value of approximately 0 °C for increased BDM fractions higher than 15 mol%. This decrease shows that the mobility of the amorphous PBT chain segments increases due to swelling by molten BDM monomer.

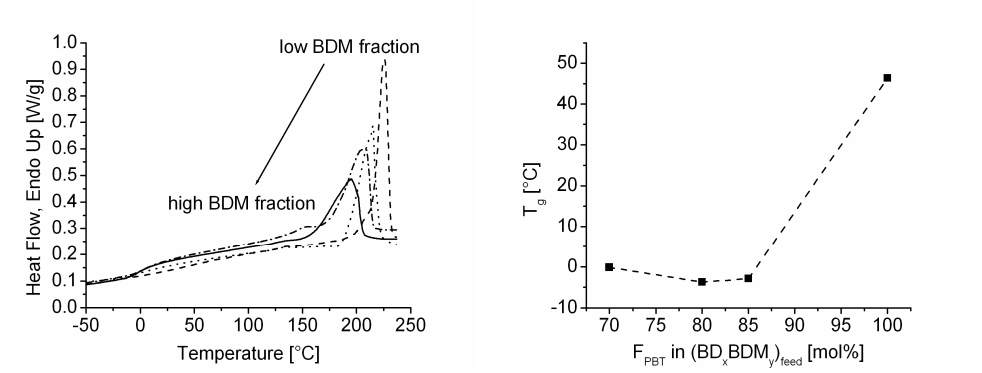

(a) (b)

Figure 7.2. (a) DSC heating traces of $(BD_xBDM_y)_{feed}$ mixtures: $(BD_{100}BDM_0)_{feed}$ (– – –), $(BD_{85}BDM_{15})_{feed}$ (·····), $(BD_{80}BDM_{20})_{feed}$ (·–·–·), $(BD_{70}BDM_{30})_{feed}$ (——) and (b) T_g of the $(BD_xEG_y)_{feed}$ mixtures as a function of PBT fraction (F_{PBT}) present in the mixtures.

The limited T_g value indicates that the concentration of BDM in the amorphous phase becomes constant. A similar effect was also observed for the $(BD_xDi_y)_{feed}$ mixtures (see **Chapter 5**). Retaining a limited value for the T_g for increasing amounts of BDM can only occur when the fraction of swollen amorphous PBT chain segments concomitantly increases. Only then, the BDM concentration in the amorphous PBT phase remains unchanged and thus a constant T_g value is obtained. The mechanism of this continuous increase of swollen PBT chain segments for increasing fractions of BDM can be explained by application of the three-phase model to represent the morphology of the $(BD_xBDM_y)_{feed}$ mixtures. This three-phase model consists of a crystalline phase (fraction: $\chi_{heating}$) and an amorphous phase which can be subdivided in a rigid amorphous fraction (α_{rigid}) and a mobile amorphous fraction (α_{mobile}).[9] The fractions $\chi_{heating}$, α_{mobile} and α_{rigid} can be calculated using the following equations:

$$\alpha_{mobile} = \Delta c_p / \Delta c_p{}^0{}_\alpha \tag{7.1a}$$

$$\chi_{heating} = \Delta H_{melting} / \Delta H^0{}_{fuse} \tag{7.1b}$$

Hence, α_{rigid} can be described by:

$$\alpha_{rigid} = 1 - \chi_{heating} - \alpha_{mobile} \tag{7.1c}$$

where Δc_p is the heat capacity increase at half-step T_g and $\Delta c_p{}^0{}_\alpha$ is the heat capacity increase for 100% amorphous PBT at the half-step T_g ($\Delta c_p{}^0{}_\alpha$ is 0.35 J/g K at T_g = 47 °C).[9,11] $\Delta H^0{}_{fuse}$ is the crystallinity of 100% crystalline PBT ($\Delta H^0{}_{fuse}$ = 145 J/g).[11-13]

It was already shown in **Chapter 5**, that mixing PBT with Dianol via dissolution in HFIP results in a large increase of the rigid amorphous fraction after evaporation of the HFIP. When the $(BD_xDi_y)_{feed}$ mixtures are heated above the T_m of Dianol monomer ($T_{m,\ Dianol}$ = 110 °C), the molten Dianol monomer acts as a plasticizer by swelling the rigid amorphous PBT chain segments. These swollen PBT chain segments have an increased mobility and can therefore no longer be considered as rigid amorphous. Instead, it was assumed that these swollen chain segments contribute to the mobile amorphous fraction of the $(BD_xDi_y)_{feed}$ mixture. Hence, the fraction of rigid amorphous chain segments are gradually transformed into mobile amorphous chain segments due to swelling of Dianol. This mechanism is also applicable to the $(BD_xBDM_y)_{feed}$ mixtures.

To calculate the total mobile amorphous fraction of the $(BD_xBDM_y)_{feed}$ mixtures used as feed for SSP, the Δc_p value at the half-step T_g, obtained from the DSC traces shown in Figure 7.2a, was used in eq 7.1a. For convenience, the value of $\Delta c_p^{\ 0}{}_{\alpha}$ for 100% amorphous PBT was assumed to be independent of the added BDM monomer and hence used to calculate α_{mobile} of the $(BD_xDi_y)_{feed}$ mixtures. In practice, the $\Delta c_p^{\ 0}{}_{\alpha}$ value of 100% amorphous PBT may be influenced by the presence of BDM monomer. However, this difference may be small as was also observed for the Dianol monomer. The fractions $\chi_{heating}$, α_{rigid} and α_{mobile} of the non-transesterified $(BD_xBDM_y)_{feed}$ mixtures, calculated using eqs 7.1a-7.1c, are plotted in Figure 7.3 as a function of F_{PBT}.

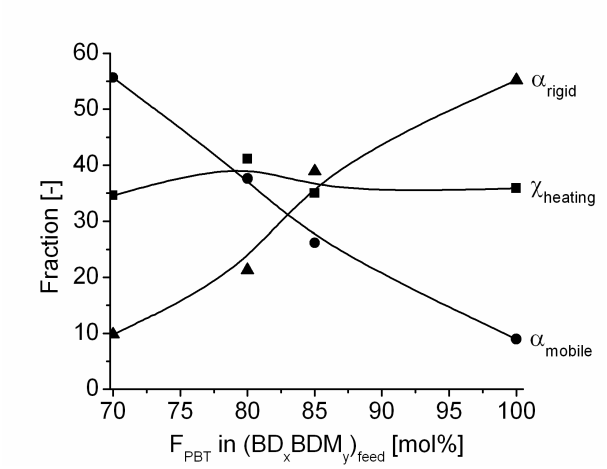

Figure 7.3. Crystalline ($\chi_{heating}$ ■), rigid amorphous (α_{rigid} ▲) and mobile amorphous (α_{mobile} ●) fraction as a function of F_{PBT} in the non-transesterified $(BD_xBDM_y)_{feed}$ mixtures.

For the observed composition range, the distribution of $\chi_{heating}$, α_{rigid} and α_{mobile} as a function of F_{PBT} is similar to that of the $(BD_xDi_y)_{feed}$ copolymers (see **Chapter 5**). The molten BDM

monomer swells the rigid amorphous chain segments which subsequently increase in mobility. As a consequence, α_{mobile} increases whereas α_{rgid} concomitantly decreases for increasing fractions of BDM monomer used for mixing. $\chi_{heating}$ is not significantly influenced by the presence of the BDM-monomer. Similarly to the $(BD_xDi_y)_{feed}$ mixtures, BDM may further dissolve PBT crystals as soon as α_{rigid} has decreased to zero.

7.3.2 Synthesis of PBT-BDM copolymers

A $(BD_{80}BDM_{20})_{feed}$ mixture was initially used to study the incorporation of BDM into PBT via SSP and MP. Thermogravimetric Analysis (TGA) measurements showed that BDM monomer is more volatile than BHET and Dianol, which were earlier used for incorporation into PBT via SSP. The obtained $(BD_{80}BDM_{20})_{ssp}$ and $(BD_{80}BDM_{20})_{mp}$ copolymers were characterized by ^{1}H-NMR spectroscopy and SEC. The results are shown in Table 7.1. ^{13}C-NMR sequence distribution analysis could not give information about the chemical microstructure of both $(BD_{80}BDM_{20})_{ssp}$ and $(BD_{80}BDM_{20})_{mp}$ copolymer. The reason is that one of the carbon atoms of the biphenyl group gives a ^{13}C-NMR peak signal which overlaps with the multiple peaks originating from peak splitting of the quaternary carbon atom signal. However, in view of the results obtained for the (BD_xDi_y) copolymers, it is expected that the $(BD_xBDM_y)_{mp}$ copolymers have a fully random distribution whereas the $(BD_xBD_y)_{ssp}$ copolymers have a non-random and more blocky distribution.

Table 7.1. Characterization of the $(BD_xBDM_y)_{ssp}$ and $(BD_xBDM_y)_{mp}$ copolymer by ^{1}H-NMR spectroscopy and SEC.

Copolymer	Composition feed[a]		Composition after reaction[b]		SEC	
	$F_{PBT,\ feed}$ [mol%]	$F_{BDM,\ feed}$ [mol%]	$F_{BD\text{-}T,\ total}$ [mol%]	$F_{BDM\text{-}T,\ total}$ [mol%]	$\overline{M}_n$ [kg/mol]	PDI
$(BD_{80}BDM_{20})_{ssp}$	79.9	20.1	86.4	13.6	16	3.1
$(BD_{80}BDM_{20})_{mp}$	80.0	20.0	82.2	17.8	16	2.5
$(BD_{85}BDM_{15})_{mp}$	85.0	15.0	86.2	13.8	18	2.6

[a] Composition of the $(BD_xBDM_y)_{feed}$ mixtures is obtained by accurately weighing of the amount of PBT and BDM.

[b] Composition of the $(BD_xBDM_y)_{ssp}$ is obtained via ^{1}H-NMR spectroscopy measurements.

When all BDM monomer present in the $(BD_{80}BDM_{20})_{feed}$ mixture is incorporated via SSP or MP, the final copolymer composition should theoretically consist of 75 mol% BD-T and 25 mol% BDM-T (20 equivalents BD-T units are replaced by 20 equivalents monomeric BDM-T units; the total copolymer consists of 80 repeat units after SSP). However, it can be seen from

Table 7.1 that for the synthesized $(BD_{80}BDM_{20})_{ssp}$ copolymer only 13.6 mol% BDM-T is present. Hence, a considerable amount of BDM monomer has evaporated during the SSP reaction prior to its incorporation. The amount of incorporated BDM in the $(BD_{80}BDM_{20})_{mp}$ copolymer is 17.8 mol%. The higher temperature used for MP-reactions results in an increased transesterification rate of BDM monomer with PBT. Once the BDM monomer has been incorporated into the PBT chain, evaporation will not occur easily. Moreover, the high viscosity of the polymer melt will slow down evaporation of the BDM monomer. The low reactivity of BDM is due to the limited flexibility of the hydroxymethyl groups which are connected to the aromatic ring via sp2-hybridization ("in plane" geometry).

Because the composition of the synthesized $(BD_{80}BDM_{20})_{ssp}$ copolymer deviate significantly from the $(BD_{80}Di_{20})_{mp}$ copolymer, also a $(BD_{85}BDM_{15})_{feed}$ mixture was polymerized in the melt. The characteristics of the resulting $(BD_{85}BDM_{15})_{mp}$ copolymer are also shown in Table 7.1. It can be seen that the composition and $\overline{M}_n$ of the $(BD_{85}BDM_{15})_{mp}$ copolymer are almost equal to those of the $(BD_{80}BDM_{20})_{ssp}$ copolymer. An equal composition and $\overline{M}_n$ is necessary for comparison of the thermal properties of the $(BD_{80}BDM_{20})_{ssp}$ and $(BD_{85}BDM_{15})_{mp}$ as will be carried out in the next paragraph.

7.3.3 Thermal properties of PBT-BDM copolymers

The thermal properties of the $(BD_xBDM_y)_{ssp}$ and $(BD_xBDM_y)_{mp}$ copolymers were determined by DSC. The DSC-trace of the first heating run of the $(BD_{80}BDM_{20})_{ssp}$ copolymer is shown in Figure 7.4. For comparison, the DSC heating runs of a $(BD_{85}Di_{15})_{ssp}$ copolymer (from **Chapter 5**), $(BD_{70}EG_{30})_{ssp}$ copolymer (from **Chapter 6**) and $(BD_{100}Di_0)_{ssp}$ (i.e. PBT homopolymer after SSP; from **Chapters 5** and **6**) are also plotted in Figure 7.4.

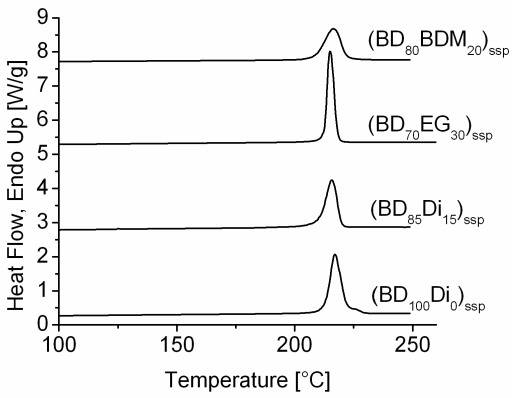

Figure 7.4. Thermal behavior of a $(PBT)_{ssp}$, $(BD_{85}Di_{15})_{ssp}$, $(BD_{80}EG_{20})_{ssp}$ and $(BD_{80}BDM_{20})_{ssp}$ copolymer.

The end compositions including the $\overline{M}_n$ values and polydispersity indices (PDI) of the selected copolymers and PBT homopolymer are given in Table 7.2.

Table 7.2. End compositions, $\overline{M}_n$ and PDI values for PBT homopolymer and several PBT copolymers obtained by SSP and MP.

Copolymer	End composition[a]		SEC[b]	
	$F_{BD\text{-}T,\ total}$ [mol%]	$F_{diol\text{-}total}$ [mol%]	$\overline{M}_n$ [kg/mol]	PDI [-]
$(BD_{80}BDM_{20})_{ssp}$	86	14	16	3.1
$(BD_{70}EG_{30})_{ssp}$	84	16	76	3
$(BD_{85}Di_{15})_{ssp}$	84	16	35	3
$(BD_{100}Di_0)_{ssp}$	100	0	42	2.7
$(BD_{85}BDM_{15})_{mp}$	86	14	18	2.6
$(BD_{80}EG_{20})_{mp}$	84	16	22	2.8
$(BD_{85}Di_{15})_{mp}$	81	19	12	2.3
$(BD_{100}Di_0)_{mp}$	100	0	15	2.3

[a] End compositions were determined by 1H-NMR spectroscopy.

[b] $\overline{M}_n$ and PDI were determined by Size Exclusion Chromatography (SEC).

It can be seen that the copolymers have an approximately equal fraction of incorporated diol. Furthermore, the $\overline{M}_n$ values for copolymers obtained by SSP are generally higher than for the copolymers obtained by MP. The higher $\overline{M}_n$ values are due to the efficient chain coupling occurring during the SSP reaction. The thermal properties derived from the DSC measurements are summarized in Table 7.3. It can be seen from Figure 7.4 that the T_m value of the $(BD_{100}Di_0)_{ssp}$ copolymer is significantly lower than generally reported in literature.[9] It was already mentioned that α_{mobile} of $(BD_{100}Di_0)_{ssp}$ copolymer was close to 0.15. Apparently, this small fraction of mobile amorphous PBT chain segments does not result in the reorganization process, leading to melting and recrystallization of the PBT crystals, which normally occurs during heating. This reorganization process results in a PBT melting temperature of approximately 225 °C. It can be observed from the second heating run (shown in Figure 7.5a and 7.5b, respectively) that the $(BD_{100}Di_0)_{ssp}$ homopolymer has a double melting endotherm and a T_m value which is in agreement with the values found in literature.

Table 7.3. Thermal properties of several PBT copolymers obtained by SSP and MP.

Copolymer	Heating run 1[a,b,c]			Cooling run 1[b,c]		Heating run 2[a,b,c]		
	T_g [°C]	$\Delta H_{melting}$ [J/g]	T_m [°C]	$\Delta H_{crystallization}$ [J/g]	T_c [°C]	T_g [°C]	$\Delta H_{melting}$ [J/g]	(T_m-T_c) [°C]
$(BD_{80}BDM_{20})_{ssp}$	67.5	50.4	216.3	35.7	180.2	58.5	35.2	23.6
$(BD_{70}EG_{30})_{ssp}$	60.1	64.5	215.0	40.3	162.8	46.7	43.5	39.8
$(BD_{85}Di_{15})_{ssp}$	67.1	56.2	215.8	17.1	112.1	49.0	24.9	72.1
$(BD_{100}Di_0)_{ssp}$	54.9	68.6	217.1	44.1	185.2	40.7	44.7	35.7
$(BD_{85}BDM_{15})_{mp}$				40.2	167.6	55.0	38.6	25.6
$(BD_{80}EG_{20})_{mp}$				45.2	165.7	43.5	45.8	37.8
$(BD_{85}Di_{15})_{mp}$				31.4	128.2	54.9	26.1	55.2
$(BD_{100}Di_0)_{mp}$				57.4	188.3	39.1	54.9	34.8

[a] The T_g values were determined in modulated DSC mode.

[b] The $\Delta H_{melting}$, T_m, $\Delta H_{crystallization}$ and T_c values were determined in normal DSC mode using heating/cooling rates of 10 °C/min.

[c] The T_m and T_c values shown are the peak values of the melting endotherms respectively crystallization exotherms.

The cooling runs of the $(BD_{80}BDM_{20})_{ssp}$, $(BD_{70}EG_{30})_{ssp}$, $(BD_{85}Di_{15})_{ssp}$ and $(BD_{100}Di_0)_{ssp}$ PBT_{ssp} are shown in Figure 7.5a together with the cooling runs of $(BD_{85}BDM_{15})_{mp}$, $(BD_{80}EG_{20})_{mp}$, $(BD_{85}Di_{15})_{mp}$ and $(BD_{100}Di_0)_{mp}$. The second heating runs of these copolymers are shown in Figure 7.5b. Despite the similarity in composition (see Table 7.2), it can be observed from Figure 7.5 and from the (T_m-T_c) values shown in Table 7.3 that PBT copolymers obtained by MP generally crystallize faster during cooling from the melt than copolymers obtained by SSP. This difference in crystallization behavior is mainly due to the $\overline{M}_n$ values of the MP copolymers which are generally lower than those of the SSP copolymers. It was already mentioned in **Chapters 5** and **6** that for both (BD_xDi_y) and (BD_xEG_y) copolymers the unmodified homopolymer PBT chain segments are fully miscible with the modified PBT chain segments when the copolymers are in the molten state. As a consequence, nucleation during cooling is delayed resulting in decreased T_c values. Also the growth of the lamellar crystals is slower due to the hindered diffusion process of homopolymer PBT chain segments from the melt to the crystal surface growth front. However, it can be seen that for both $(BD_{80}BDM_{20})_{ssp}$ and $(BD_{85}BDM_{15})_{mp}$ copolymers a high nucleation rate is observed. Apparently, the presence of the rigid biphenyl moieties results in some ordering in the melt, thereby reducing the minimum of free energy necessary for the formation of stable nuclei. The result is a high T_c value.

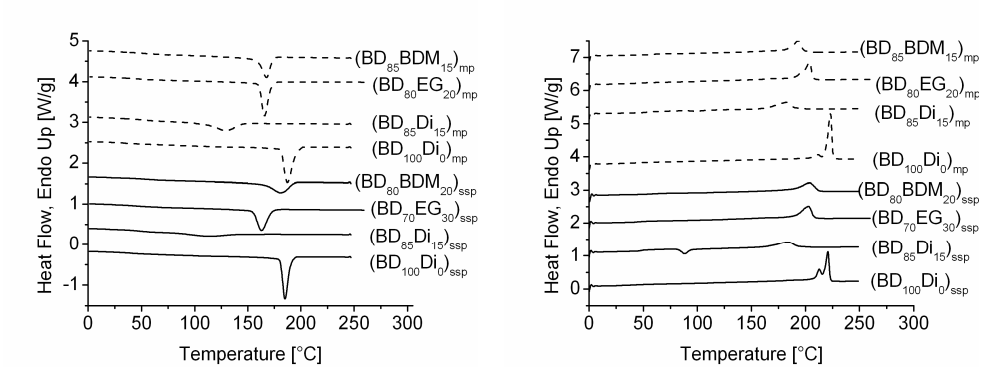

Figure 7.5. Thermal behavior of $(BD_{100}Di_0)_{ssp}$, $(BD_{85}Di_{15})_{ssp}$, $(BD_{70}EG_{30})_{ssp}$, $(BD_{80}BDM_{20})_{ssp}$, $(BD_{100}Di_0)_{mp}$, $(BD_{85}Di_{15})_{mp}$, $(BD_{80}EG_{20})_{mp}$ and $(BD_{85}BDM_{15})_{mp}$ (a) DSC cooling runs (b) second DSC heating runs. All runs were performed at a heating/cooling rate of 10 °C.

Furthermore, it can be observed from Table 7.3 that the $(BD_{80}BDM_{20})_{ssp}$ copolymer has a T_c value which is more than 10 °C higher than the T_c value of the $(BD_{85}BDM_{15})_{mp}$ copolymer (T_c = 180.2 °C and T_c = 167.6 °C, respectively), whereas the compositions and $\overline{M}_n$ values of these two copolymers are almost equal (see Table 7.2). Hence, the non-random distribution of BDM in the $(BD_{85}BDM_{15})_{ssp}$ copolymer results in a more efficient nucleation and thus in a higher T_c value compared to the $(BD_{85}BDM_{15})_{mp}$ copolymer in which the BDM is randomly distributed. The crystal growth process is for both $(BD_{80}BDM_{20})_{ssp}$ and $(BD_{85}BDM_{15})_{mp}$ copolymer rather slow as can be concluded from the broad crystallization peaks obtained during cooling from the melt (see Figure 7.5a). Apparently, the diffusion of PBT chain segments to the crystal growth front is hindered by the presence of the rigid biphenyl moieties which will not fit in the crystal phase. Furthermore, the PDI of the $(BD_{80}BDM_{20})_{ssp}$ copolymer and the $(BD_{85}BDM_{15})_{mp}$ copolymer are 3.1 and 2.6, respectively. Consequently, a slightly higher melt viscosity is expected for the $(BD_{80}BDM_{20})_{ssp}$ copolymer which may be the explanation for the broader crystallization peak of the $(B_{80}DBDM_{20})_{ssp}$ copolymer compared to that of the $(BD_{85}BDM_{15})_{mp}$ copolymer (see Figure 7.5).

From Table 7.3, it can be observed that the T_g values of the copolymers obtained by SSP are lower for the second heating run compared to the first heating run (directly after SSP). The copolymers obtained by SSP have a relatively high crystallinity due to annealing occurring simultaneously during the SSP-reaction. It was already explained for the $(BD_xDi_y)_{ssp}$ and $(BD_xEG_y)_{ssp}$ copolymers, once in the molten state, that the modified copolyester chain

segments are fully miscible with the unmodified PBT chain segments. This miscibility hinders the crystal growth process during cooling from the melt resulting in a decreased crystallinity compared to the crystallinity present directly after SSP. As a consequence, PBT homopolymer chain segments, originally part of the crystalline phase, subsequently contribute to the amorphous phase, resulting in a decreased value of the T_g for the second heating run. For the $(BD_{85}BDM_{15})_{ssp}$ copolymer, the crystallinity after cooling from the melt is not significantly different than the crystallinity present directly after SSP. Consequently, the T_g value of the $(BD_{80}BDM_{20})_{ssp}$ copolymer is considerably higher for the second heating run than the T_g values of the $(BD_{70}EG_{30})_{ssp}$ and $(BD_{85}Di_{15})_{ssp}$ copolymer (see Table 7.3).

For the $(BD_{80}BDM_{20})_{ssp}$ copolymer, the lower T_g value for the second heating can be explained by the decrease of the rigid amorphous fraction after cooling from the melt. The presence of a rigid amorphous fraction results in a constraint mobility of polymer chain segments, which are part of the mobile amorphous fraction. The influence of the rigid amorphous fraction can be clearly observed from the T_g of the $(BD_{100}Di_0)_{ssp}$ (i.e. PBT) homopolymer. Directly after SSP, the fraction of rigid amorphous phase is large resulting in a constrained mobile amorphous phase. Consequently, a T_g value of 54.9 °C is obtained for the first heating run (see Table 7.2). Crystallization during cooling from the melt and subsequent reheating results in a decrease of the rigid amorphous fraction and consequently in a T_g value which is almost 15 °C lower (T_g = 40.7 °C). A similar effect occurs for the $(BD_{80}BDM_{20})_{ssp}$ copolymer resulting in a lower T_g value for the second heating run compared to the first heating run.

7.4 Conclusions

BDM was successfully incorporated into PBT via SSP and MP. A miscibility study showed that BDM monomer swells the rigid amorphous PBT chain segments, which subsequently become more mobile. The mobility of the swollen chain segments is now sufficiently high to participate in the transesterification reactions during SSP. The methanol groups of the BDM monomers have a low flexibility resulting in a rather slow transesterification rate during the SSP-reaction. The relatively high volatility of the BDM monomer results in a significant evaporation of the monomer prior to its incorporation. DSC measurements showed that the T_g values obtained from the second heating run are more than 15 °C higher for both synthesized $(BD_{80}BDM_{20})_{ssp}$ and $(BD_{85}BDM_{15})_{mp}$ copolymers compared to the T_g of PBT homopolymer. Furthermore, both (BD_xBDM_y) copolymers have higher T_c values than the PBT-Dianol (BD_xDi_y) and PBT-BHET (BD_xEG_y) copolymers. Most likely, once (BD_xBDM_y) copolymers are molten, the rigid rod-like BDM segments induce some ordering in the melt. This ordering promotes nucleation of PBT segments upon cooling from the melt. Although, the random

$(BD_{85}DM_{15})_{mp}$ copolymer and $(BD_{80}BDM_{20})_{ssp}$ have almost equal values for composition and $\overline{M}_n$, the nucleation process is more efficient for the non-random $(BD_{80}DM_{20})_{ssp}$ copolymer as can be observed from the higher T_c value (180 °C versus 168 °C). Apparently, the non-random distribution of the BDM moieties in the $(BD_{80}BDM_{20})_{ssp}$ copolymers enhances the ordering in the melt. The polydispersity index (PDI) of the $(BD_{80}BDM_{20})_{ssp}$ copolymer is higher compared to that of the $(BD_{85}Di_{15})_{mp}$ copolymer and may result in a higher viscosity in the melt. Consequently, a lower crystal growth rate (i.e. broader crystallization peak) is obtained for the $(BD_{80}BDM_{20})_{ssp}$ copolymer compared to the growth rate of the $(BD_{85}BDM_{15})_{mp}$ copolymer.

7.5 References and notes

1. Fakirov, S. In *Solid State Behavior of Linear Polyesters and Polyamides*; Schultz, J. M., Fakirov, S., Eds.; Prentice-Hall: Englewood Cliffs, NJ, 1990; Chapter 2, p 19-43.
2. Jansen, M. A. G.; Goossens, J. G. P.; de Wit, G.; Bailly, C.; Koning, C. E. *Macromolecules* **2005**, *38*, 2659-2664.
3. Jansen, M. A. G.; Goossens, J. G. P.; de Wit, G.; Bailly, C.; Koning, C. E. *Anal. Chim. Acta* **2005**, in press.
4. Jansen, M. A. G.; Goossens, J. G. P.; de Wit, G.; Bailly, C.; Schick, C.; Koning, C. E. *Macromolecules* **2005***,* accepted.
5. Cheng, S. Z. D.; Cao, M.-Y.; Wunderlich, B. *Macromolecules* **1986**, *19*, 1868-1876.
6. Cheng, S. Z. D.; Wunderlich, *Macromolecules* **1987**, *20*, 1630-1637.
7. Cheng, S. Z. D.; Wu, Z. Q.; Wunderlich, B. *Macromolecules* **1987**, *20*, 2802-2810.
8. Cheng, S. Z. D.; Wunderlich, B. *Macromolecules* **1988**, *21*, 789-797.
9. Cheng, S. Z. D.; Pan, R.; Wunderlich, B. *Makromol. Chem.* **1988**, *189*, 2443-2458.
10. Sakaguchi, Y.; Okamoto, M.; Tanaka, I. *Macromolecules* **1995**, *28*, 6155-6160.
11. ATHAS database: Wunderlich B. *Pure and Applied Chemistry* **1995**, *67*, 1019-1026.
12. Conix, A.; Van Kerpel, R. *J. Polym. Sci.* **1959**, *40*, 521-532.
13. Kirshenbaum, I. J. *J. Polym. Sci., Part A* **1965**, *3*, 1869-1875.

Technology assessment

The aim of this study was to examine whether it is possible to modify poly(butylene terephthalate) (PBT) in such a way that its high crystallization rate is retained whereas the thermal and mechanical properties are enhanced. One condition for crystallization to occur is the presence of homopolymer chain segments of sufficient length. Traditionally, properties of polyesters are modified by reactive blending with other polycondensates. However, the transesterification reactions occurring in the melt result in shorter and more irregular homopolymer blocks. Hence, when semi-crystalline polyesters such as PBT are modified via reactive blending, a decreased crystallinity and crystallization rate will be obtained.

Solid-state polymerization (SSP) was recently used to prepare copolyesters from semi-crystalline oligomers. With SSP, the transesterification reactions only occur in the amorphous phase and consequently, crystallizable homopolymer blocks are retained.

In this study, SSP was used to modify PBT by selective incorporation of diol monomers into the amorphous phase, whereas the crystalline PBT phase remained unchanged. In this way, PBT copolymers may be obtained with a crystallization rate similar to that of pure PBT, whereas other properties can be enhanced. For PBT, it is desired that the rather low T_g of approximately 45 °C, can be increased. Unfilled PBT with a higher T_g can be used at higher temperatures without loosing dimensional stability. In this way, a broader application window for PBT may be achieved.

It was shown that diol monomers could be successfully incorporated into PBT via SSP. A blocky microstructure with sufficiently large PBT blocks, necessary for crystallization, could be obtained. For comparison, diol monomers were incorporated into PBT via melt copolymerization (MP). The MP copolymers have a random microstructure and consequently shorter PBT blocks. However, it was observed for PBT-Dianol and PBT-BHET copolymers (**Chapters 3-5** and **Chapter 6**, respectively) that the non-random chemical microstructure of the SSP copolymers did not result in a better crystallization behavior compared to the MP copolymers. This result showed that crystallization behavior of a semi-crystalline copolymer is not only determined by the presence of large homopolymer PBT blocks. Once the PBT-Dianol copolymers and PBT-BHET copolymers obtained via SSP were molten, the modified parts appeared to be fully miscible with the former crystalline homopolymer PBT parts. As a consequence, the nucleation and subsequent crystal growth were both hindered when the copolymers were cooled from the melt. To retain a high crystallization rate, the modified PBT parts should be immiscible with the non-modified homopolymer PBT parts. Another option is that diol monomers are used which are able to induce some ordering in the melt. One can think of monomers with hydrogen bonding such as amides and comonomers with phenol groups. Also rod-like monomers are known to induce some ordering in the melt. Such a

monomer is 2,2'-biphenylmethanol (BDM), described in **Chapter 7**. A high nucleation rate was obtained. In addition, it was shown that the nucleation was even more efficient for a blocky PBT-BDM copolymer obtained via SSP than for a PBT-BDM copolymer obtained via MP having a similar chemical but more random composition and molecular weight. However, it was also observed that these rod-like moieties delay the crystal growth process, because these moieties have to be excluded from the crystal phase during the crystallization process. In addition, high melt viscosities, resulting in a decreased diffusion of homopolymer PBT to the crystal growth front, also have a hindering effect on the crystal growth process.

The mixing procedure of PBT and diol monomer prior to SSP is important because the diol incorporation can only occur when the diol is homogeneously present in the amorphous PBT phase. In this thesis, the PBT and the diol monomers were mixed by dissolution in 1,1,1,3,3,3-hexafluoro-2-propanol (HFIP). After complete dissolution, the HFIP was evaporated and the obtained lump was ground into powder, which was subsequently used as feed for SSP.

The research described in this thesis showed that the initial morphology of the PBT/diol powder mixture, obtained via mixing in HFIP, has a significant influence on the final microstructure of the copolymer obtained after SSP. It appeared that only part of the amorphous PBT phase was available for incorporation of diol monomer. The part not available for incorporation is denoted as the rigid amorphous fraction. The HFIP mixing method gives a large initial rigid amorphous fraction limiting the amount of diol monomer to be incorporated. This limitation was clearly shown for the BHET monomer (**Chapter 6**). However, other diols are able to swell this rigid part, as observed for Dianol monomer (**Chapters 3-5**) and BDM monomer (**Chapter 7**). The swelling makes the rigid amorphous PBT part sufficiently mobile so that diol also can be incorporated in this part. It has to be remarked that HFIP is a corrosive and toxic solvent. Moreover, HFIP is expensive and relatively large volumes are needed for dissolution of PBT. It can be concluded that solution mixing of PBT and the diol monomer in HFIP is not a suitable method for use in an industrial process. An alternative method for mixing PBT and diol monomer, which can be easily applied in industry, is pre-melt mixing in an extruder. Short extrusion times have to be used in order to prevent extensive transesterification reactions. When extrusion is used as the method for mixing PBT and the diol monomer, the resulting blend will have a lower initial rigid amorphous part and consequently monomers like BHET can be incorporated to a larger extent.

Preliminary experiments showed that low molecular weight PET homopolymers can also be incorporated into PBT via SSP. It is known that both components of PBT-PET blends crystallize from the melt as separate crystal phases. The PBT-PET copolymer obtained via SSP retains a high crystallization rate upon cooling from the melt. The T_g is approximately 10

°C higher than for pure PBT, depending on the PET fraction used. Also an oligomer, based on terephthalate and the earlier used Dianol, was incorporated into PBT via SSP. Also here, a higher T_g is found whereas a high crystallization rate is obtained. The latter result is remarkable considering the earlier obtained results for the PBT-Dianol copolymers, synthesized via SSP.

It can be concluded from the results described in this thesis that SSP can be used to selectively incorporate comonomers into the amorphous phase of PBT. Whether a retained crystallization rate is obtained mainly depends on the miscibility in the melt of the modified PBT fraction with the unmodified homopolymer PBT fraction. When these fractions are immiscible, copolymers obtained by SSP may give a high nucleation and crystal growth rate compared to random copolymers obtained by MP.

Samenvatting

Poly(butyleen tereftalaat) (PBT) is een semi-kristallijn polycondensatie polymeer dat gekenmerkt wordt door een hoge kristallisatiesnelheid in combinatie met goede thermische en mechanische eigenschappen. De hoge kristallisatiesnelheid maakt PBT vooral geschikt voor spuitgiettoepassingen. De glasovergangstemperatuur is echter laag ($T_g \approx 45$ °C), waardoor de vormvastheid afneemt wanneer ongevuld PBT gebruikt wordt bij hogere temperaturen. Het is algemeen bekend dat de materiaaleigenschappen van PBT kunnen worden gemodificeerd door het bijvoorbeeld in de smelt te mengen met andere polycondensaten. Door transesterificatiereacties zullen in eerste instantie blokcopolymeren gevormd worden die bij het voortschrijden van de reactie worden omgezet in 'random' copolymeren. Deze random copolymeren hebben kortere homopolymeerblokken met een onregelmatige lengte hetgeen leidt tot een lagere smelttemperatuur en kristalliniteit en een langzamere kristallisatiesnelheid ten opzichte van ongemodificeerde PBT.

Het doel van het onderzoek zoals beschreven in dit proefschrift is het ontwikkelen van een modificatiemethode waarbij de hoge kristallisatiesnelheid van PBT behouden blijft, terwijl andere eigenschappen worden verbeterd. Hierbij valt te denken aan een verhoging van de T_g, maar ook verbetering van de slagvastheid en de compatibiliteit met andere polymeren. Een modificatiemethode die sinds kort gebruikt wordt om copolymeren te maken van polycondensatie homopolymeren en diol comonomeren is vaste-fase ('solid-state') (co)polymerisatie (SSP). Bij SSP wordt een reactietemperatuur gebruikt die net onder de smelttemperatuur van het homopolymeer ligt. Het gevolg is dat de polymere ketendelen die zich in de amorfe fase bevinden voldoende mobiel worden om te participeren in transesterificatiereacties met het in te bouwen comonomeer. De polymere ketendelen die zich in de kristallijne fase bevinden, zijn niet mobiel genoeg bij deze temperatuur en blijven dus onveranderd. Vaste-stof modificatie kan dus worden gebruikt om comonomeren selectief in te bouwen in de amorfe fase, zonder dat de kristallijne fase verandert. Op deze manier blijven relatief lange homopolymere PBT ketendelen die nodig zijn voor kristallisatie behouden, terwijl de thermische en mechanische eigenschappen aangepast kunnen worden.

Drie diolen zijn geschikt gebleken voor inbouw in PBT via SSP: 2,2-bis[4-(2-hydroxyethoxy)fenyl]propaan (Dianol 220®), bis(2-hydroxyethyl)tereftalaat (BHET) en 2,2'-bifenyldimethanol (BDM). PBT en diol werden in verschillende verhoudingen gemengd via een oplossingroute om zo copolymeren te verkrijgen met variërende samenstellingen. Ter vergelijking zijn deze diolen ook ingebouwd in PBT via copolymerisatie in de smelt (MP), hetgeen resulteert in een meer random structuur.

De reactiekinetiek van de Dianol-inbouw in de PBT ketens via SSP is in detail bestudeerd. Het is gebleken dat de inbouw van Dianol via twee opeenvolgende eerste orde-reacties verloopt. Het Dianol monomeer reageert eerst via één hydroxyl groep met de PBT ketendelen

(eerste reactie) hetgeen resulteert in ketenbreuk waardoor een lager molecuul gewicht wordt verkregen. The PBT keteneinden die nu een Dianol molecuul als eindgroep hebben, reageren vervolgens via de nog vrije Dianol hydroxyl groep met nieuwe PBT ketendelen wat weer resulteert in ketenrecombinatie (tweede reactie). Bij de ketenrecombinatie ontstaat 1,4-butanediol als condensatie product. Verder is aangetoond dat de eerste reactie sneller verloopt dan de tweede reactie.

De morfologie van de PBT-Dianol copolymeren kan het best worden beschreven met een drie-fasen model, bestaande uit een kristallijne fase en een amorfe fase, die weer onderverdeeld is in een rigide amorfe fractie en een mobiele amorfe fractie. Een speciaal ontwikkelde berekeningsmethode liet zien dat bij SSP alleen de mobiele amorfe fractie toegankelijk is voor inbouw van Dianol door transesterificatie en dat het Dianol in deze fase volledig random wordt ingebouwd. Bij aanvang van de SSP reactie bestaat het PBT-Dianol mengsel vrijwel uitsluitend uit een kristallijne en een rigide amorfe fractie. Tijdens de SSP-reactie zwelt een deel van de rigide amorfe ketendelen door Dianol waardoor de mobiliteit van deze ketens sterk toeneemt. Deze gezwollen mobiele fractie vormt samen met de initiële aanwezige fractie aan mobiele PBT ketens de totale mobiele fractie van het PBT-Dianol mengsel. De PBT ketendelen in deze totale mobiele fractie kunnen met Dianol transesterificeren gedurende SSP. Het gevolg is dat random gemodificeerde ketendelen ontstaan na SSP. Deze random gemodificeerde ketendelen kunnen niet meer kristalliseren door hun onregelmatige ketenstructuur. Het gedeelte van de rigide amorfe fractie dat niet gezwollen is door Dianol, transformeert gedurende de SSP reactie in de kristallijne fase hetgeen leidt tot verhoogde kristalperfectie. Naarmate meer Dianol gebruikt wordt voor de inbouw, neemt bij aanvang van de SSP reactie de fractie aan gezwollen ketendelen toe en daarmee dus ook de fractie waarin transesterificatie optreedt. Wanneer geen rigide ketendelen meer beschikbaar zijn, lost het overgebleven vrije Dianol de kristallijne PBT-ketens op. Dit oplossen gaat echter langzaam. Het uiteindelijke gevolg is dat voor voldoende hoge fracties Dianol niet meer kan worden gesproken van polymerisatie in de vaste fase, maar dat de situatie vergelijkbaar is met polymerisatie in de smelt. De chemische microstructuur is dan ook blokachtig voor lage fracties ingebouwd Dianol, maar wordt uiteindelijk volledig random voor grote hoeveelheden ingebouwd Dianol. Dit resultaat is daarmee in overeenstemming met de random chemische microstructuur van de PBT-Dianol copolymeren die verkregen zijn door polymerisatie in de smelt.

Ondanks verschillen in chemische microstructuur, zijn de thermische eigenschappen van de PBT-Dianol copolymeren verkregen door SSP vrijwel identiek aan die van de copolymeren gemaakt via MP. De T_g van de PBT-Dianol copolymeren die verkregen werden via SSP, hebben direct na SSP een hogere T_g dan bulk PBT. Als deze copolymeren na opsmelten en

afkoelen tot onder de T_g vervolgens weer verwarmd worden, zijn de T_g waarden echter veel lager. Deze afname van de T_g voor de tweede opwarmrun is te verklaren doordat de ketendelen die via SSP gemodificeerd werden, in de smelt volledig mengbaar bleken te zijn met de niet-gemodificeerde homopolymere ketendelen. De kristallisatiesnelheid en de kristalliniteit nemen hierdoor sterk af. De fractie niet gemodificeerde homopolymere PBT ketendelen in de amorfe fase neemt dus toe na kristallisatie vanuit de smelt wat dus resulteert in verlaging van de T_g voor de tweede opwarmrun.

In tegenstelling tot de PBT-Dianol copolymeren, neemt voor de PBT-BHET copolymeren die verkregen zijn via SSP het blokachtige karakter toe naarmate meer comonomeer gebruikt wordt voor inbouw. Door de aanwezigheid van zowel hydroxyl- als carbonylgroepen, kan BHET met andere BHET monomeren transesterificeren hetgeen resulteert in de vorming van PET homopolymeer. Het blijkt dat BHET maar beperkt mengbaar is met PBT. Alleen deze mengbare fractie kan transesterificeren met de mobiele amorfe fase van PBT. De BHET fractie die niet mengbaar is, vormt een aparte fase en reageert gedurende de SSP reactie tot PET homopolymeer. Wanneer de niet mengbare BHET fractie bij aanvang van de SSP reactie voldoende groot is, worden PET homopolymeren gevormd die kristalliseren gedurende de SSP reactie. Ook voor de PBT-BHET copolymeren die verkregen werden via SSP zijn thermische eigenschappen weinig verschillend met de eigenschappen van de copolymeren die verkregen werden via MP. De gemodificeerde ketendelen en niet gemodificeerde ketendelen van de copolymeren die werden verkregen via SSP zijn volledig mengbaar in de smelt.

Ten slotte werd BDM ingebouwd in PBT via SSP en MP waarbij copolymeren verkregen werden met een identieke samenstelling. BDM is net als Dianol volledig mengbaar met de mobiele amorfe PBT fase. Door de relatief hoge vluchtigheid van BDM kon niet meer dan ongeveer 15 mol% via SSP worden ingebouwd in de mobiele amorfe PBT fractie. Onderzoek naar de thermische eigenschappen van PBT-BDM copolymers die werden verkregen via SSP en MP, laat zien dat voor beide materialen een hoge kiemvormingssnelheid wordt verkregen wanneer deze copolymeren kristalliseren vanuit de smelt. Bovendien nam voor beide copolymeren de T_g met ongeveer 15 °C toe in vergelijking met de T_g van bulk PBT. De hoge kiemvormingssnelheid is mogelijk het gevolg van de rigide en staafachtige struktuur van het BDM monomeer. Het is gevolg is dat een geordende structuur van de polymere PBT ketendelen gevormd wordt wanneer de copolymeren zich in gesmolten toestand bevinden. Voor het PBT-BDM copolymeer dat verkregen werd via SSP, was de kristallisatietemperatuur zelfs meer dan 10 °C hoger in vergelijking met dat van het PBT-BDM copolymeer, verkregen via MP. Het molecuulgewicht van het PBT-BDM copolymer, verkregen via SSP, was zelfs iets hoger in vergelijking met dat van het PBT-BDM copolymeer, verkregen via MP. De niet random verdeling van BDM in het copolymeer verkregen via SSP resulteert in een hogere

ordening in de smelt dan voor de copolymeren verkregen via MP. Deze hogere mate van ordening verhoogt de kiemvormingssnelheid wanneer het copolymeer gekoeld wordt vanuit de smelt. Dit resultaat toont aan dat SSP gebruikt kan worden om eigenschappen van semi-kristallijne polymeren te verbeteren in combinatie met een beter kristallisatiegedrag ten opzichte van MP.

Dankwoord / Acknowledgements

De laatste bladzijden van het proefschrift. Vele promovendi zijn blij als ze hier aangekomen zijn. En dat geldt ook voor mij!

Vier mensen waren altijd nauw betrokken bij mijn promotieonderzoek. Deze personen, door mij heimelijk “De Grote 4” genoemd, hadden natuurlijk allemaal hun eigen inbreng in het onderzoek. De meetings die meestal in de kamer van Cor Koning plaats vonden, hadden dan ook regelmatig het karakter van een wetenschappelijk “koffiekransje” waarbij toch iedereen graag wilde meebabbelen over zaken die (al dan niet) met het onderzoek te maken hadden. Gelukkig hield Cor de teugels strak in handen en greep hij tijdig in als we te ver afdwaalden. Wie zijn nu ”De Grote 4”? Laat ik beginnen om de eerste persoon van dit gezelschap nader toe te lichten: Gert de Wit *alias* “monomeer selecteur”. Ik wil jou hartelijk danken voor de interesse en de vele nuttige adviezen die je hebt aangedragen. Ook heb je het mogelijk gemaakt om vrijwel alle SEC-metingen te laten verrichten bij GE Plastics waarvoor ook mijn dank aan Barry van Hooff en Ruud van Hout (beide werkzaam bij GE Plastics) voor het uitvoeren van de metingen. Op de TUe bleek het toch niet zo gemakkelijk om een SEC-apparaat met HFIP als eluens altijd in werkende staat te hebben. Gert, ik weet nog dat je tijdens één van onze eerste meetings “wilde” ideeën had over welke monomeren we wel allemaal niet konden inbouwen. Dat was een hele waslijst. We begonnen met Dianol en BHET. Achteraf bleek dat we, zuiver wetenschappelijk gezien, een goede keuze hadden gedaan omdat beide monomeren een verschillend gedrag vertoonden. Voor industriële toepassingen bleken ze helaas minder geschikt, tenzij je natuurlijk amorfe copolymeren wilt hebben.

De tweede persoon van “De grote 4” was Christian Bailly *alias* “wetenschappelijk filosoof”. Christian, bedankt voor je inbreng in de discussies en voor het doorworstelen van mijn proefschrift. Met betrekking tot jou wil ik hier nog even een anekdote aanhalen. Ik weet nog dat we ooit aan de hand van een ^{1}H-NMR spectrum aan het filosoferen waren over hoe zuiver het monomeer nu was na purificatie. Er was echter één piekje dat we niet konden toekennen. Jouw oplossing was doeltreffend: gewoon wegvegen met Tipp-Ex. Ja, Belgische humor is leuk!

Aangekomen bij de derde persoon van “De Grote 4”, onze eigen Han Goossens *alias* “de man van de duizend en één technieken”. Als er iemand nog ooit een real-time multipurpose combinatorial karakteriseringsapparaat voor polymeren uitvindt, dan is dat ongetwijfeld Han: SAXS, WAXD, DSC, FTIR, RAMAN, SALS, DIS, DSC, DMTA om maar “een paar” karakteriseringtechnieken te noemen. Han gebruikt ze allemaal. Wat zou onze vakgroep moeten beginnen zonder de kennis van Han. Het nadeel van het beschikken over zoveel kennis is dat iedereen daar ook gebruik van wil maken. Zo kan het dus wel eens voorkomen dat Han in bespreking is. Han, ik wil jou bedanken voor het veelvuldig doorlezen en

corrigeren van alle tekst die ik je heb aangeleverd. Je geduld en vertrouwen toen het even allemaal wat minder ging, heb ik zeer gewaardeerd. Het is uiteindelijk toch helemaal goed gekomen!

Drie mensen gehad, dus “one to go”: mijn promotor Cor Koning *alias* “de compatibilizer”. Toen ik bij jou begon als promovendus wilde je wel dat ik *full commitment* gaf. Ik hoop dat ik aan je verzoek/eis (?) heb voldaan. Het was op het laatst nog redelijk kort dag om het maar even als een understatement uit te drukken: geen uitstel want van uitstel komt afstel was jouw credo. Gelukkig heb je altijd alle vertrouwen in mij gehad. De DSM meeting in Vaalsbroek was mooi: een presentatie geven en daarna lekker eten en drinken en nog later gezellig naborrelen aan de bar. Jij een whiskey en ik een Grand Marnier en allebei een lekker Hajenius sigaartje erbij. Ook de BASF meeting, met het vele Weissbier ’s avonds en daarna nog het stadje in om te kijken of er nog wat barretjes open waren (wat inderdaad het geval was). En natuurlijk niet te vergeten de Lunteren meetings waar jij ’s avonds steevast te vinden was in “De Onderwereld”.

An dieser Stelle möchte ich auch recht gerne Herrn Prof. Schick danken für seine kritischen Kommentaren meine Doktorarbeit betreffent und seine Teilnahme in meinem Promotionskomitee. Auch seine Bereitheit um DSC Messungen in seinem Labor zu verrichten, habe ich sehr geschätzt.

También querría agradeceder al Prof. Muñoz-Guerra por ser parte del comité y por sus valiosos comentarios sobre esta tesis. Sé, que el tiempo para leer todo el material era un poco escaso. Por ello me complace que estuviese dispuesto a leer todos los capítulos.

Verder wil ik Prof. Lemstra bedanken voor het tolereren van mijn aanwezigheid in SKT gedurende de afgelopen 4½ jaar, terwijl ik eigenlijk bij SPC hoorde.

Gedurende mijn promotie, heb ik het genoegen gehad om 2 stagiaires te mogen begeleiden. De eerste was Roy Lensen die na een spoedcursus polymeerchemie vele copolymeertjes heeft gemaakt. Zo veel zelfs, dat hij daarna nooit meer iets met polymeren wilde doen en zijn geluk heeft gezocht in de richting van de organische chemie. The second research student was imported from Shanghai (China) via the Asia-Link project of PLEM & Co: Lue Hong Wu *alias* “Sjakie”. Lue, although your interests were more related to business, chatting and sleeping, you obtained some nice scientific results. Together, we went for a few days to the ESRF in Grenoble (France) for doing some X-ray measurements. However, we almost ended up in jail before we arrived at ESRF. Next time, remember where you put your passport when you are on an international train trip! Also the mini-holiday in Paris afterwards was nice. I know that you really liked the location of the hotel I arranged (at approximately 100 meters from the Moulin Rouge).

Natuurlijk wil ik mijn collega's bedanken voor de gezellige tijd die ik binnen SKT heb gehad gedurende de afgelopen jaren (in alfabetische volgorde): Anastasia, Anne, Bert, Blanca, Bob, Carmen, Cees W., Chris, David, Edgar, Emile, Ester, Ilse, Irina (*Kleine*), Joost, Jules H., Jules K., Ken, Lijing, Luigi, Mano, Marjolein, Mark, Maya, Merina, Nilesh, Pauline, Pit, Peter (ja, omdat je het zo graag wilt), Rob, Roy, Sachin, Sanjay, Soney, Thierry, Vid en Wouter.

Het is natuurlijk al een hele eer om met naam vermeld te mogen worden in het dankwoord, maar voor een paar collega's wil ik toch nog even een bijzonder woord van dank uitspreken:

Allereerst mijn kamergenoot en paranimf Jules. Ik wil jou bijzonder hartelijk danken voor het meehelpen met het lay-outen en invoeren van door mij voorgestelde correcties gedurende de laatste weken van het schrijven van mijn proefschrift. Uiteraard maak ik dit nog goed met een avondje "onbeperkt eten en drinken". Het MACRO 2004 congres in Parijs was geweldig (en je weet nu dat ze 's nachts om 2 uur geen shoarma verkopen in Parijs en in Heythuysen wel!). Ook tijdens de Lunteren meetings hebben we 's avonds veel lol gehad. Vooral toen de drank voor iedereen gratis was maar niet voor jou: "Dat is dan 20 euro a.u.b!".

Mijn andere paranimf Mark: Mark, bedankt dat je mijn paranimf wilde zijn. Ook jij was bij MACRO 2004, of nee, eigenlijk toch niet want jij was Joep van Dijk(!) of was ik dat? Het eten vond je niet geweldig die donderdagavond in Parijs maar de wijn maakte veel goed.

Ook mijn oud-collega "mama" Ilse(tje) wil ik hier nog even noemen. Toen ik begon met afstuderen, heb je je al snel over mij ontfermd en moest je altijd al mijn gezever aanhoren over de experimenten die ik van "papa" Hans Wilderbeek moest doen en die vervolgens niet lukten. Daarna heb je deze moederrol nog trouw volgehouden toen ik begon met promoveren. Tevens kreeg je een tweede "zoon": onze enige echte Jules Kierkels.

Our Man in China: Edgar, bedankt voor gezellige RPK-tripjes naar Utrecht, de terrasjes die we aldaar pakten (als het goed weer was en de RPK-sprekers minder goed; aan welke van deze twee voorwaarden het vaakst voldaan werd, mag jij zelf beoordelen) en de etentjes die we regelmatig na werktijd hadden waarbij de hele vakgroep traditiegetrouw werd doorgelicht.

Mijn (oud)-kamergenootjes: Isabelle, Vid (meestal inclusief Sanja), Jules (ja, die is al uitgebreid besproken), Blanca en part-time Maya (alhoewel haar aanwezigheid soms doet vermoeden alsof er 10 personen in STO 0.24 aan 'het werk' zijn in plaats van 4) wil ik bedanken voor de gezellige tijd.

I also would like to thank Sun Chunxia, Li Juan, Ao Yong and Cui Ning for the nice conversations and the "pleasant smell" of the Chinese food during lunch time. The Chinese dinners which I had with Li Juan and Ao Yong and later with Sun were very nice.

Ook de vele secretaresses die Piet inmiddels versleten heeft, wil ik bij deze bedanken met in

het bijzonder: Emma (nu SMN), Marleen (nu PTN), Ineke (huidige secretaresse) en Elly (huidige secretaresse en volgens mij onverslijtbaar). Verder de secretaresses van Cor: Helly (vertrokken naar Duitsland), Caroline en niet te vergeten Pleunie. Pleunie, hartelijk dank voor alle koffie die je met liefde en plezier (of met *full commitment* op zijn "Coriaans" gezegd) hebt gebracht tijdens de al eerder genoemde wetenschappelijke "koffiekransjes" op de kamer van Cor.

De laatste woorden wil ik wijden aan mijn kleine zusje Marjolein en mijn grote zwager-in-spé Dick, maar bovenal aan mijn ouders. Bedankt voor alle steun die ik van jullie de afgelopen 4½ jaar heb gekregen. Het is niet altijd gemakkelijk geweest en vooral het laatste jaar was het flink afzien, maar uiteindelijk is het toch allemaal goed gekomen.

Martijn Jansen,

Oktober 2005

Curriculum Vitae

The author of this thesis was born in Helmond, the Netherlands, on April 28th 1975. After finishing secondary school, (VWO, Carolus Borromeus College, Helmond) in 1993, he studied Chemical Engineering at the 'Fontys Hogeschool Eindhoven'. He obtained his Bachelor's degree in 1997. In the same year, he started with the shortened Master education program Chemical Engineering at the Eindhoven University of Technology. During 2000, he completed his thesis entitled 'Synthesis and UV-polymerization of liquid crystalline thiol-ene biphenyl monomers' in the 'Polymer Technology' group of prof.dr. P.J. Lemstra and successfully obtained his Master's degree.

He continued working as a research assistant on the synthesis of thiol-ene monomers for a period of 3 months. At the beginning of 2001, he started his PhD-study in the 'Polymer Technology' group of prof.dr. P.J. Lemstra under the supervision of prof.dr. C.E. Koning (Department of Chemical Engineering and Chemistry, Eindhoven University of Technology). During his PhD-study, the author completed four modules of the course 'Registered Polymer Technologist' (RPK, Register PolymeerKundige) organized by the 'National Dutch Graduate School of Polymer Science and Technology' (PTN, PolymeerTechnologie Nederland).